# MOLECULAR BASIS OF PORCINE REPRODUCTIVE AND RESPIRATORY SYNDROME VIRUS-MEDIATED INNATE IMMUNE SUPPRESSION

BY

MINGYUAN HAN

DISSERTATION

Submitted in partial fulfillment of the requirements
for the degree of Doctor of Philosophy in VMS-Pathobiology
in the Graduate College of the
University of Illinois at Urbana-Champaign, 2015

Urbana, Illinois

Doctoral Committee:

Professor Dongwan Yoo, Chair, Director of Research
Professor Daniel Rock
Professor Federico Zuckermann
Professor Joanna Shisler
Professor Rex Gaskins

## ABSTRACT

Porcine reproductive and respiratory syndrome (PRRS) is an emerged and re-emerging swine disease featured by severe reproductive losses, post-weaning pneumonia, and increased mortality. During infection of PRRS virus, poor induction of pro-inflammatory cytokines and type I IFNs are observed, and PRRSV seems to have a capacity to escape the immune surveillance for survival. Non-structural protein (nsp) 1 of PRRSV has been identified as a viral IFN antagonist, and nsp1 has been shown to degrade the CREB-binding protein (CBP) and to inhibit the formation of enhanceosome thus resulting in the suppression of IFN production. Nsp1 is auto-processed into nsp1α and nsp1β subunits, and individual subunits (nsp1α and nsp1β) of nsp1 suppress type I IFN production. In the present study, the nsp1α subunit was shown to be responsible for CBP degradation. PRRSV-nsp1β was mainly distributed in the nucleus and played roles for host cell mRNA nuclear retention leading to subversion of host protein synthesis and suppression of type I IFN production. This study was expanded to other member viruses in the family Arteriviridae, and all subunits of arterivirus nsp1 presented the IFN suppressive activity. Similar to PRRSV-nsp1α, CBP degradation was evident in cells expressing LDV-nsp1α and SHFV-nsp1γ. PRRSV-nsp1β-mediated mRNA nuclear accumulation was also observed for LDV-nsp1β and SHFV-nsp1β, but for EAV-nsp1. To study the structure function of PRRSV-nsp1 and its IFN antagonism, motifs for PLP1α (papain-like proteinase 1α), ZF1 (zinc-finger domain 1), and ZF2 within the nsp1α subunit were individually mutated and the mutant proteins were examined for their IFN suppressive ability. Single or double mutations of C8S, C10S, C25S, and/or C28S for the ZF1 motif impaired the IFN antagonism, demonstrating that ZF1 is the essential element of nsp1α for IFN suppression. The ZF1 mutants did not induce CBP degradation and nor IFN suppression. For nsp1β, a SAP motif was identified with the consensus

sequence of 126-LQxxLxxxGL-135 by bioinformatics analysis. Cytoplasmic staining was observed for SAP mutants L126, R129A, L130A, and L135A, and these mutants did not cause the nuclear retention of host cell mRNAs, and were unable to inhibit IFN signaling. Using reverse genetics, SAP mutant viable viruses vK124A, vL126A, vG134A, and vL135A were recovered. nsp1β protein was retained in the cytoplasm in cells infected with vL126A and vL135A. Accordingly, no mRNA nuclear retention was observed in these cells, and also no suppression of IFN production was identified. My study demonstrates nsp1 as the type I IFN antagonist in the family Arteriviridae and the molecular basis for this antagonism.

## ACKNOWLEDGMENTS

First and foremost, I would like to give my respectful gratitude to my advisor, Dr. Dongwan Yoo, for continued guidance and encouragement throughout my entire PhD program! I appreciate all his contributions of time, ideas, and funding to make my research experience productive and stimulating. I am also thankful for the excellent example he has provided as a successful virologist and professor.

Many thanks to my committee members, Dr. Daniel Rock, Dr. Federico Zuckermann, and Dr. Joanna Shisler, for their supports, patience, and encouragements. My special thanks to Dr. Mariangela Segre for being so gracious and generous with her endless helps and encouraging smile. Thank you also to Mrs. Paula Moxley, Mrs. Julia Thomas, Mrs. Karen Nichols, and Mrs. Linda Rohl, without whom my graduate program would not have been nearly so successful.

I would like to express my sincere gratitude to my labmates, Chi Yong Kim, Qingzhan Zhang, Hanzhong Ke, Dr. Cheng Song, Dr. Yan Sun, Dr. Sungsik Yu, and Dr. Kaichuang Shi, for their friendship, cooperation, and assistance. A big thank-you to Wei-Yu Chen, Jinjun Lin, and Dr. Luchang Zhu, for always being so willing to help.

I wish to thank all faculty members, staff, and students in the Department of Pathobiology, University of Illinois at Urbana-Champaign.

Last but not least, special recognition goes out to my family, for their love, support, encouragement, and patience during my studies. To my lovely wife, Dr. Shuaizhen Yuan, who has inspired me and provided constant encouragement during the entire process. To my parents, Wendeng Han and Yuying Xue, as you are the source of my strength and motivation. To my lovely daughter, Talia Han. I thank all of you for your patience and I love you more than you will ever know.

## TABLE OF CONTENTS

# CHAPTER 1: LITERATURE REVIEW

## 1. 1. INTRODUCTION

Porcine reproductive and respiratory syndrome (PRRS) was first reported in the United States in 1987 and subsequently in Europe in 1990 and quickly became endemic in most pig producing countries worldwide (Benfield et al., 1992; Chand et al., 2012; Murakami et al., 1994; Shimizu et al., 1994; Wensvoort et al., 1991). The clinical manifestation of PRRS is complicated but is characterized by severe reproductive losses including abortions, mummified fetuses, weak born and stillborn young, post-weaning pneumonia, increased mortality, and growth retardation of young pigs. The etiological agent is PRRS virus (PRRSV). PRRSV belongs to the family Arteriviridae together with lactate dehydrogenase-elevating virus (LDV) of mice, equine arteritis virus (EAV), and simian hemorrhagic fever virus (SHFV). The family Arteriviridae is grouped in the order Nidovirales together with Coronaviridae, Roniviridae, and Mesoniviridae (Nga et al., 2011; Zirkel et al., 2011). The wobbly possum disease virus (WPDV) has recently been discovered to infect Australian brush-tail possums and is believed to be most closely related to the current members of the family Arteriviridae (Dunowska et al., 2012), and three additional SHFV isolates have been identified in Africa that appear to be distantly related to SHFV of Southeast Asia (Lauck et al., 2013).

The PRRSV genome is a single-strand positive-sense RNA of 15 Kb in length with a 5′ cap and 3′-polyadenylated tail (Fig. 1.1A) (Meulenberg et al., 1993; Murtaugh et al., 1995; Nelsen et al., 1999; Wootton et al., 2000). The PRRSV genome is polycistronic and harbors two

This chapter previously appeared as articles in Veterinary Microbiology and Virus Research. The original citations are as follows: Han, M. and Yoo, D. 2014. Engineering the PRRS virus genome: Updates and perspectives. Veterinary Microbiology 174:279-295; Han, M. and Yoo, D. 2014; Modulation of innate immune signaling by nonstructural protein 1 (nsp1) in the family Arteriviridae. Virus Research 194:100-109. 

large open reading frames (ORFs; ORF1a and ORF1b), followed by ORF2a, ORF2b, and ORFs 3 through 7, plus ORF5a within ORF5 (Firth et al., 2011; Johnson et al., 2011; Meulenberg et al., 1993; Murtaugh et al., 1995; Nelsen et al., 1999; Wootton et al., 2000). A -2 ribosomal frame-shifting has recently been identified for expression of nsp2TF in the nsp2-coding region. The nsp2TF coding sequence is conserved in PRRSV, LDV, and SHFV but absent in EAV (Fang et al., 2012). The coding sequences in the viral genome are flanked by the 5′ and 3′ un-translated regions (UTRs) involved in translation, replication, and transcription (see review in Snijder et al., 2013).

By comparative genome sequence analysis, PRRSV isolates are divided into two distinct genotypes: the European type (genotype I) and North American type (genotype II), represented by Lelystad virus (LV) and VR-2332 as the prototype virus for each genotype, respectively (Benfield et al., 1992; Wensvoort et al., 1991). The sequence similarities between two genotypes are approximately 60% (Allende et al., 1999; Nelsen et al., 1999; Wootton et al., 2000). Amino acid (aa) sequence alignments indicate that the major differences between two genotypes exist in the open reading frame (ORF) 1a region and the structural protein region (Kapur et al., 1996; Murtaugh et al., 1995; Nelsen et al., 1999). Natural deletions and insertions are observed in some isolates, especially in the ORF1a region (Fang et al., 2004; Gao et al., 2004; Shen et al., 2000; Tian et al., 2007).

ORF1a and ORF1b code for two large polyproteins, pp1a and pp1ab, with the expression of the latter mediated by the -1 frame-shifting in the ORF1a/ORF1b overlapping region (Fig. 1.1B; den Boon et al., 1991; Snijder and Meulenberg, 1998). Thus, the pp1b portion is expressed always as a fusion with pp1a. The pp1a and pp1ab proteins are further processed to generate 14 non-structural proteins (nsps). The polyprotein processing scheme involves the rapid auto-

proteolytic release of three N-terminal nsps, nsp1α, nsp1β, and nsp2, mediated by papain like proteinase (PLP) residing in each of them. The subsequent processing for the remaining portion of polyproteins is mediated by the serine protease in nsp4 resulting in 14 individual nsps (den Boon et al., 1995; van Aken et al., 2006; Ziebuhr et al., 2000). The proteolytic cleavages for individual nsps were initially predicted by sequence comparisons in combination with some experimental data from EAV, the prototype virus of the family Arteriviridae (Fang and Snijder, 2010; Ziebuhr et al., 2000). The exact cleavage sites for PRRSV nsp1α↓nsp1β and nsp1β↓nsp2 have recently been confirmed to be M180↓A181 and G383↓A384 mediated by PRRSV-PLP1α and PRRSV-PLP1β, respectively (Chen et al., 2010a; Sun et al., 2009; Xue et al., 2010).

A set of 3′-coterminal nested subgenomic (sg) mRNAs, from which structural proteins are translated, is produced during infection (Fig. 1.1B). Each mRNA contains a common 5′-end leader sequence identical to the 5′-proximal part of the genome and this sequence is referred to as transcription-regulatory sequence (TRS). The fusion of the common 5′ sequence (leader TRS) to the different 3′-body segments of sg mRNAs is mediated by discontinuous transcription which is a common strategy of nidoviruses (Sawicki et al., 2007; Snijder et al., 2013; Sola et al., 2011). During the negative-strand sg RNA synthesis, transcription is attenuated at different body TRS regions of the genomic template. The nascent subgenome-length minus-strand RNA, having an anti-body TRS at its 3′ end, will then move and base-pair with the leader TRS and completes the extension of sg RNA. Minus-strand sg RNAs subsequently serve as a template for plus-strand sg mRNA which is subsequently translated for structural protein (Music and Gagnon, 2010; Sawicki et al., 2007; Snijder et al., 2013). The SHFV genome contains a duplication of the ORFs 2a, 2b, 3, and 4 downstream of ORF1b, and this gene duplication has been confirmed in the recent African isolates of SHFV (Lauck et al., 2011; Lauck et al., 2013).

## 1.2. IMMUNE MODULATION BY PRRSV

During infection of PRRSV, poor induction of pro-inflammatory cytokines and type I IFNs are observed, and PRRSV seems to have a capacity to escape the immune surveillance for survival. At least six viral proteins have been identified as IFN antagonists regulating the innate immune signaling during infection; nsp1α, nsp1β, nsp2, nsp4, nsp11, and N proteins. Among these proteins, nsp1α and nsp1β are two most potent IFN antagonists (Beura et al., 2010; Chen et al., 2010; Kim et al., 2010; Song et al., 2010; Sun et al., 2012a; Yoo et al., 2010). nsp1 is cleaved into two subunits of nsp1α and nsp1β, and both subunits suppress the type I IFN induction. In order for IFN gene expression, enhanceosome is first assembled to recruit CREB (cyclic AMP responsive element binding)-binding protein (CBP) as the key component of the IFN enhanceosome. CBP has been found to be degraded in the presence of PRRSV-nsp1α (Han et al., 2013), which is likely the basis for IFN suppression by nsp1α.

### 1.2.1. Modulation of innate immune signaling by Arteriviruses

The host range of arteriviruses is narrow and their infection is restricted to suids, mice, equids, and non-human primates for PRRSV, LDV, EAV, and SHFV, respectively. Macrophages appear to be primary target cell for their infection (Snijder and Meulenberg, 1998). Arterivirus infection may cause persistence in infected animals. PRRSV may persist up to 6 months in pigs and EAV may persist for life-long in horses. LDV infection is typically asymptomatic and the virus persists for life-long in infected mice (Anderson et al., 1995; Plagemann et al., 1995). For SHFV, fatal hemorrhagic fever occurs in macaques, but asymptomatic persistent infection is observed in baboons (Vatter and Brinton, 2014)

**Arterivirus-mediated type I interferon modulation**

The type I IFN system is a key component of the innate immunity and represents a first line of defense against viral infection (Samuel, 2001). PRRSV is sensitive to anti-viral effects of type I IFNs, and the treatment with porcine IFN-α impedes the growth of PRRSV significantly (Albina et al., 1998; Buddaert et al., 1998). The sensitivity of PRRSV to IFN-α varies and dose-dependent (Lee et al., 2004). LDV is resistant to anti-viral effects of IFN-α in mice, which is probably a reason for its life-long persistence (Ammann et al., 2009). Arteriviruses do not trigger effective innate immune responses upon infection, and it may explain the weak adaptive response and viral persistence. Unlike other respiratory viruses such as swine influenza and porcine respiratory coronavirus, whose infections induce high concentrations of IFN-α, PRRS causes minimal expression of IFN-α which is a hallmark for PRRSV infection in cells and pigs (Van Reeth et al., 1999), even though considerable variations are observed for different isolates (Lee et al., 2004; Miller et al., 2004; Nan et al., 2012). Dendritic cells (DCs) play an important role in anti-viral immunity by providing early innate protection against viral replication and by presenting antigens to T cells for initiation of the adaptive immune response (Clark et al., 2000), and thus IFN response in DCs by PRRSV has been studied. Monocyte-derived DCs are susceptible for PRRSV, and the expression of IFN-α/β mRNA is elevated in time-dependent and transient manners. However, a little or no detectable levels of IFNs are found in the supernatants and cell lysates (Loving et al., 2007; Zhang et al., 2012). IFN production is observed in plasmacytoid dendritic cells (pDCs) after infection (Baumann et al., 2013). pDC is the primary cell type that produces IFN-α during LDV infection (Ammann et al., 2009). For EAV infection, poor induction of IFN is seen in pulmonary endothelial cells (Go et al., 2014). For SHFV, IFN response is host cell-dependent. Up-regulation of IFN-β production is detected in myeloid

dendritic cells (mDCs) and macrophages in macaques, but a low and no detectable levels of IFN-β response is seen in macrophages and mDCs of baboons, respectively (Vatter and Brinton, 2014).

The suppression of IFN-α is observed in PRRSV-infected macrophages (Albina et al., 1998; Lee et al., 2004), and the suppression occurs likely at the post-transcriptional level since IFN-α mRNA is increased after stimulation (Lee et al., 2004; Miller et al., 2009). On the contrary, a decrease of IFN transcripts is observed in PRRSV-infected MARC-145 cells (Miller et al., 2004). Plasmacytoid DCs (pDCs) are characterized by rapid and mass production of type I IFNs upon infection (Mildner and Jung, 2014), and porcine pDCs appear to be non-susceptible for PRRSV. In these cells, IFN production is blocked in the presence of TLR agonists when incubated with PRRSV, and the inhibitory effect is not altered by UV-inactivated PRRSV, suggesting the inhibition likely occurs on the cell surface (Calzada-Nova et al., 2011). IRF7 is not up-regulated by PRRSV in pDCs compared to other TLR (toll-like receptor) agonists. Another study shows no inhibition of IFN-α in porcine pDCs by PRRSV (Baumann et al., 2013). In that study, both genotypes of PRRSV were used, and all test isolates of both genotypes induced IFN-α production in pDCs by both infectious and non-infectious PRRSV (Baumann et al., 2013). It is possible that PRRSV prevents the paracrine loop of IFN induction and shuts off the IFN-boosted IRF7 expression while still inducing IFN production during the early stage of infection. Besides PRRSV, EAV has also recently been reported to inhibit IFN production with decreased IFN-β transcripts in EAV-infected equine pulmonary artery endothelial cells (Go et al., 2014).

**Regulation of IFN signaling pathway**

Production of type I IFNs is an important component of the host innate immunity against viral infection, and activation of IFN cascade starts from recognition of viral components by two distinct pattern recognition receptors (PRRs); TLRs and retinoic acid inducible gene I (RIG-I)-like receptors (RLRs) including melanoma differentiation associated protein 5 (MDA5) and RIG-I. TLR3, TLR7/8, and TLR9 function at either cell surface or endosomal membranes and are involved in antiviral response (Baccala et al., 2007). When pathogen-associated molecular patterns (PAMPs) are sensed by PRRs, signal transduction is turned on to activate IFN regulatory factor 3 (IRF3) and activating protein (AP)-1, and release of NF-κB from its inhibitor IκB (Baccala et al., 2007). Activated AP-1, IRF3 and NF-κB are translocated to the nucleus and bind their positive regulatory domains (PRDs) within the IFN promoter region and instigate the production of IFNs by recruiting CREB (cyclic AMP responsive element binding)-binding protein (CBP) to form an enhanceosome complex for IFN transcription (Randall and Goodbourn, 2008). Impaired production of type I IFNs has been observed during infection of arteriviruses.

Minimal IFN production is noticeable under arterivirus infection, but PRRs still senses invading arteriviruses. An increased activation of IFN-β promoter has been noticed in PRRSV-infected PAMs and MARC-145 cells, and TLR3 seems to be involved (Miller et al., 2004; Miller et al., 2009; Shi et al., 2010). TLR7 is also thought to be essential for IFN production in LDV- and PRRSV-stimulated IFN response in pDCs (Ammann et al., 2009; Baumann et al., 2013). A study using EAV in specific gene-knockout mouse embryonic fibroblasts suggests that both MDA-5 and RIG-I play a role in counteracting viral infection (van Kasteren et al., 2013). In PRRSV-infected PAMs and DCs, expression of TLR3 and TLR7 is inhibited at early infection but restored later (Chaung et al., 2010). The TLR3 and TLR7 expressions are delayed in

PRRSV-infected tracheobronchial lymph nodes (Liu et al., 2009), but no difference is observed in PAMs among different isolates of PRRSV for transcription of TLR3, TLR7, and TLR9 (Kuzemtseva et al., 2014).

To investigate the modulation of IFN signaling by arteriviruses, poly(I:C) as a dsRNA analog or Sendai virus (SeV) has been used for IFN activation. The dsRNA analog induced full activation of IRF3 in MARC-145 cells. When these cells were infected with PRRSV, only a partial activation was seen for Toll/IL-1R (TIR) domain-containing adaptor inducing IFN-β (TRIF) which is an adaptor molecule of TLR3 (Luo et al., 2008). For PRRSV-mediated IFN suppression, the suppression of NF-κB activity seems to be involved during early in infections, even though PRRSV activates NF-κB later in infection (Lee and Kleiboeker, 2005; Song et al., 2013; Sun et al., 2010). Reduction of CBP is observed during infection of PRRSV, and this inhibits the formation of enhanceosome to result in transcription inhibition of IFN expression (Kim et al., 2010). PRRSV also inhibits the JAK-STAT signaling pathway. In PRRSV-infected cells, nuclear translocation of IFN-stimulated gene factor 3 (ISGF3) is blocked (Patel et al., 2010), and this is due to the disruption of nuclear pores by nsp1β. The PRRSV function to inhibit IFN induction seems to be redundant by different viral proteins including nsp1α, nsp1β, nsp2, nsp4, nsp11, and N proteins (Table 1.1.). nsp1 and nsp2 of LDV and SHFV also possess IFN suppressive activities. It seems that arteriviruses tend to employ a combination of modulatory function for innate immunity.

**Regulation of other cytokines by PRRSV**

While type I IFN is suppressed by PRRSV, other cytokines such as TNF-α, IL-6, IL-8, and IL-10 are stimulated (Darwich et al., 2010). Association of three serum cytokines (IL-8, IL-

1β, IFN-γ) is significantly correlated with PRRSV persistence (Lunney et al., 2010). For EAV, virulent and avirulent strains differed in the induction of TNF-α, IL-1β, IL-6, and IL-8 (Moore et al., 2003). For SHFV, pro-inflammatory cytokines including IL-1β, IL-6, IL-12/23(p40), and TNF-α are efficiently induced in macaques but not in baboons, which is consistent with the scenario of IFN production (Vatter and Brinton, 2014). TNF-α is produced mainly by monocytes and macrophages. It is a pleiotropic cytokine important for induction and regulation of inflammatory responses (Hawiger, 2001). TNF-α inhibits PRRSV replication in PAMs (Ait-Ali et al., 2007; Lopez-Fuertes et al., 2000), and thus induction of TNF-α by PRRSV is controversial. An early study showed impaired production of TNF-α in PRRSV-infected PAMs, and this was consistent with the findings in bronchoalveolar fluids after infection (Thanawongnuwech et al., 2001; Van Reeth et al., 1999). However, TNF-α is still detectable in PAMs, peripheral blood mononuclear cells (PBMCs), and bronchoalveolar cells (Aasted et al., 2002; Ait-Ali et al., 2007; Johnsen et al., 2002), along with the virus in the lesions of lungs, lymph nodes, and serum of infected pigs (Choi et al., 2002; Miguel et al., 2010; Rowland et al., 2001). Different breeds and ages of pigs also lead to differential expression of TNF-α (Ait-Ali et al., 2007; Johnsen et al., 2002). In a study using 39 different isolates of PRRSV, various patterns of TNF-α expression are observed (Gimeno et al., 2011). Another study also shows that TNF-α expression was strain-dependent; a lower level expression of TNF-α by highly pathogenic (HP)-PRRSV compared to the conventional strains of PRRSV (Hou et al., 2012). TNF-α induction has been linked to activation of the ERK (extracellular signal-regulated kinase), MAPK (p38 mitogen-activated protein kinase), or NF-κB pathway (Mathur et al., 2004; Saccani et al., 2002), and PRRSV has been shown to induce a robust but transient activation of ERK (Lee and Lee, 2010). A later study shows that the ERK pathway, rather than the p38-MAPK and NF-κB pathways, is associated

with differential expression of TNF-α in macrophages. HP-PRRSV suppresses the release of TNF-α by inactivating the ERK pathway (Hou et al., 2012). This may explain the reduction of TNF-α by PRRSV (Lopez-Fuertes et al., 2000).

IL-10 is a pleiotropic cytokine with a potent immune-suppressive function (Conti et al., 2003; Darwich et al., 2010), and thus its expression during PRRSV infection has been studied (Thanawongnuwech et al., 2001; Wang et al., 2007). No response or minimal response is reported in some studies but a significant up-regulation of IL-10 expression is also reported in other studies. The up-regulation of IL-10 is observed in PBMCs, bronchoalveolar cells, and tissues including lungs and lymph nodes in PRRSV-infected pigs of different ages (Feng et al., 2003; Johnsen et al., 2002; Rowland et al., 2001; Suradhat et al., 2003). A significant increase of IL-10 is also observed in bone marrow-derived immature DCs (BM-imDCs) of PRRSV-infected pigs (Chang et al., 2008) and in PRRSV-infected monocyte derived mature DCs isolated from pigs (Flores-Mendoza et al., 2008). In PAMs, the induction of IL10 is time-dependent and dose-dependent (Genini et al., 2008; Song et al., 2013). During PRRSV infection, stress-activated protein kinases (SAPKs) including p38 MAPK and c-Jun N-terminal kinases (JNK) are activated, probably through a post-entry process leading to activation of transcription factors such as activator protein-1 (AP-1) (Lee and Lee, 2012). A later study confirms that the p38 MAPK and NF-κB pathways are responsible for IL-10 up-regulation in PAMs (Song et al., 2013). For NF-κB activation, MyD88 is essential and thus the TLR-MyD88-NF-κB signaling cascade is speculated to be involved in PRRSV-induced IL-10 expression. The N (nucleocapsid) protein is able to trigger NF-κB activation and has been demonstrated to up-regulate the IL-10 expression in PAMs, and thus N-mediated IL-10 induction may rely on NF-κB activation (Luo et al., 2011;

Wongyanin et al., 2012). Indeed, NF-κB activation by the N protein has been demonstrated (Luo et al., 2011; Fu et al., 2012; Pujhari et al., 2014).

### 1.2.2. Arterivirus nsp1-mediated innate immune modulation

**Multifunctional nature of PLPs**

nsp1 is the first viral protein synthesized during infection of arteriviruses and it functions in viral genome replication. Important domains have been identified for PRRSV-nsp1, which includes papain-like proteinase (PLP), two zinc finger (ZF) motifs, and a nuclease motif (Fang and Snijder, 2010; Sun et al., 2009; Xue et al., 2010). The PLP-like domain is found in the N-terminal region of viral polyproteins of many other positive-sense RNA viruses including picornaviruses, coronaviruses, arteriviruses, and pestiviruses, The PLP activity is essential for polyprotein processing (Chen et al., 1996; den Boon et al., 1995; Gorbalenya et al., 1989; Gorbalenya et al., 1991; Guarne et al., 2000; Harcourt et al., 2004; Karpe and Lole, 2011; Lim et al., 2000; Mielech et al., 2014a; Snijder et al., 1994). The PLP motifs exist in nsp1 of all arteriviruses and are responsible for cleaving nsp1 off from pp1a and pp1ab, and also for internal cleavage of nsp1 to generate nsp1α and nsp1β in PRRSV and LDV. Depending on the number of PLP motifs in nsp1, PLP is designated as PLP1α, PLP1β, or PLP1γ (Fig. 1.2). Correct processing of nsp1 by PLP1 is essential for viral genomic RNA and mRNA syntheses, and an impaired activity of PLP is lethal for PRRSV replication (Kroese et al., 2008). Unlike the leader proteinase (Lpro) of foot-and-mouth disease virus (FMDV), which cleaves the host cell eukaryotic initiation factor 4G (eIF4G) as well as itself from the nascent viral polypeptide, PLPs in arteriviruses hardly maintain their protease activities after self-cleavage (Guarne et al., 1998; Sun et al., 2009; Xue et al., 2010). The structural studies for PRRSV-nsp1α and PRRSV-nsp1β indicate stable

interactions between the C-terminal extension (CTE) and the PLP1α and PLP1β domains, hence further proteolytic processing is hardly conducted due to the inhibition of access to other potential substrates (Sun et al., 2009; Xue et al., 2010). In comparison with FMDV Lpro, a large interaction surface is observed for PRRSV-PLP1α and CTE, which enables to stabilize the intramolecular complex in PRRSV-nsp1α (Steinberger et al., 2013).

Besides acting as a protease, PLP2 in nsp2 functions as a deubiquitinating (DUB) enzyme which removes ubiquitin modification from a cellular target. The DUB activity is identified in the PLP of coronaviruses and the DUB activity overlaps with a de-ISGylating activity in some of these protease domains, (Chen et al., 2007; Clementz et al., 2010; Lindner et al., 2005; Mielech et al., 2014b; Wojdyla et al., 2010; Xing et al., 2013; Zheng et al., 2008). For PRRSV and EAV, DUB and de-ISGylating activities are identified in the PLP2 domain, and these activities are essential for viral modulation on innate immunity (Frias-Staheli et al., 2007; Sun et al., 2010; Sun et al., 2012b; van Kasteren et al., 2013; van Kasteren et al., 2012). There is no report about the association of PLP1 with the DUB and de-ISGylating activities.

Computer-based sequence alignments of nsp1 from different arteriviruses reveal a conserved zinc finger (ZF) motif in the N-terminal region, and the crystal structure of PRRSV-nsp1α suggests that the topology of the N-terminal ZF domain is generally similar to that of the ββα ZF family of over 1,000 known transcription factors (Sun et al., 2009; Tijms et al., 2001). The zinc ion coordinating the C-terminal zinc motif is identified in PRRSV-nsp1α but the biological function of this motif is unknown. Mutations in the N-terminal zinc finger domain of nsp1α selectively abolish the viral transcription whereas the genome replication is not affected (Tijms et al., 2007; Tijms et al., 2001). For PRRSV-nsp1β, no ZF is found according to the crystal structure. Instead, a nuclease activity is identified to degrade either double-stranded (ds)

DNA or ssRNA (Xue et al., 2010). Recent studies show the involvement of arterivirus nsp1 in viral gene transcription and translation (Li et al., 2014; Nedialkova et al., 2010). EAV-nsp1 involves in controlling the accumulation of genome-length and subgenome-length minus-strand RNA for mRNA synthesis (Nedialkova et al., 2010), whereas PRRSV-nsp1β functions as a transactivator to induce -1/-2 frameshifting in nsp2 region to produce nsp2TF and nsp2N (Li et al., 2014).

**Biogenesis of nsp1 subunits in arteriviruses**

For EAV, the PLP motif in the N-terminal region of nsp1 was initially predicted to somewhere between amino acid positions 158 and 178 (den Boon et al., 1991). Later by in vitro translation and mutagenesis studies, the PLP motif was confirmed to mediate a self-cleavage of nsp1 from nsp2 (Snijder et al., 1993). Cys164 and His230 of the EAV polyprotein are catalytic residues for PLP, and Gly260↓Gly261 was determined as the cleavage site (Snijder et al., 1993). Unlike EAV-nsp1, two adjacent PLP domains, PLP1α and PLP1β, are found in nsp1 of PRRSV and LDV. PLP1α mediates the internal cleavage of nsp1 to release nsp1α, and PLP1β mediates the cleavage between nsp1β and nsp2 to release nsp1β. Their catalytic sites are predicted to Cys76 and His146 for PRRSV-PLP1α, and Cys76 and His147 for LDV-LP1α (Fig. 1.2) (den Boon et al., 1995). The presence of two PLP motifs may reflect an ancient duplication during viral evolution (Snijder et al., 2013). The cleavage between PRRSV-nsp1α and PRRSV-nsp1β was initially predicted to occur near residues 164 to 168 (den Boon et al., 1995), and later shown to be Gln166↓Arg167 based on the prediction from sequence alignments (Allende et al., 1999). Recent studies by X-ray crystallography (Sun et al., 2009) and mass spectrometric analysis (Chen et al., 2010) have corrected the cleavage site to Met180↓Ala181, and this cleavage site of

Met180/Ala181 is conserved in type II PRRSV. The corresponding cleavage site of H180/S181 in type I PRRSV still needs to be confirmed experimentally. The cleavage site of Gly203↓Ala204 between nsp1β and nsp2 was also determined by protein sequencing (Xue et al., 2010).

For LDV, cleavage sites and PLP domains in nsp1 were predicted on the basis of sequence alignments with other arteriviruses. In our study, a consensus sequence CPFxxAxAT(N)V was identified in the adjacent region between nsp1α and nsp1β of both PRRSV and LDV, and the cleavage by LDV-PLP1α was predicted to Arg181↓Ala182. The sequence alignments also suggest that the cleavage for nsp1 and nsp2 locates at Gly381↓Tyr382 according to comparisons with PRRSV and EAV sequences (Han et al., 2014).

The structural characteristic of SHFV-nsp1 is rather complicated. SHFV-nsp1 contains an array of three potential PLP domains tentatively designated PLP1α, PLP1β, and PLP1γ, and each domain is presumed to generate nsp1α, nsp1β, and nsp1γ, respectively (Fig. 1.2; Snijder et al., 2013). SHFV-PLP1α contains Cys115 and His130 and these residues constitute a putative PLP1α by comparisons with PRRSV, LDV, and the remnants of inactive PLP1α in EAV. Interestingly, the SHFV-PLP1β sequence is rather similar to that of SHFV-PLP1γ, suggesting the evolutionary gene duplication.

Both SHFV-PLP1β and SHFV-PLP1γ sequences are well aligned with the sequences of PRRSV-PLP1β, LDV-PLP1β, and EAV-PLP1. For cleavage of SHFV-nsp1, a 39 kD band is identified in SHFV-nsp1 gene-transfected cells. This band is much larger than the prediction of SHFV-nsp1α and is rather similar to the sum of nsp1α and nsp1β. It suggests that SHFV-PLP1α may be non-functional. To verify this premise, a set of deletion constructs for nsp1 were made using a tag at the N-terminus of each construct. SHFV-PLP1α appears to be inactive, whereas

SHFV-PLP1β is functional and cleaves off nsp1β, thus producing nsp1a and nsp1β as a single protein (Han et al., 2014). We have termed this protein SHFV-nsp1αβ. SHFV-PLP1γ appears to be normally functional and cleaves off nsp1γ from nsp2. Compared to PRRSV, discontiguous deletions of 55 amino acids between two catalytic residues of Cys115 and His130 are noticeable in the SHFV-nsp1α region. These deletions in the relatively conserved region of nsp1α may likely contribute to the functional impairment of SHFV-PLP1α. Another study shows that PLP1α is predicted to constitute Cys63 and His130, and is functional to cleave off nsp1α at Gly164↓Gly165 (Vatter et al., 2014). This study was conducted in the cell-free translation system, and the reason for difference remains to be clarified. PLP1γ is functional and generates SHFV-nsp1γ by cleaving at either Tyr479↓Gly480 or Gly484↓Gly485 depending on the experimental system (Han et al., 2014; Vatter et al., 2014). For SHFV-PLP1β and SHFV-PLP1γ, cleavage occurs at Gly350↓Gly351 and Gly480↓Arg481, respectively (Han et al., 2014).

**Subcellular localization of individual nsp1 subunits in arteriviruses**

Cellular localization of nsp1 of arteriviruses has been investigated in virus-infected cells and gene-transfected cells. For EAV, nsp1 is localized in the nucleus in addition to the cytoplasmic distribution during infection (Tijms et al., 2002). For PRRSV, both nsp1α and nsp1β localize in the nucleus and cytoplasm with distinct patterns (Song et al., 2010). PRRSV-nsp1β shows two different distribution patterns; a punctate, perinuclear localization early in infection and predominantly a nuclear distribution later in infection (Li et al., 2012). In gene-transfected cells, both EAV-nsp1 and PRRSV-nsp1β are predominantly nuclear, whereas PRRSV-nsp1α shows the nuclear-cytoplasmic distributions (Chen et al., 2010; Han et al., 2013; Song et al., 2010; Tijms et al., 2002).

In our study, the subcellular localization of LDV-nsp1 and SHFV-nsp1 have been investigated (Fig. 1.3A) LDV-nsp1α localizes in the both nucleus and cytoplasm, and distribution patterns are similar to those of PRRSV-nsp1α in gene-transfected cells. Identical to PRRSV-nsp1β, predominantly nuclear distribution appears in cells expressing LDV-nsp1β, SHFV-nsp1αβ, and SHFV-nsp1γ. Three different types of perinuclear staining, nuclear aggregation, and predominantly nuclear staining are observed for SHFV-nsp1αβ and SHFV-nsp1γ, and the proportion of each type varies depending on the cell types (Han et al., 2014). Sequence analysis of nsp1 does not show the presence of nuclear localization signal (NLS), suggesting that the nuclear transport of nsp1 may be mediated through the interaction with a cellular protein containing such a signal or by the passive transport.

**Arterivirus nsp1-mediated innate immune modulation**

Among IFN antagonists of PRRSV, nsp1 and its two subunits are potent modulators for IFN production and signaling (Fang and Snijder, 2010; Sun et al., 2012a). The nsp1α and nsp1β subunits of PRRSV suppress IFN-β activation (Beura et al., 2010; Chen et al., 2010; Kim et al., 2010; Song et al., 2010). Individual elements in the IFN production pathway including RIG-1, IPS-1, MDA-5, TBK1, IKKε, and IRF3 are unaffected, suggesting that inhibition occurs downstream of IRF3 activation possibly in the nucleus (Chen et al., 2010). The total amount of IRF3 and its nuclear localization are not affected by nsp1. Instead, CBP is degraded in the nucleus and the CBP degradation is proteasome-dependent (Kim et al., 2010). Further studies show that the nsp1α subunit is responsible for CBP degradation (Han et al., 2013). PRRSV-nsp1α also reduces NF-κB activation (Song et al., 2010). For LDV, EAV, and SHFV, nsp1 subunits suppress IFN production by inhibiting the IFN promoter activities (Fig. 1.3B, and 1.3C;

Go et al., 2014). The motif for IFN down-regulation in SHFV-nsp1αβ resides in the nsp1β portion (Fig. 1.3D). The CBP degradation is also true for LDV-nsp1α but is not seen in cells expressing nsp1β. The molecular basis for IFN suppression by nsp1β or EAV-nsp1 remains to be determined (Han et al., 2014). Besides, all subunits of arterivirus nsp1 possess the suppressive activity for ISRE promoter. PRRSV-nsp1β interrupts the phosphorylation of STAT1 and the nuclear translocation of ISGF3 of the JAK (Janus kinase)-STAT (signal transducer and activator of transcription) pathway (Chen et al., 2010; Patel et al., 2010). The inhibition of ISGF3 nuclear localization by PRRSV-nsp1β is due to the degradation of karyopherin-α1 (KPNA1) which is a nuclear import protein (Wang et al., 2013). Both PRRSV-nsp1α and PRRSV-nsp1β involve in the suppression of TNF-α promoter activity through inhibiting the NF-κB activation and Sp1 transactivation (Subramaniam et al., 2010). The functional domains in PRRSV-nsp1 for IFN regulation have been identified by mutational studies. Critical residues have been identified in nsp1α and nsp1β by alanine scanning (Beura et al., 2012; Subramaniam et al., 2012), and a highly conserved motif in PRRSV-nsp1β appears to be imporant for IFN suppression (Li et al., 2013). In our studies, PRRSV-PLP1α and the C-terminal ZF motif in PRRSV-nsp1α are not impoortant for IFN suppression, but the N-terminal ZF motif in PRRSV-nsp1α is critical for this activity. This is consistent with the finding that some of the N-terminal ZF mutants of PRRSV-nsp1α are not able to induce CBP degradation (Han et al., 2013).

## 1.3. REVERSE GENETICS FOR PRRS VIRUS GENOME

The reverse genetics system has been developed for many RNA viruses, and infectious clones have been utilized for the study of biology and the vaccinology of viruses. The availability of such a powerful molecular tool has revolutionized the structure function studies

for viral genome and proteins and has facilitated the studies for virulence, pathogenesis, immune responses, and vaccine development. The first full-length genomic cDNA clone was constructed for poliovirus more than three decades ago and its infectivity was demonstrated (Racaniello and Baltimore, 1981). Infectious clones have since been constructed for picornaviruses, caliciviruses, flaviviruses, togaviruses, influenza viruses, paramyxoviruses, rhabdoviruses, and coronaviruses to name a few (Almazan et al., 2000; Boyer and Haenni, 1994; Pu et al., 2011; Scobey et al., 2013; Sosnovtsev and Green, 1995; Yount et al., 2003). For arteriviruses, EAV and PRRSV are the first for which the reverse genetics system has been developed (Meulenberg et al., 1998; van Dinten et al., 1997).

### 1.3.1 Construction of PRRSV infectious clones

The genome of negative-strand RNA viruses is non-infectious, and its replication in permissive cells requires the ribonucleoprotein (RNP) complex as the infectious unit. In contrast, the genome from positive-strand RNA viruses is fully infectious, and thus the assemly of full-length cDNA clones corresponding to the RNA genome is the kernel to the construction of infectious clones (Boyer and Haenni, 1994; Meyers et al., 1997; Moormann et al., 1996; Sosnovtsev and Green, 1995; van Dinten et al., 1997). Non-retroviral RNA viruses do not undergo a DNA intermediate step in their replication cycle. To obtain a template which can be manipulated by molecular techniques, a full-length cDNA clone is first generated using the reverse transcriptase and DNA polymerase. Once generated, two strategies have been established to generate virus progeny from the full-length copy of viral genome: RNA transfection and DNA transfection. In the RNA transfection strategy, viral RNA is synthesized by in vitro transcription using T7 or SP6 RNA polymerase coupled with the respective promoter located immediately

upstream of the viral genome. The synthesized RNA genome is then introduced into cells to initiate an infection cycle. In the DNA launch strategy, a full-length genomic clone is placed under a eukaryotic promoter such as a cytomegalovirus (CMV) promoter and the entire plasmid is introduced to cells for transcription by exploiting the nuclear function of the cell. The transcribed viral genome in the nucleus is exported to the cytoplasm where viral genome translation and replication occur. This strategy omits the steps of in vitro synthesis of genomic RNA and RNA transfection, thus the risk of RNA degradation during transfection is reduced and transfection efficiency becomes consistent (Yoo et al., 2004).

An arterivirus infectious clone was first made for EAV. The pEAV030 full-length clone containing the 12.7 kb cDNA copy of the EAV genome was infectious (van Dinten et al., 1997), and the first PRRSV infectious clone pABV437 was developed for the genotype I PRRSV Lelystad virus (Meulenberg et al., 1998). Subsequently, infectious clones for VR-2332 which is the genotype II PRRSV, and the European-like genotype I PRRSV SD01-08 circulating in the US was developed (Fang et al., 2006a; Fang et al., 2006b; Nielsen et al., 2003). Numerous clones have additionally been developed including the highly-pathogenic PRRSV that emerged in China in 2006 (Guo et al., 2013; Lv et al., 2008; Zhou et al., 2009). To date, at least 14 different infectious clones are available for PRRSV (Table 1.2).

PRRSV infectious clones have mostly been developed based on the RNA launch strategy. BHK-21, MA-104, and MARC-145 cells are cells of choice for transfection and progeny production. Although BHK-21 cells are non-permissive for PRRSV infection, they provide a high efficiency of transfection and a good production of progeny (Meulenberg et al., 1998). To eliminate the need for in vitro transcription and consistency associated with RNA transfection, the CMV promoter has been used for construction of the P129 infectious clone. The P129 virus

is an isolate recovered from an outbreak of highly virulent atypical PRRS in the mid-Western USA in 1995 (Lee et al., 2005; Yoo et al., 2004). The CMV promoter-based infectious clone is convenient and simple to use and provides a consistency of transfection and recovery of progeny virus (Lee et al., 2005).

An infectious clone should genetically be identical to the parental virus. However, non-viral nucleotides are occasionally added to the viral genome at the 5′ or 3′ end to meet the engineering needs without impeding the infectivity of the clones (Meulenberg et al., 1998; Truong et al., 2004). To differentiate the reconstituted progeny virus from the parental virus, genetic markers of either restricted enzyme recognition sequences or certain nucleotide mutations have been introduced to infectious clones, and such modifications should be non-lethal and stable. To assure the starting position of the RNA polymerase II-mediated transcription, 24 nucleotides are placed between the TATA box and the genome start when constructing pCMV-S-P129 (Lee et al., 2005). The PRRSV genome is usually divided to several fragments flanked by restriction sites for subsequent assembly (Meulenberg et al., 1998; Nielsen et al., 2003). As a cloning vector, a low-copy-number plasmid is generally preferred as suggested in some studies (Meulenberg et al., 1998; Sumiyoshi et al., 1992; Nielsen et al., 2003) but has appeared unnecessary. Progeny virus generated from an infectious clone should ideally retain the biological properties of the parental virus, such as growth rate, virulence, and transmissibility (Kwon et al., 2008; Lee et al., 2005; Meulenberg et al., 1998; Nielsen et al., 2003; Truong et al., 2004; Yuan and Wei, 2008).

### 1.3.2 Engineering PRRSV infectious clones

Like most RNA viruses, PRRSV genome has evolved to optimal fitness, and most of the genetic information seems to be essential (Verheije et al., 2001). Notably, the 3′-proximal portion of the genome is compact and organized to contain eight genes, most of which overlap with neighboring genes (Snijder et al., 2013). The PRRSV genome is complex and the engineering of such a compact viral genome is a challenge. In addition, minor alternations in conserved regions or functional domains in the genome almost inevitably lead to non-viable consequences (Ansari et al., 2006; Kroese et al., 2008; Lee et al., 2005). Despite such difficulties, some genetic manipulations for PRRSV have been successful.

**Strategies for infectious clone engineering**

Mutation, deletion, insertion, and substitution are major approaches to viral genome manipulation. Due to the large genome of PRRSV, shuttle plasmids have been used as an intermediate platform to contain the target viral genomic sequence with a pair of unique enzyme sites at each end. Mutations are introduced to target sites or sequences in the shuttle plasmid. The biological functions of PLP1α and PLP1β in nsp1, conserved cysteine residues at C49 and C54 in the E protein, N-linked glycosylation sites in GP3 at N131 and GP5 at N34, N44, and N51, cysteines at C23, C75, and C90 for homo-dimerization of N protein, and the motif for nuclear localization signal (NLS) of N have been mutated to produce PRRSV mutants (Ansari et al., 2006; Kroese et al., 2008; Lee et al., 2005; Lee et al., 2006; Lee and Yoo, 2005; Pei et al., 2009; Vu et al., 2011). Alanine scanning and protein surface accessibility predictions were conducted for identification of residues for type I IFNs or TNF-α antagonism of nsp1, and specific residues have been mutated in the infectious clones (Beura et al., 2012; Li et al., 2013; Subramaniam et

al., 2012). Mutations have also been introduced to knockout genes by changing the translation initiation codon, and this approach destroys the expression of nsp1 and E protein (Lee and Yoo, 2006; Tijms et al., 2001).

Deletion of genomic sequences has been applied to identifying non-essential regions for PRRSV replication or to obtaining attenuated live vaccine candidates (Verheije et al., 2001). Inter-genotypic sequence alignments between genotype 1 and genotype 2 reveal the regions of sequence heterogeneity suggesting the potential to tolerate the deletions, and non-essential regions in the N gene and 3′-UTR (Table 1.3; Sun et al., 2010b; Tan et al., 2011). The hypervariable regions have been observed in the nsp2 gene (Fang et al., 2004; Gao et al., 2004; Ni et al., 2013; Shen et al., 2000; Tian et al., 2007), suggesting the existence of a non-essential region in nsp2 (Chen et al., 2010b; Han et al., 2007; Ran et al., 2008; Xu et al., 2012b). Deletion of ORF2 or ORF4 results in the absence of infectivity, suggesting the requirement of GP2 and GP4 proteins for PRRSV infectivity (Welch et al., 2004).

Insertion of additional nucleotides to the viral genome expands the scope of modifications. An attempt was made to separate overlapping regions of PRRSV structural protein genes, and three restriction enzyme sites were inserted between ORFs 5/6 and ORFs 6/7 (Yu et al., 2009), which produced viable viruses. The possibility of expressing foreign genes using PRRSV has been explored; the nsp2 gene was utilized as an insertion site for expressions of green fluorescent protein (GFP) and FLAG tag (Fang et al., 2006b; Kim et al., 2007). An alternate approach was taken to insert foreign genes within a structural gene; for example, a small portion of the influenza virus hemagglutinin (HA) gene into the 5′ or 3′ end of ORF7 of PRRSV (Bramel-Verheije et al., 2000). However, the insertion of HA to N gene resulted in a nonviable virus. A strategy utilizing the mechanism of transcription of PRRSV for foreign gene

expression is of particular interest. Using an infectious clone, two unique enzyme sites have been introduced between ORF1b and ORF2, and a copy of the TRS6 sequence was inserted to replace the TRS designed to synthesize the mRNA for foreign gene expression (Fig. 1.6) (Lee et al., 2005; Pei et al., 2009; Yoo et al., 2004). The foreign genes including GFP, capsid protein of porcine circovirus type 2 (PCV2), Discosoma sp. (sea anemone) red fluorescent protein (DsRED), Renilla luciferase (Rluc), IFN-α1, IFN-β, IFN-δ3, and IFN-ω5 have all been expressed as an independent transcript using this approach (Table 1.4; Pei et al., 2009; Sang et al., 2012).

Multiple genes, a single gene, or partial sequence of the viral genome have been substituted with corresponding sequences from other arteriviruses for chimeric arterivirus construction. The first chimeric arterivirus was generated using an EAV infectious clone as a backbone, and ectodomains of two membrane proteins, GP5 and M, were substituted with the corresponding sequences from PRRSV or LDV (Dobbe et al., 2001). These chimeric viruses were viable, and additional chimeric arteriviruses have been constructed (Table 1.5). The construction of intra- or inter-genotypic PRRSV chimeras is maneuverable, and the regions of 5′-UTR, non-structural genes, and structural genes have been replaced (Gao et al., 2013; Lu et al., 2012; Tian et al., 2012; Tian et al., 2011; Vu et al., 2011; Zhou et al., 2009). To facilitate the intra-genotypic substitution, a gene-swapping mutagenesis technique has been used to substitute the structural genes (Kim and Yoon, 2008). Using this technique, individual replacement of ORF2a and ORF2 through ORF6 of VR-2332 was successfully carried out with corresponding ORFs from other strains of PRRSV including JA142, SDSU73, PRRS124, and 2M11715 (Kim and Yoon, 2008).

## Identification of modification-limited genomic regions

### *nsp2*

PRRSV nsp2 is a multifunctional protein that undergoes remarkable genetic variations. The nsp2 protein consists of five regions: hypervariable region I (HV-I), PLP2 cysteine protease core, hypervariable region II (HV-II), transmembrane regions, and a C-terminal tail (Fig. 1.4A; Han et al., 2009). The PLP2 cysteine protease domain possesses cis-acting and trans-acting cleavage activities and mediates its rapid release from pp1a and pp1ab (Han et al., 2009; Snijder et al., 1995). Two sites were initially predicted for nsp2/nsp3 cleavage at 981G/982G and somewhere at 1196G/1197G/1198G, and recent studies showed the actual cleavage occurs at 1196G/1197G for VR-2332 (Allende et al., 1999; Han et al., 2009; Nelsen et al., 1999). The corresponding cleavage for EuroPRRSV SD01-08 likely occurs at 1445GG/1447A (Fang and Snijder, 2010). PLP2 is as a member of the ovarian tumor domain (OTU) family of deubiquitinating enzymes, and has shown to deconjugate ubiquitin (Ub) and IFN-stimulated gene (ISG) 15 from cellular targets. This is an important viral strategy inhibiting the Ub-dependent and ISG15-dependent host innate immune responses (Frias-Staheli et al., 2007; Sun et al., 2010a; Sun et al., 2012b; van Kasteren et al., 2012)

Besides the proteinase and deubiquitinase functions, nsp2 contributes to the major genetic differences between genotypes I and II, sharing only less than 40% similarity at the amino acid level (Allende et al., 1999; Nelsen et al., 1999). The nsp2 gene also contains naturally inserted sequences and deletions (Fig. 1.4A) in the hypervariable region (Fang et al., 2004; Gao et al., 2004; Ni et al., 2011; Shen et al., 2000; Tian et al., 2007). The deletion of 12 amino acids in nsp2 was first found in a Chinese PRRSV isolate, HB-2(sh)/2002, in comparison with other North American isolates (Gao et al., 2004). Sequence analysis of PRRSV MN184 reveals three

discontinuous deletions of 111, 1, and 19 amino acids at the corresponding positions 324-434, 486, and 505-523 of VR-2332, respectively (Han et al., 2006). Discontinuous deletions were also identified in the highly pathogenic PRRSV (HP-PRRSV) associated with the 2006 outbreaks of porcine high fever disease in China (Tian et al., 2007). The 30 amino acids discontinuous deletion consists of 1 aa deletion at position 482 and 29 aa deletions at 534-562, and the deletion region contains B-cell epitopes (de Lima et al., 2006) and T-cell epitopes (Chen et al., 2010b). Strikingly, cell culture passages of PRRSV may generate a deletion in nsp2, and a study shows the generation of a large deletion of 135 aa at 581-725 in nsp2 during passages (Ni et al., 2011). A deletion in nsp2 is also found in genotype I PRRSV. The EuroPRRS SD-01-08 virus in the US shows a 17 aa deletion at positions 349-365 of nsp2 when compared to Lelystad virus (Fang et al., 2004). Biological significance of the genetic deletion in nsp2 remains to be determined. Besides deletions, a 36 aa insertion was also observed in the SP strain of PRRSV, which is a vaccine strain, located between G812 and T849 of the SP nsp2 (Shen et al., 2000).

Given the tolerance of deletions and insertions in the hypervirable region of nsp2, this region is considered as a site for foreign gene insertion (Fig. 1.4B and 1.4C). The GFP gene was inserted into nsp2 of the SD01-08 strain and fully infectious virus was rescued (Fang et al., 2006b). The GFP insertion did not affect the growth of the virus, and the infectivity was comparable to that of parental virus. The capacity of deletion in nsp2 was determined by introducing a series of in-frame deletions (Han et al., 2007). The PLP2 domain, the PLP2 downstream flanking region, and the transmembrane domain were crucial for virus replication but deletions of 13 to 35 aa from the N-terminal portion of the hypervariable region and 324 to 813 aa from the hypervariable region appeared to be tolerable for viability. In the hypervariable region, the largest deletion that can be achieved was about 400 aa at positions 324-726, although

a deletion of up to 200 aa is preferable for infectivity (Fig. 1.4B). The insertion of GFP or other genes such as New Castle disease virus nucleoprotein (NP) gene has been successful as long as insertions reside in the hypervirable regions (Fig. 1.4C) (Kim et al., 2007; Xu et al., 2012a). The deletion of inmmunodominant linear B-cell epitopes (ES2-ES7) were attempted; deletion of ES3, ES4, or ES7 allowed the generation of an infectious virus (Chen et al., 2010b; Oleksiewicz et al., 2001).

***N protein***

PRRSV N is a mutilfunctional protein. The specific domains and residues critical for virus replication have been identified in N (Fig. 1.5A). The N protein is comprised of 123 or 128 aa for the North American and European genotypes, respectively (Music and Gagnon, 2010). N consists of the N-terminal RNA-binding domain (RBD) at positions 41-47 and the C-terminal dimerization domain comprising a four-stranded antiparallel β-sheet floor flanked by α-helices (Doan and Dokland, 2003; Yoo et al., 2003). As the sole component of viral capsid, N interacts with itself via covalent or noncovalent interactions (Doan and Dokland, 2003; Wootton and Yoo, 2003). The cysteine at position 23 is responsible for the formation of an intermolecular disulfide bond, and aa 30-37 are essential for mediating noncovalent homodimers (Wootton and Yoo, 2003). A crystallographic study on N shows the imprtance of the C-terminal dimerization domain for N (Doan and Dokland, 2003; Spilman et al., 2009). PRRSV N is a serine phosphoprotein which is a common property for N of EAV and coronaviruses (Music and Gagnon, 2010; Wootton et al., 2002). One of the phosphorylation sites of N is at position 120, but its biological significance is still unknown. N contains NLS in a stretch of basic amino acids 41-PGKKNKK-47 which is overlapping with the RNA-binding domain and particially with a

nucleolar localization signal (NoLS) at aa 41-72 (Rowland et al., 1999; Rowland et al., 2003). The nuclear export signal (NES) is found at positions 106-117 and is responsible for the nucleolar-cytoplasmic shuttling of N (Rowland and Yoo, 2003) .

The functional structure of N is compact and thus N is sensitive to structural modification. The secondary structure in the C-terminal residues 112-123 is an important determinant for conformational epitopes, and the mutations in this region change the monoclonal antibody (MAb) reactivity (Wootton et al., 2001). Insertion of a foreign sequence into the N gene was attemped and the influenza virus HA epitope was added at the N-terminus or C-terminus. Despite the initial rescue of the infectious virus, the HA expression was unsuccessful (Bramel-Verheije et al., 2000). The GFP tag was inserted between ORF6 and ORF7 to moniter the ORF7 mRNA synthesis, but no mRNA was made, indicating the 5′ end of the ORF7 gene is essential for mRNA synthesis (Yoo et al., 2004). The N protein is inter-genotypically conserved but shares only 60% of its identity between LV and VR-2332 (Dea et al., 2000). The C-terminus of N is heterogenous, and truncation of up to 6 aa is tolerable (Verheije et al., 2001). In another study, deletions were made at the inter-genotypic variable region or conserved region of N, and 4 regions at 5-13, 39-42, 48-52, and 120-123, were found to be dispensible for viability (Fig. 1.5B) (Tan et al., 2011). No foreign gene can be incorporated in these rgions.

***Non-conding regions***

The PRRSV genome is flanked by 5′- and 3′-UTR, and the UTR sequences play a vital role for genomic replication, mRNA transcription, and protein translation (Pasternak et al., 2006; Snijder et al., 2013). The non-coding regions of the genome have been investigated. By serial deletions, the first 3 nucleotides in 5′-UTR appears to be dispensible for viability in type II

PRRSV (Gao et al., 2012). For 3′-UTR, the first 11 nucleotides are unique for each genotype, and a stretch of 38 nucleotides is present in VR-2332 but is absent in LV (Allende et al., 1999; Verheije et al., 2001). A deletion study shows that 7 nucleotides at the 5′ end of the 3′-UTR is tolerable for genotype I PRRSV (Verheije et al., 2001). The 3′-UTR of genotype II has also been studied, and at least 40 nucleotides immediately following ORF7 is dispensable for virus viability (Sun et al., 2010b).

The genetic information on the structural region of arteriviruses is organized in an extremely efficient manner. The genes for GP2, GP3, and GP4 overlap each other, and similarly the genes for GP5, M, and N overlap each other for PRRSV. This structural complexicity hampers the genetic manipulation of infectious clones. The importance of the overlapping gene arrangement for the life-cycle of virus has been studied (Verheije et al., 2002; Yu et al., 2009). A series of full-length clones were engineered to separate overlapping genes for EAV ORFs 4/5 or ORFs 5/6 by inserting small additional sequences containing a termination codon for the upstream gene, a unique restriction site, and a translation initiation codon for the downstream gene. The insertions result in the functional separation of overlapping ORFs, and do not impair infectivity (de Vries et al., 2000). The ORFs 5/6 separation in genotype I PRRSV is also possible and progeny virus is produced (Verheije et al., 2002). For the North American PRRSV, restriction sites were inserted between ORFs 1/2, ORFs 4/5, ORFs 5/6, ORFs 6/7, and ORFs 7/3′-NTR, and progeny viruses are generated from these modifications. This indicates that gene overlap is dispensable for infectivity and that separation of each gene does not interrupt mRNA synthesis (Yu et al., 2009).

### 1.3.3 Applications of PRRSV infectious clone

#### Chimeric viruses and cell tropism

The development of infectious clones allows the construction of chimeric arteriviruses. An attempt was made to swab the ectodomains of GP5 and M. In engineered chimeric viruses using the EAV clone as a backbone, the ectodomains were replaced by corresponding sequences from other arteriviruses. Chimeric viruses containing the GP5 ectodomain from LDV and PRRSV were infectious. These chimeric viruses however retain their cell tropism for BHK-21 cells, which are susceptible for EAV but non-susceptible for LDV and PRRSV (Dobbe et al., 2001). Replacement of the M ectodomain of EAV with the corresponding sequence from other arteriviruses does not produce infectious virus, but replacement of the M ectodomain of PRRSV with the corresponding sequence from LDV, EAV, and genotype II PRRSV produced an infectious virus. Using the LV infectious clone as a backbone, substitutions with the EAV M ectodomain or VR-2332 M ectodomain is impossible, but removal of the gene overlap between the M and GP5 genes is required before swapping, indicating that the VR-2332 M ectodomain and EAV M ectodomain are incompatible with the remaining part of LV M. It is also possible that unintended mutations may have been introduced to GP5 during the ectodomain swap (Verheije et al., 2002). Substitution of structural genes between arteriviruses has been extremely useful to identify viral factors for viral tropism. The substitution of GP5 or/and M do not alter their cell tropism (Dobbe et al., 2001; Lu et al., 2012; Verheije et al., 2002). In contrast, the substitution of minor envelope proteins and E protein using the PRRSV infectious clone as a backbone allows the chimeric PRRSV to acquire a broad cell tropism but to lose the ability to infect PAMs. It indicates that the GP2/GP3/GP4 minor proteins are determinants for cell entry and tropism (Tian et al., 2011).

**Chimeric viruses and virulence immunogenicity**

Intra-genotypic or inter-genotypic gene-swapping have been conducted between EAV and PRRSV to study the genetic compatibility and viral-specific phenotypes, including neutralization, virulence, and pathogenesis. For neutralization, 9 chimeric EAVs were generated in which each construct contained individual ORF5 from different isolates (Balasuriya et al., 2004). Also, the role of individual envelope proteins of GP2 through M for cross-neutralization was studied using the VR-2332 infectious clone as a backbone (Kim and Yoon, 2008). The PRRSV-01 strain is highly susceptible to serum neutralization and induces atypically rapid and robust neutralizing antibodies in pigs. Analysis of structural genes of PRRSV-01 reveals the absence of two N-linked glycosylation sites each in GP3 and GP5. The significance of missing glycans for neutralization has been determined by replacing GP3 and GP5 genes from PRRSV-01 (Vu et al., 2011). The major virulence determinants have also been identified by gene swapping experiments to locate in nsp3 through nsp8 and GP5 (Kwon et al., 2008). Highly pathogenic PRRSV contains the 30 aa deletion in nsp2 sequence (Tian et al., 2007). By gene swapping studies using nsp2 from an avirulent PRRSV, the deletion in nsp2 was shown to be irrelevant to virulence and pathogenicity (Zhou et al., 2009). A recent study identified nsp9- and nsp10-coding regions together were essential for increased pathogenicity and fatal virulence for HP-PRRSV by swapping these regions between the highly and low pathogenic strains (Li et al., 2014). The inter-genotypic 5′-UTR swap between genotypes I and II was investigated and shows that the 5′-UTR of genotype II may be substituted with the corresponding sequence from genotype I, while the substitution of 5′- UTR of genotype I with its corresponding sequence from genotype II is lethal (Gao et al., 2013). Using this approach, the envelope proteins representing

GP2 through GP5 of genotype I are shown to be fully functional for genotype II when using genotype II as a backbone (Tian et al., 2011).

**Rational design for a new PRRS vaccine**

A random sequence shuffling has been employed to generate immunologic variants of PRRSV (Ni et al., 2013; Zhou et al., 2013; Zhou et al., 2012). GP3 sequences representing immunologically diverse strains of PRRSV are randomly shuffled, and the shuffled gene is incorporated in the infectious clone to generate a new virus that contains a new GP3 gene, which may improve the cross neutralization (Zhou et al., 2012). The breeding of GP4 and M have also been tried, and the rescued virus induces a broad spectrum of cross-neutralizing antibodies (Zhou et al., 2013). The GP5 sequence from 7 genetically diverse strains of PRRSV and the GP5-M sequence from 6 different strains were subjected to breeding, and the shuffled genes were cloned in infectious clones for the generation of new viruses. Two representative chimeric viruses, DS722 by GP5 shuffling and DS5M3 by GP5-M shuffling, were found to be clinically attenuated (Ni et al., 2013). This approach allows rapid generation of an attenuated virus and may be useful for vaccine development for antigenetically variable viruses (Ni et al., 2013; Zhou et al., 2012). Another approach to the rapid generation of attenuated PRRSV is referred to as SAVE (synthetic attenuated virus engineering). Codon-pair bias is a phenomenon that certain codon pairs appear in a higher frequency in comparison to other synonymous codon pairs for the same amino acid, and the codon-pair bias is host species-dependent related to the efficiency of protein synthesis (Coleman et al., 2008; Moura et al., 2007; Mueller et al., 2010). By deoptimizing the codon pair of a virulence gene, an expression level of this protein decreases. The computer-aided deoptimization of codon-pairs modifies only naturally optimized pairs of codons and does not

change the amino acid sequence (Mueller et al., 2010). Using this approach, the GP5 gene was codon-pair deoptimized, and a new virus was generated. The modified GP5 sequence did not affect the viability of PRRSV and the engineered virus was clinically attenuated in pigs (Ni et al., 2014).

To fulfill serological discrimination between naturally infected and vaccinated animals, removing an immunodominant epitope has been applied to developing a live-attenuated differentiating infected from vaccinated animals (DIVA) vaccine against PRRSV (de Lima et al., 2008; Vu et al., 2013). The serologic marker antigen selected for DIVA vaccine should be highly immunodominant without disrupting protective well-conserved epitopes among PRRSV isolates and stability during passages. Besides, the removal of a selected epitope should not adversely affect the growth property or virulence of the mutant virus (de Lima et al., 2008; Vu et al., 2013). Two epitopes residing in nsp2 and M have been identified fulfilling the requirements for PRRSV DIVA vaccine (de Lima et al., 2008; Vu et al., 2013). Two mutants, FLdNsp2/44 with a deletion of residues 431-445 within nsp2, and Q164R disrupting antigenicity of epitope M201 in M protein have been designed and constructed accordingly (de Lima et al., 2008; Vu et al., 2013). The immunogenicity of those two epitopes has been eliminated during infection of PRRSV mutants, and both epitopes may be used as an immunologic marker for DIVA vaccine development (de Lima et al., 2008; Vu et al., 2013).

**PRRSV as a foreign gene expression vector**

PRRSV may serve as a vaccine vector. PRRSV infectious clones have been developed as a gene delivery vector for foreign gene expression. Identification of gene insertion sites in the viral genome and viral infectivity is critical for gene delivery. GFP and B-cell epitopes of the

Newcastle disease virus (NDV) nucleoprotein have been inserted into non-essential regions of nsp2 of PRRSV (Fang et al., 2008; Fang et al., 2006b; Kim et al., 2007; Xu et al., 2012a). In this approach however, the stability of the inserted gene was of a concern. When PRRSV expressing GFP in nsp2, PRRSV SD01-08-GFP, was cell-culture passaged, a population of GFP-expression negative-virus appears by the 7th passage. Sequencing shows a deletion of GFP at the N-terminal half (1 to 159), leading to the loss of GFP expression. Insertion of 2 amino acids at position 160 of GFP was also observed in some viral clones (Fang et al., 2006b). The stability of the GFP gene in this recombinant virus was improved by deleting the ES4 epitope located downstream of the GFP gene, and the GFP expression in this virus was stable for 10 passages. However, R97C mutation was found in GFP, and this mutation caused the loss of florescence (Fang et al., 2008). The loss of fluorescence was also observed in two other GFP recombinant viruses during serial passages. In another study, the GFP-coding sequence remained intact but point mutations were identified and these mutations caused amino acid changes to R96C and N106Y (Kim et al., 2007). The expression of 49 aa B-cell epitope of the NDV nucleoprotein in PRRSV nsp2 remained stable in cell culture up to 20 passages (Xu et al., 2012a; Zhang et al., 2011). The instability of foreign gene insertion in nsp2 is not fully understood. The length of insertion may be important for stability.

An attempt was made to produce an additional mRNA for foreign gene expression. The GFP gene was inserted between ORF1b and ORF2a for PRRSV along with a copy of TRS (Lee et al., 2005; Pei et al., 2009; Sang et al., 2012; Yoo et al., 2004). Compared to insertion in nsp2, this site is suitable for foreign gene insertion since the recombinant virus was stable for up to at least 37 passages without the loss of gene or fluorescence (Pei et al., 2009). The genetic stability of genes inserted at this site has been confirmed by expressing other genes including DsRed,

Renilla luciferease, IFNα1, IFNβ, IFNδ3, and IFNω5 (Sang et al., 2012). This approach has the particular advantage of eliminating the need to alter the coding sequence of a viral gene and also of minimizing the effects on expression and post-translational modification of viral proteins (Pei et al., 2009).

**Application of infectious clones to structure function studies**

Infectious clones are important molecular tools to study structure function relationships of proteins and genomic sequences at the infectious virus level in vivo. Specific sequence motifs may be mutated or deleted from the virus and their phenotypes may be examined to determine their functions. The removal of N-linked glycosylation at N34 and N51 of GP5 results in a mutant virus with its phenotype of enhanced sensitivity to serum neutralization and high level induction of neutralizing antibodies (Ansari et al., 2006). Elimination of N44-linked glycan is not in concert with a high-level neutralizing antibody response to wild type PRRSV (Wei et al., 2012). Meanwhile, introduction of multiple mutations at these N-linked glycosylation sites could significantly reduce virus yields (Wei et al., 2012). The E gene knock-out mutation allows for genome replication and transcription but does not produce infectious progeny, indicating that the E protein is essential for virion assembly (Lee and Yoo, 2006). PRRSV nsp1 is a multifunctional protein regulating the accumulation of genomic RNA and mRNAs. It also has the ability to modulate the host innate immunity by suppressing the type I IFN production (Nedialkova et al., 2010; Sun et al., 2012a; Yoo et al., 2010). The motifs for zinc fingers, PLPs, and nuclease have been identified in nsp1 (Fang and Snijder, 2010; Snijder et al., 2013; Xue et al., 2010). By deleting from the genome, nsp1 is shown to be dispensable for genome replication but crucial for mRNA transcription. Mutation in the catalytic sites of PLP1 impairs both viral genome and

mRNA synthesis as well as the cleavage between nsp1 and nsp2. Mutations in the zinc finger motif abolished the mRNA transcription, whereas genome replication was not affected (Tijms et al., 2007; Tijms et al., 2001). When the catalytic sites of PLP1α are mutated using a PRRSV infectious clone, the proteinase activity disappears and mRNA synthesis is completely blocked. In contrast, mutations at the PLP1β catalytic sites result in no mRNA synthesis and no viral infectivity, indicating that the normal cleavage of nsp1 and nsp2 is critical for viral replication (Kroese et al., 2008).

To design effective vaccine candidates that may be useful to overcoming antigenic heterogeneity of PRRS, extensive studies have been conducted to eliminate the IFN antagonistic function from the virus (see reviews Snijder et al., 2013; Sun et al., 2012a; Yoo et al., 2010). Among viral proteins, nsp1α and nsp1β have been identified as potent IFN analogists (Beura et al., 2010; Chen et al., 2010a; Han et al., 2013; Han et al., 2014; Kim et al., 2010; Song et al., 2010). Subsequent studies have identified specific residues regulating the IFN antagonism, and a mutant virus with a stretch of alanine substitution at positions 16-20 of nsp1β showed the loss of IFN suppression (Beura et al., 2012). In another study, K124 and R128 were mutated to release the surface accessibility of nsp1β, and mutant PRRSV impaired the IFN antagonism (Li et al., 2013).

Motifs in the N protein have broadly been studied using mutant viruses. The importance of N protein dimerization has been examined by mutating C23S which is responsible for the covalent interaction between N proteins. Mutant viruses of C23S, C75S, and C90S were constructed, and with the exception of C75S, both C23S and C90S completely lost their infectivity. In another study however, the replacement of cysteines within N protein, either singly or in combination, did not impair the growth PRRSV according (Zhang et al., 2012). Genome

replication and mRNA transcription were normal for both mutants, suggesting the dimerization of N may be important for particle assembly or maturation (Lee et al., 2005). The nuclear localization signal (NLS) of N was also mutated to examine the biological consequence of N in the nucleus in PRRSV-infected cells. Compared to wild-type PRRSV, NLS-null mutant PRRSV was attenuated in pigs and produced a significantly shorter mean duration of viremia and higher titers of neutralizing antibodies (Lee et al., 2006; Pei et al., 2008), demonstrating that the N protein nuclear localization is a virulence factor.

## 1.4. HYPOTHESIS AND OBJECTIVES OF THE THESIS

### 1.4.1. Introduction

The existence of a virus in a host requires a balance between replication of the virus and the antiviral defense of the host. The antiviral defense of the host is armed with a variety of immune surveillance mechanisms to eliminate invading viruses, and viruses in turn have evolved to subvert these barriers. RNA viruses with a small coding capacity have been evolved to constrain antiviral reactions of host cells. To compensate the small coding capacity of RNA viruses, these proteins are often multifunctional.

Production of type I IFNs is an important component of the host innate immunity against viral infection, and impaired production of type I IFNs has been observed during infection of arteriviruses. For PRRSV-mediated IFN suppression, the suppression of NF-κB activity and the reduction of CREB (cyclic AMP responsive element binding)-binding protein (CBP) are observed during infection of PRRSV. PRRSV also inhibits the JAK-STAT signaling pathway. In PRRSV-infected cells, nuclear translocation of IFN-stimulated gene factor 3 (ISGF3) is blocked, and this is due to KPNA degradation by nsp1β. Nsp1α, nsp1β, nsp2, nsp4, nsp11, and N proteins participate in the IFN inhibition, and therefore the PRRSV function to inhibit IFN induction seems to be redundant.

In this study, the viral evasion strategies from the host innate immunity will be focused and the role of nsp1 as an IFN antagonist for cellular processes would be investigated. The functional motifs of PRRSV nsp1 subunits will be identified and removed from the virus by genetic manipulation using infection clones. Genetically modified PRRSV mutants will be generated and their phenotypes will be examined in cells and pigs. The mutant PRRSV will no longer be able to modulate the normal host innate immunity but will become attenuated and mount desired immune responses during vaccination. This study will pave a way to the design of

an effective vaccine strain for PRRS.

### 1.4.2. Principle hypothesis

PRRSV carries an ability to counteract the host antiviral innate immunity. PRRSV modifies the IFN production and IFN signaling pathways so as to survive and establish a persistent infection in pigs. As the first product among viral proteins, PRRSV nsp1 plays an important role in modulating innate immune responses, and both nsp1 subunits nsp1α and nsp1β are proved to be essential for IFN suppression. IFN-down-regulation gene knock-down mutant viruses would be constructed by genetic manipulation on essential motifs of PRRSV nsp1α and nsp1β without losing the infectivity.

### 1.4.3. Specific aims

**Specific aims 1:** Molecular dissection of the PRRSV strategies for immune evasion. The functional roles of nsp1α and nsp1β for type I IFN production and downstream expression of IFN responsive genes will be elaborated with emphases on the IFN signaling and its key elements such as CBP.

**Specific aims 2:** Remove IFN modulatory functions from PRRSV by genetic manipulation and construct IFN-down-regulation gene knock-down mutant viruses. We will identify functional motifs by fine mapping studies on nsp1α or nsp1β and construct genetically altered PRRSV mutants using infectious clones. Determine the phenotypes of mutant PRRSV in vitro in various cell types.

**Specific aims 3:** Exploration of the biogenesis of arterivirus nsp1 subunits and their roles in innate immune suppression. The PLP1 motifs-mediated arterivirus nsp1 cleavages will be studied. The roles of arterivirus nsp1 subunits for type I IFN production and downstream expression of IFN responsive genes will be elaborated with emphases on the IFN signaling. CBP degradation and mRNA nuclear export will be examined for each arterivirus nsp1 subunits.

## 1.5. FIGURES AND TABLES

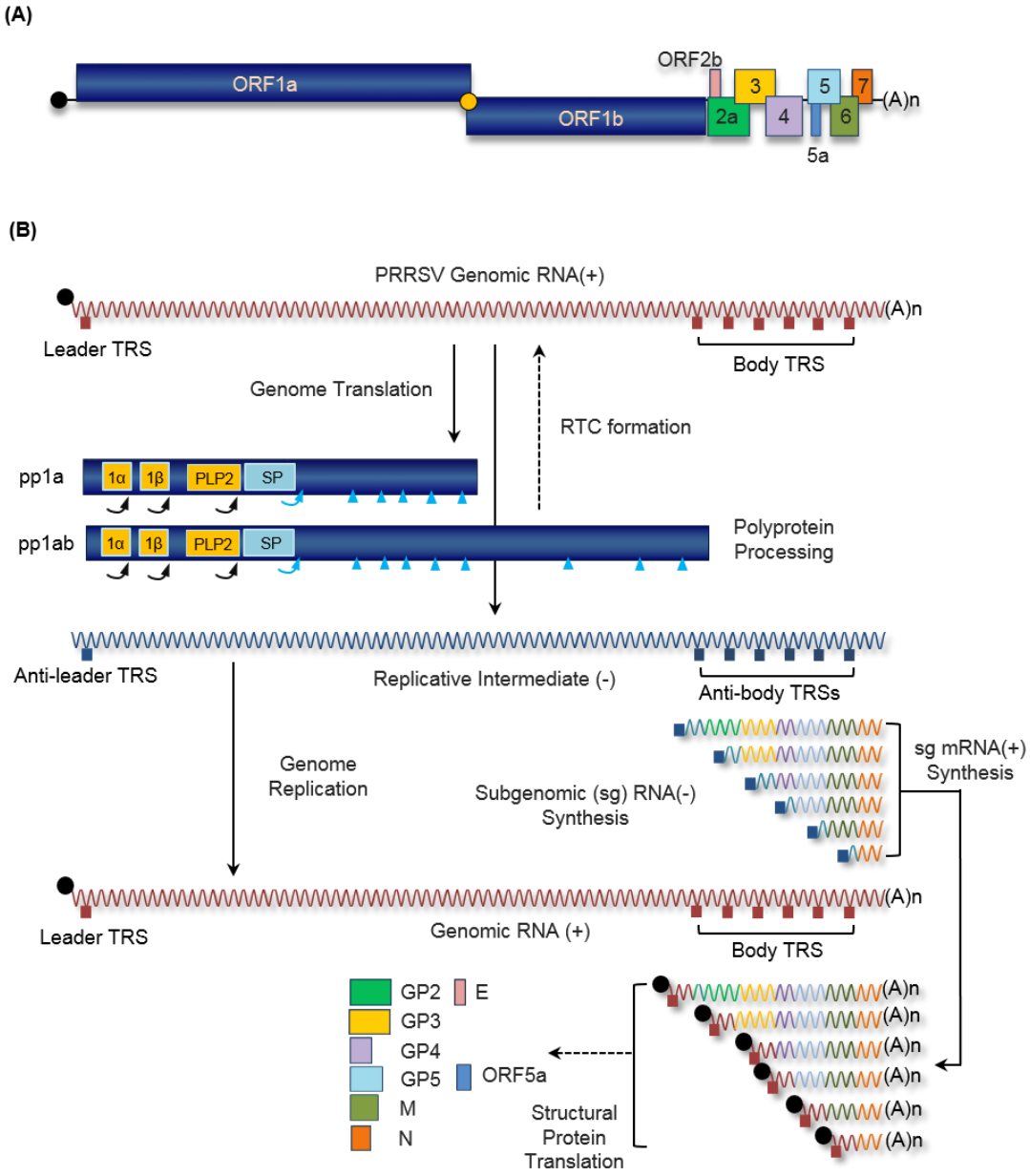


**Fig.1.1. Transcription and translation of PRRSV genome**. (A), PRRSV genome organization. PRRSV possesses a single-stranded positive-sense RNA genome of 15 Kb in length with a 3′-polyadenylated tail and the 5′-cap (grey). The viral genome is polycistronic, harboring ORF1a and ORF1b, and structural genes of ORF2a, ORF2b, and ORFs 3 through 7, plus ORF5a within ORF5. (B), Viral gene expression. Non-structural proteins (black) are produced from pp1a and pp1ab after proteolytic processing. The PRRSV replicase-processing scheme involves the rapid auto-proteolytic release of nsp1α, nsp1β, and nsp2 (yellow boxes), mediated by papain-like proteinase (PLP) domains residing in each of them. The remaining polyproteins are processed by nsp4, resulting in a set of 14 individual nsps. The cleavage sites by PLPs and nsp4 are annotated by curved arrows and blue triangles, respectively. Structural proteins (color-coded) are expressed from the subset of sg mRNA. The 3′-co-terminal nested set of minus-strand RNAs is produced as a template for plus-strand sg mRNA synthesis. TRS, transcription regulatory sequence.

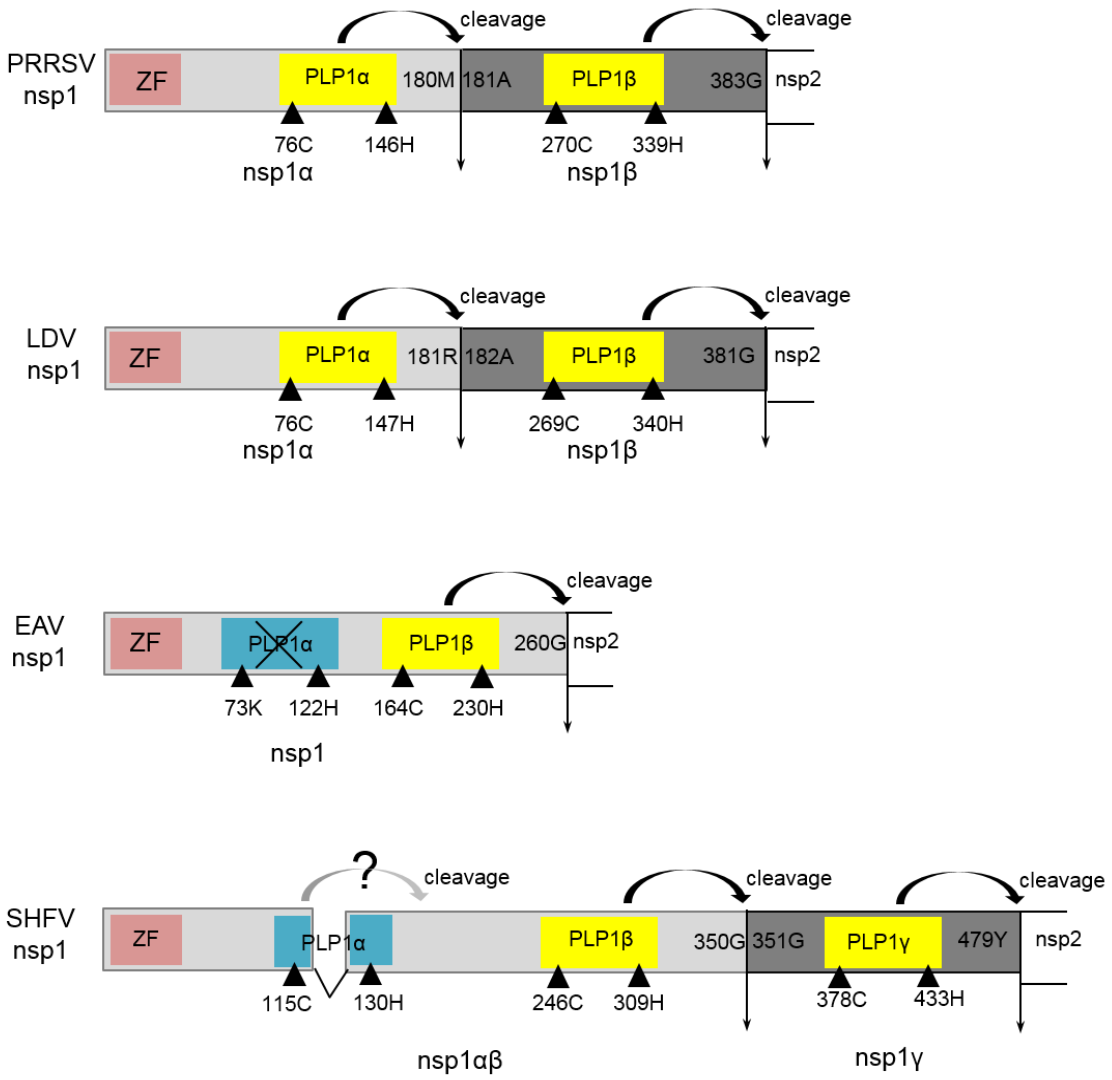


**Fig. 1.2. Schematic presentation of nsp1 of arteriviruses.** nsp1 protein of PRRSV, LDV, EAV, and SHFV is constituted of 384, 381, 260, and 479 amino acids, respectively. PRRSV-nsp1 is cleaved into PRRSV-nsp1α and PRRSV-nsp1β, and similarly, LDV-nsp1 is cleaved into LDV-nsp1α and LDV-nsp1β. For SHFV, two subunits of SHFV-nsp1αβ and SHFV-nsp1γ are produced from SHFV-nsp1. EAV-nsp1 remains uncleaved. Biologically active PLP domains are indicated in yellow and inactive PLP domains in EAV is shown in blue with crossing-outs. A question mark is labeled for SHFV PLP1α due to its unclear function. Catalytic residues for PLPs are indicated by blue triangles. Vertical arrows represent PLP-mediated cleavage sites (Han et al., 2014). Numbers indicate amino acid positions. Cleavage site 180M/181A is for the internal cleavage of type II PRRSV nsp1. Sequences from PRRSV PA8 strain (GenBank accession NO.: AF176348), LDV Plagemann strain (GenBank accession NO.: U15146.1), EAV Bucyrus strain (GenBank accession NO.: DQ846750), and SHFV (GenBank accession NO.: AF180391) are used to make the figure.

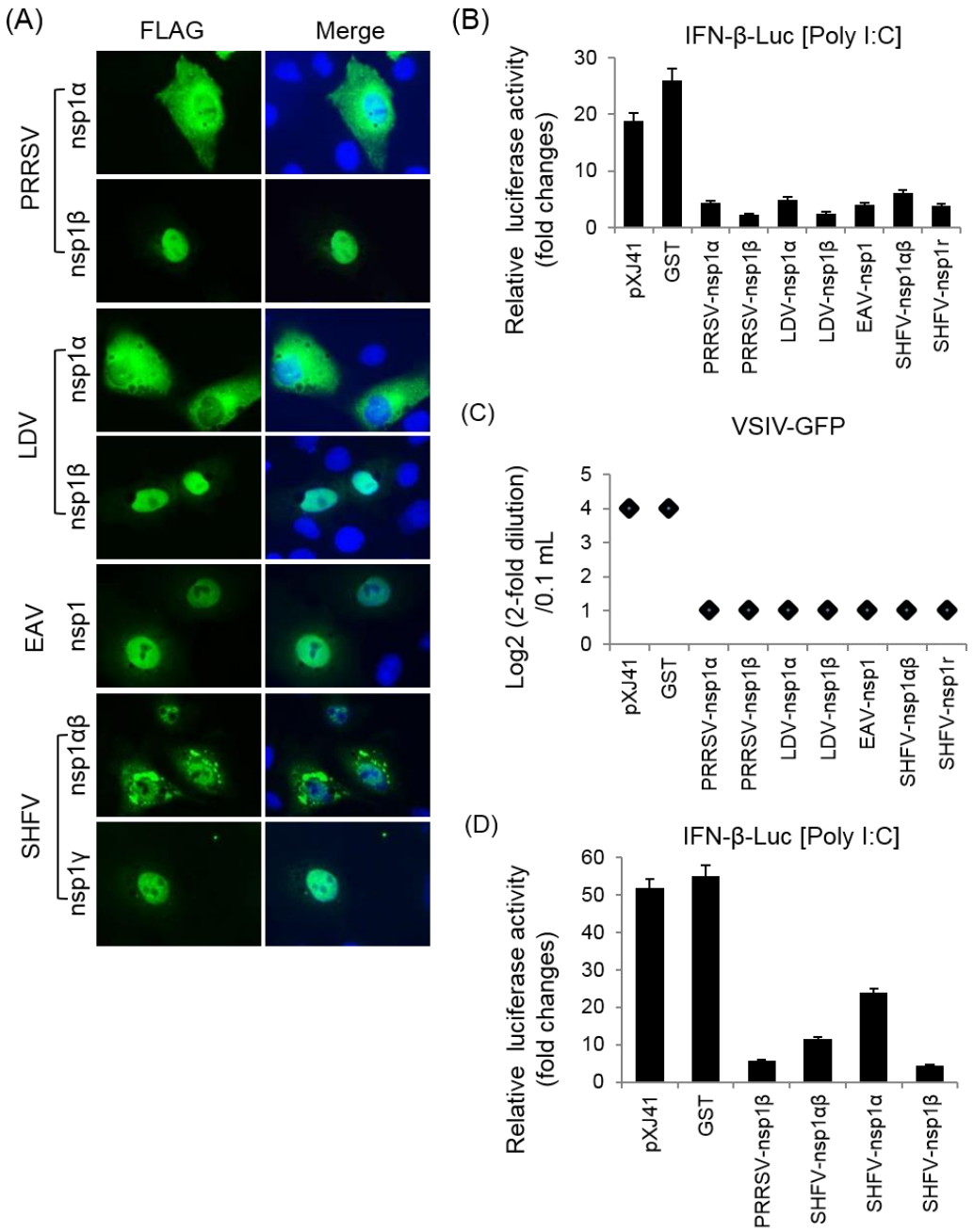


**Fig. 1.3. Suppression of IFN-β production by individual subunits of nsp1 of arteriviruses. (**A) Subcellular localization of individual nsp1 subunits of arteriviruses in MARC-145 cells. Cells were grown to 40% confluency and transfected with indicated genes for 24 h. Cells were stained with anti-FLAG Ab followed by staining with Alexa 488-labeled anti-mouse Ab and DAPI. Cellular localization of individual subunits was examined by fluorescent microscopy. (B) HeLa cells were seeded in 12-well plates and co-transfected with pIFN-β-Luc along with individual genes and pTK-RL as an internal control at a ratio of 1:1:0.1. (C) IFN bioassays using VSIV-GFP (vesicular stomatitis Indiana virus expressing GFP). (D) Identification of the functional region for IFN-β suppression in SHFV-nsp1αβ. SHFV-nsp1α and SHFV-nsp1β were separated according to Vatter et al. (2014) to make SHFV-nsp1α as 164 aa in length and SHFV-nsp1β as 186 aa.

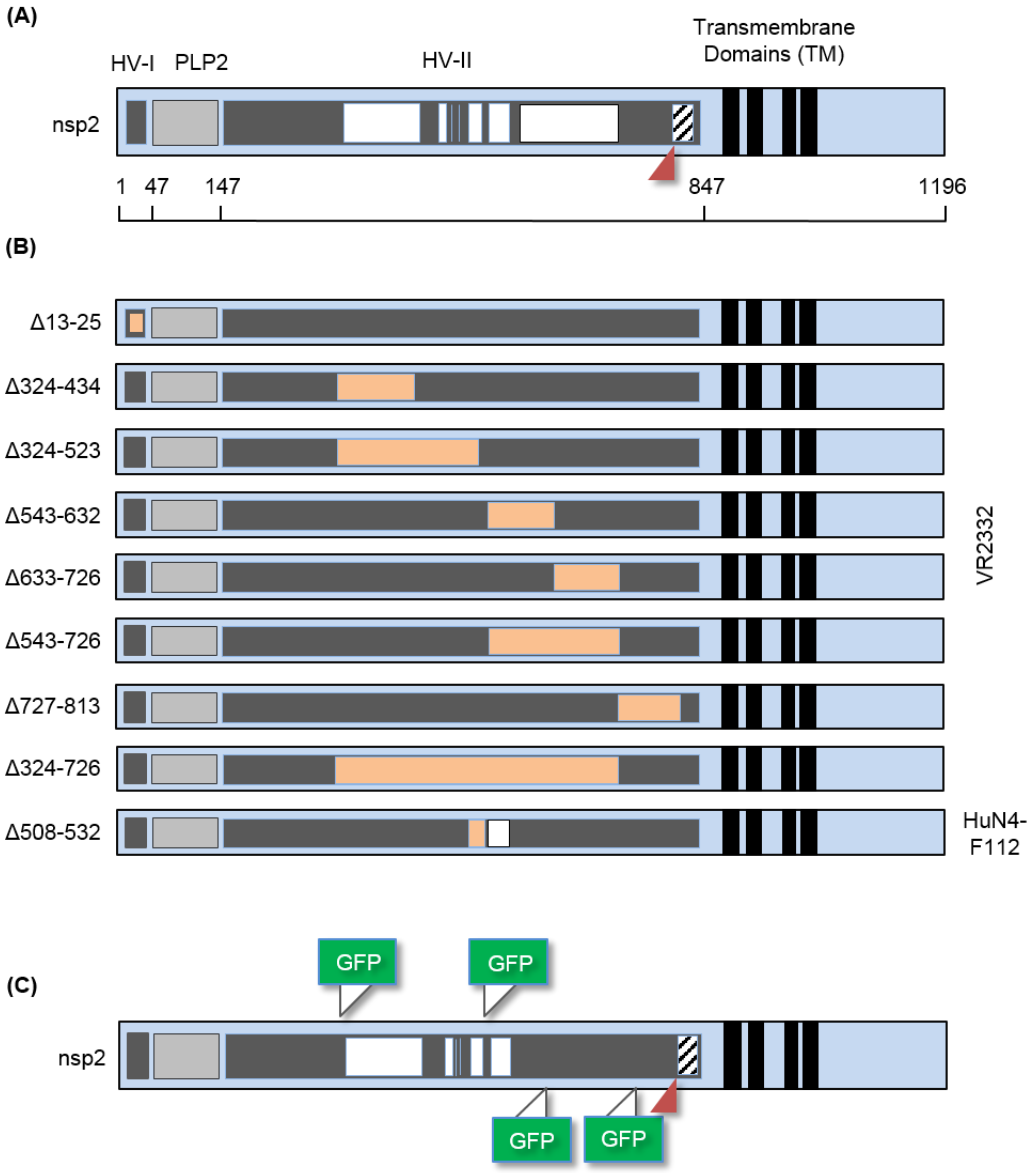


**Fig. 1.4. Engineering of infectious clones for nsp2 region.** (A), Schematic presentation of the nsp2 protein. The nsp2 protein consists of five regions: hypervariable region I (HV-I), PLP2 cysteine protease core, hypervariable region II (HV-II), transmembrane regions, and the C-terminal tail. White areas indicate natural deletions. A triangle indicates the position of natural insertion. (B), Location of experimental sequence deletions (Orange). (C), Foreign gene insertion sites. Triangles indicate the position of insertion. GFP, green fluorescent protein; HV, hypervariable region; PLP, papain-like proteinase. Numbers indicate amino acid positions of nsp2.

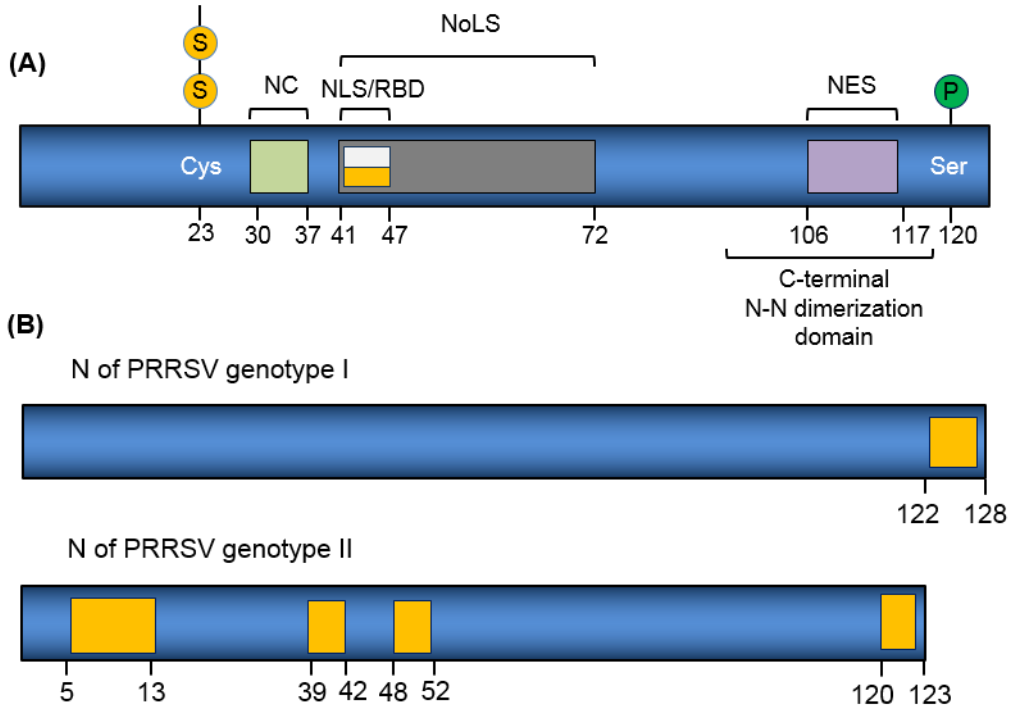


**Fig. 1.5. Engineering of infectious clones in N gene.** (A), Schematic presentation of the nucleocapsid (N) protein. NLS and RBD overlap each other. (B), Deletion tolerance regions (yellow) in N protein. NLS, nuclear localization signal; NES, nuclear export signal; P, phophorylation site; S, disulfide bridge, RBD, RNA-binding domain; NoLS, nucleolar localization signal. NCI, non-covalent interaction motif. Numbers indicate amino acid positions of N.

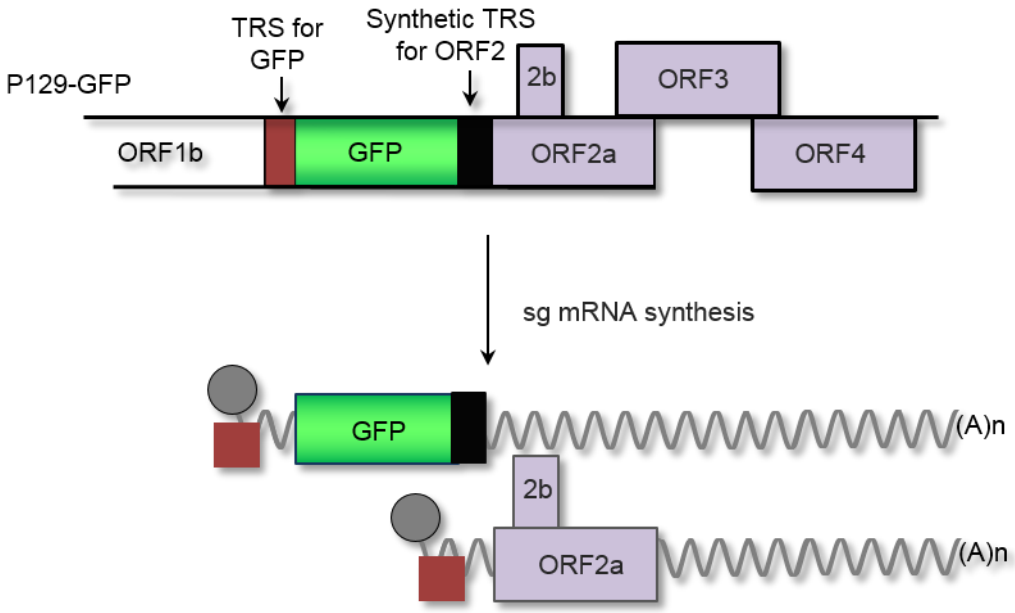


**Fig. 1.6. PRRSV infectious clone for foreign gene expression.** A copy of TRS (Black bar) is inserted between ORF1b and ORF2. Two kinds of sg mRNAs are produced from this construction. The GFP or other foreign genes is inserted between the synthetic TRS (Black bar) and the original TRS (Brown bar), and the original TRS leads to generation of mRNA for GFP expression. The inserted TRS drives the synthesis of sg mRNA for ORF2 expression.

## Table 1.1. Arterivirus proteins modulating innate immune signaling

| Virus | Protein | Modulatory function for innate immunity | Reference |
|---|---|---|---|
| PRRSV | nsp1α | Inhibits production of type I IFNs and impairs IFN promoter activity | (Chen et al., 2010) |
| | | Suppresses NF-κB activation | (Song et al., 2010; Subramaniam et al., 2010) |
| | | Induces CBP degradation | (Han et al., 2013; Kim et al., 2010) |
| | | Suppresses TNF-α promoter activity | (Subramaniam et al., 2010) |
| | nsp1β | Inhibits production of type I IFNs and impairs IFN promoter activity | (Chen et al., 2010) |
| | | Impairs IRF3 phosphorylation and IRF3 nuclear localization | (Beura et al., 2010) |
| | | Interferes with IFN-α induction and ISG expression | (Patel et al., 2010) |
| | | Blocks nuclear translocation of ISGF3 by inducing KPNA1 degradation | (Wang et al., 2013) |
| | | Suppresses TNF-α promoter activity | (Subramaniam et al., 2010) |
| | nsp2 (PLP2) | Antagonizes type I interferon induction<br>Interferes with NF-κB signaling pathway<br>Prevents IκBα degradation by OTU domain | (Sun et al., 2010) |
| | | Inhibits ISG15 production and ISGylation | (Sun et al., 2012b) |
| | | Activates NF-κB | (Fang et al., 2012a) |
| | nsp4 | Inhibits IFN-β promoter activity<br>Suppresses NF-κB mediated signaling pathway in the nucleus | (Chen et al., 2014) |
| | nsp11 | Impair IFN promoter activity<br>Participates in suppression of RIG-I signaling<br>Degrades mRNA of IPS-1 | (Sun et al., 2012a) |
| | N | Inhibits production of type I IFNs and impairs IFN promoter activity<br>Impairs IRF3 phosphorylation and IRF3 nuclear localization | (Sagong and Lee, 2011) |
| | | Upregulates IL-10 gene expression | (Wongyanin et al., 2012) |
| | | Activates NF-κB | (Luo et al., 2011;<br>Pujhari et al., 2014) |
| EAV | nsp1 | Inhibits production of type I IFNs and impairs IFN promoter activity | (Han et al., 2014)<br>(Go et al., 2014) |
| | nsp2 (PLP2) | Inhibits RIG-I-mediated innate immune signaling<br>inhibits RIG-I ubiquitination by its DUB activity | (van Kasteren et al., 2012; 2013) |
| LDV | nsp1α | Inhibits production of type I IFNs and impairs IFN promoter activity<br>Induces CBP degradation | (Han et al., 2014) |
| | nsp1β | Inhibits production of type I IFNs and impairs IFN promoter activity | (Han et al., 2014) |
| SHFV | nsp1αβ | Inhibits production of type I IFNs and impairs IFN promoter activity | (Han et al., 2014) |
| | nsp1γ | Inhibits production of type I IFNs and impairs IFN promoter activity | (Han et al., 2014) |

## Table 1.2. Construction of PRRSV infectious clone

| Name | Year[a] | Genotype[b] | Isolate | GenBank # | Cell type for | | Vector | Promoter | Genetic marker[d] | Reference |
|---|---|---|---|---|---|---|---|---|---|---|
| | | | | | Transfection | Passage | | | | |
| pABV414[e] | 1998 | I | *Ter Huurne* (TH) | N/A | BHK-21 | PAM/ CL2621 | pOK12 | T7 | N/A | (Meulenberg et al., 1998) |
| pABV416[e] | 1998 | I | *Ter Huurne* (TH) | N/A | BHK-21 | PAM/ CL2621 | pOK12 | T7 | N/A | (Meulenberg et al., 1998) |
| pABV437 | 1998 | I | *Ter Huurne* (TH) | N/A | BHK-21 | PAM/ CL2621 | pOK12 | T7 | pacI(3′UTR) | (Meulenberg et al., 1998) |
| N/A | 2003 | II | VR-2332 | AY150564 | BHK-21C | PAM/ MARC-145 | pOK12 | T7 | BstZ17I (ORF1a)/ HpaI(3′UTR) | (Nielsen et al., 2003) |
| pFL12 | 2004 | II | NVSL#97-7895 | AY545985 | MARC-145 | PAM/ MARC-145 | pBR322 | T7 | BsrGI(ORF1a) | (Truong et al., 2004) |
| pT7-P129 | 2005 | II | P129 | AF494042 | MARC-145 | MARC-145 | pCR2.1 | T7 | C1559T/ A12622G | (Lee et al., 2005) |
| pCMV-S-P129 | 2005 | II | P129 | AF494042 | MARC-145 | MARC-145 | pCMV | hCMV | C1559T/ A12622G | (Lee et al., 2005) |
| pSD01-08 | 2006 | NA I[f] | SD 01-08 (P34) | DQ489311 | BHK-21 | PAM/ MARC-145 | pACYC177 | T7 | ScaI(ORF7) | (Fang et al., 2006a; Fang et al., 2006b) |
| pPP18 | 2006 | II | Prime Pac (PP) | DQ779791 | MARC-145 | PAM/ MARC-145 | pOK12 | T7 | SpeI(ORF1a) | (Kwon et al., 2006) |
| pVR-V7 | 2007 | II | VR2332 | DQ217415 | MA-104/ MARC-145 | MA-104/ MARC-145 | pOK12HDV-PacI | T7 | G7329A/ T7554 C | (Han et al., 2007) |
| pWSK-DCBA | 2007 | II | BJ-4 | EU360128 | MARC-145 | PAM/ MARC-145 | pWSK29 | SP6 | VspI(ORF1b) | (Ran et al., 2008) |
| pAPRRS | 2008 | II | APRRS | N/A | MA-104 | MA-104 | pBluescript SK(+) | T7 | N/A | (Yuan and Wei, 2008) |
| pORF5M | 2008 | II | APRRS | N/A | MA-104 | MA-104 | pBluescript SK(+) | T7 | MluI (ORF5) | (Yuan and Wei, 2008) |
| pJX143 | 2008 | II | JX143 | EF488048 | MA-104 | MA-104 | pBlueScript II SK (+) | T7 | N/A | (Lv et al., 2008) |
| pJX143M | 2008 | II | JX143 | N/A | MA-104 | MA-104 | pBlueScript II SK (+) | T7 | MluI (ORF6) | (Lv et al., 2008) |
| pWSK-JXwn | 2009 | II | JXwn06 | N/A | BHK-21 | MARC-145 | pWSK29 | SP6 | BstBI(ORF1a) | (Zhou et al., 2009) |
| pWSKHB-1/3.9 | 2009 | II | HB-1/3.9 | N/A | BHK-21 | MARC-145 | pWSK29M | SP6 | MluI (ORF1a) SifI (ORF1b) | (Zhou et al., 2009) |
| pHuN4-F112 | 2011 | II | HuN4-F112 | N/A | BHK-21 | MARC-145 | pBlueScript II SK (+) | SP6 | MluI (ORF6) | (Zhang et al., 2011) |
| pACYC-VR2385-CA | 2011 | II | VR2385-CA | N/A | BHK-21 | MARC-145 | pACYC177 | T7 | Sph I(ORF1a) | (Ni et al., 2011) |
| pIR-VR2385-CA | 2011 | II | VR2385-CA | N/A | BHK-21 | MARC-145 | pIRES-EGFP2 | CMV | Sph I(ORF1a) | (Ni et al., 2011) |
| pSHE | 2013 | I | SHE(AMER-VAC-PRRS/A3) | GQ461593 | BHK-21 | MARC-145 | pB-ZJS | CMV | N/A | (Gao et al., 2013) |
| pCMV-SD95-21 | 2013 | II | SD95-21 | KC469618 | BHK-21 | MARC-145 | pACYC177 | CMV | N/A | (Li et al., 2013) |

N/A is the abbreviation of not application a. The individual time of PRRSV infectious clones construction referred to the date of each publication. b. Genotype I and II PRRSV represents European and North America strains, respectively. c. Sequences of full-genome cDNA clone rather than complete genome sequences of parental virus are listed. d. The genome area in which the restricted enzyme sites are introduced is indicated with brackets. The position where single mutations are introduced is given. e. Genome-length cDNA clones of pABV414 and pABV416 encode identical viral protein sequences except for one amino acid at position 1084 in ORF1a, which are a Pro in pABV414 and a Leu in pABV416. f. The abbreviation, NA I, in the genotype column represents genotype I PRRSV isolated in North America.

## Table 1.3. Identification of non-essential regions of PRRSV genome

| Genotype and gene | | Mutation/deletion (nts or aa) | Motif | Infectious clone | Growth [d] | GenBank |
|---|---|---|---|---|---|---|
| II | 5′UTR | 1-3 nts | N/A | pAPRRS | N/A | GQ330474.2 |
| II | nsp2 | 13-35 aa | hypervariable | pVR-V7 | ↓ | DQ217415 |
| II | nsp2 | 324-726 aa | hypervariable | pVR-V7 | ↓ | DQ217415 |
| II | nsp2 | 727-813 aa | hypervariable | pVR-V7 | ↓ | DQ217415 |
| II | nsp2 | 480-667 aa | hypervariable | pHuN4-F112 | N/A | EF635006 |
| I | nsp2 | 691-722 aa | ES3[a] | pSD01-08 | ↑ | DQ489311 |
| I | nsp2 | 736–790 aa | ES4 [a] | pSD01-08 | nc | DQ489311 |
| I | nsp2 | 1015–1040 aa | ES7 [a] | pSD01-08 | ↓ | DQ489311 |
| II | ORF7 | 5-13 aa | N/A | pAPRRS | ↓ | GQ330474.2 |
| II | ORF7 | 39-42 aa | N/A | pAPRRS | ↓ | GQ330474.2 |
| II | ORF7 | 48-52 aa | N/A | pAPRRS | nc | GQ330474.2 |
| II | ORF7 | 120-123 aa | N/A | pAPRRS | nc | GQ330474.2 |
| II | ORF7 | 43,44 aa | NLS [b] | pCMV-S-P129 | ↓ | AF494042 |
| II | ORF7 | 43,44,46 aa | NLS [b] | pCMV-S-P129 | ↓ | AF494042 |
| II | ORF7 | 46,47 aa | NLS [b] | pCMV-S-P129 | ↓ | AF494042 |
| I | ORF7 | 123-128 aa | N/A | pABV437 | nc | N/A |
| I | 3′UTR | 14989-14995 nts | N/A | pABV437 | nc | N/A |
| II | 3′UTR | 15370-15409 nts | N/A | pAPRRS | N/A | GQ330474.2 |

N/A is the abbreviation of not application. a. The abbreviation, ES, stands for the immunodominant B-cell epitopes identified in type I PRRSV.ES2-ES7 are identified in nsp2 encoding regions (Oleksiewicz et al., 2001). b. NLS stands for the nuclear localization signal which mediates the nuclear localization of PRRSV N protein. c. Ref. Seq. is the abbreviation of reference sequence, and GenBank accession numbers for each construct are provided. d. Symbols "↑" and "↓" indicate increased or reduced virus growth respectively. "nc" stands for no change.

## Table 1.4. Insertion tolerable regions in PRRSV genome

| Genotype | Genomic region | | Position | | foreign sequence | Infectious clone | Growth rate[a] | GenBank |
|---|---|---|---|---|---|---|---|---|
| | | | nt | aa | | | | |
| II | ORF1a | nsp2 | 3219/3220 | N/A | GFP | pCMV-S-P129 | nc | AF494042 |
| II | ORF1a | nsp2 | 3219/3220 | N/A | FLAG-tag | pCMV-S-P129 | ↓ | AF494042 |
| II | ORF1a | nsp2 | 3614/3615 | N/A | GFP | pCMV-S-P129 | ↓ | AF494042 |
| I | ORF1a | nsp2 | N/A | 348/349 | GFP | pSD01-08 | ↓ | DQ489311 |
| II | ORF1a | nsp2 | N/A | 507/508 | B-cell epitope in NDV NP | pSK-F112-D508–532 | nc | N/A |
| II | ORF1b/ORF2 | | N/A | N/A | TRS6+GFP | pCMV-S-P129 | nc | AF494042 |
| II | ORF1b/ORF2 | | N/A | N/A | TRS6+PCV2 C | pCMV-S-P129 | nc | AF494042 |
| II | ORF1b/ORF2 | | N/A | N/A | TRS6+DsRED | pCMV-S-P129 | nc | AF494042 |
| II | ORF1b/ORF2 | | N/A | N/A | TRS6+Rluc | pCMV-S-P129 | nc | AF494042 |
| II | ORF1b/ORF2 | | N/A | N/A | IFNα1 | pCMV-S-P129 | ↓ | AF494042 |
| II | ORF1b/ORF2 | | N/A | N/A | IFNβ | pCMV-S-P129 | ↓ | AF494042 |
| II | ORF1b/ORF2 | | N/A | N/A | IFNδ3 | pCMV-S-P129 | nc | AF494042 |
| II | ORF1b/ORF2 | | N/A | N/A | IFNω5 | pCMV-S-P129 | ↓ | AF494042 |
| II | ORF1b/ORF2 | | N/A | N/A | AscI ,SwaI, PacI | pAPRRS | nc | GQ330474.2 |
| II | ORF4/ORF5 | | N/A | N/A | NdeI | pAPRRS | nc | GQ330474.2 |
| II | ORF5/ORF6 | | N/A | N/A | AscI ,SwaI, PacI | pAPRRS | ↓ | GQ330474.2 |
| II | ORF6/ORF7 | | N/A | N/A | AscI ,SwaI, PacI | pAPRRS | nc | GQ330474.2 |
| II | ORF7/3'UTR | | N/A | N/A | NdeI | pAPRRS | nc | GQ330474.2 |

N/A is the abbreviation of not application. a. Symbols "↑" and "↓" indicate increased or reduced virus growth respectively. "nc" stands for no change.

## Table 1.5. Constructions of chimeric viruses

| Swapped region [a] | | | | | Substituent [b] | | | | Viability |
|---|---|---|---|---|---|---|---|---|---|
| **Virus** | **strain** | **Infectious clone [c]** | **Genome region** | **Position aa** | **Virus** | **Strain** | **Genome region** | **Position aa** | |
| EAV | Bucyrus | pA45 | ORF5 | 1-114 | LDV | P | GP5 | 1-64 | + |
| | | | | | PRRSV | IAF-Klop | GP5 | 1-64 | + |
| | | | | | SHFV | LVR 42-0/M6941 | GP7 | 1-138 | - |
| | | | | | SinV | San Juan | E1 | 1-428 | - |
| | | | | | VSV | HR | G | 1-402 | - |
| | | | | Whole | EAV | A45-80.4 | GP5 | Whole | + |
| | | | | | | 5rUCD | GP5 | Whole | + |
| | | | | | | 5r6D10 | GP5 | Whole | + |
| | | | | | | 5rVAC | GP5 | Whole | + |
| | | | | | | 5rKY84 | GP5 | Whole | + |
| | | | | | | 5rIL93 | GP5 | Whole | + |
| | | | | | | 5rCA95 | GP5 | Whole | + |
| | | | | | | 5rWA97 | GP5 | Whole | + |
| | | | | | | 5rATCC | GP5 | Whole | + |
| | | | | | | 5r10B4 | GP5 | Whole | + |
| | | | ORF6 | 17-162 | PRRSV | IAF-Klop | M | 1-16 | - |
| | | | | | LDV | P | M | 1-14 | - |
| | ARVAC | prMLVB4/5 | ORF5 | 115-255 | PRRSV | IA-1107 | ORF5 | 1-64 | + |
| | | prMLVB4/5 | ORF5 | N/A[d] | PRRSV | IA-1107 | ORF5 | Whole | - |
| | | prMLVB5/6 | ORF6 | N/A[d] | PRRSV | IA-1107 | ORF6 | Whole | - |
| | | prMLVB4/5/6 | ORF6 | 17-162 | PRRSV | IA-1107 | ORF6 | 1-17 | + |
| PRRSV | LV | pABV437 | ORF6 | 1-16 | PRRSV | V2332 | M | 1-16 | - |
| | | | | | LDV | P | M | 1-14 | + |
| | | | | | EAV | Bucyrus | M | 1-17 | - |
| | | pABV871 | ORF6 | 1-16 | PRRSV | V2332 | M | 1-16 | + |
| | | | | | EAV | Bucyrus | M | 1-17 | + |
| | VR2332 | N/A | ORF2 | Whole | PRRSV | JA142 | ORF2 | Whole | + |
| | | | ORF3 | Whole | PRRSV | JA142 | ORF3 | Whole | + |
| | | | | 1-194 | PRRSV | JA142 | ORF3 | 1-194 | + |
| | | | | 183-255 | PRRSV | JA142 | ORF3 | 183-255 | + |
| | | | ORF4 | Whole | PRRSV | JA142 | ORF4 | Whole | + |
| | | | ORF5 | Whole | PRRSV | JA142 | ORF5 | Whole | + |
| | | | | | | SDSU73 | ORF5 | Whole | + |
| | | | | | | 2M11715 | ORF5 | Whole | + |
| | | | | | | PRRS124 | ORF5 | Whole | + |
| | | | ORF6 | Whole | PRRSV | JA142 | ORF6 | Whole | + |
| | | | ORFs5-6 | Whole | PRRSV | JA142 | ORFs5-6 | Whole | + |
| | | | ORFs4-6 | Whole | PRRSV | JA142 | ORFs4-6 | Whole | + |
| | | | ORFs3-6 | Whole | PRRSV | JA142 | ORFs3-6 | Whole | + |
| | | | ORFs2-6 | Whole | PRRSV | JA142 | ORFs2-6 | Whole | + |
| | APRRS | pAPRRS asc | ORFs2a-4 | Whole | PRRSV | SHE | ORFs2a-4 | Whole | + |
| | | | | | EAV | vEAV030 | ORFs2a-4 | Whole | + |
| | | | ORFs2a-5 | Whole | PRRSV | SHE | ORFs2a-5 | Whole | + |
| | | | ORF5 | Whole | PRRSV | SHE | ORF5 | Whole | + |
| | NVSL# 97-7895 | FL12 | ORFs2a-7 | Whole | PRRSV | PRRSV01 | ORFs2a-7 | Whole | + |

N/A is the abbreviation of not application. Whole represents the full sequence of a specific region. a This section provides information of the regions replaced by the counterparts, including the virus, virus strains, the infectious clone used for swapping, and the exact position in which region is changed. b. The substituent section indicates the sequences used for substitutions. c. Infectious clone construct provided here includes both prototypes and modified constructs.

## CHAPTER 2: DEGRADATION OF CREB-BINDING PROTEIN AND MODULATION OF TYPE I INTERFERON INDUCTION BY THE ZINC FINGER MOTIF OF THE PRRSV NSP1-ALPHA SUBUNIT

### 2.1. ABSTRACT

Non-structural protein (nsp) 1 of PRRS virus is a viral antagonist for type I interferons (IFNs), and in cells expressing nsp1, CREB-binding protein (CBP) is degraded. Nsp1 is auto-processed into nsp1α and nsp1β subunits and in the present study we show that the nsp1α subunit was responsible for CBP degradation. The nsp1α subunit contains three distinct functional motifs; a papain-like cysteine protease α (PCPα) motif, an N-terminal zinc finger motif (ZF1), and a newly reported C-terminal zinc finger motif (ZF2). To study the structure function of nsp1α and its IFN antagonism, these motifs were individually mutated and the mutants were examined for their IFN suppression ability. The mutations that destroyed the PCPα activities (C76S, H146Y, and C76S/H146Y) did not affect the IFN suppressive activity of nsp1α, indicating that the cysteine protease activity did not participate in IFN suppression. The mutations of C70S, C76S, H146Y, and/or M180I which coordinated the ZF2 motif also did not alter IFN suppression. However, the mutations of C8S, C10S, C25S, and/or C28S for the ZF1 motif impaired the IFN antagonism of nsp1α, demonstrating that ZF1 was the essential element of nsp1α for IFN suppression. Wild-type nsp1α localized in the both nucleus and cytoplasm, but the ZF1 mutants that lost the IFN suppressive activity did not localize in the nucleus and remained in the cytoplasm. Consistent with their cytoplasmic distribution, CBP was not degraded by these mutants. Our results indicate that the ZF1 motif of nsp1α plays an important role for IFN

This chapter previously appeared as article in Virus Research. The original citation is as follows: Han, M., Du, Y., Song, C., Yoo, D. 2013. Degradation of CREB-binding protein and modulation of type I interferon induction by the zinc finger motif of the porcine reproductive and respiratory syndrome virus nsp1alpha subunit. Virus Research172:54-65. 

regulation and further demonstrate that the CBP degradation is likely the key mechanism for IFN suppression mediated by the nsp1α subunit protein of PRRS virus.

## 2.2. INTRODUCTION

The type I interferon (IFN) system is considered a key component of the innate immune response and represents one of the first lines of defense against virus infection (Samuel, 2001). The IFN-induced signal transduction leads to the expression of more than 300 IFN-stimulated genes (ISG) that contribute to the antiviral state of host cells, directly or indirectly (Sadler and Williams, 2008). Type I IFNs are induced directly in response to virus infection and viral components are recognized by two distinct pattern recognition receptors (PRRs); toll-like receptors (TLRs) and RIG-like receptors (RLRs) (reviewed in Yoo et al., 2010). After the binding of pathogen-associated molecular patterns (PAMPs) to PRRs, ensuing signal transduction leads to the activation of IFN regulatory factor 3 (IRF3) and the release of nuclear factor-kappa B (NF-κB) from its inhibitor IκB (Baccala et al., 2007). IRF3 is activated through phosphorylation by IKKε and/or TBK1 kinases, and the phosphorylation results in the IRF3 dimerization and conformational switch, exposing nuclear localization signal (NLS) for subsequent nuclear translocation. By phosphorylation, an auto-inhibitory (feature of IRF3 that prevents its interaction with CREB (cyclic AMP responsive element binding)-binding protein (CBP) is removed) (Panne et al., 2007 and Takahasi et al., 2010). For NF-κB-mediated signaling, it is normally held in the cytoplasm by association with the inhibitor of NF-κB (IκB). Once the signaling cascade contributes to the phosphorylation of IκB and its subsequent ubiquitination and degradation by proteasomes, NF-κB is detached from IκB and translocates to the nucleus (Murray, 2007). After nuclear translocation, activated IRF3 and NF-κB exert modulation on the

activation of IFN-β promoter. Within the IFN-β promoter, four regulatory cis elements are found, namely, the positive regulatory domains (PRDs) I, II, III, and IV. PRD I/III, PRD II and PRD IV are binding sites for IRFs, NF-κB, and ATF-2/c-Jun (AP-1), respectively (Honda et al., 2006). The expression of IFN-β requires the assembly of these regulatory factors on PRDs to form an enhanceosome complex, which recruits CBP to instigate IFN production (Randall and Goodbourn, 2008).

Porcine reproductive and respiratory syndrome (PRRS) is an emerged and re-emerging swine disease featured by severe reproductive losses, post-weaning pneumonia and increased mortality. PRRS was first reported in the Unites States in 1987 and subsequently in Europe in 1990, and has since become the most economically significant disease to pig production worldwide (Chand et al., 2012). PRRS virus (PRRSV) is the etiological agent placed in the family Arteriviridae in the order Nidovirales, together with equine arteritis virus (EAV), lactate dehydrogenase-elevating virus (LDV), and simian hemorrhagic fever virus (SHFV). PRRSV possesses a single-stranded positive-sense RNA genome of 15 kb in length, harboring 10 ORFs: ORF1a, ORF1b, ORF2a, ORF2b, and ORFs 3 through 7 (Meulenberg et al., 1993 and Wootton et al., 2000), plus a newly identified ORF5a (Firth et al., 2011 and Johnson et al., 2011). Mediated by the ribosomal frame-shifting signal in the ORF1a/ORF1b overlapping region, ORF1a and ORF1b synthesize two polyproteins, pp1a and pp1ab, which are proteolytically cleaved into 14 non-structural proteins (nsp) by papain-like cysteine protease (PCP) α and PCPβ in nsp1, poliovirus 3C-like cysteine protease (CP) in nsp2, and serine protease (SP) in nsp4 (reviewed by Fang and Snijder, 2010). The remaining ORFs code for eight different structural proteins: glycoprotein (GP) 2, small envelopes (E), GP3, GP4, GP5, ORF5a, membrane (M), and

nucleocapsid (N) proteins (Firth et al., 2011, Johnson et al., 2011, Meulenberg et al., 1993 and Wootton et al., 2000).

PRRSV seems to suppress the production of type I IFNs in infected pigs (Albina et al., 1998). IFNs are negligible in the lungs of pigs where PRRSV actively replicate in vivo, and the induction of IFN is poor in virus-infected PAMs (porcine alveolar macrophages) and MARC-145 cells in vitro. PRRSV can establish a persistent infection for up to 6 months. It seems that PRRSV has evolved to modulate the host antiviral response via several strategies such as delayed generation of neutralizing antibody and suppressed IFN production (Allende et al., 2000, Diaz et al., 2005, Lee et al., 2004 and Luo et al., 2008). The molecular basis for modulation of type I IFN production by PRRSV has recently been studied and five viral proteins have been identified to date as IFN antagonists: N as a structural protein and four non-structural proteins, nsp1α, nsp1β, nsp2 and nsp11 (Beura et al., 2010, Chen et al., 2010, Kim et al., 2010, Sagong and Lee, 2011, Sun et al., 2010 and Yoo et al., 2010).

Among these, nsp1α is the first viral protein synthesized during virus-infection. nsp1α is a multifunctional regulatory protein, containing an N-terminal zinc finger (ZF) motif, designated as ZF1 in the present study, and the papain-like cysteine protease (PCP) α domain. The ZF1 motif of nsp1α belongs to the 4-Cys (4-C) ZF superfamily, and mutations in the ZF1 motif selectively eliminate subgenomic (sg) mRNA synthesis, while genomic RNA synthesis is either not affected or even increased (Sun et al., 2009 and Tijms et al., 2007). The PCPα domain conducts self-processing of nsp1, yielding nsp1α and nsp1β subunits. This auto-cleavage is essential for synthesis of PRRSV sg mRNA but does not affect viral genome replication (Kroese et al., 2008). The crystallographic study for nsp1α has identified a second zinc finger motif in the C-terminal region, designated ZF2 in the present study, and that the active site residues for PCPα

participate in the ZF2 configuration to coordinate a zinc atom (Sun et al., 2009). The biological function of ZF2 is unknown.

Recent studies have shown that PRRSV nsp1 suppresses the production of type I IFNs in PRRSV-infected cells and gene-transfected cells, and its cleavage products, nsp1α and nsp1β, are capable of blocking the induction of type I interferon by targeting both IRF3- and NF-κB-mediated production pathways (Beura et al., 2010, Chen et al., 2010 and Song et al., 2010). Further investigations showed CBP degradation in the presence of nsp1, and the degradation was proteasome-dependent (Kim et al., 2010). In the present study, we investigated the basis for the type I IFN suppression mediated by nsp1 and showed that nsp1α subunit alone was responsible and sufficient for CBP degradation. We also determined the importance of ZF1 for IFN suppression and provided evidence that the CBP degradation was likely the basis for IFN suppression mediated by nsp1α of PRRSV.

## 2.3. MATERIALS AND METHODS

**Cells and viruses:** HeLa cells (NIH AIDS Research and Reference Reagent Program, Germantown, MD) were grown in Dulbecco′s modified Eagle′s medium (DMEM; Mediatech Inc., Manassas,VA) supplemented with 10% heat-inactivated fetal bovine serum (FBS; HyClone, Logan, UT) in a humidified incubator with 5% $CO_2$ at 37 °C. The PA8 strain of the North American genotype PRRSV (Wootton et al., 2000) was used throughout the study. The full-length genomic sequence of PA8 shares 99.2% identity with the prototype PRRSV VR2332 of the North American genotype (Nelsen et al., 1999).

**Plasmids and DNA cloning:** The plasmids pFLAG-nsp1 and pFLAG-nsp1α contain the full-length nsp1 and nsp1α genes, respectively, fused with an N-terminal FLAG tag (Song et al., 2010). The full sequence of nsp1β including the N-terminal FLAG tag was amplified by PCR using pFALG-nsp1 as a template using the upstream primer (5′-CCGAATTCACCATG*GATTACAAGGATGACGACGATAAG*GCTACTGTCTATGACATTGGTCATGGCTAC-3′, where the EcoRI recognition sequence is underlined and the FLAG tag is italicized and underlined) and the downstream primer (5′-GGCTCGAGCTAGCCGTACCACTTGT-3′, where the XhoI sequence is underlined). The PCR fragment was cloned into pXJ41 mammalian expression vector after digestion with XhoI and EcoRI (Xiao et al., 1991). Mutant plasmids were generated using PCR-based site-directed mutagenesis as described below using plasmid pFLAG-nsp1α as a template and a set of primers listed in Table 2.1. pIFN-β-Luc, p4xIRF3-Luc and pTATA-Luc, were kindly provided by Stephan Ludwig (Ehrhardt et al., 2004; Institute of Molecular Medicine, Heinrich Heine Universtät, Düsseldorf, Germany). The pIFN-β-luc plasmid contains the luciferase reporter gene placed under the IFN-β promoter. The p4xIRF3-Luc construct contains four copies of the IRF3 specific PRDI/III domain of the IFN-β promoter in front of the luciferase reporter gene. The plasmid pPRDII-Luc contains 2 copies of the NF-κB binding region PRD II of the IFN-β promoter in front of the luciferase gene and was kindly provided by Stanley Perlman (University of Iowa, IA; Zhou and Perlman, 2007). The plasmid pISRE-Luc contains the IFN stimulated response element (ISRE) binding sequence upstream of the luciferase reporter gene (Stratagene, La Jolla, CA). The pRL-TK plasmid (Promega) contains the renilla luciferase reporter under control of the herpes simplex virus thymidine kinase (HSV-tk) promoter and was included in all experiments to serve as an internal control.

**Antibodies and chemicals:** Polyinosinic:polycytidylic [poly (I:C)] and anti-Flag MAb (M2) were purchased from Sigma (St. Louis, MO). Anti-β-actin MAb (sc-47778), anti-CBP MAbs (sc-7300), and anti-PML PAb (sc-5621) were purchased from Santa Cruz Biotechnologies Inc. (Santa Cruz, CA). Anti-ISG15 PAb was purchased from Thermo Scientific Pierce (Rockford, IL). The peroxidase-conjugated Affinipure goat anti-mouse IgG and peroxidase-conjugated Affinipure goat anti-rabbit IgG were purchased from Jackson Immuno Research (West Grove, PA). Alexa-red conjugated goat anti-rabbit antibody and Alexa-green conjugated goat anti-mouse antibody were purchased from Invitrogen (Carlsbad, CA).

**Transfection and protein expression:** Transfection was conducted using Lipofectamine 2000 according to the manufacturer′s instructions (Invitrogen; Carlsbad, CA). HeLa cells were plated in 6-well plates and grown to 80% confluency. Transfection mix containing 2 μg of DNA and 2 μl of Lipofectamine 2000 in OPTI-MEM® I (Invitrogen; Carlsbad, CA) was incubated at room temperature (R/T) for 20 min and added to each well. After 4 h, the transfection mix was replaced with a fresh medium, and cells were incubated for 24 h for protein expression.

**Luciferase reporter assay:** HeLa cells were seeded in 12-well plates one day prior to transfection. When cells were grown to a density of $5 \times 10^4$ cells/well, 0.5 μg of pFLAG-nsp1α plasmid or its mutant derivatives, 0.5 μg of pIFN-β-Luc, p4xIRF3-Luc, pPRDII-Luc, or pTATA-Luc, and 0.05 μg of pLR-TK were co-transfected using Lipofectamine. At 24 h post-transfection, cells were transfected again with 0.5 μg of poly (I:C) for 16 h and cell lysates were prepared for luciferase assays. For pPRDII-Luc, cells were incubated with 20 ng of TNFα for 16 h and for

pISRE-Luc, cells were incubated with 1,000 units of IFN (Calbiochem) for 16 h. Luciferase activities were measured using the Dual-Glo Luciferase Assay System according to the manufacturer′s instructions (Promega). The values were normalized with respect to renilla luciferase activities and the results were expressed as relative luciferase activities. All assays were repeated at least three times, each experiment in triplicates.

**Western blot analysis:** Gene-transfected HeLa cells were lysed in lysis buffer (20 mM Tris [pH 7.5], 150 mM NaCl, 1 mM EDTA, 1 mM EGTA, 1% Triton X-100, 1% NP-40) containing the protease inhibitor cocktail (P-8340 Sigma). Insoluble materials were removed by centrifugation at 4°C for 10 min at 13,200 x relative centrifugal force in a microcentrifuge (Eppendorf 5415R). The cell lysates were resolved by 7.5% or 12% SDS-PAGE, followed by transfer to Immobilon-P membrane (Millipore). After blocking with 5% skim milk powder in TBS-T (10 mM Tris–HCl [pH 8.0], 150 mM NaCl, 1% Tween 20), membranes were incubated with primary antibody for 1 h at R/T followed by incubation with horseradish peroxidase-conjugated secondary antibody for 1 h at R/T. After three washes with TBS-T, proteins were visualized using the Enhanced Chemiluminescence system (Pierce, Rockford, IL).

**Immunofluorescence analysis (IFA):** Cells were grown on cover slips to 40% confluency and transfected with indicated plasmids for 24 h. Cells were then fixed with 4% paraformaldehyde for 10 min at R/T in phosphate-buffered saline (PBS) and permeabilized using 0.1% Triton X-100 for 10 min at R/T. After blocking with 1% BSA in PBS for 30 min, cells were incubated with primary antibody in PBS containing 1% BSA for 2 h followed by incubation with Alexa Fluor 488- and/or 594-conjugated secondary antibody for 1 h. Nuclear staining was performed

with DAPI (4′,6-diamidino-2-phenylindol) for 3 min at R/T. After washing with PBS, coverslips were mounted onto slides using Fluoromount-G mounting medium (Southern Biotech, Birmingham, AL), and examined under a fluorescence microscope (Nikon Eclipse TS100). Degradation of CBP and reduction of PML were quantified by calculating the percentage of cells for visible reduction of CBP or PML-NB using the following formula; (Number of cells showing more than 50% reduction of the CBP or PML staining intensity compared to the control CBP or PML staining intensity out of total 50 cells expressing nsp1 or its mutant derivatives) / (50 cells expressing nsp1α or its mutant derivatives) x 100.

## 2.4. RESULTS

**CBP degradation by Nsp1α:** A previous report has shown the CBP degradation in the presence of nsp1 in gene-transfected cells and PRRSV-infected cells (Kim et al., 2010). Since nsp1 is cleaved into nsp1α and nsp1β, it was of interest to determine the role of each subunit for CBP degradation. For this, Western blot was conducted to examine CBP in HeLa cells expressing nsp1α or nsp1β (Fig. 2.1A). Empty vector pXJ41, pFLAG-nsp1, pFLAG-nsp1α, pFLAG-nsp1β, and pXJ41-GST plasmids were individually transfected into cells for 24 h. Cell lysates were then prepared and subjected to Western blot using the CBP antibody and FLAG antibody. Nsp1α and nsp1β were expressed as 19 kD and 26 kD proteins, respectively. The molecular weight of the nsp1 precursor was detected as 19 kD since a FLAG tag was attached to the N-terminus of nsp1 which was then cleaved to generate FLAG-nsp1α (Fig. 2.1A, middle panel, arrows). A decreased amount of CBP was shown in the FLAG-nsp1-expressing and FLAG-nsp1α-expressing cells (Fig. 2.1A, upper panel, lanes 2, 3, asterisks) compared with pXJ41-transfected cells and GST-expressing cells (upper panel, lanes 1, 5). In contrast, virtually no detectable reduction of CBP

was observed in the FLAG-nsp1β-expressing cells (upper panel, lane 4), suggesting that nsp1α may be the subunit responsible for CBP degradation. GST served as a negative control to eliminate the possibility of non-specific CBP degradation. To further confirm the CBP degradation by nsp1α, immunofluorescence analysis (IFA) was employed. The endogenous levels of CBP were determined by staining cells with CBP antibody (Fig. 2.1B, panels B, F, J, and N). Both FLAG-nsp1-expressing (panel F) and FLAG-nsp1α-expressing (panel J) cells showed significantly reduced signals of CBP (arrows) in comparison to cells without nsp1 or nsp1α expression. Cells expressing FLAG-nsp1β did not appear to show detectable reduction of CBP (Fig. 2.1B, panel N, arrowhead), indicating that nsp1β did not affect CBP degradation. CBP degradation by nsp1α or nsp1β was quantified by calculating the numbers of cells exhibiting reduced CBP out of the number of cells expressing nsp1, nsp1α, or nsp1β. Approximately 82% of nsp1-expressing cells and 84% of nsp1α-expressing cells showed appreciable reduction of CBP, while no single cell expressing FLAG-nsp1β exhibited CBP reduction (Fig. 2.1C). The IFA results were consistent with the Western blot data demonstrating that only the nsp1α subunit contributed to the CBP degradation.

**Cysteine protease activity of nsp1α is not required for IFN-β suppression:** Since nsp1α was shown to down-regulate type I IFN production (Song et al., 2010) and caused CBP degradation (Fig. 2.1), it was of interest to determine the functional domain responsible for the suppression of type I IFN. Since nsp1α contains the PCPα domain, the protease activity of this domain was examined for CBP degradation. To examine the role of the protease activity for IFN modulation, three PCPα mutants (C76S, H146Y, and C76S/H146Y) were constructed by site-directed mutagenesis to subvert the catalytic sites, since C76 and H146 were previously shown to destroy

the proteolytic activity of PCPα (Kroese et al., 2008). The IFN-β suppression of the mutants was then examined using IFN-β-Luc, 4xIRF3-Luc, and pRD II-Luc reporters. Upon poly(I:C) stimulation of IFN-β-Luc-transfected cells, the reporter suppression was still significant for all three mutants (Fig. 2.2A), suggesting that the PCPα activity did not contribute to IFN suppression. This result was subsequently substantiated by luciferase assays using 4xIRF3-Luc (Fig. 2.2B) and pRD II-Luc (Fig. 2.2C) reporters in PCPα mutant-expressing cells. Neither IRF3 activity nor NF-κB activity was subverted by PCPα mutants since the levels of reporter gene expression determined for the IRF3 and NF-κB promoter activities were similar to that of cells expressing wild-type nsp1α.

**ZF2 is dispensable for IFN suppression:** The nsp1 cleavage site directed by PRRSV PCPα was initially predicted to somewhere at positions Gln166-Pro168 (den Boon et al., 1995), while it was specifically indicated to Gln166↓Arg167 (Allende et al., 1999). Recent studies however identified Met180↓Ala181 as the authentic cleavage site (Chen et al., 2010; Sun et al., 2009), making the nsp1α subunit to be 14 aa longer than the previous prediction. The crystallographic study identified a second zinc finger (ZF2) motif in nsp1α, and M180 which is the most C-terminal residue participates in the ZF2 configuration together with C70, C76, and H146. Subsequently, the importance of the structural integrity of nsp1α for IFN regulation was demonstrated (Song et al., 2010). Since the 14 aa-deletion would destabilize the ZF2 configuration and the 14-aa deletion mutant lost IFN suppressive activity, it was postulated that the ZF2 motif may play an important role for IFN regulation. To examine this possibility, single or double mutations were introduced to C70, C76, H146, and M180, and a set of ZF2 mutants were constructed (Fig. 2.3A). Mutants C70S, C76S, H146Y, and M180I were predicted to

destroy the ZF2 configuration, while C to H substitution would maintain the ZF2 motif, since both C and H function interchangeably to hold a zinc atom, and thus the optional use of C and H gives rise to different types of zinc finger motifs such as C2H2, C2HC, or C4 (Iuchi, 2001). To ensure the complete destruction of ZF2 configuration, double substitutions were also introduced (Fig. 2.3A), and using the ZF2 mutant genes, IFN suppressive activity was examined by reporter assays. After poly(I:C) stimulation of cells expressing individual mutants, virtually all constructs exhibited comparable levels of luciferase response to that of wild-type nsp1α for IFN-β-Luc (Fig. 2.3B). Similarly, these mutants maintained the suppressive activity for IRF3-Luc (Fig. 2.3B) and PRDII-Luc (Fig. 2.3B). These results indicated that ZF2 of nsp1α did not affect the IRF3-mediated or PRDII-mediated IFN suppression.

**Suppression of IFN induction by ZF1:** Since both ZF2 and PCPα motifs appeared not to participate in IFN suppression, the N-terminal ZF1 motif was examined for its possible role. The ZF1 motif comprised of C8-C10-C25-C28, and single or double mutations were introduced to this motif as illustrated in Fig. 2.3A. C8S, C10S, C25S, or C28S would destabilize the ZF1 configuration whereas C8S/C25S, C8S/C28S, or C10S/C25S would completely dissolve the ZF1 structure. C8H, C10H, and C8H/C10H would maintain the zinc-coordinating ability of the motif as shown previously (Tijms et al., 2007). These mutants were then examined for IFN suppression in HeLa cells after co-transfection of individual mutant plasmids with the IFN-β-Luc reporter. The plasmid pXJ41-GST encoding the GST protein was used as a negative control. After poly(I:C) stimulation, C8H, C10H, and C8H/C10H were found to retain the IFN suppression as anticipated, whereas all other double mutants lost their suppressive activities for IFN induction (Fig. 2.3C). C28S was of noteworthy since it was the only single mutant that lost the suppressive

activity. Our results indicate that ZF1 of nsp1α was the important element for modulating IFN-β promoter activation. To study signaling released from constraints, the 4xIRF3-Luc and pRD II-Luc reporter activities were also examined for these mutants after poly(I:C) stimulation and TNF-α stimulation, respectively. The ZF1 mutants whose IFN suppressive activity was subverted did not suppress IRF3-mediated or NF-κB-mediated promoter activities (Fig. 2.3C). Considered together, the data suggests a possibility that both IRF3-dependent and NF-κB-dependent IFN pathways were probably exempted from repression.

**Cellular localization of ZF1 mutants:** Nsp1α is a nuclear-cytoplasmic protein distributed in both the nucleus and cytoplasm (Song et al., 2010). To explore the basis for IFN suppression mediated by nsp1α subunit, the individual ZF1 mutants were expressed in HeLa cells for 24 h, stained with anti-FLAG MAb, and their subcellular distributions were examined. The results of their staining patterns are summarized in Table 2.2, and Fig. 2.4 shows the staining patterns of C8S/C25S, C8H/C10H, and C70S/C76S mutants representing three distinct groups; ZF1-destruction mutants, ZF1-retaining mutants, and ZF2-destruction mutants, respectively. A perinuclear punctate staining was observed for C8S/C25S (Fig. 2.4, panel J), whereas the staining patterns for C8H/C10H (panel G) and C70S/C76S (panel M) were consistent with that of wild-type nsp1α (panel D). The ZF1 mutants whose IFN suppressive activity was lost were unanimously cytoplasmic with a punctate pattern (Table 2.2). In contrast, the ZF1 mutants that maintained suppressive activity showed cellular distribution patterns identical to that of nsp1α. Similarly, the mutants that maintained their suppressive activity were nucleocytoplasmic regardless of mutations at ZF1, ZF2, or PCPα (Table 2.2). These results show that destruction of the ZF1 configuration caused the change of subcellular distribution and the staining pattern of

nsp1α. These observations also demonstrate that type I IFN suppression was attributed to the cellular distribution of nsp1α.

**CBP degradation and ZF1 mutants:** Since CBP was degraded by the nsp1α subunit (Fig. 2.1), and that nsp1α caused the IFN suppression, it was of interest to determine if nsp1α mutants that lost the IFN suppressive activity still caused CBP degradation. For this, HeLa cells were transfected with empty vector pXJ41, pFLAG-nsp1α, or ZF mutant plasmids for 24 h, and their lysates were subjected to Western blot using CBP antibody. The mutants C8S/C25S, C8H/C10H, and C70S/C76S were chosen to represent three distinct mutant groups; ZF1-destruction mutants, ZF1-retaining mutants, and ZF2-destruction mutants as a control, respectively. C76S/H146Y was included as an additional control as a PCPα-destruction mutant. C8H/C10H, C70S/C76S, C76S/H146 mutants caused a notable reduction of CBP (Fig. 2.5A, lanes 5, 6, 7) when compared to that of empty vector-transfected cells (lane 1). In contrast, C28S and C8S/C25S did not cause the notable reduction of CBP (Fig. 2.5A, lanes 3, 4). These results revealed the correlation of ZF1-mediated IFN suppression and CBP degradation. CBP degradation was also visualized by co-staining of cells expressing wild-type nsp1α (Fig. 2.5B, panel F, arrow), C8H/C10H (panel R, arrow), C70S/C76S (panel V, arrow), and C76S/H146Y (panel Z, arrow) by using CBP antibody and anti-FLAG antibody. While CBP degradation was evident in cells expressing C70S/C76S (panel V, arrow) and C76S/H146Y (panel Z, arrow), it was not degraded in C28S-expressing cells (panel J, arrowhead) and C8S/C25S-expressing cells (panel N, arrowhead). CBP degradation by nsp1α and its mutants was quantified by calculating the numbers of cells exhibiting reduced CBP over the given number of cells expressing nsp1α. Approximately 80% of cells expressing C8H/C10H, C70S/C76S, and 86% of cells expressing C76S/H146Y showed

significant levels of CBP degradation, whereas no single cells expressing C28S and C8S/C25S mutants exhibited the CBP reduction (Fig. 2.5C). These observations reveal that CBP degradation was consistent with the IFN suppressive activity of nsp1α ZF1 mutants. Together with the Western blot data, it further confirms that IFN suppression by nsp1α was due to CBP degradation and that CBP degradation was associated with the ZF1 configuration in nsp1α.

**Suppression of ISRE by nsp1α:** The cooperation between signal transducers and activators of transcription (STAT) and CBP is an important process for ISG production in the Janus kinase (JAK)-STAT signal transduction pathway (Wojciak et al., 2009). Since CBP was degraded by nsp1α, it was postulated that the JAK-STAT pathway might also be affected by nsp1α. Thus to examine the level of ISRE activity, ISRE-Luc reporter assays were employed whose activation required the binding of interferon-stimulated gene factor 3 (ISGF3) complex (Schindler and Darnell, 1995). HeLa cells were co-transfected with ISRE-Luc and empty vector pXJ41, nsp1α, or indicated ZF mutant plasmids for 24 h and stimulated with IFN-β. Nsp1β was used as a positive control since its JAK-STAT suppression was previously reported (Patel et al., 2010). Significant levels of ISRE suppression was observed in nsp1β-, nsp1α-, and C70S/C76S-expressing cells whereas no ISRE suppression was observed in C8S/C25S-expressing cells (Fig. 2.6A). The inhibition of the JAK-STAT pathway by nsp1α and its mutant derivatives were correlated with their ability to cause CBP degradation. These results show that nsp1α-mediated JAK-STAT inhibition was likely due to CBP degradation. To further confirm the inhibition of JAK-STAT by nsp1α, promyelocytic leukemia (PML), of whose expression is ISRE promoter-dependent (Chelbi-Alix et al., 1995), was examined. The results of Western blot in Fig. 2.6B showed reduced expression of PML in cells FLAG-nsp1α-expressing cells and C70S/C76S-

expressing cells (upper panel, lanes 4 and 6, asterisks). The expression level of another ISG, ISG15, was examined for further confirmation, and suppressed expression of ISG15 appeared in cells expressing FLAG-nsp1α and C70S/C76S (Fig. 2.6B, middle upper panel, lanes 4 and 6, asterisks). Since PML is a component of the nuclear bodies (NBs) (Dyck et al., 1994), we examined PML by the staining of nsp1α-expressing and its individual mutants-expressing cells (Fig. 2.6C). Compared to cells without nsp1α and its mutants (panels I, M, Q, U), the decrease of PML-NBs was evident in cells expressing nsp1β (panel I, arrow), nsp1α (panel M, arrow), and C70S/C76S (panel U, arrow), whereas no PML-MB reduction was observed in C8S/C25S-expressing cells (panel Q, arrowhead). The reduction of PML by nsp1α and its mutants was quantified by calculating the numbers of cells exhibiting the reduced CBP out of the total given number of cells expressing nsp1α or its mutants (Fig. 2.6D). Approximately 82% of cells expressing nsp1β, 78% of cells expressing nsp1α, and 82% of cells expressing C70S/C76S showed the reduction of PML-NB, while only 4% of cells expressing C8S/C25S exhibited the PML reduction (Fig. 2.6D). Taken together, our results demonstrate that nsp1α subunit induced CBP degradation which leads to the inhibition of ISRE-dependent ISG expressions.

## 2.5. DISCUSSION

To counteract viral infections, host cells are armed with a variety of immune surveillance mechanisms to elicit antiviral defense. Among these mechanisms, type I IFNs exert a wide range of antiviral functions during early infection, including the initiation of antiviral effectors synthesis, mediation of apoptosis, and driving differentiation and maturation of certain leukocytes (Koyama et al., 2008; Samuel, 2001). The survival of infecting viruses in hosts requires a set of counteractions to avoid the host′s antiviral status, and the blocking of type I IFN

production has been identified as an important strategy adopted by many viruses. Activation of IRF3 and NF-κB is necessary for activation of IFN-β promoter. After nuclear translocation of these factors and binding to the IFN-β promoter, enhanceosome is formed to recruit RNA polymerase II (Pol II) via the CBP transcriptional co-activator. Among various evasion strategies utilized by different viruses, modulation of IRF3 is one commonly employed by many viral IFN antagonists. IE62 of varicella-zoster virus (VZV) blocks the phosphorylation of IRF3 (Sen et al., 2010), Npro of classical swine fever virus (CSFV), vpr and vif of human immunodeficiency virus 1, NSP1 of rotavirus, and ORF61 of VZV to name a few can induce IRF3 degradation (Bauhofer et al., 2007; Okumura et al., 2008; Sen et al., 2009; Zhu et al., 2011). NP1 of human bocavirus, ORF36 of murine gamma-herpesvirus 68 (MHV-68), and human respiratory syncytial virus can also bind to the activated IRF3 and interrupt the interaction of IRF3 with CBP (Hwang et al., 2009; Ren et al., 2011; Zhang et al., 2012).

It is intriguing that PRRSV nsp1α subunit is able to degrade CBP in cells. CBP is the KAT3 histone acetyltransferase which is the key factor in the transcription regulatory network, and almost 400 proteins are known to interact with CBP functionally or physically, including the IRF family, STATs, and PIAS1 (Bedford and Brindle, 2012; Goodman and Smolik, 2000; Long et al., 2004; Weaver et al., 1998). CBP and its paralog p300 regulate cellular transcription by acetylating the lysine on histones or other transcriptional regulators, recruiting components of the Pol II machinery, and by functioning as adaptors binding to other cofactors (Bedford et al., 2010). Proteasome-dependent CBP degradation seems to be a unique tactic used by viruses to inhibit IFN-β production and in the current study, the suppression of IFN promoter and ISRE promoter by CBP degradation was verified. CBP degradation may cause negative effects on other CBP-dependent transcriptions, which needs to be studied. A recent study on the ML protein of

Thogoto virus however shows that the function of RNA polymerase II transcription factor IIB (TFIIB) was interfered by the ML protein but host cell gene expression was limitedly influenced by ML-TFIIB interaction, whereas a negative impact was significant on the IRF3-regulated and NF-κB-regulated promoter activities (Vogt et al., 2008). In our study, both IFN production (Fig. 2.1) and IFN signaling pathways (Fig. 2.6) were affected by nsp1α-mediated CBP degradation. Thus it is plausible that PRRSV nsp1α-induced CBP degradation may have some additional effects for other cellular gene transcription.

The CBP degradation by PRRSV nsp1 is proteasome-dependent (Kim et al., 2010), and thus degradation of CBP by the nsp1α subunit is also likely proteasome-dependent. Since proteasome-mediated CBP degradation is a nuclear event and because nsp1α exists in both the cytoplasm and nucleus, it is presumed that the nuclear form of nsp1α is responsible for CBP degradation. Our study showed no direct binding of nsp1 to CBP, suggesting that the nsp1α-induced CBP degradation is likely indirect. CBP is subjected to a range of posttranslational modifications including acetylation, phosphorylation, ubiquitinylation, and SUMOylation, which modulates its function and/or stability (Kuo et al., 2005; Tanaka et al., 2006; Thompson et al., 2004). Activated Ras signaling pathway also leads to CBP degradation via ubiquitinylation (Sanchez-Molina et al., 2006), and SUMOylated CBP can co-localize with PML nuclear bodies where proteasome-mediated CBP degradation can occur (Ryan et al., 2010). Thus, it is possible that nsp1α may modulate the Ras-signaling pathway or mediate CBP SUMOylation to lead to CBP degradation. Alternatively, nsp1α may utilize other mediators or modulate other signaling pathways to complete the degradation process.

According to previous reports, it seems clear that nsp1β-mediated IFN suppression is via either IFR3 or NF-κB pathways (Beura et al., 2010; Chen et al., 2010; Sanchez-Molina et al.,

2006). In our study, no notable CBP degradation was identified in nsp1β-expressing cells even though the majority of nsp1β was localized to the nucleus (Fig. 2.1). Therefore, it is possible that the molecular basis for IFN suppression by nsp1β may differ substantially from that of nsp1α.

Among the functional motifs present in nsp1α, ZF1 appeared to be the important element for regulating IFN induction, while ZF2 and PCPα did not participate in this process. A previous study showed that PCPα played a role in IFN suppression (Shi et al., 2011). In our study however, the protease activity of PCPα did not participate in the type I IFN suppression and the PCPα mutants retained the identical phenotype of IFN modulation to that of wild-type nsp1α (Fig. 2.2). Our result is supported by the previous study on the tertiary structure of nsp1α that a stable cohesion is formed between the C-terminal extension (CTE) and PCPα motif immediately after proteolytic processing and thus further proteolytic reaction is hardly conducted because no substrate is allowed to access the PCPα domain (Sun et al., 2009). A similar PCP-substrate interaction was found for nsp1β when it freed itself from the nascent polypeptide chain by cleavage, thereby suggesting the disruption of PCP activity (Xue et al., 2010).

A second zinc finger motif (ZF2) has been identified in the C-terminal region of nsp1α (Sun et al., 2009), in addition to the first zinc finger motif (ZF1) identified in the N-terminus. ZF2 exhibits a novel feature that C76 and H146, which are the catalytic residues for PCPα, participate to comprise the ZF2 configuration. The newly identified C-terminal zinc finger structure requires two additional residues of C70 and M180 for stable configuration. Although the biological function of ZF2 is unknown, considering the differential suppression of IFN-β between nsp1α and nsp1α-Δ14 which is short by 14 aa at the C-terminus and thus lacking the ZF2 configuration (Song et al., 2010), the ZF2 domain may be associated with a potential regulatory capacity. According to the present study, however, the pattern of cellular distribution

(Fig. 2.4), IFN regulation (Fig. 2.3B), and CBP degradation (Fig. 2.5) of the ZF2 mutants were similar to those of wild-type nsp1α, suggesting that the regulatory capacity of the ZF2 domain may be more complex than a mere zinc finger structure.

ZF1 mutants selectively suppresses sg mRNA synthesis but the basis of suppression is unknown (Tijms et al., 2007). Functions of zinc finger proteins are extremely diverse, ranging from transcription activation and apoptotic regulation to protein folding and assembly (Laity et al., 2001). ZF1 in nsp1α belongs to the 4-C zinc finger superfamily (Sun et al., 2009; Tijms et al., 2007), and many ZF proteins in this family are transcription factors that function by recognition of specific DNA sequences. In the present study, mutations in nsp1α ZF1 failed to induce CBP degradation, indicating its participation in regulating CBP functions. Furthermore, the cellular distribution of nsp1α ZF1 mutants was altered significantly and their staining pattern was changed to the punctate pattern in the perinuclear region (Fig. 2.4). Since CBP degradation did not occur by these mutants, it is possible that the destruction of the ZF1 motif may have caused a conformational change of nsp1α, which in turn may have destroyed the normal biological function of nsp1α. Such studies are in progress to dissect the role of ZF1. Taking the findings all together, we show that ZF1 is a key determinant for IFN suppression mediated by nsp1α.

## 2.6. FIGURES AND TABLES

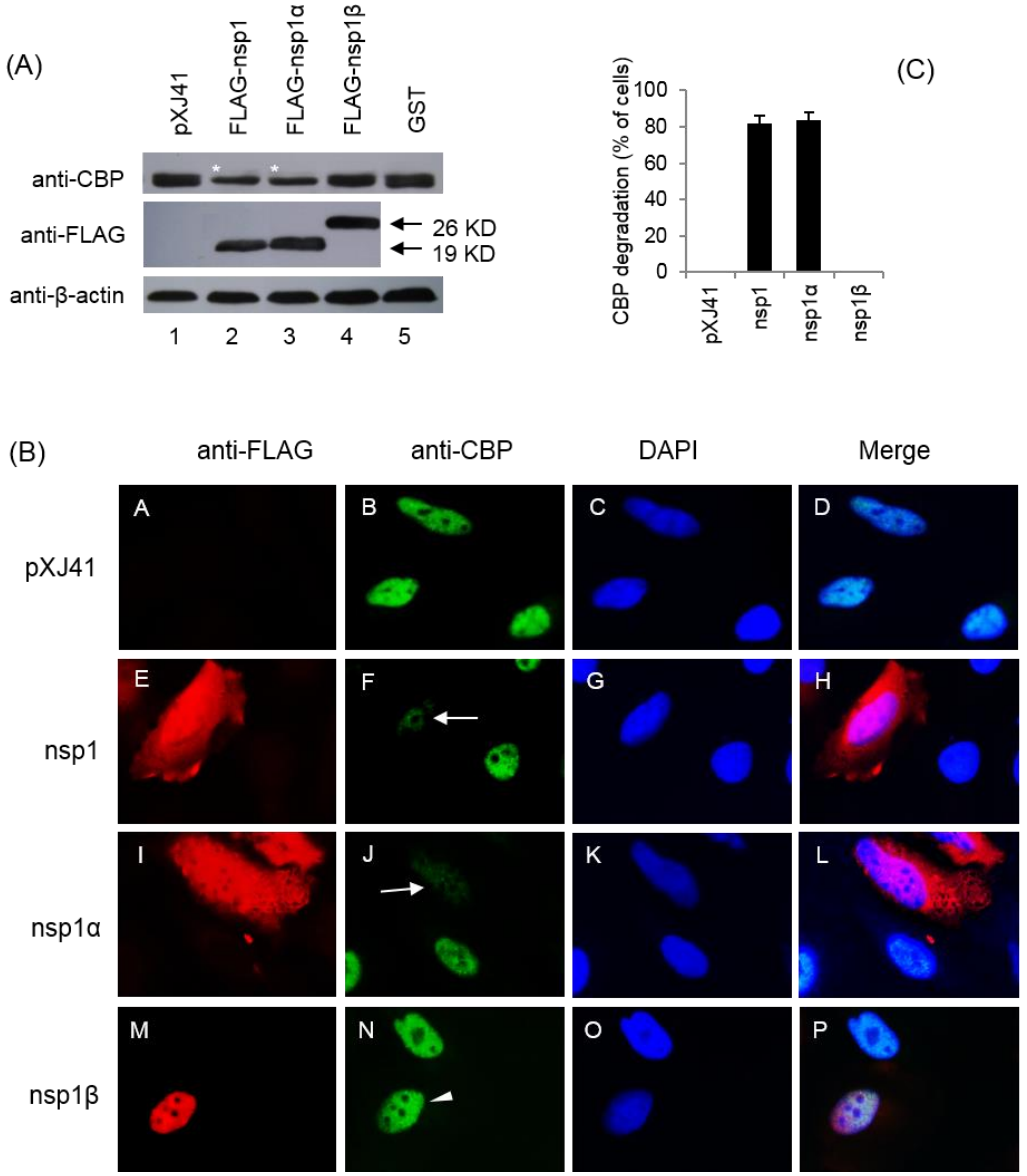


**Fig. 2.1. Degradation of CBP in cells expressing nsp1 and the nsp1α subunit.** (A) HeLa cells were transfected with empty vector pXJ41, pFLAG-nsp1, pFLAG-nsp1α, pFLAG-nsp1β, or pFLAG-GST for 24 h, and cell lysates were subjected to Western blot using anti-FLAG antibody to detect the expression of FLAG-tagged proteins (upper panel) or anti-CBP antibody to measure the endogenous expression of CBP (middle panel). Stars indicate reduced amounts of CBP, and arrows indicate the nsp1α subunit (19 kD) and the nsp1β subunit (26 kD). β-actin (lower panel) is indicated as a loading control. (B) CBP degradation was examined by IFA in cells expressing nsp1, nsp1α, or nsp1β. HeLa cells were grown to 40% confluency and transfected with pXJ41, pFLAG-nsp1, pFLAG-nsp1α, or pFLAG-nsp1β for 24 h. Cells were washed with PBS, fixed with 4% paraformaldehyde, and incubated with rabbit anti-FLAG Ab and mouse anti-CBP Ab, followed by incubation with Alexa Fluor 594-conjugated (red) and 488-conjugated (green) secondary antibodies, respectively, along with DAPI for nucleus staining (blue). Arrows indicate cells where CBP is degraded, and arrowheads indicate cells where CBP is intact. (C) The percentage of cells showing significant reduction of CBP was calculated using the following formula; (Number of cells showing more than 50% reduction of the CBP staining intensity compared to the control CBP staining intensity out of 50 nsp1-positive cells/ (50 cells expressing nsp1, nsp1α, or nsp1β) x 100.

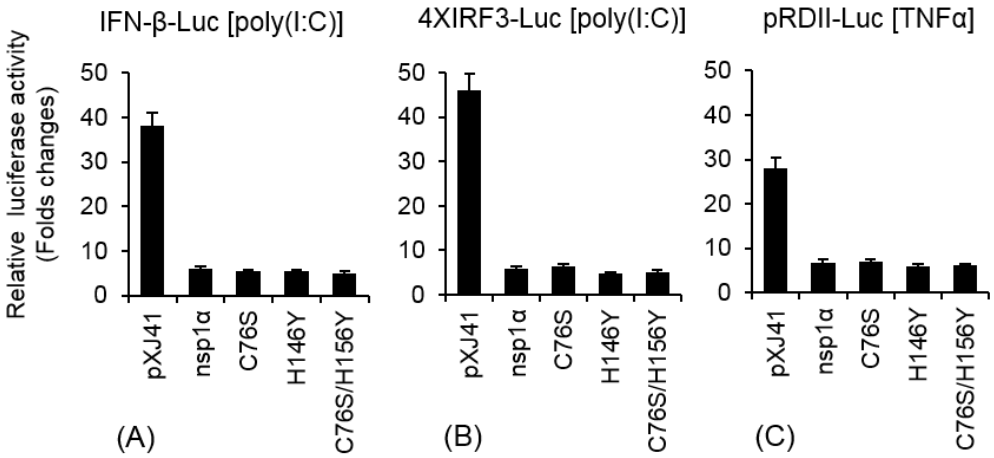


**Fig. 2.2. Suppression of IFN-β induction by PCPα mutants of nsp1α**. HeLa cells were seeded in 12-well plates and co-transfected with 500 ng of pIFN-β-Luc (Fig. 2A), p4×IRF3-Luc (Fig. 2B), or pRD II -Luc (Fig. 2C), and 500 ng of pXJ41, pFLAG-nsp1α, C76S, H146Y, or C76S/H146Y plasmids along with 50 ng of pTK-RL as an internal control. At 24 h post-transfection, cells were either stimulated with 1 μg/ml of poly(I:C) or untreated for 12 h. For pRD II -Luc, cell were stimulated by TNFα incubation. Cells were lysed and the reporter expressions were examined using the Dual Luciferase assay system (Promega). Relative luciferase activities were calculated by normalizing the firefly luciferase to renilla luciferase activities according to the manufacturer′s protocol. The data represent the means of three independent experiments, each experiment in triplicate.

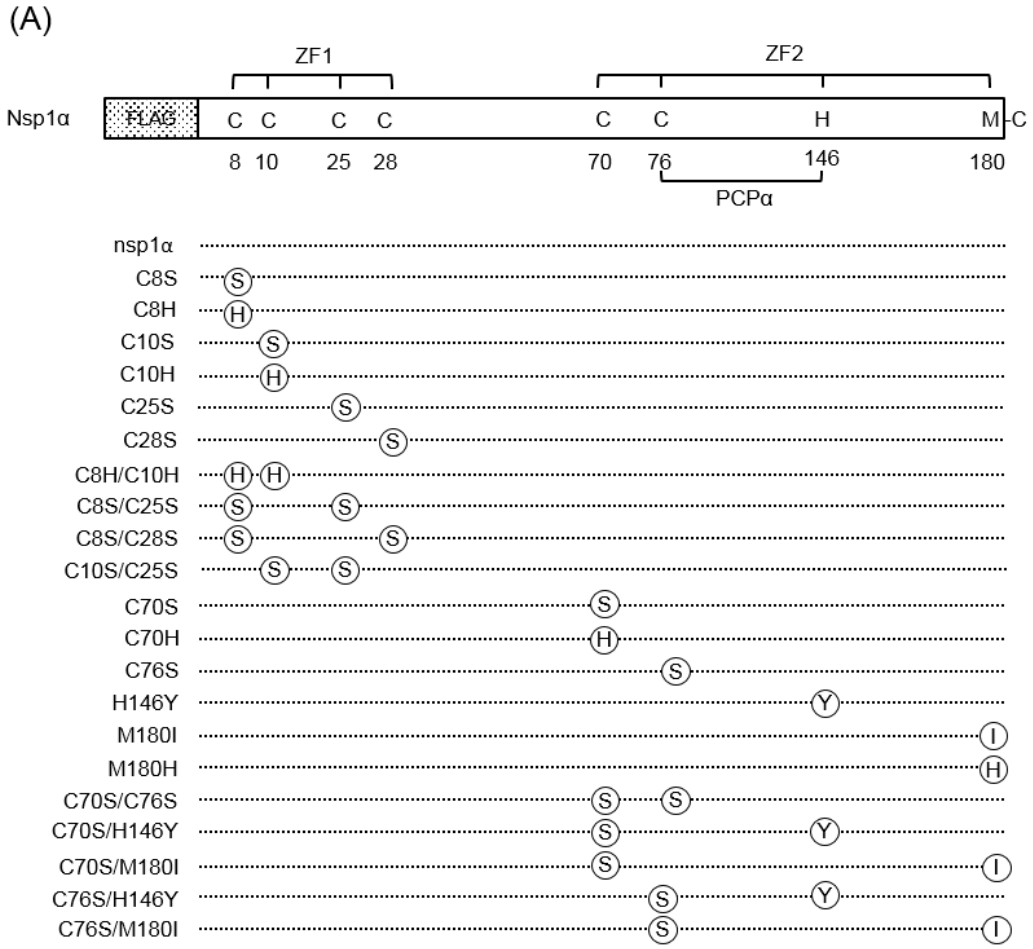


**Fig. 2.3. Identification of the functional domain of nsp1α for IFN modulation.** (A) Structural illustration of domains in nsp1α and introduction of mutations. The full-length protein of nsp1α is 180 amino acids and a FLAG tag is fused at its N-terminus. The catalytic sites of PCPα and the zinc ion coordinating residues for ZF1 and ZF2 are indicated. Single letter alphabets indicate amino acids, and numbers indicate positions. Encircled letter indicates substituted amino acids. (B) Suppression of type I IFN induction by ZF2 mutants of nsp1α. HeLa cells were seeded in 12-well plates and co-transfected with 500 ng of pIFN-β-Luc, p4×IRF3-Luc, or pRD II -Luc, and 500 ng of pXJ41, pXJ41-GST, pFLAG-nsp1α, or indicated mutant plasmid along with 50 ng of pTK-RL as an internal control. At 24 h post-transfection, cells transfected with pIFN-β-Luc or p4×IRF3-Luc were treated with 1 μg/ml of poly(I:C) for 12 h or left untreated, while cells transfected with pRD II -Luc were stimulated with 20 ng/ml of TNFα for 12 h or untreated. Cells were lysed and reporter expressions were examined using the Dual Luciferase assay system (Promega). Relative luciferase activities were calculated by normalizing the firefly luciferase to renilla luciferase according to the manufacturer′s protocol. The data represent the means of three independent experiments, each experiment in triplicate. (C) Modulation of type I IFN induction by ZF1 mutants of nsp1α.

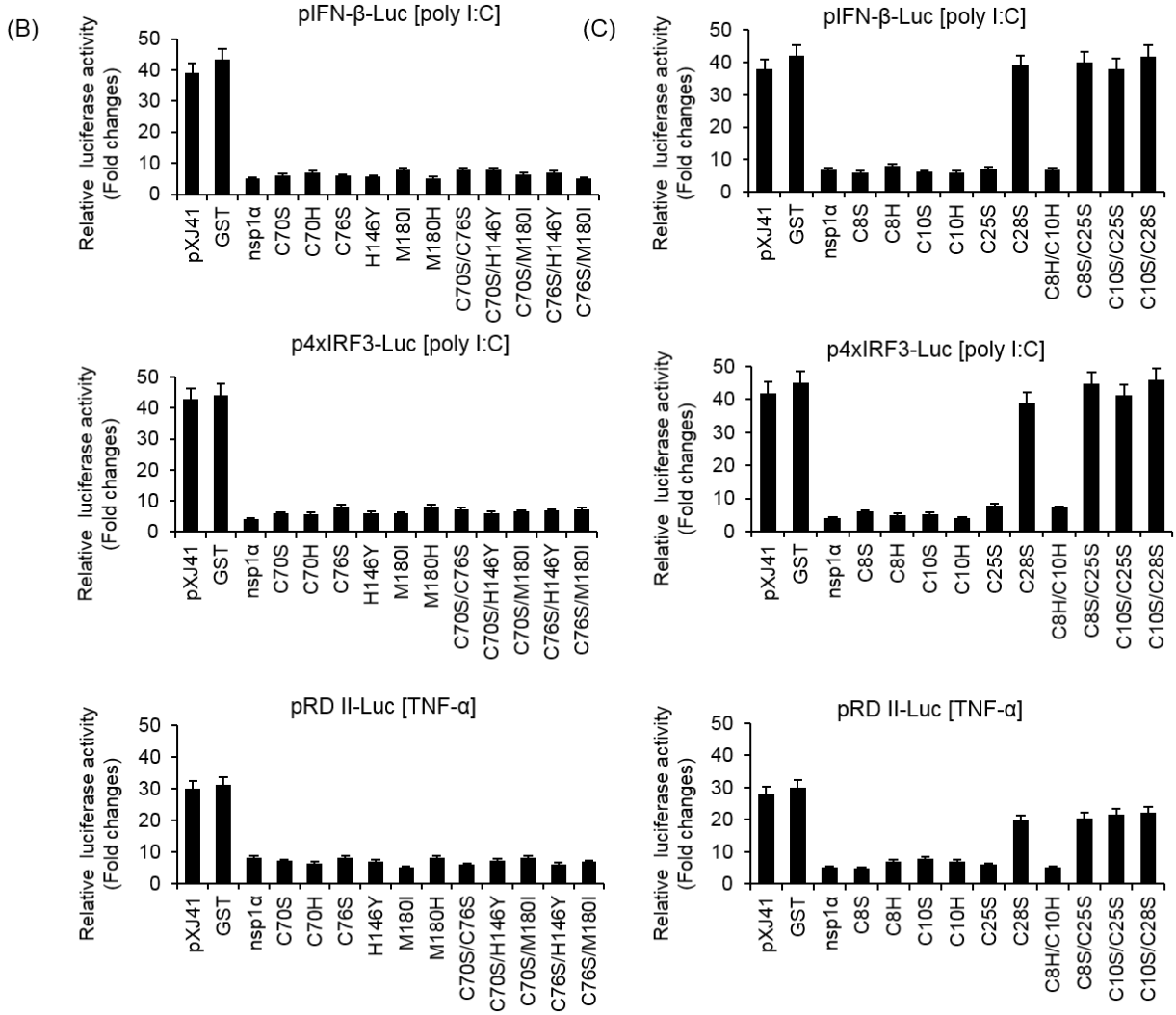
(B)
(C)
pIFN-β-Luc [poly I:C]
p4xIRF3-Luc [poly I:C]
pRD II-Luc [TNF-α]
Relative luciferase activity (Fold changes)
0
10
20
30
40
50
pXJ41
GST
nsp1α
C70S
C70H
C76S
H146Y
M180I
M180H
C70S/C76S
C70S/H146Y
C70S/M180I
C76S/H146Y
C76S/M180I
C8S
C8H
C10S
C10H
C25S
C28S
C8H/C10H
C8S/C25S
C10S/C25S
C10S/C28S

**Fig. 2.3. (conti.)**

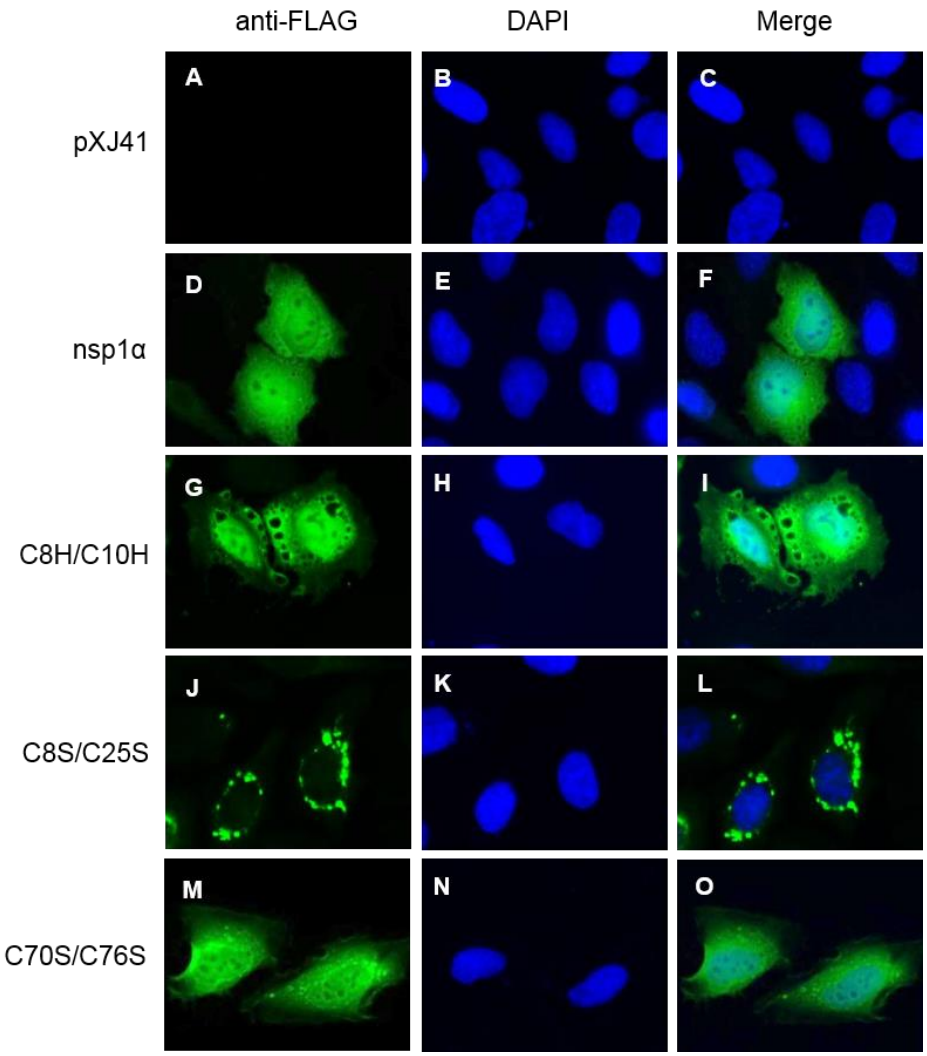


**Fig. 2.4. Subcellular distribution of ZF mutants of nsp1α in HeLa cells.** Cells were grown to 40% confluency and transfected with indicated plasmids for 24 h. Cells were washed with PBS, fixed with 4% paraformaldehyde and stained with mouse anti-FLAG Ab followed by Alexa 488-labeled anti-mouse Ab. Cellular localization of nsp1α and its mutants was examined by fluorescence microscopy. Nuclei were stained using DAPI.

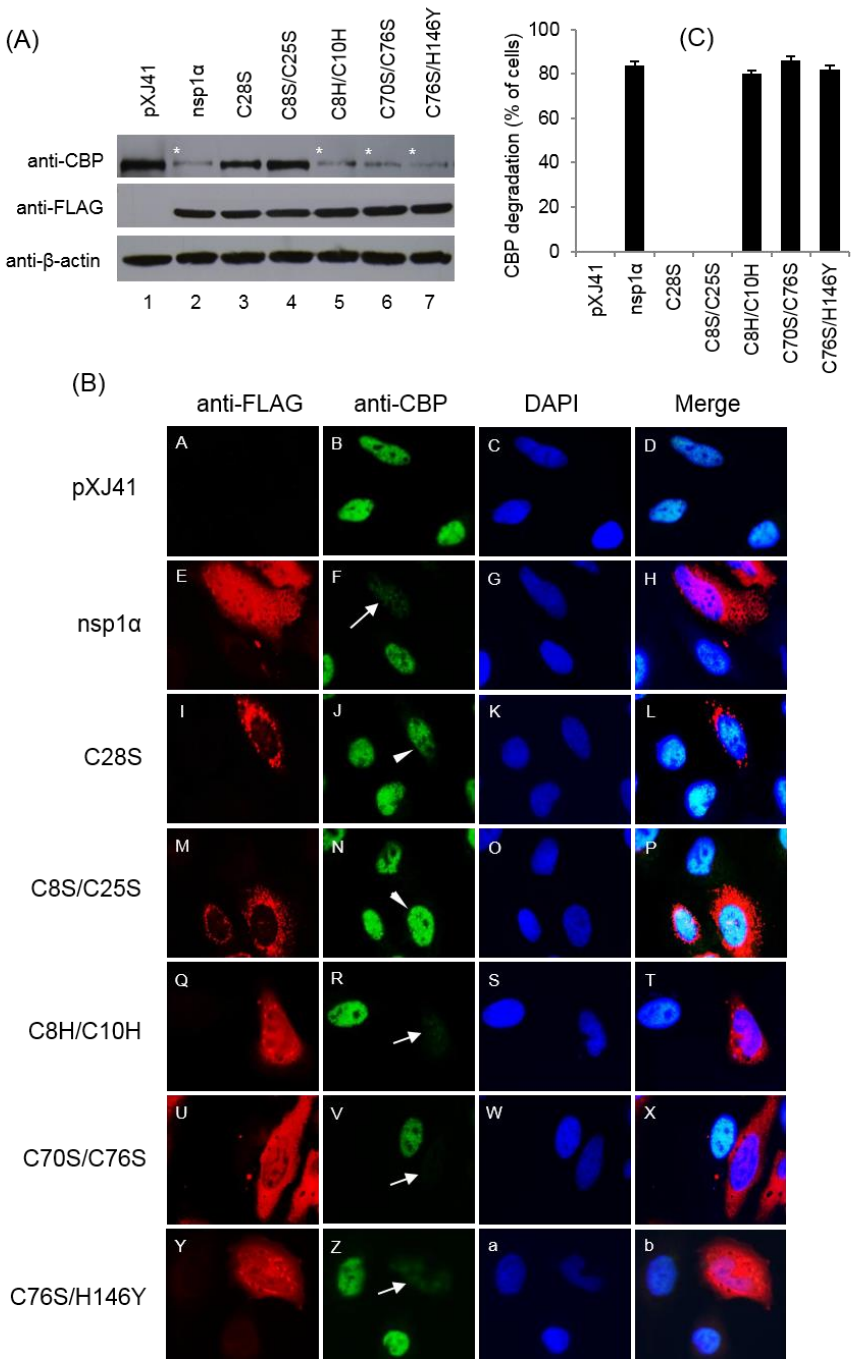


**Fig. 2.5. CBP degradation in the presence of ZF1 mutants of nsp1α.** (A) HeLa cells were transfected with empty vector pXJ41, pFLAG-nsp1α, or ZF1 individual mutants of nsp1α for 24 h, and cell lysates were subjected to Western blot analyses. Stars indicate reduction of CBP. (B) Degradation of CBP in nsp1α- or nsp1α mutant-expressing cells examined by IFA. HeLa cells were grown to 40% confluency and transfected with pXJ41, pFLAG-nsp1α, or indicated plasmids representing mutated ZF1 (C28S, C8S/C25S, and C8H/C10H) and ZF2 (C70S/C76S and C76S/H146Y) for 24 h. Arrows indicate cells where CBP is degraded, and arrowheads indicate cells where CBP is intact. (C) Percentage of cells showing CBP degradation.

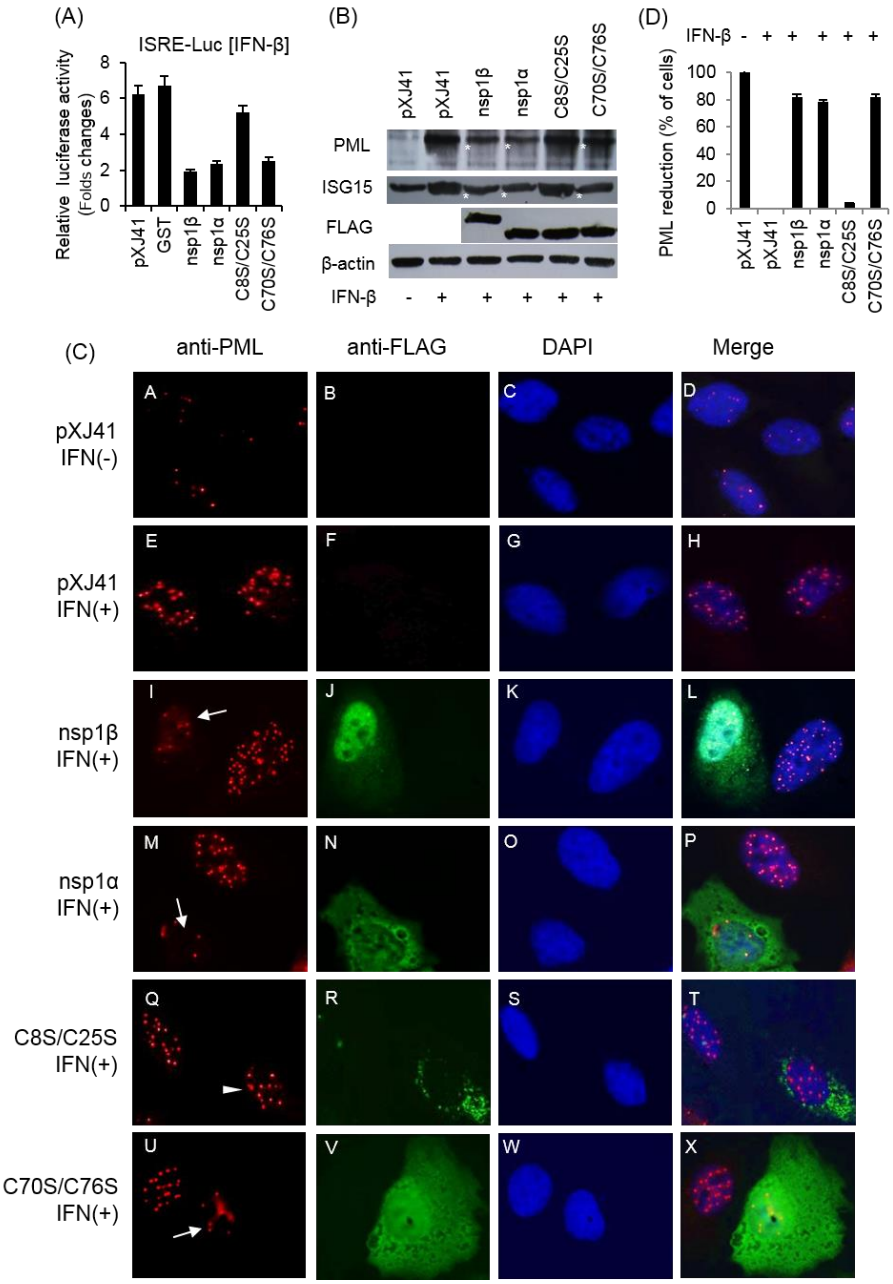


**Fig. 2.6. Suppression of ISRE activity by nsp1α.** (A) HeLa cells were seeded in 12-well plates and co-transfected with 500 ng of pISRE-Luc, 500 ng of pXJ41 empty vector, pFLAG-nsp1β, pFLAG-nsp1α, C8S/C25S, or C70S/C76S plasmids along with pTK-RL. (B) HeLa cells were transfected with empty vector pXJ41, pFLAG-nsp1β, pFLAG-nsp1α, or ZF1 individual mutants of nsp1α for 24 h followed by IFN treatment for 12 h. Cell lysates were subjected to Western blot analyses using anti-PML antibody to detect the expression of PML (top panel) and anti-ISG15 antibody to determine the levels of ISG15 (second panel). β-actin was used as a loading control (bottom panel). Stars indicate reduction of PML and ISG15. (C) Reduced expression of PML in nsp1α-expressing cells.. Arrows indicate the reduction of PML expression, and arrowheads indicate the normal expression of PML. (D) Percentage of cells showing reduced production of PML

## Table 2.1. Oligonucleotides and their sequences

| Oligonucleotides | Primer sequence |
|---|---|
| nsp1α-C8S-Fwd | 5′-CTGGGATACTTGATCGGAGTACGTGCACCCCCAATG-3′ |
| nsp1α-C8S-Rev | 5′-CATTGGGGGTGCACGTACTCCGATCAAGTATCCCAG-3′ |
| nsp1α-C8H-Fwd | 5′-CTGGGATACTTGATCGGCATACGTGCACCCCCAATG-3′ |
| nsp1α-C8H-Rev | 5′-CATTGGGGGTGCACGTATGCCGATCAAGTATCCCAG-3′ |
| nsp1α-C10S-Fwd | 5′-GATACTTGATCGGTGCACGAGTACCCCCAATGCCAGGG-3′ |
| nsp1α-C10S-Rev | 5′-CCCTGGCATTGGGGGTACTCGTGCACCGATCAAGTATC-3′ |
| nsp1α-C10H-Fwd | 5′-GATACTTGATCGGTGCACGCATACCCCCAATGCCAGGG-3′ |
| nsp1α-C10H-Rev | 5′-CCCTGGCATTGGGGGTATGCGTGCACCGATCAAGTATC-3′ |
| nsp1α-C25S-Fwd | 5′-GGAGGGCCAAGTCTACAGTACACGATGTCTCAGTGC-3′ |
| nsp1α-C25S-Rev | 5′-GCACTGAGACATCGTGTACTGTAGACTTGGCCCTCC-3′ |
| nsp1α-C28S-Fwd | 5′-AAGTCTACTGCACACGAAGCCTCAGTGCACGGTCTC-3′ |
| nsp1α-C28S-Rev | 5′-GAGACCGTGCACTGAGGCTTCGTGTGCAGTAGACTT-3′ |
| nsp1α-C70S-Fwd | 5′-ATTCCCCACTGTTGAGAGTTCCCCCGCCGGGGCCT-3′ |
| nsp1α-C70S-Rev | 5′-AGGCCCCGGCGGGGGAACTCTCAACAGTGGGGAAT-3′ |
| nsp1α-C70H-Fwd | 5′-ATTCCCCACTGTTGAGCATTCCCCCGCCGGGGCCT-3′ |
| nsp1α-C70H-Rev | 5′-AGGCCCCGGCGGGGGAATGCTCAACAGTGGGGAAT-3′ |
| nsp1α-C76S-Fwd | 5′-TCCCCCGCCGGGGCCAGTTGGCTTTCTGCGATCTT-3′ |
| nsp1α-C76S-Rev | 5′-AAGATCGCAGAAAGCCAACTGGCCCCGGCGGGGGA-3′ |
| nsp1α-H146Y-Fwd | 5′-TTTTGCCAACTCCCTATACGTGAGTGATAAACCTT-3′ |
| nsp1α-H146Y-Rev | 5′-AAGGTTTATCACTCACGTATAGGGAGTTGGCAAAA-3′ |
| nsp1α-M180I-Fwd | 5′-CCCTTTTGAGTGTGCTATAGCTGACGTCTATGATA-3′ |
| nsp1α-M180I-Rev | 5′-TATCATAGACGTCAGCTATAGCACACTCAAAAGGG-3′ |
| nsp1α-M180H-Fwd | 5′-CCCTTTTGAGTGTGCTCATGCTGACGTCTATGATA-3′ |
| nsp1α-M180H-Rev | 5′-TATCATAGACGTCAGCATGAGCACACTCAAAAGGG-3′ |

## Table 2.2. Summary of various phenotypes of nsp1α and its mutants

| | nsp1α mutant | Suppression | | | Cellular distribution | CBP degradation |
|---|---|---|---|---|---|---|
| | | IFN | IRF3 | PRD II | | |
| Wt | nsp1α | + | + | + | Cyto/Nuc | + |
| ZF1 | C8S | + | + | + | Cyto/Nuc | + |
| | C8H | + | + | + | Cyto/Nuc | + |
| | C10S | + | + | + | Cyto/Nuc | + |
| | C10H | + | + | + | Cyto/Nuc | + |
| | C25S | + | + | + | Cyto/Nuc | + |
| | C28S | - | - | - | Cyto | - |
| | C8H/C10H | + | + | + | Cyto/Nuc | + |
| | C8S/C25S | - | - | - | Cyto | - |
| | C8S/C28S | - | - | - | Cyto | - |
| | C10S/C25S | - | - | - | Cyto | - |
| ZF2 | C70S | + | + | + | Cyto/Nuc | + |
| | C70H | + | + | + | Cyto/Nuc | + |
| | M180I | + | + | + | Cyto/Nuc | + |
| | M180H | + | + | + | Cyto/Nuc | + |
| | C70S/C76S | + | + | + | Cyto/Nuc | + |
| | C70S/H146Y | + | + | + | Cyto/Nuc | + |
| | C70S/M180I | + | + | + | Cyto/Nuc | + |
| PCPα | C76S | + | + | + | Cyto/Nuc | + |
| | H146Y | + | + | + | Cyto/Nuc | + |
| | C76S/H146Y | + | + | + | Cyto/Nuc | + |

The symbol "+" denotes the presence of indicated phenomena and "-" denotes the absence of indicated phenomena. Cyto and Nuc are abbreviations of cytoplasm and nucleus, respectively. Cyto/Nuc indicates the both cytoplasm and nucleus.

# CHAPTER 3: BIOGENESIS OF NON-STRUCTURAL PROTEIN 1 (NSP1) AND NSP1-MEDIATED TYPE I INTERFERON MODULATION IN ARTERIVIRUSES

## 3.1. ABSTRACT

Type I interferons (IFNs-α/β) play a key role for the antiviral state of host, and the porcine arterivirus, porcine reproductive and respiratory syndrome virus (PRRSV), has been shown to down-regulate the production of IFNs during infection. Non-structural protein (nsp) 1 of PRRSV has been identified as a viral IFN antagonist, and the nsp1α subunit of nsp1 has been shown to degrade the CREB-binding protein (CBP) and to inhibit the formation of enhanceosome thus resulting in the suppression of IFN production. The study was expanded to other member viruses in the family Arteriviridae: equine arteritis virus (EAV), murine lactate dehydrogenase-elevating virus (LDV), and simian hemorrhagic fever virus (SHFV). While PRRSV-nsp1 and LDV-nsp1 were auto-cleaved to produce the nsp1α and nsp1β subunits, EAV-nsp1 remained uncleaved. SHFV-nsp1 was initially predicted to be cleaved to generate three subunits (nsp1α, nsp1β, and nsp1γ), but only two subunits were generated as SHFV-nsp1αβ and SHFV-nsp1γ. The papain-like cysteine protease (PLP) 1α motif in nsp1α remained inactive for SHFV, and only the PLP1β motif of nsp1β was functional to generate SHFV-nsp1γ subunit. All subunits of arterivirus nsp1 were localized in the both nucleus and cytoplasm, but PRRSV-nsp1β, LDV-nsp1β, EAV-nsp1, and SHFV-nsp1γ were predominantly found in the nucleus. All subunits of arterivirus nsp1 contained the IFN suppressive activity and inhibited both interferon regulatory factor 3 (IRF3) and NF-κB mediated IFN promoter activities. Similar to PRRSV-nsp1α, CBP degradation was evident in cells expressing LDV-nsp1α and SHFV-nsp1γ, but no

This chapter previously appeared as article in Virus Research. The original citation is as follows: Han, M., Kim, C. Y., Rowland, R., Fang, Y., Kim, D., Yoo, D. 2014. Biogenesis of non-structural protein 1 (nsp1) and nsp1-mediated type I interferon modulation in arteriviruses. Virology 458-459:136-150.

such degradation was observed for EAV-nsp1. Regardless of CBP degradation, all subunits of arterivirus nsp1 suppressed IFN-sensitive response element (ISRE)-promoter activities. Our data show that the nsp1-mediated IFN modulation is a common strategy for all arteriviruses but their mechanism of action may differ from each other.

## 3.2. INTRODUCTION

The family *Arterividae* in the order *Nidovirales* consists of a group of enveloped, single-stranded, positive-sense RNA viruses including porcine reproductive and respiratory syndrome virus (PRRSV), lactate dehydrogenase-elevating virus (LDV) of mice, equine arteritis virus (EAV), and simian hemorrhagic fever virus (SHFV). The arterivirus genome varies between 12.7-15.7 kb in length but their genome organization is relatively consistent with some minor variations (Snijder et al., 2013). At least 10 functional open reading frames (ORFs) have been identified in the PRRSV genome: ORF1a, ORF1b, ORF2a, ORF2b, and ORFs 3 through 7, plus recently identified ORF5a within ORF5 (Firth et al., 2011; Johnson et al., 2011; Meulenberg et al., 1993; Snijder et al., 1999; Wootton et al., 2000). For SHFV, four additional ORFs (2a, 2b, 3, and 4) immediately downstream of the replicase gene are duplicated (Godeny et al., 1998), and the gene duplication was confirmed in four newly identified SHFV isolates (Lauck et al., 2011; Lauck et al., 2013). In addition, a -2 ribosomal frame-shifting has been reported for expression of transframe (TF) ORF in the nsp2-coding region, and TF ORF is conserved in PRRSV, LDV and SHFV (Fang et al., 2012). The structural proteins encoded by ORFs 2a through 7 are expressed from the 3′-co-terminal nested set of subgenomic (sg) mRNAs (Firth et al., 2011; Godeny et al., 1998; Johnson et al., 2011; Meulenberg et al., 1993; Snijder et al., 1999). Mediated by the -1 frame-shifting in the ORF1a/ORF1b overlapping region, two polyproteins pp1a and pp1ab are

synthesized (den Boon et al, 1991), and these polyproteins are proteolytically processed by two papain-like cysteine proteinases (PLPs) 1α and 1β in nsp1, a papain-like proteinase (PLP2) in nsp2, and a serine protease (SP) in nsp4. Thus, the proteolytic processing of pp1a and pp1ab generates 13 nsps for EAV and 14 nsps for PRRSV and LDV (reviewed by Fang and Snijder, 2010; Snijder et al., 2013).

Arterivirus nsp1 is a multifunctional regulatory protein. For EAV, nsp1 is thought to regulate the accumulation of the viral genomic RNA and subgenomic (sg) mRNAs in a manner by determining the levels at which their negative-stranded templates are produced (Nedialkovaet al., 2010). An N-terminal zinc finger (ZF) domain was indispensable for this function but other domains are also important (Tijms et al., 2001). Arterivirus nsp1 harbors several important motifs: two motifs of PLP1α and PLP1β, two zinc finger motifs of ZF1 and ZF2, and a nuclease domain (Xue et al., 2010; reviewed in Fang and Snijder, 2010; Snijder et al., 2013). The PLP1α and PLP1β motifs are relatively well conserved among arteriviruses with some variations. Both motifs are found in nsp1 of PRRSV, LDV and EAV, but PLP1α is inactive in EAV (den Boon et al., 1995; Ziebuhr et al., 2000). The PLP1α activity directs the internal cleavage of nsp1 to produce nsp1α, and the PLP1β activity is thought to release nsp1β from nsp2 of pp1a and pp1ab. In PRRSV, failure of the PLP1α-mediated nsp1 cleavage impairs the synthesis of viral mRNA but does not affect the genome replication. In contrast, no evidence of viral RNA synthesis was detected in PLP1β-impaired PRRSV mutants, indicating that the correct cleavage of nsp1β from nsp2 is essential for PRRSV genome replication (Kroese et al., 2008). Interestingly, the protease activities of PRRSV nsp1α and PRRSV nsp1β become inactive once cleaved due to the stable cohesion between the C-terminal extensions (CTE) and PLP1 motifs according to the X-ray crystallographic studies (Sun et al., 2009; Xue et al., 2010). The functional existence of ZF1 at

the N-terminal region of nsp1 has been confirmed for EAV, and the presence of ZF2 in the C-terminal region of nsp1α has been described for PRRSV (Sun et al., 2009; Tijms et al., 2001). For SHFV, the nsp1 sequence reveals an array of three potential domains for PLP1α, PLP1β, and PLP1γ (Snijder et al., 2013), but these motifs have not experimentally been confirmed for their functions.

Restricted tropism of arteriviruses limits their host range to suids, mice, equids, and non-human primates for PRRSV, LDV, EAV, and SHFV, respectively, and macrophages appear to be the primary target cells for their infections. Arteriviruses establish persistent infection in certain circumstances, and LDV in particular causes a life-long persistence in infected mice (Anderson et al., 1995; Plagemann et al., 1995). Arteriviruses seem to have evolved to escape the host immune surveillance and suppress the antiviral response. The type I interferon (IFN) system is a key component of the innate immunity and represents the first lines of defense against virus infection (Samuel, 2001). Subsequently, antiviral actions from IFN-stimulated gene (ISG) expression contribute to the antiviral state of cells (Sadler and Williams, 2008). For PRRSV however, IFN production is negligible in virus-infected cells and pigs, and the virus seems to suppress the IFN cascade (Albina et al., 1998). The molecular basis for IFN suppression by PRRSV has recently been explored and at least five viral proteins has been identified as an IFN antagonist, which includes four non-structural proteins (nsp1α, nsp1β, nsp2, and nsp11) and a structural protein (nucleocapsid, N) (Reviewed in Sun et al., 2012; Yoo et al., 2010).

Extensive studies have accentuated nsp1α and nsp1β as IFN modulators for PRRSV, and the inhibition of both IFN production and JAK-STAT (Janus Kinase-Signal Transducers and Activators of Transcription) signaling pathways have been shown in virus-infected cells and gene-transfected cells (Yoo et al., 2010; Sun et al., 2012). Both IRF3-mediated and NF-κB-

mediated IFN production pathways are affected by nsp1α and nsp1β (Beura et al., 2010; Chen et al., 2010; Song et al., 2010), and the functional domains have been identified (Beura et al., 2012; Han et al., 2013; Li et al., 2013). It was reported that PRRSV nsp1α reduced the NF-κB activity (Song et al., 2010), and also nsp1α degrades the CREB (cyclic AMP responsive element binding)-binding protein (CBP) in a proteasome-dependent manner, leading to the suppression of IFN production (Han et al., 2013). In contrast, PRRSV nsp1β degrades karyopherin-α1 (KPNA1) and blocks nuclear translocation of interferon-stimulated gene factor 3 (ISGF3) (Patel et al., 2010; Wang et al., 2013). Besides PRRSV, no such study has been conducted for other member viruses in the family Arteriviridae. In the current study, we have investigated the biogenesis of nsp1 of arteriviruses and the role of nsp1 cleavage products for IFN synthesis and suppression. We report that the IFN modulation by nsp1 is a common strategy in arteriviruses for immune modulation. The molecular bases of immune evasion however may differ among arteriviruses.

### 3.3. MATERIALS AND METHODS

**Cells and viruses:** HeLa cells (NIH AIDS Research and Reference Reagent Program, Germantown, MD) and MARC-145 cells (Kim et al., 1993) were grown in minimum essential medium (MEM) and Dulbecco′s modified Eagle′s medium (DMEM; Mediatech Inc., Manassas,VA), respectively, supplemented with 10% heat-inactivated fetal bovine serum (FBS; HyClone, Logan, UT) in a humidified incubator with 5% $CO_2$ at 37 °C. The PA8 strain of the North American genotype PRRSV (Wootton et al., 2000) was used. The full-length genomic sequence of PA8 shares 99.2% identity with the prototype PRRSV VR2332 of the North American genotype (Nelsen et al., 1999). Vesicular stomatitis Indiana virus expressing green fluorescent protein (VSIV-GFP; Dalton and Rose, 2001) was kindly provided by Adolfo García-

Sastre (Mt. Sinai School of Medicine, New York, NY). LDV was provided by Steve Jennings (Charles River Laboratories, Wilmington, MA). This virus was isolated from a mice breeding colony and designated LDV-Urbana. The SHFV nsp1 gene was cloned from the cDNA library provided by Eric Snijder (Leiden University Medical Center, Leiden, Netherlands). The nsp1 sequence from SHFV cDNA shared 99.2% nucleotide and 98.3% amino acid identity with the nsp1 sequence from GenBank (GenBank accession NO.: NC_003092).The EAV nsp1 gene was cloned from the Bucyrus strain of EAV.

**Antibodies and chemicals:** Polyinosinic:polycytidylic [poly (I:C)], DAPI (4′,6-diamidino-2-phenylindol), anti-Flag MAb (F3165), and anti-FLAG PAb (F7425) were purchased from Sigma (St. Louis, MO). Anti-β-actin MAb (sc-47778), anti-CBP MAb (sc-7300), anti-IRF3 PAb (sc-9082), anti- HSP90 MAb (sc-69703), anti-PARP PAb (sc-7150) and anti-PML PAb (sc-5621) were purchased from Santa Cruz Biotechnologies Inc. (Santa Cruz, CA). Anti-ISG15 PAb was purchased from Thermo Scientific Pierce (Rockford, IL). Phospho-IRF-3 (Ser396) mAb was purchased from Cell Signaling (Danvers, MA). The peroxidase-conjugated Affinipure goat anti-mouse IgG and peroxidase-conjugated Affinipure goat anti-rabbit IgG were purchased from Jackson Immuno Research (West Grove, PA). Alexa-Flour 488-conjugated and Alexa-Flour 594-conjugated secondary antibodies were purchased from Invitrogen (Carlsbad, CA).

**Plasmids and DNA cloning:** The plasmids pFLAG-nsp1, pFLAG-nsp1α and pFLAG-nsp1β contain the full-length nsp1, nsp1α, and nsp1β genes of PRRSV, respectively, fused with an N-terminal FLAG tag (Han et al., 2013; Song et al., 2010). The full sequence of LDV nsp1, EAV nsp1, SHFV nsp1 and their subunits including the N- or C-terminal FLAG tag were amplified by

PCR using cDNA clones of LDV, EAV and SHFV and primer sets listed in Table 3.1. The SHFV- nsp1 gene was kindly provided by Eric Snijder (Leiden University Medical Center, Leiden, Netherlands). The PCR fragments were cloned into the pXJ41 mammalian expression vector using the indicated restriction enzymes (Xiao et al., 1991). Mutant genes were generated by PCR-based site-directed mutagenesis using primers listed in Table 3.2. Reporter plasmids, pIFN-β-Luc and p4xIRF3-Luc were kindly provided by Stephan Ludwig (Ehrhardt et al., 2004; Institute of Molecular Medicine, Heinrich Heine Universtät, Düsseldorf, Germany), and used for luciferase assays. The p4xIRF3-Luc construct contains four copies of the IRF3-specific PRDI/III domain of the IFN-β promoter in front of the luciferase reporter gene. The plasmid pPRDII-Luc contains two copies of the NF-κB-specific PRDII binding region of the IFN-β promoter in front of the luciferase gene and was kindly provided by Stanley Perlman (University of Iowa, IA; Zhou and Perlman, 2007). The plasmid pISRE-Luc contains the IFN stimulated response element (ISRE) binding sequence and was purchased from Stratagene (La Jolla, CA). The *Renilla* luciferase plasmid pRL-TK contains the herpes simplex virus thymidine kinase (HSV-*tk*) promoter and was included to serve as an internal control in luciferase reporter assay (Promega).

**DNA transfection and protein expression:** DNA transfection was performed in HeLa or MARC-145 cells using Lipofectamine 2000 according to the manufacturer′s instructions (Invitrogen; Carlsbad, CA). HeLa or MARC-145 cells were seeded in 6-well plates a day prior to transfection and grown to 80% confluency. A transfection mix containing DNA and Lipofectamine 2000 in OPTI-MEM® I (Invitrogen; Carlsbad, CA) was incubated at room temperature (R/T) for 20 min and added to each well. After incubation, the transfection mix was replaced with a fresh medium, and cells were incubated for 24 h to allow gene expression.

**Western blot analysis:** Cells were lysed in lysis buffer (20 mM Tris [pH 7.5], 150 mM NaCl, 1 mM EDTA, 1 mM EGTA, 1% Triton X-100, 1% NP-40) supplemented with a cocktail of protease inhibitors (P-8340 Sigma). Cell lysates were centrifuged and supernatants were resolved by 7.5%, 10%, or 12% SDS-PAGE, followed by transfer to Immobilon-P membrane (Millipore). After blocking with 5% skim milk powder in TBS-T (10 mM Tris–HCl [pH 8.0], 150 mM NaCl, 1% Tween 20), membranes were incubated with primary antibody dissolved in TBS-T containing 5% skim milk powder for 1 h at R/T followed by washing and incubation with horseradish peroxidase-conjugated secondary antibody for 1 h at R/T. After three washes with TBS-T, proteins were visualized using the Enhanced Chemiluminescence system (Pierce, Rockford, IL). Digital signal acquisition and analysis were conducted using GraphPad Prism 5.0 (GraphPad).

**Immunofluorescence analysis (IFA):** Cells were seeded on cover slips and transfected with individual plasmids for 24 h. After washing with phosphate-buffered saline (PBS), cells were fixed with 4% paraformaldehyde for 10 min at R/T in (PBS), and then permeabilized using 0.1% Triton X-100 for 10 min at R/T. After blocking with 1% BSA in PBS for 30 min, cells were incubated with primary antibody in PBS containing 1% BSA for 2 h followed by incubation with Alexa Fluor 488- and/or Alexa Fluor 594-conjugated secondary antibody for 1 h. Nuclear staining was performed with DAPI for 3 min at R/T. After washing with PBS, coverslips were mounted onto microscope slides using Fluoromount-G mounting medium (Southern Biotech, Birmingham, AL), and examined under a fluorescence microscope (Leitz Laborlux 12). To

quantify degradation of CBP and reduction of PML, the formula described previously (Han et al., 2013) were used to calculate the percentage of cells with visible reduction of CBP or PML-NB.

**Luciferase reporter assay:** HeLa cells were grown to a density of $5 \times 10^4$ cells/well in 12-well plates and transfected with various combination of plasmid DNA: 0.5 μg of plasmid encoding the subunit protein of nsp1, 0.5 μg of pIFN-β-Luc, pPRDII-Luc, p4xIRF3-Luc, or pISRE-Luc, and 0.05 μg of pLR-TK were co-transfected using Lipofectamine. At 24 h post-transfection, cells were stimualted with 0.5 μg of poly (I:C) for 16 h and cell lysates were prepared for luciferase assays. For pISRE-Luc, cells were incubated with 1,000 units of human IFN (bioWORLD, Dublin, OH) for 16 h. Luciferase activities were measured using the Dual-Glo Luciferase assay system according to the manufacturer′s instructions (Promega). Values for each sample were normalized using *Renilla* luciferase activities and the results were expressed as relative luciferase activities. All assays were repeated at least three times, and each sample was analyzed in triplicates.

**VSIV-GFP bioassay:** HeLa cells in 6-well plates were transfected with 2 μg of plasmids expressing individual subunit of arterivirus nsp1. At 24 h post-transfection, cells were stimulated with 1 μg of poly (I:C) by transfection and continued incubation for 12 h. Supernatant was harvested and serially diluted by 2-folds. MARC-145 cells were grown in 96-well plates and incubated for 24 h with 100 μl of each dilution of the supernatant. Cells were then infected with 100 μl of VSIV-GFP of $10^4$ PFU/ml and incubated for 16 h. Cells were fixed with 4% paraformaldehyde, and GFP expression was examined under an inverted fluorescence microscopy (Nikon Eclipse TS100).

## 3.4. RESULTS

**PLP domains in SHFV-nsp1:** Two separate PLP domains, PLP1α and PLP1β, have been identified in nsp1 of PRRSV. These domains consist of catalytic residues C76 and H146, and C270 and H339, respectively. Both PLP1α and PLP1β domains are functional and generate nsp1α and nsp1β, respectively (Sun et al., 2009; Xue et al., 2010). For LDV, PLP domains in nsp1 resemble those of nsp1 of PRRSV, and their activities and cleavages may likely mimic those of PRRSV-nsp1. For EAV, PLP1α is composed of K73 and H122, and the K-H motif instead of the C-H motif in PRRSV has been shown to be inactive. As a result, EAV-nsp1α is not cleaved off from EAV-nsp1β, and thus uncleaved nsp1 is produced by the PLP1β activity (den Boon et al., 1995; Snijder et al., 1992). For SHFV, three potential PLP domains (PLP1α, PLP1β, and PLP1γ) are found according to sequence comparisons and each domain is presumed to be functional to generate nsp1α, nsp1β, and nsp1γ, respectively (Fig. 3.1A). The SHFV-PLP1α domain consists of C115 and H130, and resembles PRRSV-PLP1α and LDV-PLP1α. SHFV-PLP1β however is rather similar to SHFV-PLP1γ, suggesting gene duplication. Both SHFV-PLP1β and SHFV-PLP1γ are aligned well with PRRSV-PLP1β, LDV-PLP1β, and EAV-PLP1β (Fig. 3.1B).

To examine the cleavage products of nsp1 for each arterivirus, nsp1 genes were individually cloned and expressed in cells (Fig. 3.1D). A FLAG-tag was added to the N-terminus of each construct and thus only N-terminal cleavage product would be detected when using anti-FLAG antibody. LDV-nsp1α was identified as a 22 kD protein (lane 2), and the molecular size was slightly larger than 21 kD of PRRSV-nsp1α (lane 1), reflecting the predicted molecular weights of 21.1 kD and 20.8 kD for LDV-nsp1α and PRRSV-nsp1α, respectively. EAV-nsp1 was detected as a 30 kD protein (lane 3). In cells expressing SHFV-nsp1, a 39 kD protein was

observed (Fig. 3.1D, lane 4), which was much larger than the predicted size of 21 kD for SHFV-nsp1α and was rather similar to the sum of nsp1α and nsp1β. This result suggests that the SHFV-PLP1α domain may be non-functional and instead SHFV-PLP1β cleaves off SHFV-nsp1β to generate a single protein of nsp1α and nsp1β.

To confirm the proteolytic activity of each PLP of SHFV-nsp1, different sets of nsp1 constructs were made using a FLAG tag at the N-terminus of each construct (Fig. 3.2A, left panel). Then, either single or double amino acid mutations were introduced to the catalytic sites to subvert the function of respective PLP. PRRSV-nsp1 and PRRSV-nsp1α were included as a cleavage control. To determine the enzymatic activity of SHFV-PLP1α, individual constructs were transfected to cells for 24 h and their cleavage patterns were examined using anti-FLAG antibody. To exclude a possible influence by the N-terminal tag on the PLP1α activity, a C-terminal-tagged construct was made and designated SHFV-nsp1αβ/F. The nsp1αAA/β mutant was made to destroy the PLP1α motif by substituting C115 and H130 to C115A and H130A, respectively. After transfection, cell lysates were prepared and subjected to Western blot using FLAG antibody. SHFV-nsp1α and SHFV-nsp1β were expressed as 21 kD and 18 kD proteins, respectively (Fig. 3.2A, right panel, lanes 4, 5). Expressions of SHFV-nsp1, SHFV-nsp1αβ, SHFV-nsp1αβ/F, and SHFV-nsp1αAA/β produced a 39 kD protein which was the sum of nsp1α and nsp1β (lanes 6, 7, 8, 9), demonstrating that the cleavage did not occur between nsp1α and nsp1β, and suggesting that SHFV-PLP1α was most likely inactive.

To study the role of PLP1β, SHFV-nsp1β/γ and three additional PLP1β mutants (nsp1βAH/γ, nsp1βCA/γ, and nsp1βAA/γ) were constructed (Fig. 3.2B, left panel). When they were expressed in cells, an 18 kD protein was identified in SHFV-nsp1β/γ expressing cells (Fig. 3.2B, right panel, lane 6), and it resembled the predicted size of SHFV-nsp1β (Fig. 3.2B, right

panel, lane 4), indicating that PLP1β was enzymatically functional to release SHFV-nsp1β from SHFV-nsp1. In contrast, a 33 kD protein was identified in PLP1β mutants expressing cells, and this size was consistent with the predicted size of the sum of nsp1β and nsp1γ (Fig. 3.2B, right panel, lanes 7-9). This finding shows that the PLP1β activity was responsible for the generation of SHFV-nsp1β. Taken altogether, our data showed that SHFV-PLP1α was non-functional and thus SHFV-nsp1 was cleaved by PLP1β in between nsp1αβ and nsp1γ, and so only two cleavage products were generated from SHFV-nsp1. We designated the N-terminal cleavage product of nsp1 as SHFV-nsp1αβ for the following studies.

To study the role of SHFV-PLP1γ for the nsp1↓nsp2 cleavage, the nsp1γ gene was fused with the 5′ partial sequence of nsp2, which was then named SHFV-nsp1γ/2P. Three mutants of PLP1γ (nsp1γAH/2P, nsp1γCA/2P, and nsp1γAA/2P) were constructed to destroy the potential PLP1γ activity by replacing catalytic amino acids (Fig. 3.2C, left panel). A 15 kD band was identified in SHFV-nsp1γ expressing and SHFV-nsp1γ/2P expressing cells (Fig. 3.2C, right panel, lanes 4, 5). In contrast, in PLP1γ mutants expressing cells, a 23 kD protein was identified (Fig. 3.2C, right panel, lanes 6-8). This size was the sum of nsp1γ and the 5′ terminal partial sequence of nsp2. These results indicate that the SHFV-PLP1γ domain was functional and cleaved the sequence between nsp1↓nsp2 for the generation of nsp1γ.

**PLP-specific cleavages of SHFV-nsp1:** Since PLP1α was functional for PRRSV and LDV but non-functional for EAV and SHFV, sequence specificity of the nsp1α-nspβ cleavage sites were examined for PRRSV and LDV (Fig. 3.1C, upper panel). CPFxxAxAT(N)V was identified as a consensus sequence, in which x for any amino acids. Since the PRRSV-PLP1α-mediated nsp1 cleavage occurs at M180↓A181, the cleavage site for LDV-PLP1α was predicted to R181↓A182

which is an immediate upstream of the second ′A′ (Sun et al., 2009). Previously, the nsp1↓nsp2 cleavage sites were determined to G260↓G261 for EAV and G383↓A384 for PRRSV (Snijder et al., 1992; Xue et al., 2010). Both the SHFV-PLP1β and SHFV-PLP1γ sequences were aligned well with the PLP1β sequence of PRRSV, LDV, and EAV (Fig. 3.1B), and thus based on the sequence similarities, the cleavages sites by SHFV-PLP1β and SHFV-PLP1γ were relatively easily predictable. A consensus sequence of H(R/K)K(T)Y(W)Y(F)G was identified at the C-terminal region of PRRSV-nsp1β, LDV-nsp1β, and SHFV-nsp1αβ (Fig. 3.1C, lower panel), and because the PRRSV-PLP1β cleavage occurs immediately after G384, the LDV-PLP1β and SHFV-PLP1β cleavage sites were predicted to G381↓Y382 and G350↓G351, respectively. For SHFV-PLP1γ, the C-terminal four amino acid residues of SHFV-nsp1γ were highly conserved with the arterivirus consensus sequence, and thus the cleavage site by PLP1γ was predicted to G480↓R481 (Fig. 3.1C). To confirm the cleavage by SHFV-PLP1β and SHFV-PLP1γ, mutations were introduced to substitute G350, G351, Y479, G480, and R481 to either serine (S) or valine (V) (Fig. 3.3A and 3.3B, left panels). Y479 served as a functionally silent control. Cleavage of the mutant constructs was then analyzed by expressing each construct in cells followed by Western blot using anti-FLAG antibody. Compared to PLP1β cleavage of nsp1β/γ (Fig. 3.3A, right panel, lane 3), mutants nsp1βAA/γ, G350S, G350V, and G351V (Fig. 3.3A, right panel, lanes, 4-7) were less effective for cleaving nsp1 whereas G351S as a silent control efficiently released nsp1γ as anticipated (Fig. 3.3B, right panel, lane 8). These findings support the cleavage of G350↓G351 by PLP1β. To further determine the PLP1γ cleavage, the mutants Y479S, Y479V, G480S, G480V, R481S, and R481V were made and examined. No cleavage was found for Y479S, G480S, and G480V (Fig. 3.3B, right lane 5, 7 and 8), and the size of the uncleaved protein was identical to the size of nsp1γAA/2P (Fig. 3.3B, right panel, lane 4). Full cleavage of

SHFV-nsp1γ/2P was observed for Y479V (Fig. 3.3B, right panel, lane 6) suggesting Y to V substitution at aa 479 did not block the cleavage by PLP1γ. The SHFV-nsp1γ subunit was normally produced by any substitution of R481, R481S, and R481V (Fig. 3.3B, right panel, lanes 9 and 10), supporting the cleavage site by PLP1γ as Y479↓G480.

**Cellular localization of arterivirus nsp1 individual subunits:** PRRSV-nsp1α is a nuclear-cytoplasmic protein distributed in the both nucleus and cytoplasm, whereas PRRSV-nsp1β and EAV-nsp1 are predominantly found in the nuclear and perinuclear regions (Li et al., 2012; Chen et al., 2010; Song et al., 2010; Tijms et al., 2002). Thus, it was of interest to determine the cellular distribution of each subunit of LDV-nsp1 and SHFV-nsp1. Plasmids coding for individual subunits of nsp1 were transfected into MARC-145 or HeLa cells for 24 h, and the subcellular distribution of each nsp subunit was determined by staining with anti-FLAG antibody (Table 3.3). LDV-nsp1α was localized in the both nucleus and cytoplasm (Fig. 3.4A, panel G), and its distribution patterns were similar to those of PRRSV-nsp1α (Fig. 3.4A, panel A). A predominant nuclear distribution was observed for LDV-nsp1β, SHFV-nsp1αβ, and SHFV-nsp1γ (Fig. 3.4A, panels M, P, S). For SHFV-nsp1αβ in particular, three staining patterns were observed: perinuclear staining (Fig. 3.4B, A-type), nuclear aggregation (Fig. 3.4B, B-type), and predominantly nuclear staining (Fig. 3.4B, C-type). In HeLa cells, 74% of cells showed A-type staining and 10% of cells appeared to be of C-type (Fig. 3.4C, upper panel, black bars). In MARC-145 cells, the A-type staining pattern decreased to 54% while B-type staining increased to 38% and C-type to be 8% (Fig. 3.4C, upper). For SHFV-nsp1γ, a majority of cells (74%) showed A-type staining in HeLa cells (Fig. 3.4C, lower), whereas in MARC-145 cells, three patterns were relatively evenly distributed by 30% each, suggesting a possible variation of their roles depending on cell types.

**Suppression of IFN production by nsp1 subunits of arteriviruses:** Both PRRSV-nsp1α and PRRSV-nsp1β have been reported to participate in the suppression of IFN production, and thus it was of interest to determine whether nsp1 of other arteriviruses plays a similar role to antagonize the IFN activity. To examine this possibility, a luciferase reporter assay was employed. Plasmids coding for individual subunits of different arterivirus nsp1 were individually co-transfected with the reporter plasmids, followed by poly(I:C) stimulation for IFN induction. Virtually all subunits exhibited comparable levels of IFN responses to those of PRRSV-nsp1α and PRRSV-nsp1β (Fig. 3.5A, left panel). Similar to IFNβ-Luc, every subunit of arterivirus nsp1 showed the suppression of IRF3-Luc activity (Fig. 3.5A, middle panel) and NF-κB-Luc activity (Fig. 3.5A, right panel). To further confirm the suppression of IFN by nsp1, an IFN bioassay was conducted using vesicular stomatitis Indiana virus expressing GFP (VSIV-GFP). HeLa cells were transfected with a plasmid expressing each of the nsp1 subunit gene, and then stimulated with poly(I:C). The supernatants were collected, serially-diluted, and incubated with MARC-145 cells. After incubation, cells were infected with VSIV-GFP. The presence of IFN in the supernatant will inhibit the replication of VSIV-GFP, resulting in the absence of GFP expression. If IFN suppression occurs by arterivirus nsp1, a reduced amount of IFN secreted in the supernatants will allow the replication of VSIV-GFP and so the GFP expression will be visible. In the present study, two folds-dilution of supernatant exhibiting the minimum 50% GFP expression was calculated as the end point for IFN-directed inhibition of VSIV replication. Control cells transfected with the empty vector pXJ4 and GST, and then stimulated with poly(I:C) resulted in efficient production of IFN in the supernatant, and the VSIV-GFP replication was limited as anticipated. For these control, the end points for GFP expression were determined as 1:16 (Fig.

3.5B, second and third panels from top). Cells transfected with pXJ41 without stimulation resulted in the absence of IFN production, and thus VSIV-GFP did replicate normally and the end point was determined as 1 (Fig. 3.5B, top panels). Cells incubated with the supernatant from nsp1 subunit-expressing cells showed a very little inhibition of VSIV-GFP and the end point was determined to be 1:2 for each of the subunits. The inhibition level was 8-folds lower than that of the control (1:16), indicating that each of nsp1 subunits strongly suppressed the IFN production in transfected cells (Fig. 3.5B). These observations were consistent with the luciferase assay data and demonstrate the IFN suppression by arterivirus nsp1 subunits.

**Phosphorylation and nuclear translocation of IRF3 in the presence of nsp1 subunits:** When stimulated for IFN induction, IRF3 is phosphorylated by IKKε and/or TBK1 kinases, and the phosphorylated IRF3 results in dimerization and conformational switch, exposing the nuclear localization signal (NLS) for subsequent translocation to the nucleus (Baccala et al., 2007). Some viral IFN antagonists degrade IRF3, inhibit IRF3 phosphorylation, or block IRF3 nuclear translocation (Ren et al., 2011; Sen et al., 2010; Zhu et al., 2011). Since our results showed the IRF3-mediated IFN suppression by nsp1 subunits, and because for PRRSV, nsp1α- and nsp1β-mediated IFN suppressions were IRF3-independent (Chen et al., 2010; Kim et al., 2010), it was of interest to examine whether IRF3 function was altered by nsp1 of other arteriviruses. The amounts of total IRF3 (Fig. 3.6A, middle panel) and phosphorylated IRF3 (pIRF3, Fig. 3.6A, upper panel) were examined after expression of individual subunits of nsp1. No significant changes were observed for levels of IRF3 and pIRF3 in comparison to those of control, suggesting that IRF3 inhibition occurred at steps after phosphorylation. We thus explored the nuclear localization of IRF3 by cell fractionation (Fig. 3.6B) and fluorescence staining (Fig.

3.6C). After poly(I:C) stimulation, IRF3 was partly accumulated in the nuclear fraction, and this was not affected by expression of nsp1 subunits (Fig. 3.6B, right upper panel). HSP90 and PARP as the cytosolic and nuclear proteins markers, respectively, remained in their respective compartments (Fig. 3.6B, middle upper panel, lanes 1-9; middle lower panel, lanes 10-18), indicating that the results were not due to the cross-contamination during fractionation. To confirm the cell fractionation result, immunofluorescence of endogenous IRF3 was conducted after poly(I:C) stimulation. Without stimulation, IRF3 was distributed normally in the cytoplasm with some nuclear diffusion (Fig. 3.6C, panel A), but when stimulated, it was translocated to the nucleus (Fig. 3.6C, panel D). In cells expressing the nsp1 subunits (Fig. 3.6C, middle column, white arrows), IRF3 was found to normally translocate to the nucleus after stimulation (Fig. 3.6C, left column, white arrows). These results suggest that the nsp1-mediated IFN suppression occurs at the downstream of IRF3 nuclear localization.

**CBP degradation and nsp1 subunits:** In our studies, all subunits of arterivirus nsp1 appear to suppress the IFN production. Since CBP is degraded by PRRSV-nsp1α in the nucleus (Han et al., 2013), we examined whether CBP degradation was a common mechanism in arteriviruses. For this, HeLa cells were transfected with plasmids expressing individual nsp1 subunits, and the CBP degradation was determined by immunofluorescence and Western blot assays (Fig. 3.7). PRRSV-nsp1α was used as a CBP degradation control and PRRSV-nsp1β was used as a negative control. LDV-nsp1α caused a notable reduction of CBP, and the level of reduction was comparable to that of PRRSV-nsp1α (Fig. 3.7A, lanes 2, 4). In cells expressing LDV-nsp1α and SHFV-nsp1γ, CBP degradation was also evident in immunofluorescence assay (Fig. 3.7B, panels M, c), even though SHFV-nsp1γ-mediated CBP degradation was less evident in Western blot. In

contrast, no CBP degradation was observed for LDV-nsp1β (panel Q), EAV-nsp1 (panel U), and SHFV-nsp1αβ (panel Y). The CBP degradation was quantified by counting the numbers of cells exhibiting the reduced CBP and the number of cells expressing the respective nsp expression. Approximately 80% of cells expressing PRRSV-nsp1α and 78% of cells expressing LDV-nsp1α showed a significant reduction of CBP whereas only approximately 30% of cells expressing SHFV-nsp1γ exhibited the CBP reduction (Fig. 3.7C). Together with the data from Western blot, it further confirmed that LDV-nsp1α and SHFV-nsp1γ caused CBP degradation, resulting in the inhibition of enhanceosome formation and thus suppression of IFN production.

**Suppression of ISRE by nsp1 subunits of arteriviruses:** In addition to suppression of the IFN production pathway, PRRSV-nsp1α and PRRSV-nsp1β have been shown to suppress the JAK-STAT signaling pathway (Chen et al., 2010; Patel et al., 2010). We thus further examined whether nsp1 subunits of other arteriviruses would also suppress the IFN signaling. HeLa cells were co-transfected with a plasmid expressing individual subunit of arterivirus nsp1 and the ISRE-Luc reporter plasmid, followed by stimulation with IFN-β. As shown in Fig. 3.8A, ISRE-dependent luciferase expression was suppressed by each subunit of all arteriviruses. To further confirm their suppressive effects on IFN stimulated gene (ISG) expression through the JAK-STAT pathway, ISG15 and promyelocytic leukemia (PML), whose expression is ISRE-dependent, were examined by Western blot (Fig. 3.8B; Chelbi-Alix et al., 1995). The reduction of ISG15 (middle panel, lanes 3 through 9) and PML (upper panel, lanes 3 through 9) was identified in cells expressing individual nsp1 subunit, in comparison to those in mock-transfected cells. The suppression of ISG15 expression by SHFV nsp1 was relatively weaker than those of PRRSV-nsp1β, LDV-nsp1β, and EAV-nsp1 but was still significant. The reduction of PML was

also confirmed by the staining of nsp1-expressing cells (Fig. 3.8C). PML is a component of the nuclear bodies (NBs) (Dyck et al., 1994), and thus is stained as a punctate pattern in the nucleus. Compared to cells where no viral protein was expressed, the reduction of PML-NBs was evident in cells expressing PRRSV-nsp1α (panel G, arrow), PRRSV-nsp1β (panel J, arrow), LDV-nsp1α (Panel M, arrow), LDV-nsp1β (Panel P, arrow), EAV-nsp1 (panel S, arrow), SHFV-nsp1αβ (panel V, arrow), and SHFV-nsp1γ (panels Y, arrow). The reduction of PML was quantified by counting the number of cells exhibiting the reduced CBP out of 200 cells expressing viral nsp1 (Fig. 3.8D). Approximately, 80% of cells showed the reduction of PML-NBs for PRRSV-nsp1α, PRRSV-nsp1β, LDV-nsp1α, and LDV-nsp1β, whereas 60% of cells showed the reduction of PML-NBs for SHFV-nsp1αβ. In contrast, only 40% of cells showed the reduction of PML for EAV-nsp1 and SHFV-nsp1γ (Fig. 3.8D). Taken together, our results demonstrate that each subunit of all arterivirus nsp1 contained the inhibitory activity for ISRE and ISRE-dependent antiviral protein expression.

### 3.5. DISCUSSION

During the processing of pp1a and pp1ab polyproteins in arteriviruses, PLP1α/β-mediated proteolytic cleavages are unique characteristics for nsp1 biogenesis, and the role of PLP1α/β for polyproteins processing and viral genome replication has been elucidated for PRRSV and EAV (For a review, see Fang and Snijder, 2010; Snijder et al., 2013). With an exception of SHFV, catalytic sites for nsp1 of other arteriviruses have been either predicted or confirmed by experiments (den Boon et al., 1995; Snijder et al., 1992). In the current study, we show that the processing of LDV-nsp1 is similar to that of PRRSV-nsp1, while SHFV-PLP1α in SHFV-nsp1 is non-functional as that of EAV-PLP1α. For EAV, the displacement of C73 by K73 in nsp1

explains the functional deficiency of PLP1α (Fig. 3.1A). For SHFV, two residues of C115 and H130 are critical for the catalytic activity of PLP1α, and these residues are conserved. However, a contiguous deletion of 55 amino acids is notable in the region between two catalytic residues of C115 and H130 when compared to PRRSV (Fig. 3.1A), thus likely contributing to the impaired function of SHFV-PLP1α.

To study the biogenesis of nsp1, the cleavage sites were first determined. The PRRSV-nsp1 cleavage site was initially predicted to Q166↓R167 in the case of North American genotype PRRSV or somewhere between Q166 and F173 for European genotype PRRSV (Allende et al., 1999; den Boon et al., 1995). Recent studies however, identified the cleavage at M180↓A181 for North American PRRSV, and similarly a corresponding site of H180↓S181 was predicted as the cleavage site for European genotype PRRV according to our sequence analysis (Chen et al., 2010; Sun et al., 2009). The discovery of authentic cleavage site results in addition of 14 amino acids to the C-terminus of PRRSV-nsp1α in contrast to the initial prediction. A crystallographic study shows that these additional 14 residues constitute the C-terminal extension (CTE) of PRRSV-nsp1α and are essential for formation of the newly described C-terminal zinc finger motif (Sun et al., 2009). We have previously shown that these 14 residues are essential for the nsp1α function for IFN suppression and cellular distribution (Song et al., 2010). Hence, keeping the structural integrity of nsp1α seems to be critical to retain its biological function for PRRSV replication. Thus, among the PLP1α homologs in arteriviruses, only PRRSV-PLP1α and LDV-PLP1α appear to be active and functional. When compared the nsp1α-nsp1β junction sequence of LDV to that of PRRSV, CPFxxAxAT(N)V (where x is any amino acid) is conserved between the two viruses, and thus, nsp1α↓nsp1β cleavage site for LDV-PLP1α is readily predictable. In fact, the junction sequence is highly conserved among LDV, PRRSV, and SHFV, and therefore, R181↓A182 is

likely the correct cleavage site for LDV-PLP1α, and G381↓Y382 for LDV-PLP1β. Similarly, G350↓G351 is predicted to be the cleavage site for SHFV-PLP1β (Fig. 3.1C). According to our mutational studies, the cleavage site for SHFV-PLP1γ is reasonably predicted to Y479↓G480 rather than the previous prediction of G480↓R481.

It is intriguing that all subunits of arterivirus nsp1 have the ability to suppress the type I IFN production despite the limited sequence similarities. However, some critical functional motifs appeared to be conserved. The results from luciferase reporter assays indicate that either the IRF3-mediated or NF-κB-mediated signaling pathway are inhibited. In the current study, no changes were identified for both phosphorylation and nuclear localization of IRF3 in cells expressing arterivirus nsp1 subunits, which is in agreement with a previous study by Chen et al. (2010). Thus, it is proposed that the IFN inhibition by arterivirus nsp1 subunits may be a nuclear event. All subunits of arterivirus nsp1 are found to localize in the nucleus, but their role in the nucleus seems variable. PRRSV-nsp1α degrades CBP which is a crucial co-factor for IFN-β transcription (Han et al., 2013), and CBP degradation is also observed for LDV-nsp1α (Fig. 3.7). The subcellular distribution of PRRSV-nsp1α and LDV-nsp1α are both nuclear-cytoplasmic, and their distribution patterns are similar (Fig. 3.4). Since the PRRSV-nsp1α-mediated CBP degradation is a nuclear event and proteasome-dependent and also because of the lack of direct binding of PRRSV-nsp1α to CBP (Kim et al., 2010), the nuclear form of PRRSV-nsp1α is likely responsible for CBP degradation through utilizing a mediator or other signaling pathway to complete the degradation process.

In contrast to the nuclear-cytoplasmic distribution of nsp1α, PRRSV-nsp1β, LDV-nsp1β, and EAV-nsp1 are predominantly nuclear without cytoplasmic distribution (Table. 3.3). IFN synthesis is inhibited by these proteins but a notable CBP degradation is absent, suggesting a

novel strategy by nsp1β for IFN suppression. For SHFV-nsp1γ, CBP degradation was less pronounced but apparent by immunofluorescence in some SHFV-nsp1γ expressing cells, suggesting that a certain form of nsp1γ is probably responsible for CBP degradation. In addition to suppression of the IFN production pathway, all subunits of arterivirus nsp1 are found to inhibit the JAK-STAT signaling pathway. The basis for ISRE inhibition by LDV-nsp1α is similar to that of PRRSV-nsp1α as for CBP degradation. For PRRSV-nsp1β, the KPNA1 degradation has been reported to cause the inhibition of ISGF3 nuclear translocation thus to result in the inhibition of JAT-STAT pathway. Whether LDV-nsp1β and EAV-nsp1 also block the ISGF3 nuclear translocation remain to be determined. Different types of subcellular distribution are found for SHFV-nsp1αβ and SHFV-nsp1γ, suggesting that their nuclear localization is crucial for IFN suppression. The molecular basis for IFN suppression by SHFV-nsp1αβ and SHFV-nsp1γ needs to be further explored.

In summary, we have shown that the nsp1 subunits of all four arteriviruses are able to modulate the IFN production either through the production pathway or the signaling pathway, and their biological function seems to be corresponding to their cellular distributions. Taking together, nsp1 subunits of all viruses in the family *Arteriviridae* are important IFN antagonists, and their IFN modulatory function seems to be a common strategy for evading the host immune system.

## 3.6. FIGURES AND TABLES

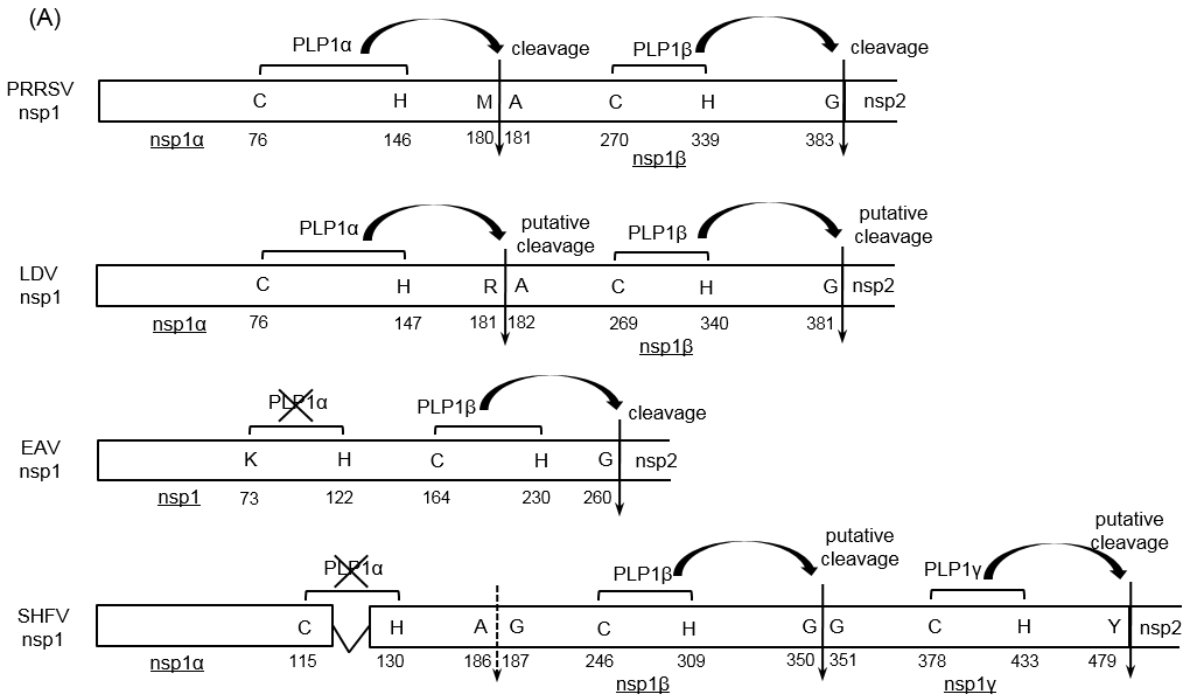


**Fig. 3.1. Schematic presentation and sequence alignments of arterivirus nsp1.** (A) Structures and potential cleavage sites of nsp1 of PRRSV, LDV, EAV, and SHFV. The nsp1 protein for PRRSV, LDV, EAV, and SHFV is of 384, 381, 260, and 479 amino acids (aa), respectively. The catalytic residues for PLPs are indicated. Solid vertical arrows represent the PLP-mediated cleavage sites and dotted arrows indicate predicted cleavage sites. Crossing-outs indicate non-functional PLPs. Numbers indicate amino acid positions in nsp1. The "V" shape connector between aa 115 and 130 in SHFV nsp1 indicates the deletion within the conserved PLP1α domain of arteriviruses..

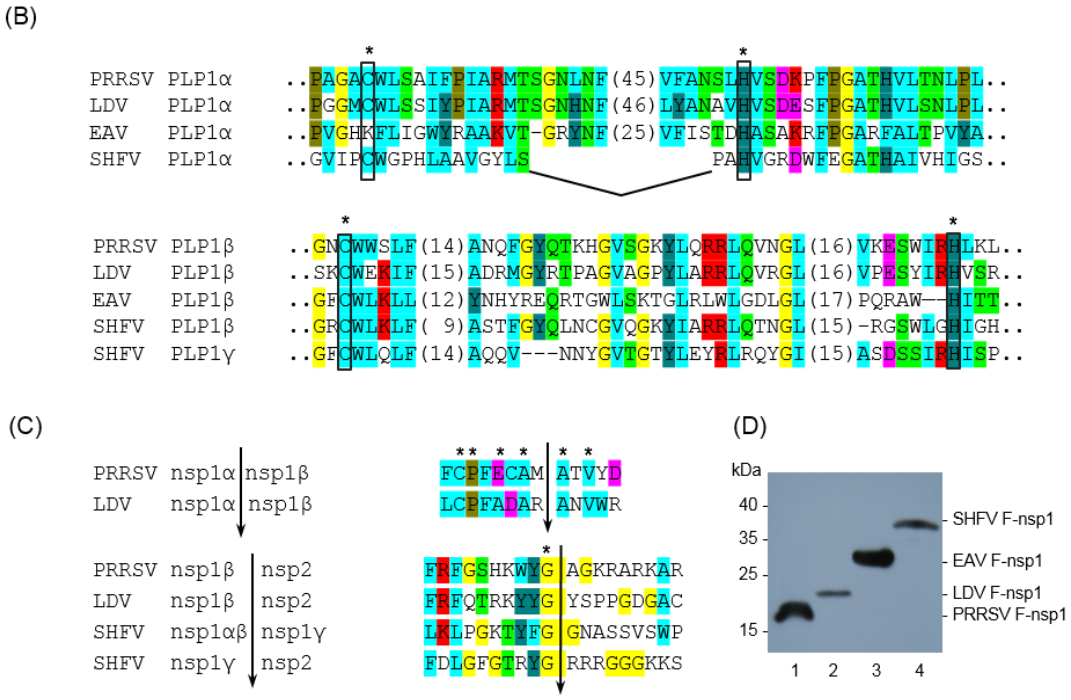


**Fig. 3.1. (Conti.)** (B) Multiple sequence alignments of the PLP domains of nsp1 of arteriviruses. Conserved residues are shown in colors. PLP catalytic sites are boxed and indicated with asterisks. Dotted and solid lines indicate amino acid deletions. Numbers in parenthesis indicate the numbers of amino acids between the two sequences. (C) Sequence alignments of PLP-directed cleavage sites in nsp1 of different arteriviruses. Conserved amino acid residues are indicated in asterisks. Vertical arrows indicate cleavage sites. Sequence alignments were constructed using Clustal X2.1 and presented in reference to the previous report (van Hemert and Snijder, 2007). (D) Identification of the N-terminal cleavage product of individual arterivirus nsp1. Individual nsp1 genes were FLAG-tagged at their N-terminus and transiently

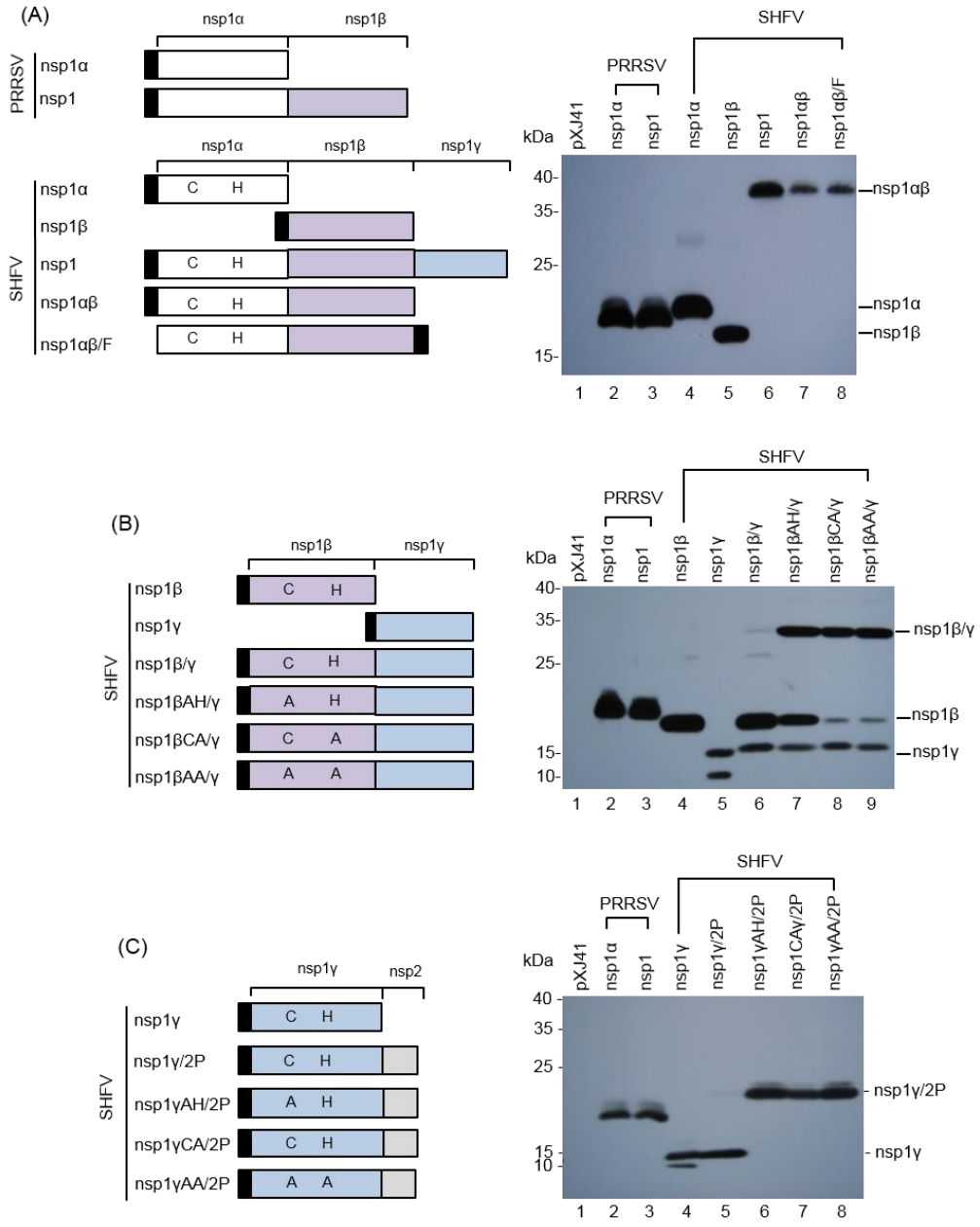


**Fig. 3.2. PLP-mediated cleavages of SHFV-nsp1.** (A) Structural illustration and self-cleavage of SHFV-nsp1 mutants and PLP1α mutants. Each construct was fused with a FLAG tag (dark areas) at the N-terminus or C-terminus. C and H residues of the catalytic dyad of PLP1α and alanine substitution are indicated (left panel). HeLa cells were transfected with indicated constructs for 24 h, and cell lysates were subjected to Western blot using anti-FLAG antibody. 21 kD, 18 kD, and 31 kD proteins represent SHFV-nsp1α, SHFV-nsp1β, and SHFV-nsp1α/β constructs, respectively (right panel). (B) Identification of SHFV-PLP1β mediated cleavage products. Schematic diagrams for constructs to determine PLP1β-mediated cleavages were shown in the left panel. 33 kD, 18 kD, and 15 kD proteins represent an uncleaved form of SHFV-nsp1β/γ, SHFV-nsp1β, and SHFV-nsp1γ, respectively (right panel). 10 kD proteins in lane 5 is a cleaved form of SHFV-nsp1γ. (C) Generation of PLP1γ-mediated nsp1γ. Structural presentations of nsp1γ constructs were shown (left panel). nsp1γ was extended to include a partial sequence of nsp2. 15 kD protein represents nsp1γ and 23 kD protein represent an uncleaved form of nsp1γ/2P (right panel).

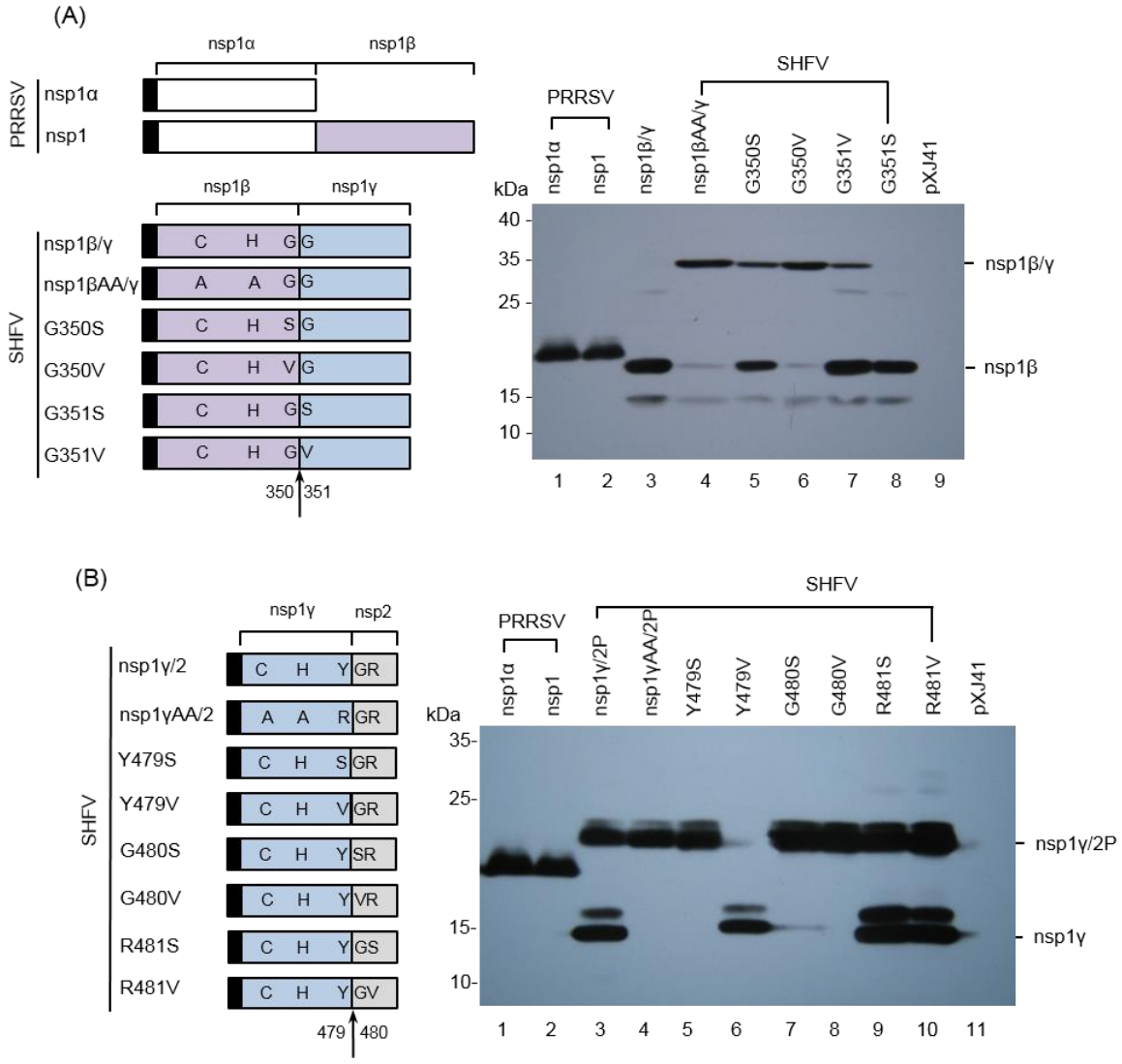


**Fig. 3.3. Identification of PLP1β-directed and PLP1γ-directed cleavages of SHFV-nsp1.** (A) Identification of PLP1β-directed cleavage products of SHFV-nsp1. Each construct was fused with a FLAG tag at the N-terminus (dark areas). The catalytic residues of PLP1β and their amino acid substitutions are indicated. PLP1β-directed nsp1 cleavage was predicted at G350↓G351 (arrows), and a mutation to G350S, G350V, G351S, or G351V is indicated (left panel). HeLa cells were transfected with individual constructs illustrated in the left panel for 24 h, and cell lysates were subjected to Western blot using anti-FLAG antibody. The 33 kD band represents the uncleaved nsp1β/γ protein and the 18 kD band represents the nsp1β subunit (right panel). (B) Identification of PLP1γ-directed nsp1 cleavage. Each construct for PLP1γ-directed nsp1 processing was fused with a FLAG tag at the N-terminus for detection by anti-FLAG antibody. The catalytic residues and amino acids at the junction of predicted cleavage sites between nsp1γ and nsp2 are indicated. These amino acids were subjected to substitution by G or S (left panel). The 23 kD band indicates the uncleaved nsp1γ/2P and the 15 kD band indicates the nsp1γ subunit (right panel).

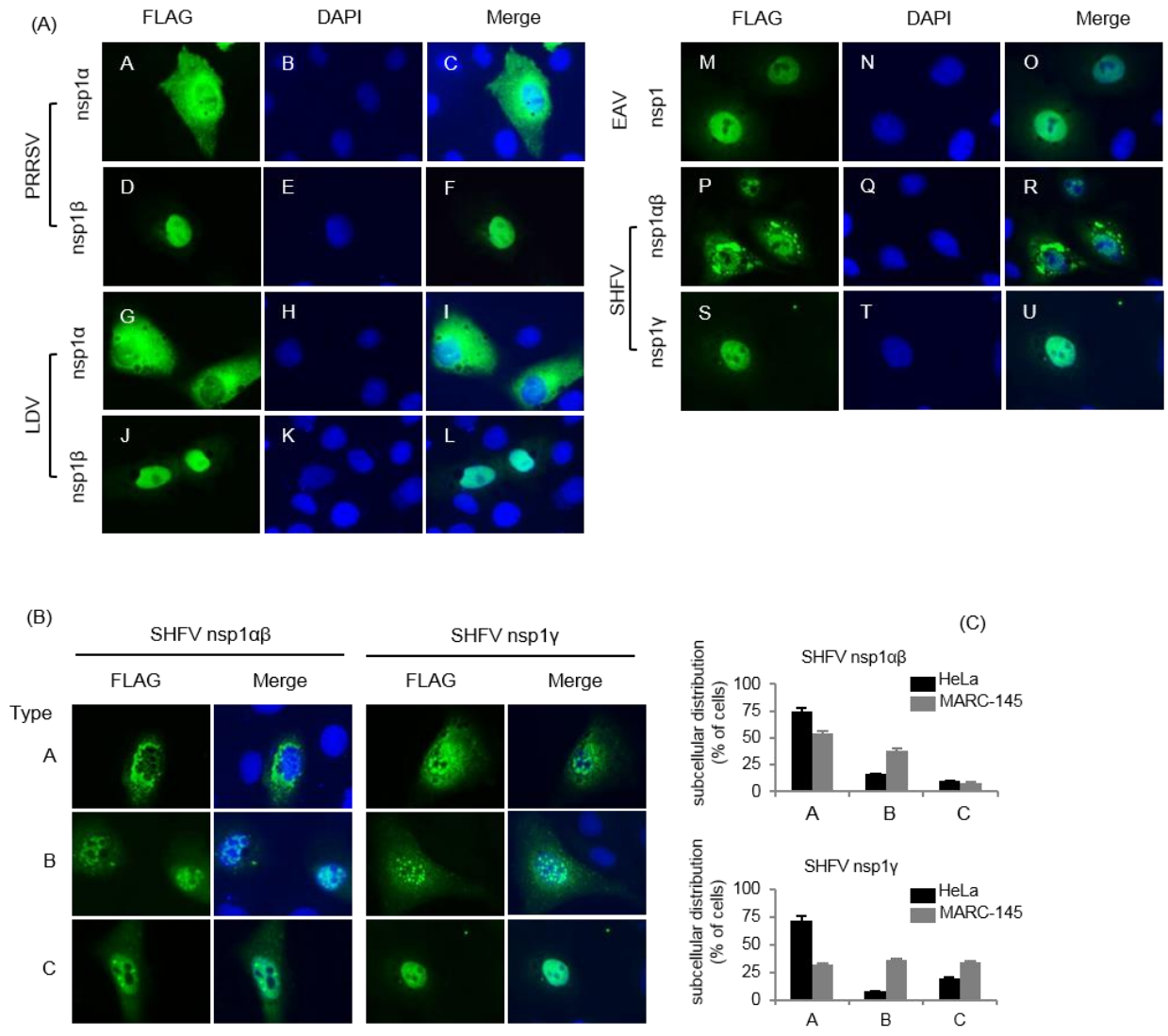


**Fig. 3.4. Subcellular localization of nsp1 subunits of arteriviruses in HeLa and MARC-145 cells.** (A) Cells were grown to 40% confluency and transfected with indicated genes for 24 h. Cells were fixed with 4% paraformaldehyde and stained with anti-FLAG Ab followed by staining with Alexa 488-labeled anti-mouse Ab and DAPI. Cellular localization of nsp1 subunits were examined by fluorescence microscopy. (B) Types of cellular distribution for SHFV-nsp1αβ and SHFV-nsp1γ. (C) The percentages of cells showing different types of subcellular distribution were calculated using the following formula; (Number of cells showing each of distribution types/ (50 cells expressing SHFV-nsp1αβ or SHFV-nsp1γ) x 100.

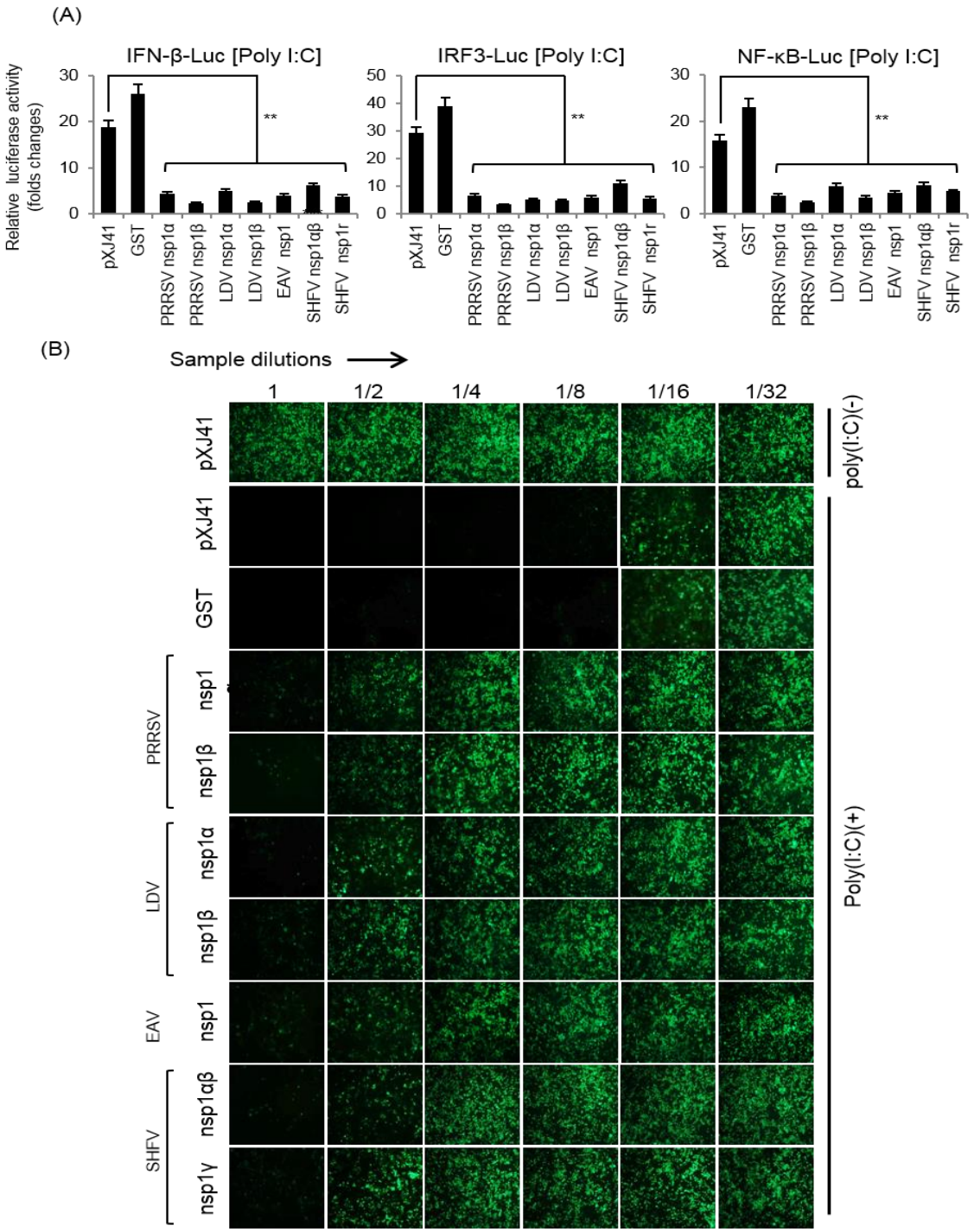


**Fig. 3.5. Suppression of IFN-β production by individual arterivirus nsp1 subunits.** (A) HeLa cells were seeded in 12-well plates and co-transfected with pIFN-β-Luc, p4×IRF3-Luc, or pRD II-Luc, along with individual arterivirus nsp1 genes and pTK-RL as an internal control at a ratio of 1:1:0.1. At 24 h post-transfection, cells were stimulated with 1 μg/ml of poly(I:C) for 12 h, and lysed for the reporter determination using the Dual Luciferase assay system (Promega). Relative luciferase activities were calculated by normalizing the firefly luciferase to renilla luciferase activities according to the manufacturer′s protocol. The data represent the means of three independent experiments, each experiment in triplicate. (B) IFN bioassay using VSIV-GFP.

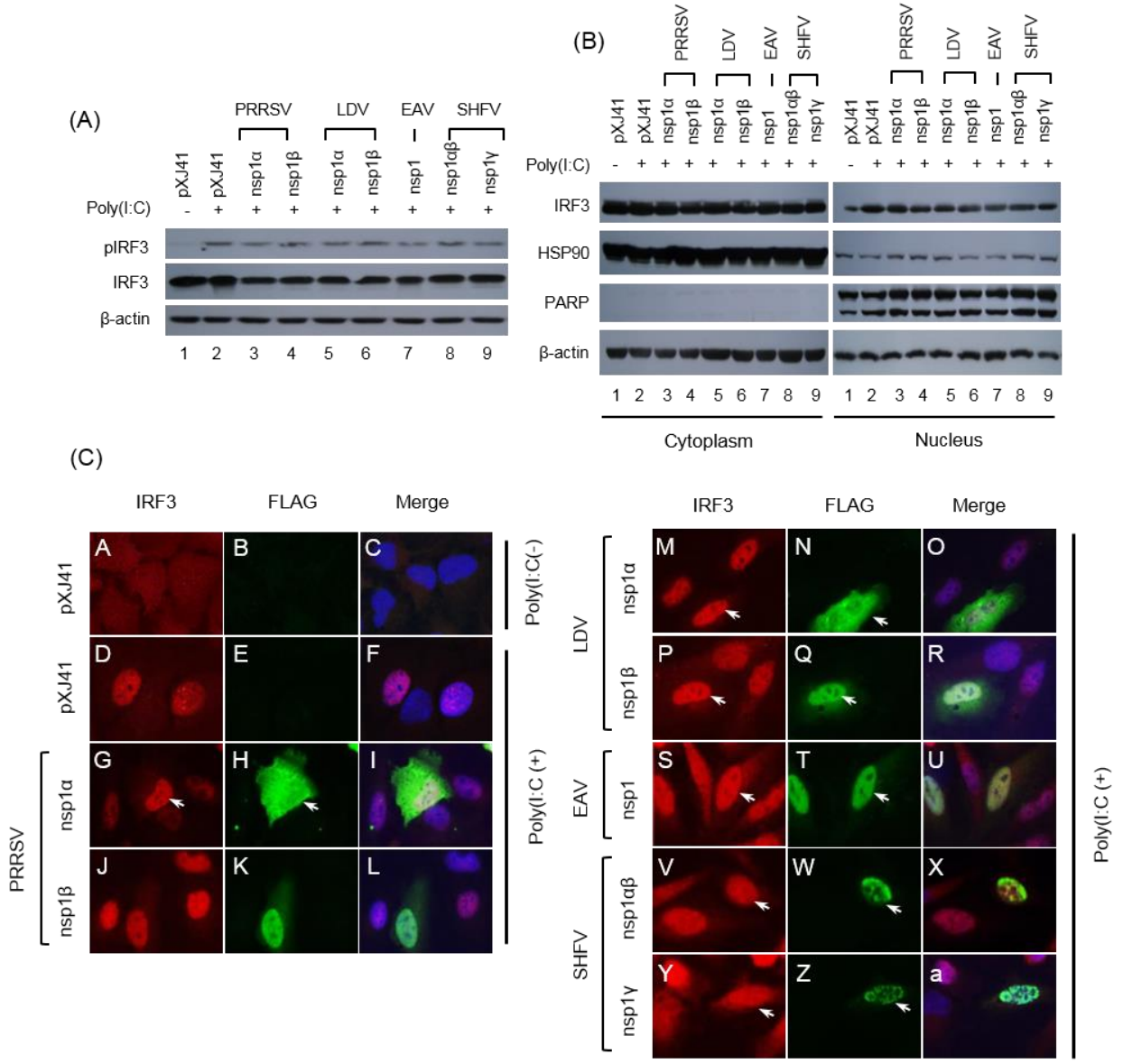


**Fig. 3.6. Activation and nuclear localization of IRF3 in cells expressing the individual arterivirus nsp1 subunits.** (A) Phosphorylation of IRF3 in the presence of arterivirus nsp1 subunits. HeLa cells were transfected with plasmids expressing each of individual arterivirus nsp1 subunits for 24 h and stimulated by poly(I:C) for 8 h. Cells were lysed and subjected to Western blot using phospho-IRF3 (Ser396) antibody (top panel), IRF3 antibody (second panel), and β-actin antibody (bottom panel). (B) Nuclear localization of IRF3 in cells expressing the individual arterivirus nsp1 subunits. HeLa cells expressing individual nsp1 subunits were fractionated followed by Western blot using IRF3 antibody (upper panel), anti-HSP90 antibody as a cytosolic marker (second panel), anti-PARP antibody as a nuclear protein marker (third panel), and β-actin antibody as a loading control (bottom panel). (C) Nuclear translocation of IRF3 in nsp1 subunit- gene transfected cells. Cells were stimulated with poly(I:C) for 8 h, fixed with 4% paraformaldehyde, and incubated with rabbit anti-IRF3 Ab and mouse anti-FLAG Ab, followed by incubation with Alexa Fluor 594-conjugated (red) and 488-conjugated (green) secondary antibodies, respectively, along with DAPI for nucleus staining (blue). pXJ41 is an empty vector and used as a control. Arrows indicate IRF3 and respective nsp1 subunit in the nucleus.

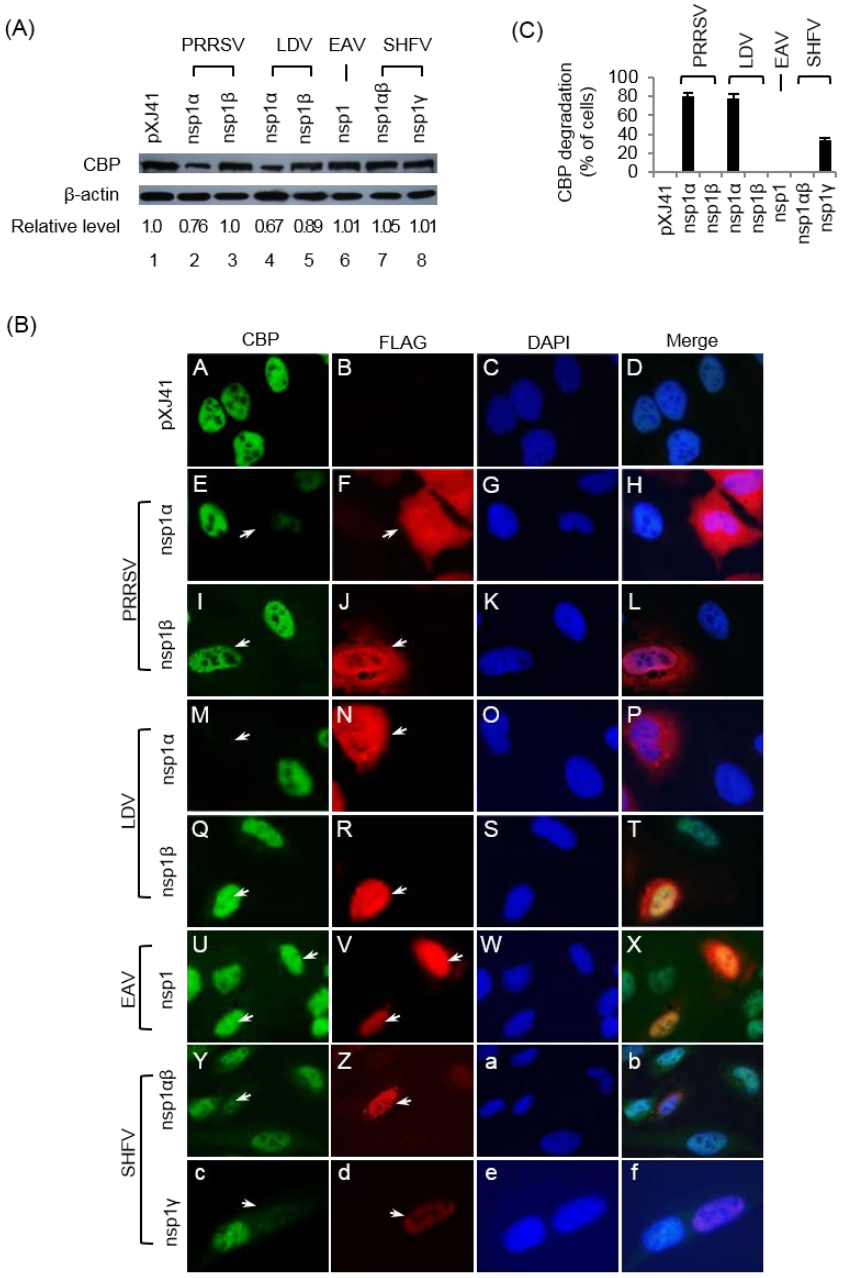


**Fig. 3.7. Degradation of CBP with expressions of arterivirus nsp1 subunits.** (A) HeLa cells were transfected with individual constructs expressing each of arterivirus nsp1 subunits for 24 h, and cell lysates were subjected to Western blot using anti-CBP antibody to examine the endogenous level of CBP (top panel). Fold changes of CBP levels were shown below the images. Digital signal acquisition and analysis were conducted using GraphPad Prism 5.0 (GraphPad). (B) Determination of CBP degradation by IFA. HeLa cells were grown to 40% confluency and transfected with individual arterivirus nsp1 subunit constructs. At 24 h, cells were co-stained with rabbit anti-FLAG Ab and mouse anti-CBP Ab, followed by incubation with Alexa Fluor 594-conjugated (red) and 488-conjugated (green) secondary antibodies, respectively, along with DAPI for nucleus staining (blue). Arrows indicate cells where CBP is degraded by nsp1. (C) The percentage of cells showing significant reduction of CBP was calculated using the following formula; (Number of cells showing more than 50% reduction of the CBP staining intensity compared to the control CBP staining intensity out of 50 nsp1-expressing cells/ (50 cells expressing each subunits of arterivirus nsp1) x 100.

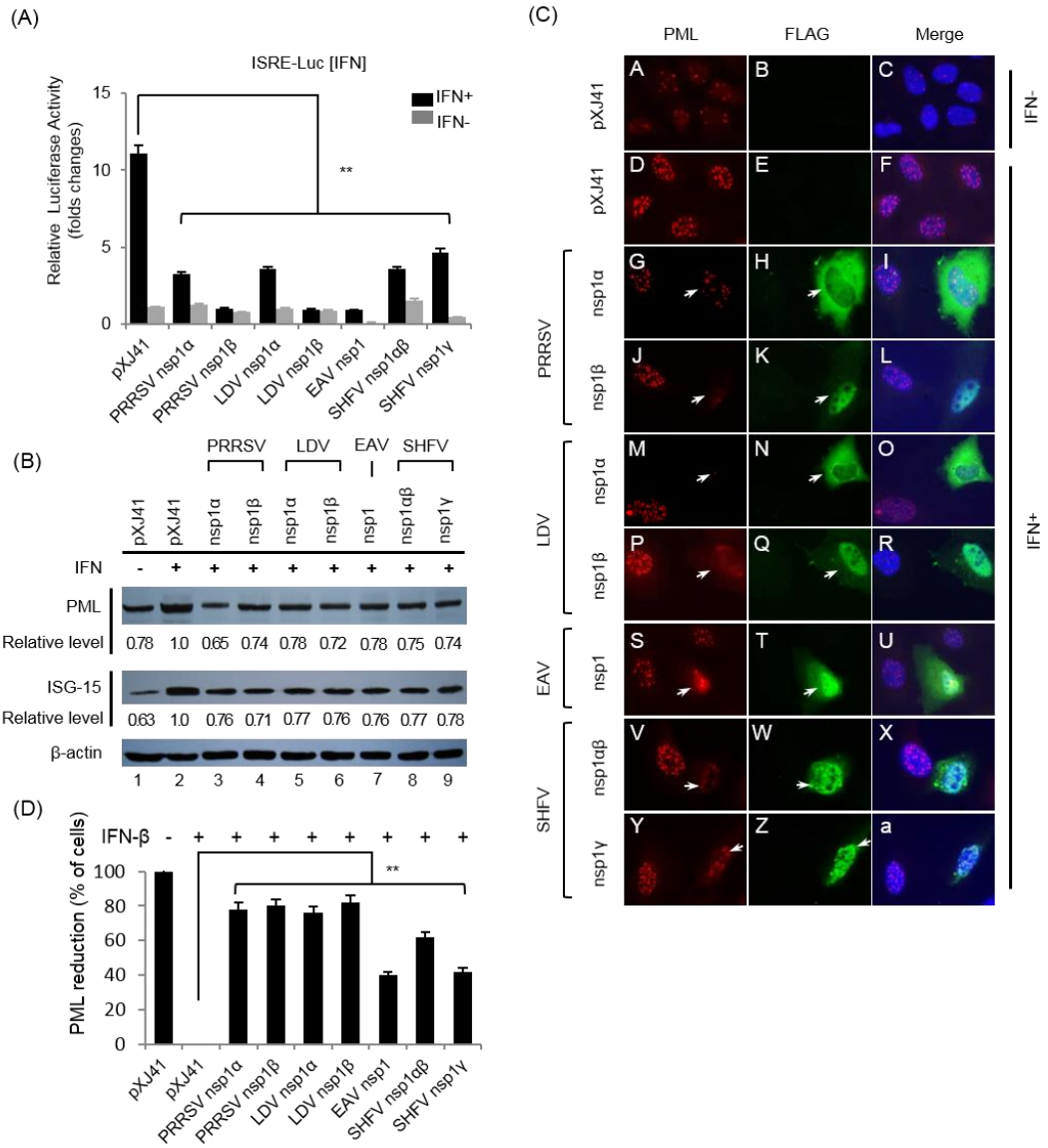


**Fig. 3.8. Suppression of ISRE activities by arterivirus nsp1 subunits.** (A) HeLa cells were co-transfected with 500 ng of pISRE-Luc, 500 ng of pXJ41 empty vector or a plasmid expressing individual arterivirus nsp1 subunit along with pTK-RL as an internal control. At 24 h post- transfection, cells were incubated with 1,000 units/ml of IFN-β for 12 h, followed by luciferase reporter assays using the Dual Luciferase assay system (Promega). Relative luciferase activities were calculated by normalizing the firefly luciferase to renilla luciferase activities. Significant differences in fold changes of relative luciferase activity between empty vector and each of the arterivirus nsp1 subunits are indicated as follows: *, P<0.05, and **, P<0.01. (B) HeLa cells were transfected with individual plasmids encoding nsp1 subunits for 24 h, followed by IFN treatment for 12 h. Cell lysates were subjected to Western blot analyses using anti-PML antibody (top panel) and anti-ISG15 antibody (second panel). β-actin was used as a loading control (bottom panel). (C) Reduced expression of PML in nsp1subunit-expressing cells. After IFN stimulation, cells were fixed with 4% paraformaldehyde and incubated with rabbit anti-FLAG Ab and mouse anti-CBP Ab for 2 h, followed by incubation with Alexa Fluor 594-conjugated (red) and Alexa Fluor 488-conjugated (green) secondary antibodies, respectively. The nuclei were stained with DAPI (blue). Arrows indicate the reduction of PML expression. Fold changes of PML and ISG-15 levels were shown below each of the images, respectively. Digital signal acquisition and analysis were conducted using GraphPad Prism 5.0 (GraphPad). (D) Percentage of cells showing reduced production of PML. Significant differences Significant differences in fold changes of relative luciferase activity between empty vector and each of the arterivirus nsp1 subunits after IFN stimulation are indicated as follows: *, P<0.05, and **, P<0.01.

## Table 3.1. Oligonucleotides used for cloning nsp1 genes and their sequences

| Oligonucleotides | Primer sequence |
|---|---|
| LDV-F-nsp1α-Fwd | 5′-GCCGAATTCCACCATG*GATTACAAGGATGACGACGATAAG*ATGCAGTCGGGATTCG-3′ |
| LDV-F-nsp1α-Rev | 5′-GCCCTCGAGCTATCGTGCATCAGCAAAAGGACAT-3′ |
| LDV-F-nsp1β-Fwd | 5′-GCCGGATCCACCATG*GATTACAAGGATGACGACGATAAG*GCGAATGTGTGGCGTTAC-3′ |
| LDV-F-nsp1β-Rev | 5′-GCCGGTACCCTACCCATAGTATTTTCTAGTTTGGAATCTA-3′ |
| EAV-F-nsp1-Fwd | 5′-GCCGAATTCACCATG*GATTACAAGGATGACGACGATAAG*ATGGCAACCTTCTCCGC-3′ |
| EAV-F-nsp1-Rev | 5′-GCCCTCGAGCTAGCCGTAGTTGCCAGCAGGC-3′ |
| SHFV-F-nsp1α-Fwd | 5′-GCCGAATTCACCATG*GATTACAAGGATGACGACGATAAG*TTCTGTGAGTGCCC-3′ |
| SHFV-F-nsp1α-Rev | 5′-GCCCTCGAGCTATGCATGCCACTCGACATGATCTATG-3′ |
| SHFV-F-nsp1β- Fwd | 5′-GCCGAATTCACCATG*GATTACAAGGATGACGACGATAAG*GGTGTTAAGCCTGG-3′ |
| SHFV-F-nsp1β-Rev | 5′-GCCCTCGAGCTAACCGAAATAAGTCTTCCC-3′ |
| SHFV-nsp1β-F-Rev | 5′-GCCCTCGAGCTA*CTTATCGTCGTCATCCTTGTAATC*ACCGAAATAAGTCTTCCC-3′ |
| SHFV-F-nsp1γ- Fwd | 5′-GCCGAATTCACCATG*GATTACAAGGATGACGACGATAAG*GGAAATGCCAGTTCGG-3′ |
| SHFV-F-nsp1γ-Rev | 5′-GCCCTCGAGCTAGTAACGCGTTCCGAATCC-3′ |
| SHFV-F-nsp1γ/2P-Rev | 5′- GCCCTCGAGCTAGTCTGTAGTGACTTTGG-3′ |

Restriction enzyme recognition sequences are underlined. The FLAG tag is italicized and underlined.

## Table 3.2. Mutagenic oligonucleotides and their sequences

| Oligonucleotides | Primer sequence |
|---|---|
| SC246A-Fwd | 5′-CTTTGAGCATGGCCGCGCCTGGCTGAAGTTGTTC-3′ |
| SC246A-Rev | 5′-GAACAACTTCAGCCAGGCGCGGCCATGCTCAAAG-3′ |
| SH309A-Fwd | 5′-ATCTTGGCTCGGGGCCATCGGTCATGCCG-3′ |
| SH309A-Rev | 5′-CGGCATGACCGATGGCCCCGAGCCAAGATC-3′ |
| SC378A-Fwd | 5′-CCCTCACTGCTGGGTTCGCTTGGTTGCAGCTATTTC-3′ |
| SC378A-Rev | 5′-GAAATAGCTGCAACCAAGCGAACCCAGCAGTGAGGG-3′ |
| SH433A-Fwd | 5′-CTAGTGATTCTTCCATCAGAGCCATTTCTCCCGTCCCTATAC-3′ |
| SH433A-Fwd | 5′-GTATAGGGACGGGAGAAATGGCTCTGATGGAAGAATCACTAG-3′ |
| SG164S-Fwd | 5′-CAGGGAAGACTTATTTCAGTGGAAATGCCAGTTCG-3′ |
| SG164S-Rev | 5′-CGAACTGGCATTTCCACTGAAATAAGTCTTCCCTG-3′ |
| SG164V-Fwd | 5′-AGGGAAGACTTATTTCGTTGGAAATGCCAGTTCGG-3′ |
| SG164V-Rev | 5′-CCGAACTGGCATTTCCAACGAAATAAGTCTTCCCT-3′ |
| SG165S-Fwd | 5′-AGGGAAGACTTATTTCGGTAGCAATGCCAGTTCGGTTAGCT-3′ |
| SG165S-Rev | 5′-AGCTAACCGAACTGGCATTGCTACCGAAATAAGTCTTCCCT-3′ |
| SG165V-Fwd | 5′-GGAAGACTTATTTCGGTGTAAATGCCAGTTCGGTTAG-3′ |
| SG165V-Rev | 5′-CTAACCGAACTGGCATTTACACCGAAATAAGTCTTCC-3′ |
| SG294S-Fwd | 5′-GGAACGCGTTACAGTCGCCGTCGGG-3′ |
| SG294S-Rev | 5′-CCCGACGGCGACTGTAACGCGTTCC-3′ |
| SG294V-Fwd | 5′-GAACGCGTTACGTTCGCCGTCGGGG-3′ |
| SG294V-Rev | 5′-CCCCGACGGCGAACGTAACGCGTTC-3′ |
| SY293S-Fwd | 5′-CGATTTAGGATTCGGAACGCGTAGCGGTCGCCGTCG-3′ |
| SY293S-Rev | 5′-CGACGGCGACCGCTACGCGTTCCGAATCCTAAATCG-3′ |
| SY293V-Fwd | 5′-CGATTTAGGATTCGGAACGCGTGTCGGTCGCCGTCG-3′ |
| SY293V-Rev | 5′-CGACGGCGACCGACACGCGTTCCGAATCCTAAATCG-3′ |
| SR295S-Fwd | 5′-TCGGAACGCGTTACGGTAGCCGTCGGG-3′ |
| SR295S-Rev | 5′-CCCGACGGCTACCGTAACGCGTTCCGA-3′ |
| SR295V-Fwd | 5′-TCGGAACGCGTTACGGTGTCCGTCGGGG-3′ |
| SR295V-Rev | 5′-CCCCGACGGACACCGTAACGCGTTCCGA-3′ |

**Table 3.3. Subcellular distribution and IFN suppression phenotypes of the individual subunits of arterivirus nsp1**

| Virus | subunits | Cellular distribution | | Activity suppression | | | |
|---|---|---|---|---|---|---|---|
| | | Cytoplasm | Nucleus | IFN | IRF3 | CBP | ISRE |
| PRRSV | nsp1α | +++ | + | +++ | - | +++ | ++ |
| | nsp1β | + | +++ | +++ | - | - | +++ |
| LDV | nsp1α | +++ | + | +++ | - | +++ | ++ |
| | nsp1β | + | +++ | +++ | - | - | +++ |
| EAV | nsp1 | + | +++ | +++ | - | - | ++ |
| SHFV | nsp1αβ | ++ | ++ | +++ | - | - | ++ |
| | nsp1γ | + | +++ | +++ | - | + | ++ |

The symbols denotes the presence (+) or absence (-) of indicated phenotypes. Intensities are expressed as + (weak), ++ (medium), and +++ (strong).

# CHAPTER 4: SUBVERSION OF HOST PROTEIN SYNTHESIS BY PRRSV NONSTRUCTURAL PROTEIN 1-BETA

## 4.1. ABSTRACT

Positive-strand RNA genomes function as mRNA for viral protein synthesis which is fully reliant on host cell translation machinery. Competing with cellular protein translation needs to ensure the productions of viral proteins but also stifles innate host defense. Picornaviruses impair cap-dependent translation and promotes internal ribosome entry site (IRES)-initiated viral protein production. Porcine reproductive and respiratory syndrome virus (PRRSV) is a positive-strand RNA virus with the genome of 5′ cap and 3′-polyadenylated tail, and thus the PRRSV protein translation is likely cap-dependent. In the present study, we found that PRRSV induced the subversion of host cell mRNA translation by blocking their nuclear export, leading to enhanced synthesis of PRRSV proteins. PRRSV-nsp1β was the protein playing a role for mRNA nuclear retention and subversion of host protein synthesis. For other arteriviruses, mRNA nuclear accumulation was also observed for LDV-nsp1β and SHFV-nsp1β, but for EAV-nsp1. By sequence analysis, a SAP motif was identified with the consensus sequence of 126-LQxxLxxxGL-135. Site-specific mutagenesis was conducted to knock off SAP function, and the phenotype of SAP mutant proteins were examined including their subcellular localization and suppression of host protein synthesis. An exclusive cytoplasmic staining was observed for SAP mutants L126, R129A, L130A, and L135A, and these mutants did not suppress host protein synthesis In site hybridization unveiled that mutants L126A, R128A, R129A, L130A, and L135A were unable to cause nuclear retention of host cell mRNAs. While PRRSV-nsp1β suppressed the IFN response significantly, SAP mutants L126A, R128A, R129A, L130A, and L135A were unable to suppress activation of the IFN production, IFN signaling, and TNF-α

production pathways. Using reverse genetics, a series of SAP mutant viruses were generated. vK124A, vL126A, vG134A, and vL135A were viable and vL126A and vL135A showed impaired growth. PRRSV-nsp1β was retained in the cytoplasm in cells infected with vL126A and vL135A, and no mRNA nuclear retention was observed by these mutant viruses. Importantly, vL126A and vL135A did not suppress IFN production. Our data show that PRRSV infection blocks mRNA nuclear export, which is mediated by nsp1β protein. The SAP motif identified in nsp1β is required for nsp1β nuclear localization and host cell mRNA nuclear retention, which leads to subversion of host protein synthesis and innate immune responses

## 4.2. INTRODUCTION

Porcine reproductive and respiratory syndrome (PRRS) emerged in the United States in 1987 and subsequently in Europe in 1990, and has since become endemic in most pig-producing countries worldwide (Benfield et al., 1992; Murakami et al., 1994; Shimizu et al., 1994; Wensvoort et al., 1991). The clinical manifestations of PRRS include mild to severe respiratory disease in young pigs whereas abortion and reproductive failures are common in pregnant pigs. The etiological agent is PRRS virus (PRRSV) that falls into the family Arteriviridae together with lactate dehydrogenase-elevating virus (LDV) of mice, equine arteritis virus (EAV), and simian hemorrhagic fever virus (SHFV). By comparative genome sequence analysis, PRRSV isolates are grouped into two distinct genotypes: European type (EU, genotype I) and North American type (NA, genotype II). Lelystad virus (LV) and VR-2332 represent two prototype viruses for two genotypes, respectively, with their sequence similarity of approximately 60% (Benfield et al., 1992; Nelsen et al., 1999; Wensvoort et al., 1991; Wootton et al., 2000). The PRRSV genome is a single-stranded positive-sense RNA of 15 Kb in length with the 5′ cap and

3′-polyadenylated [poly(A)] tail (Meulenberg et al., 1993; Murtaugh et al., 1995; Nelsen et al., 1999; Wootton et al., 2000). Two large open reading frames (ORFs), ORF1a and ORF1b, occupy the 5′ three-quarters of the genome and code for two polyproteins, pp1a and pp1ab, with the expression of the latter mediated by the -1 frame-shifting in the ORF1a/ORF1b overlapping region (Snijder and Meulenberg, 1998). The pp1a and pp1ab proteins are further processed to generate 14 non-structural proteins (nsps). The remaining sequence located in the 3′ one-quarter of the genome codes for structural genes: ORF2a, ORF2b, and ORFs 3 through 7, plus ORF5a within ORF5 (Firth et al., 2011; Johnson et al., 2011; Murtaugh et al., 1995; Nelsen et al., 1999; Wootton et al., 2000). A set of 3′-coterminal nested subgenomic (sg) mRNAs, from which structural proteins are translated, is produced during infection (Snijder et al., 2013). A -2 ribosomal frame-shifting has recently been identified for expression of nsp2TF in the nsp2-coding region (Fang et al., 2012).

Host innate immune system produces cytokines and chemokines in response to viral infection for protection (Yoo et al., 2010). Type I interferons (IFN-α/β) and the pleiotropic cytokine TNF-alpha (TNF-α) have been shown to inhibit PRRSV replication (Ait-Ali et al., 2007; Albina et al., 1998; Buddaert et al., 1998; Lopez-Fuertes et al., 2000). Therefore, such principle cytokines are ideal targets for PRRSV to disarm host surveillance, and a poor induction of proinflammatory cytokines and type I IFNs is the hallmark of PRRSV infection in cells or pigs (Han and Yoo, 2014; Sun et al., 2012; Yoo et al., 2010). Impaired production of TNF-α is noticeable in PRRSV-infected pulmonary alveolar macrophages (PAMs) and in bronchoalveolar fluids (Thanawongnuwech et al., 2001; Van Reeth et al., 1999), even though a detectable level of TNF-α has been claimed in cells, organs, and serum of PRRSV-infected pigs (Aasted et al., 2002; Ait-Ali et al., 2007; Choi et al., 2002; Johnsen et al., 2002; Miguel et al., 2010; Rowland et al.,

2001). The production of type I IFNs is also subverted during PRRSV infection. PRRSV induces a minimal expression of IFN-α in cells and in vivo (Van Reeth et al., 1999), and the induction varies among virus isolates and cell types (Baumann et al., 2013; Lee et al., 2004; Loving et al., 2007; Miller et al., 2004; Nan et al., 2012). Double-strand RNA-induced IFN-α is blocked in the presence of PRRSV. A decrease of IFN transcripts is observed in PRRSV-infected MARC-145 cells (Miller et al., 2004). On the contrary, IFN-α mRNA is augmented after stimulation in PRRSV-infected macrophages, suggesting a post-transcriptional inhibition (Lee et al., 2004; Miller et al., 2009). For the IFN production signaling, PRRSV suppresses IRF3 signaling by inactivating IFN-β promoter stimulator 1 (IPS-1) in MARC-145 cells. A partial activation has been seen for toll/IL-1R (TIR) domain-containing adaptor inducing IFN-β (TRIF), which is an adaptor molecule of TLR3 (Luo et al., 2008). In addition, the suppressed nuclear factor kappa-light-chain-enhancer of activated B cells (NF-κB) activity is likely related to down-regulation of IFN production during early infection of PRRSV. At the downstream, CREB (cyclic AMP responsive element binding)-binding protein (CBP) is degraded in the presence of PRRSV and the assembly of enhanceosome for IFN transcription is disrupted (Kim et al., 2010). Moreover, the nuclear translocation of IFN-stimulated gene factor 3 (ISGF3) is inhibited in PRRSV-infected MARC-145 cells and primary PAMs, with the subsequent inhibition of IFN signaling pathway (Patel et al., 2010). Six viral proteins to date have been identified as IFN antagonists, including five non-structural proteins (nsp1α, nsp1β, nsp2, nsp4, and nsp11) and a structural protein [nucleocapsid (N) protein] (Han and Yoo, 2014; Yoo et al., 2010).

In addition to modulation of host cell signaling, seizing the control of host protein synthesis is a complementary strategy for virus to suppress host innate defense (Walsh and Mohr, 2011). The life cycle of virus is reliant on the translation machinery of host cells, and

commandeering ribosomes to viral mRNA is essential for viral protein production, viral genome replication, and production of progeny. During infection, regulated mRNA expression also stifles host innate defense that is designed to cripple the protein production and hence the production of anti-viral molecules are be suppressed such as Type I IFNs (Walsh and Mohr, 2011). Discrete strategies for the subversion of host mRNA synthesis have been uncovered during virus infection which includes interferences on translation factors (Walsh and Mohr, 2011), mRNA nuclear imprisonment (Kuss et al., 2013), cleavages of host cellular mRNAs (Kamitani et al., 2006; Sokoloski et al., 2009), and induction of microRNAs that inhibits host translation (Abraham and Sarnow, 2011). The inhibition of cap-dependent host protein translation is well studied for members in Picornavirales. The proteases of enteroviruses (2A protease and/or 3C protease) and caliciviruses (3C protease) cleave eukaryotic translation initiation factor 4G (eIF4G), polyadenosine binding protein (PABP) (Lloyd, 2006; Smith and Gray, 2010), and eIF5B (de Breyne et al., 2008). Encephalomyocarditis virus activates the translational repressor 4EBP1 to prevent the assembly of eIF4F (Gingras et al., 1996). Besides, some picornaviruses impede host protein translation by blocking nucleo-cytoplasmic trafficking of mRNA (Kuss et al., 2013). During infection of enteroviruses, polioviruses , and rhinoviruses, their 2A proteases lead to the alternation of NPC structure by degrading Nup62, Nup98, and Nup153 (Castello et al., 2009; Gustin and Sarnow, 2001; Gustin and Sarnow, 2002; Lidsky et al., 2006; Park et al., 2010). For cardioviruses, the leader protein inhibits mRNA nuclear export (Porter et al., 2006; Ricour et al., 2009). Cap-independent translation driven by IRES has been identified for enteroviruses, cardioviruses, pestiviruses, and hepacaiviruses, which guarantees viral protein synthesis even if cap-dependent translation is impaired (Balvay et al., 2009).

For nidoviruses, the nsp1 protein of severe acute respiratory syndrome coronavirus (SARS-CoV) inhibits the expression of host genes (Huang et al., 2011b). SARS-CoV nsp1 induces endonucleolytic cleavage of host mRNAs, and binds to 40S ribosomes to inactivate their translation functions (Kamitani et al., 2009; Kamitani et al., 2006). The nsp1 proteins of mouse hepatitis virus (MHV) and transmissible gastroenteritis virus (TGEV) strongly reduce cellular mRNA expression but the strategy used by TGEV nsp1 is different from that if SARS-CoV nsp1 (Huang et al., 2011a; Tohya et al., 2009; Zust et al., 2007). Coronavirus nsp1 is a virulence factor, and the type I interferon system is impeded in the presence of coronavirus nsp1 (Narayananj et al., 2008; Tohya et al., 2009; Zust et al., 2007). For arteriviruses, suppression of host protein synthesis has not been reported yet but nsp1 or its subunits are potent modulators for IFN production and signaling (Han and Yoo, 2014). PRRSV-nsp1α and PRRSV-nsp1β suppress IFN-β production (Beura et al., 2010; Chen et al., 2010; Kim et al., 2010; Song et al., 2010), and PRRSV-nsp1α induces CREB (cyclic AMP responsive element binding)-binding protein (CBP) degradation (Han et al., 2013). A nuclear inhibition has been suggested for nsp1β-mediated IFN suppression (Chen et al., 2010). In addition, PRRSV-nsp1β interrupts the phosphorylation of STAT1 and the nuclear translocation of ISGF3 and causes inhibition of the JAK (Janus kinase)-STAT (signal transducer and activator of transcription) pathway (Chen et al., 2010; Patel et al., 2010). The inhibition of ISGF3 nuclear localization by PRRSV-nsp1β is due to the degradation of karyopherin-α1 (KPNA1) which is a nuclear import protein (Wang et al., 2013). In the present study, we investigated the regulation of host protein expression by PRRSV. We demonstrated that PRRSV blocked nucleo-cytoplasmic trafficking of host cellular mRNA by nsp1β, which leads to the subsequent shutoff of host protein synthesis. A conserved motif for SAP (SAF-A/B, Acinus, and PIAS) was identified in nsp1β and the this motif played a role for nuclear

distribution of nsp1β, nuclear retention of mRNA, subversion of host protein synthesis, innate immune responses, and PRRSV replication.

## 4.3. MATERIALS AND METHODS

**Cells and viruses:** HeLa cells (NIH AIDS Research and Reference Reagent Program, Germantown, MD), MARC-145 cells (Kim et al., 1993), and RAW 264.7 cells were grown in Dulbecco′s modified Eagle′s medium (DMEM; Mediatech Inc., Manassas,VA), supplemented with 10% heat-inactivated fetal bovine serum (FBS; HyClone, Logan, UT) in a humidified incubator with 5% $CO_2$ at 37 °C. North American (NA) type PRRSV strains VR-2332 (Collins et al., 1992), PA8 (Wootton et al., 2000), and FL12 (Truong et al., 2004), and European (EU) type PRRSV strain Lelystad virus (LV) were propagated in MARC-145 cells and used as virus stocks for the present study. For infection, MARC-145 cells were grown to approximately 70% confluency and infected at a multiplicity of infection (m.o.i.) of 0.1 to 5. Vesicular stomatitis Indiana virus expressing green fluorescent protein (VSIV-GFP) (Dalton and Rose, 2001) was kindly provided by Adolfo García-Sastre (Mt. Sinai School of Medicine, New York, NY).

**Antibodies and chemicals**: An anti-PRRSV-nsp1β rabbit polyclonal antibody (PAb) specific for NA-PRRSV nsp1β was generated at the Immunological Research Center, University of Illinois at Urbana-Champaign (Urbana, IL)**.** The anti-LV-nsp2/3 antibody was a generous gift from E. Snijder, (Leiden University Medical Center, Leiden, The Netherlands). Anti-N protein MAbs (SDOW17) was obtained from E. Nelson (South Dakota State University, Brookings, SD). olyinosinic:polycytidylic [poly (I:C)], DAPI (4′,6-diamidino-2-phenylindol), anti-Flag monoclonal antibody (MAb) (F3165), and anti-FLAG PAb (F7425) were purchased from Sigma

(St. Louis, MO). Anti-β-actin MAb (sc-47778), anti- HSP90 MAb (sc-69703), and anti-PARP PAb (sc-7150) were purchased from Santa Cruz Biotechnologies Inc. (Santa Cruz, CA). Anti-ISG15 PAb and anti-GFP PAb were purchased from Thermo Scientific (Rockford, IL). The peroxidase-conjugated Affinipure goat anti-mouse IgG and peroxidase-conjugated Affinipure goat anti-rabbit IgG were purchased from Jackson Immuno Research (West Grove, PA). Alexa-Flour 488-conjugated and Alexa-Flour 568-conjugated secondary antibodies were purchased from Invitrogen (Carlsbad, CA).

**Plasmids and DNA cloning:** The plasmids pPRRSV-F-nsp1α, pPRRSV-F-nsp1β, pLDV-F-nsp1α, pLDV-F-nsp1β, pEAV-F-nsp1, pSHFV-F-nsp1αβ, pSHFV-F-nsp1α, pSHFV-F-nsp1β, and pSHFV-F-nsp1γ were fused with the N-terminal FLAG tag as described previously (Han et al., 2013; Han and Yoo, 2014; Song et al., 2010). The genes for PRRSV-nsp1β and PRRSV-nsp1β with the C-terminal FLAG tag were amplified by PCR using primer sets listed in Table 4.1. The PCR fragments were cloned in the pXJ41 mammalian expression vector using indicated restriction enzymes and pPRRSV-nsp1β and pPRRSV-nsp1β-F were constructed (Xiao et al., 1991). Mutant genes were generated by PCR-based site-directed mutagenesis using primers listed in Table 4.2. The reporter plasmids pIFN-β-Luc and p4xIRF3-Luc were kindly provided by Stephan Ludwig (Institute of Molecular Medicine, Heinrich Heine Universtät, Düsseldorf, Germany) (Ehrhardt et al., 2004), and used for luciferase assays. Four copies of the IRF3-specific PRDI/III domain of the IFN-β promoter were placed in front of the luciferase reporter gene to make p4xIRF3-Luc construct. The plasmid pPRDII-Luc contains two copies of the NF-κB-specific PRDII binding region of the IFN-β promoter in front of the luciferase gene and was kindly provided by Stanley Perlman (University of Iowa, Ames, IA). The plasmid pISRE-Luc

contains the IFN stimulated response element (ISRE) binding sequence and was purchased from Stratagene (La Jolla, CA).The plasmid pswTNF-α-luc containing TNF-α promoter sequence was kindly provided by Fernando A. Osorio (University of Nebraska-Lincoln, Lincoln, NE). The *Renilla* luciferase plasmid pRL-TK contains the herpes simplex virus thymidine kinase (HSV-tk) promoter and was included to serve as an internal control in luciferase reporter assay (Promega).The plasmid pIRES-FF-RL contains full sequence of *firefly* gene under CMV promoter and a copy of *Renilla* gene after the IRES site. *Firefly* gene and *Renilla* gene were amplified by PCR using primer sets listed in Table 4.1, and the PCR fragments were cloned into the pIRES-neo vector (Clonetech, CA) using the indicated restriction enzymes. The plasmid pEGFP-N1 (Clontech) was used for GFP co-expression. The plasmids DsRed2-Mito and pDsRed2-ER were used as subcellular compartmental markers for mitochondria (MITO) and endoplasmic reticulum (ER), resepectively (Clontech).

**DNA transfection and protein expression:** DNA transfection was performed using Lipofectamine 2000 according to the manufacturer′s instructions (Invitrogen; Carlsbad, CA). HeLa, Raw264.7 or MARC-145 cells were seeded in 6-well plates a day prior to transfection and grown to 80% confluency. A transfection mix containing DNA and Lipofectamine 2000 in OPTI-MEM® I (Invitrogen; Carlsbad, CA) was incubated at room temperature (R/T) for 20 min and added to each well. After incubation, the transfection mix was replaced with a fresh medium, and cells were incubated for 24 h for gene expression.

**Western blot analysis:** Cells were lysed using the M-PER® mammalian protein extraction reagent (Thermo Scientific, City? IL) supplemented with a cocktail of protease inhibitors (P-

8340 Sigma). Cell lysates were centrifuged and supernatants were resolved by 10% or 12% Sodium dodecyl Sulfate (SDS)-poly-acrylamide gel electrophoresis and transferred on polyvinylidene fluoride (PVDF) membrane (Millipore). After blocking with 5% skim milk powder in TBS-T (10 mM Tris–HCl [pH 8.0], 150 mM NaCl, 1% Tween 20), membranes were incubated with primary antibody dissolved in TBS-T containing 5% skim milk powder for 1 h at R/T followed by washing and incubation with horseradish peroxidase-conjugated secondary antibody for 1 h at R/T. After three washes with TBS-T, proteins were visualized using the Enhanced Chemiluminescence system (Thermo Scientific).

**Immunofluorescence analysis (IFA):** Cells were seeded on cover slips and grown to 80% confluency. Cells were then transfected with individual plasmids for 24 h, or infected with virus for indicated times. After washing with phosphate-buffered saline (PBS), cells were fixed with 4% paraformaldehyde for 10 min at R/T in (PBS), and then permeabilized using 0.1% Triton X-100 for 10 min at R/T. After blocking with 1% BSA in PBS for 30 min, cells were incubated with primary antibody in PBS containing 1% BSA for 2 h followed by incubation with Alexa Fluor 488- and/or Alexa Fluor 568-conjugated secondary antibody for 1 h. The staining of the nucleus was performed with DAPI for 3 min at R/T. After washing with PBS, coverslips were mounted onto microscope slides using Fluoromount-G mounting medium (Southern Biotech, Birmingham, AL), and examined under LSM700 confocal laser scanning microscopy (Zeiss). Images were processed with NIH Image/J to determine florescence intensity (FI).

**Generation of SAP mutant full-length PRRSV cDNA clones:** The infectious clone pFL12 was modified in our lab to generate infectious clone pFL13 with CMV promoter. To modify the SAP

motif (124-KxLQxxLxxxGL-135 for FL12 strain) at positions K124, L126, R128, R129, L130, G134, and L135 of nsp1β, PCR-based site-directed mutagenesis was conducted to substitute codons for indicated residues using the shuttle plasmid pFL13-SP-nsp1 with primer pairs in Table 2. PCR-based mutagenesis was performed using QuikChange II XL Site-Directed Mutagenesis Kit (Agilent, Santa Clara, CA) according to the manufacturer′s instructions. The shuttle plasmid pFL13-SP-nsp1 was constructed using the vector pCITE-2b as backbone. The fragment covering nucleotide positions 1 to 2532 of ORF1a was amplified by PCR using the upstream primer (5′-gcc<u>ctcgag</u>*<u>ggcgcgcc</u>*accgtcatg-3′, where the XhoI recognition sequence is underlined and the AscI recognition sequence is italicized and underlined) and the downstream primer (5′-gcc<u>tctaga</u>*<u>actagt</u>* ttcagcagatcctcctcc-3′, where the XbaI sequence is underlined and the SpeI recognition sequence is italicized and underlined). The PCR fragment was cloned into the vector pCITE-2b after digestion with XhoI and XbaI. The wild-type full-length genomic cDNA clone was digested with AscI and SpeI, and the fragment was replaced with the corresponding fragment obtained from the shuttle plasmid. The ligated full length plasmid DNA was screened by MfeI digestion, and based on the MfeI digestion pattern, positive clones were selected. The selected clones were sequenced to confirm the presence of mutations in the full-length genome.

**Production of virus from full-length cDNA clones:** Marc-145 cells were seeded in 35-mm-diameter dishes and grown to 70% confluency. Cells were transfected for 24 h with 2 μg of the full-length cDNA plasmid using Lipofectamine 2000. Transfected cells were incubated for 5 days in DMEM supplemented with 10% FBS. The culture supernatants were harvested at 5 days post-transfection and designated ′passage-1′. The passage-1 virus was used to inoculate fresh Marc-145 cells, and the 5-day harvest was designated ′passage-2′. The ′passage-3′ virus was

prepared in the same way as for passage-2. Each passage virus was aliquoted and stored at 80°C until use. Viral titers were calculated using the Reed and Muench method in MARC-145 cells.

**Luciferase reporter assay:** HeLa cells were grown to a density of 5 x $10^4$ cells/well in 12-well plates and transfected with various combinations of plasmid DNA: 0.5 μg of viral protein coding plasmid, 0.5 μg of pIFN-β-Luc, pPRDII-Luc, p4xIRF3-Luc, or pISRE-Luc, and 0.05 μg of pLR-TK were co-transfected using Lipofectamine. At 24 h post-transfection, cells were stimulated with 0.5 μg of poly (I:C) for 16 h and cell lysates were prepared for luciferase assays. For pISRE-Luc, cells were incubated with 1,000 units of human IFN-β (bioWORLD, Dublin, OH) for 16 h. Raw264.7 cells were used for pswTNF-α-luc as described previously (Ehrhardt et al., 2004). Luciferase activities were measured using the Dual-Glo Luciferase assay system according to the manufacturer′s instructions (Promega). Values for each sample were normalized using *Renilla* luciferase activities and the results were expressed as relative luciferase activities. All assays were repeated at least three times, and each sample was analyzed in triplicates.

**Quantitative real-time-PCR (qRT-PCR):** Total cellular RNA was extracted for qRT-PCR from MARC-145 cells or HeLa cells using RNeasy mini kit (QIAGEN, Hilden) according to manufacturer′s instructions. Nuclear RNA was separated using Sureprep™ cytoplasmic and nuclear RNA purification kit (Fisher BioReagents, PA) in accordance with the manufacturer′s instructions. qRT-PCR reactions were performed in the ABI sequence detector system (ABI Prism 7000 and software; Applied Biosystems) in a final volume of 25 μL containing 2.5 μL of cDNA synthesized from the reverse transcription (RT) reaction, 2.5 pmol of each primer, 12.5 μL of SYBR® Green Master Mix (Applied Biosystems), and 5 μL of water. Primers for GAPDH,

DEPTOR, NOL6, SH2, and EGR1 are reported previously (Sun et al., 2014). The primer sequences for firefly and Renilla were as follows: Firefly forward, 5′-GGATTACCAGGGATTTCAGTC-3′; Firefly reverse, 5′-CTCACGCAGGCAGTTCTAT-3′; Renilla forward, 5′-TGCAGAAGTTGGTCGTGAGGCA-3′; Renilla reverse, 5′-TCTAGCCTTAAGAGCTGTAATTGAACTGG-3′. The mRNA levels of indicated genes were normalized to that of GAPDH mRNA. Two independent experiments were conducted in duplicate and the average of normalized values obtained from each infection and transfection were presented.

**Oligo(dT) *in situ* hybridization (ISH):** HeLa or MARC-145 cells were grown to 80% confluency, and the cells were transfected with selected plasmid DNA or infected with virus. Oligo (dT) in situ hybridization simultaneously with IFA was performed as described previously (Chakraborty et al., 2006). Briefly, the cells were fixed for 8 min with 4% paraformaldehyde, permeabilized with 0.5% Triton X-100, and labeled with primary antibodies at chosen times after transfection or infection. The primary antibodies were diluted in PBS containing 0.2% Triton X-100, 1 mM DTT, and 200 U/ml RNasin (Promega). Cells were again fixed with paraformaldehyde and washed with PBS. Oligo (dT) *in situ* hybridization was then performed at 42°C overnight with biotinylated oligo(dT) (Promega, WI). Samples were washed twice with 0.5× SSC at 42°C. Cells were then fixed with paraformaldehyde, washed in PBS, and incubated for 30 min at room temperature with cy3-streptavidin (Jackson Immuno Research, PA) and secondary antibodies. Cells were then stained with DAPI for nuclear labelling, and mounted on glass slides for subsequent examination by confocal microscopy.

**VSIV-GFP bioassay:** HeLa cells in 6-well plates were transfected with 2 μg of plasmid expressing a selected gene. For PRRSV infection, MARC-145 cells in 12-well plates were infected at an m.o.i. of 1. At 24 h post-transfection or post-infection, cells were stimulated with 1 μg of poly (I:C) by transfection and were further incubated for 12 h. Supernatants were harvested and serially diluted by 2-folds. MARC-145 cells were grown in 96-well plates and incubated for 24 h with 100 μl of each dilution of the supernatant. Cells were then infected with 100 μl of VSIV-GFP of $10^4$ PFU/ml and incubated for 16 h. Cells were fixed with 4% paraformaldehyde, and GFP expression was examined under an inverted fluorescence microscope (Nikon Eclipse TS100).

## 4.4. RESULTS

**Impaired poly(A)+ RNA nuclear-cytoplasmic trafficking by PRRSV:** To examine if PRRSV infection suppresses non-viral gene expression, two constructs of pRL-TK and pIRES-FF-RL were used for reporter assays (Fig. 4.1A). MARC-145 cells were infected with PRRSV PA8 at an m.o.i. of 5 for 24 h, and then individually transfected with indicated constructs for 12 h. PRRSV infection down-regulated the TK-promoter-driven *Renilla* expression (Fig. 4.1B, upper panel), and the expression of PRRSV N protein confirmed the PRRSV infection (Fig. 4.1B, lower panel). Using the construct pIRES-FF-RL, the *firefly* and *Renilla* expressions which were mediated by CMV promoter and IRES element, respectively, were decreased by PRRSV (Fig. 4.1C). These results suggest that PRRSV infection may inhibit host cellular protein synthesis.

Due to complicated cellular responses and host cell-virus interactions, mechanisms for PRRSV-mediated suppression of host protein synthesis may vary. The nuclear-cytoplasmic trafficking of poly(A)+ RNA was firstly examined by *in situ* hybridization in MARC-145 cells

after infection with type II (NA) PRRSV strains VR2332, FL12, and PA8 (Fig. 4.1D). Anti-nsp1β PAb was used to detect PRRSV infection (Fig. 4.1D, upper panel). PRRSV-nsp1β appeared in the both cytoplasm and nucleus (Fig. 4.1D, panels A, E, H, and L). The cellular distribution of poly(A)+ RNA (Fig. 4.1D, second panel from left) was detected using the biotinylated oligo(dT) as a probe followed by staining with cy3-streptavidin. Compared to non-infected cells, PRRSV-infected MARC-145 cells showed significant red florescent intensities (FIs) (Fig. 4.1D, second panel from left), suggesting PRRSV caused poly(A)+ RNA retention in the nucleus. To determine if this phenomenon was common for both type II and type I of PRRSV, cells were infected with Lelystad virus representing type I PRRSV and stained with anti-nsp2/3 PAb. Nsp2/3 protein was observed in the cytoplasm as anticipated (Fig. 4.1D, panel P). When the cells were hybridized with oligo(dT) probe, poly(A)+ RNA accumulation was evident in the nucleus as with type II PRRSV (Fig. 4.1D, second panel from left), indicating that nuclear retention of cellular mRNA is common for both genotypes of PRRSV.

To determine whether poly(A)+ RNA nuclear retention is time-dependent, kinetic studies were conducted hourly from 7 h post infection (hpi) to 12 hpi, and at 24 hpi (Fig. 4.1E). In MARC-145 cells infected with PRRSV PA8 virus, poly(A)+ RNA accumulation in the nucleus (Fig. 4.1E middle panel) was detectable starting from 8 hpi at least till 24 hpi, along with nsp1β nuclear staining (Fig. 4.1E upper panel). The nuclear FIs were quantified in PRRSV-infected cells, and both red [poly(A)+ RNA] and green (PRRSV-nsp1β) FIs increased significantly over time (Fig. 4.1E, right panel), suggesting the accumulation of poly(A)+ RNA was correlated with the nuclear localization of nsp1β. To verify this correlation, florescence analysis was conducted for poly(A)+ RNA nuclear staining in a group of cells upon PRRSV infection (Fig. 4.1F, upper panel; individual cells were labeled from a to i). According to the straining patterns of nsp1β,

cells were divided into three groups; cells with no nuclear nsp1β (′a′ and ′b′; group A), cells with nuclear nsp1β (′c′ to ′g′; group B), and non-infected cells (′h′ and ′i′; group C). The average nuclear FIs for both poly(A)+ RNA and nsp1β were measured and normalized using the average FIs of the background (Fig. 4.1F, yellow circles). In comparison with non-infected cells (Fig. 4.1F, lower panel, lanes h and i), no significant increase of nuclear red FIs was observed for cells in group A (lanes a and b). However, red FIs showed 2-4 folds increase in cells of group B (Fig. 4.1F, lower panel, lanes c to g), further suggesting that the nuclear retension of poly(A)+ RNA requires nsp1β in the nucleus. PRRSV-infected cells exhibited the poly(A)+ RNA nuclear retention at 24 hpi with strong red FIs (Fig. 4.1G).

**Inhibition of poly(A)+ RNA nuclear export by PRRSV-nsp1β:** To identify the viral protein responsible for blocking poly(A)+ RNA nuclear export, nsp1α, nsp1β, and N proteins of PRRSV were examined by ISH since these three proteins have been found to distribute specifically to the nucleus.(Fig. 4.2A) (Yoo et al., 2010). Protein inhibitor of activated STAT-1 (signal transducer and activator of transcription protein-1; PIAS1, is a host cell nuclear protein, and PIAS1-FLAG tag was included as a negative control (Fig. 4.2A, second upper panel). Poly(A)+RNA was found to accumulate only in the nucleus of cells expressing nsp1β (Fig. 4.2A, panels M and N) while the nuclear accumulation of poly(A)+ RNA was not seen in other cells, suggesting that PRRSV-nsp1β plays a role for the poly(A)+RNA nuclear retention. PIAS1 was localized in the nucleus exclusively, and poly(A)+ RNA nuclear retention was not seen in these cells (Fig. 4.2A, panels E and F), excluding the possibility of non-specific interactions between RNA probe and the primary Ab.

To confirm that PRRSV-nsp1β protein inhibits the cellular mRNA export from the nucleus to the cytoplasm, four host genes, DEP domain-containing mTOR-interacting protein (DEPTOR), nucleolar protein 6 (NOL6), src homology 2 (SH2), and early growth response protein 1 (EGR1) were randomly chosen to determine their mRNA levels in the nucleus by qRT-PCR (Fig. 4.2B). Initially, the total mRNA was analyzed by qRT-PCR (Fig. 4.2B, upper panel) from total cell lysates prepared from cells expressing pXJ41 (empty vector), nsp1α, nsp1β, and N. . No significant regulation was identified for chosen genes except EGR1 (Fig. 4.2B, upper panel, purple bars). In cells expressing nsp1β, EGR1 expression was upregulated by 5.4-folds compared to that of cells expressing pXJ41, while 0.47-fold downregulation was observed for N-expressing cells. Consequently, EGR1 was removed from subsequent assays. To determine the nuclear levels of indicated mRNAs, nuclear RNAs were separated followed by RT-PCR. In comparison to those of pXJ41, 2.65-, 1.60-, and 2.72-fold increases of nuclear mRNA were observed for DEPTOR, NOL6, and SH2, respectively (Fig. 4.2B, lower panel). In the presence of N, slight augments ranging from 1.1 to 1.2 folds were observed for chosen genes, whereas nsp1α did not cause significant changes compared to pXJ41. From these results, nsp1β was concluded to induce mRNA accumulation in the nucleus. Since PRRSV-nsp1β was found to inhibit the mRNA export, it was of interest to examine if nsp1β subverted host cellular protein synthesis. HeLa cells were co-transfected with individual genes for viral proteins and GFP, and GFP expression was examined by Western blot. As shown in Fig. 4.2C, nsp1β caused a notable reduction of GFP expression in comparison with pXJ41, which was consistent with the results from ISH and qRT-PCR. Taken together, it was concluded that nsp1β suppressed host protein synthesis by impairing mRNA export to the cytoplasm.

Two additional constructs of nsp1β, pPRRSV-nsp1β and pPRRSV-nsp1β-CF, were made to express nsp1β alone without tag and nsp1β with the C-terminal FLAG tag in addition to pPRRSV-NF-nsp1β which is nsp1β with the N-terminal FLAG tag (Fig. 4.2D, upper panel). NF-nsp1β and nsp1β resulted in identical patterns localized in the nucleus (Fig. 4.2D, panels A and E), and both constructs inhibited the mRNA nuclear export (Fig. 4.2D, panels B and F). On the contrary, nsp1β-CF localized in the cytoplasm (Fig. 4.2D, panel I) and this construct did not inhibit the mRNA nuclear accumulation (Fig. 4.2D, panel J). A ratio for nuclear red FIs was calculated for each construct in accordance with the formula; [(total FI $_{nucleus}$/ total FI $_{cytoplasm}$) nsp1β expressing cells/ (total FI $_{nucleus}$/ total FI $_{cytoplasm}$) nsp1β non-expressing cells]. The FI ratios for nsp1β and NF-nsp1β were approximately 2.4, while the FI ratio for CF-nsp1β was 1, indicating no mRNA accumulation in the nucleus by CF-nsp1β which was cytoplasmic (Fig. 4.2E). Inhibition of protein synthesis by each nsp1β construct was examined using the *Renilla* reporter assay (Fig. 4.2F) and GFP co-expression assay (Fig. 4.2G). In contrast to nsp1β and NF-nsp1β, CF-nsp1β did not inhibit protein expression, further demonstrating the requirement of nsp1β nuclear localization for mRNA nuclear retention.

**Suppression of mRNA nuclear export by nsp1 of arteriviruses:** Since PRRSV-nsp1β caused mRNA accumulation in the nucleus, it was plausible that nsp1 protein of other arterivirus might possess the similar inhibitory activity. To examine this, HeLa cells were co-transfected with individual subunits of arterivirus nsp1 along with the *Renilla* luciferase reporter, and total cell lysates were subjected to reporter assay. In the presence of LDV-nsp1β and SHFV-nsp1β, *Renilla* expression was reduced to the level of PRRSV-nsp1β (Fig. 4.3A). No significant reduction was observed for other constructs. In consistent with this finding, poly(A)+RNA

accumulation was evident in the nucleus of cells expressing PRRSV-nsp1β (Fig. 4.3B, panel F), LDV-nsp1β (Fig. 4.3B, panel N), and SHFV-nsp1β (Fig. 4.3B, panel Z). The average of red FIs in the nucleus was analyzed, and LDV-nsp1β and SHFV-nsp1β were shown to have similar intensities to that of PRRSV-nsp1β (Fig. 4.3C). 96%, 94%, and 90% of cells showed nuclear poly(A)+ RNA retention for PRRSV-nsp1β, LDV-nsp1β, and SHFV-nsp1β, respectively (Fig. 4.3D). These results indicate that the inhibition of mRNA nuclear export is common for PRRSV, LDV, and SHFV, but for EAV.

**nsp1β SAP mutants and inhibition of protein synthesis:** A papain-like proteinase domain (PLP1β) and a nuclease motif have been identified in the PRRSV-nsp1β protein (Xue et al., 2010). Analysis of the nsp1β sequence showed a conserved sequence at residues 123 to 138 that resembled the previously defined SAP domain for protein-nucleotide interactions (Fig. 4.4A; Aravind and Koonin, 2000). A structural motif of α-helix-turn-α-helix is found within the SAP domain, and three-dimensional structure of PRRSV-nsp1β shows an α-helix-turn-β-strand structure in the conserved sequence. The residues 124-KxLQxxLxxxGL-135 in PRRSV-nsp1β meet the SAP consensus motif in the first α-helix, xPLBxxHxxBxH, where P, B, and H indicate polar, bulky, and hydrophobic residues, respectively. Mutations introduced in the first α-helix of the SAP motif in the foot and mouth disease virus (FMDV) Lpro protein were sufficient to subvert the function of SAP. Hence, we assumed that this conserved sequence contained the SAP function, and accordingly a series of single mutation were individually introduced to the SAP motif of PRRSV-nsp1β (Fig. 4.4B).

To determine if the SAP mutants inhibited protein synthesis, the *Renilla* reporter assay and GFP co-expression were employed. With the exception of K124A and G134A, all other

mutants did not suppress *Renilla* expression in contrast to the wild-type nsp1β, and their *Renilla* expression was similar to the empty vector control (Fig. 4.5A). The GFP expression was reduced in the presence of K124A and G134A to the level of nsp1β (Fig. 4.5B, right upper panel), which was consistent with the results of *Renilla* reporter assay. Self-constraint expression was reported previously for PRRSV-nsp1β, and the R128A mutant was unable to inhibit the self-expression (Li et al., 2013). The self-expression of other SAP mutants were examined, and all of other mutants showed the comparable level expression to wild-type nsp1β with an exception of the R128A mutant (Fig. 4.5B, right middle panel), even though mutants L126A, R129A, L130A, and L135A did not inhibit host protein synthesis (Table 4.3).

The substitution of hydrophobic residues in SAP motif altered subcellular localization of FMDV $L^{pro}$ (de los Santos et al., 2009). Thus, it was of interest to determine whether their cellular distribution was also altered for SAP mutants of PRRSV-nsp1β. Plasmids for individual SAP mutants were transfected into MARC-145 cells for 24 h, and subcellular distribution of each mutant was determined by staining with anti-FLAG antibody. A predominant nuclear distribution was observed for K124A, R128A, and G134A, and their distribution patterns were identical with that of wild-type nsp1β (Fig. 4.5C, panels A, B, D, and G). In the contrast, L126A, R129A, L130A, and L135A were exclusively localized in the cytoplasm (Fig. 4.5C, panels C, E, F, and H). Their distribution patterns were confirmed by cell fractionation and Western blot (Fig. 4.5D). All mutants were detected in the cytoplasmic fraction, while nsp1β is found in the nuclear fraction for wild-type, K124A, R128A, and G134A. HSP90 and PARP were included as the cytosolic and nuclear protein controls, respectively, and they remained in their respective compartment (Fig. 4.5D, middle lower panel and middle upper panel), excluding the possibility of cross-contamination during cell fractionation. The distribution of L126A, R129A, L130A, and

L135A were not even in the cytoplasm (Fig. 4.5C, panels C, E, F, and H) but punctate, suggesting specific compartmental localization. MARC-145 cells were co-transfected with nsp1β, L126A, L130A, or G134A, together with DsRed2-Mito and pDsRed2-ER, which are specific markers for mitochondria (Fig. 4.5E, panel MITO) and endoplasmic reticulum (Fig. 4.5E, panel ER), respectively. Upon examination by confocal microscopy, L126A and L130A were found to localize in the mitochondria (Fig. 4.5E, panels, X and AB), suggesting L126A and L130A were localized in the mitochondria.

**Poly(A)+ RNA nuclear export by individual SAP mutants:** Since L126A, R128A, R129A, L130A, and L135A mutants did not suppress the protein synthesis, mRNA nuclear export was examined for each nsp1β SAP mutant. The nuclear retention of poly(A)+ RNA was evident for nsp1β (Fig. 4.6A, panel B), K124A (Fig. 4.6A, panel F), G134A (Fig. 4.6A, panel Z), while no nuclear accumulation was observed for L126A (Fig. 4.6A, panel J), R128A (Fig. 4.6A, panel N), R129A (Fig. 4.6A, panel R), L130A (Fig. 4.6A, panel V), and L135A (Fig. 4.6A, panel AD). The average nuclear FIs were measured for red and green florescence representing poly(A)+ RNA and nsp1β, respectively. nsp1β, K124A, and G134A resulted in the strong red and green FIs in the nucleus, but FIs for L126, R129, L130A, and L135A were weak. For R128A, weak red FIs but strong green FIs were observed in the nucleus, suggesting that the residue R128 was essential for poly(A)+ RNA nuclear retention but was not for its nuclear localization (Fig. 4.6B). The SAP mutants R128A and L135A were chosen to examine the relative amounts of nuclear mRNA (Fig. 4.6C). No significant regulations on selected genes were observed for the rest SAP mutants (Fig. 4.6B, upper panel). In comparison to nuclear mRNA levels by PRRSV-nsp1β, reduced levels of nuclear mRNA for DEPTOR, NOL6, and SH2 were observed by R128A and

L135A (Fig. 4.6C, lower panel), further suggesting that the SAP motif was important to retain mRNA in the nucleus.

**Suppression of innate immune signaling by SAP mutants:** PRRSV-nsp1β has been reported to participate in the suppression of IFN production pathway, IFN signaling pathway, and TNF-α production pathway, and thus it was of interest to determine whether nsp1β SAP mutants maintain the suppressive activities. To examine the modulation of IFN production, luciferase reporter assays were employed. Plasmids coding for SAP mutants were individually transfected with the reporter plasmids, followed by poly(I:C) stimulation for IFN induction. Virtually, all SAP mutants failed to suppress IFN responses compared to those by PRRSV-nsp1β with exceptions of K124A and G134A (Fig. 4.7A, left panel). R128A showed partial suppression on the IFNβ-Luc activity. L126A, R129A, L130A, and L135A did not cause the suppression on the IRF3-Luc activity (Fig. 4.7A, middle panel) and pRDII activity (Fig. 4.7A, right panel). To further confirm the modulation of IFN production by SAP mutants, IFN bioassays were conducted using VSIV-GFP as described previously (Han et al., 2014). Controls were included using the empty vector pXJ41 or pXJ41-GST, followed by poly(I:C) stimulation for production of IFN in the supernatant, which would restrict VSIV-GFP replication. For these controls, end point dilution for GFP expression was determined to be 1:16 (Fig. 4.7B). Cells incubated with the supernatant from cells expressing nsp1β, K124A, or G134A showed a limited inhibition of VSIV-GFP replication and their end points were determined to be 1:1 for each. The end point for R128A was 1:8, and for L126A, R129A, L130A, and L135A, their end points were determined to be 1:16, further confirming that SAP mutants L126A, R129A, L130A, and L135A lost the suppressive function in cells (Fig. 4.7B). The TNF-α promoter activity was also determined for

SAP mutants using luciferase reporter assay (Fig. 4.7C). Plasmids coding for SAP mutants were individually transfected with the TNF-α reporter plasmid, followed by LPS stimulation for TNF-α induction. Significant suppression of TNF-α promoter activity was identified for nsp1β, K124A, and G134A, while no suppression was determined for L126A, R129A, L130A, and L135A (Fig. 4.7C).

In addition to suppression of the production pathways of IFNs and TNF-α, PRRSV-nsp1β has been shown to suppress the JAK-STAT signaling pathway (Chen et al., 2010; Patel et al., 2010). We thus further examined the inhibitory activity of SAP mutants on the JAK-STAT signaling pathway. As shown in Fig. 4.7D, the ISRE-dependent luciferase expression was suppressed by wild type nsp1β, K124A, and G134A, and partially suppressed by R128A. In contrast, the mutants L126A, R129A, L130A, and L135A were unable to suppress ISRE-dependent luciferase expression (Fig. 4.7D). To confirm their suppressive effects on the IFN stimulated gene (ISG) expression through the JAK-STAT pathway, ISG15, whose expression is ISRE-dependent, was examined by Western blot (Fig. 4.7E). The reduction of ISG15 (upper panel) was identified in cells expressing nsp1β, L126A, and R128A, in comparison to that in mock-transfected cells. The suppression of ISG15 expression by nsp1β was relatively stronger than two other mutants. Our results demonstrate that the SAP motif is required for the inhibitory activity of nsp1β for innate immune response.

The mutant R128A did not inhibit the protein synthesis (Fig. 4.5) and mRNA nuclear export (Fig. 4.6), but partially suppressed the IFN production, TNF-α production, and IFN signaling (Fig. 4.7A to 4.7E). It was thus plausible that a complementary strategy might contribute to suppressions on innate immune responses besides nsp1β-inhibited mRNA export. A nuclease motif was found in nsp1β, and this motif was shown to degrade both single-strand RNA

and double-strand DNA (Xue et al., 2010). To determine if the nuclease motif is involved in IFN suppression, single or double mutations were introduced into the catalytic amino acid residues K18 and E32. Upon stimulation, the nuclease mutants K18A, E32A, and K18AE32A all maintained the suppressive activity on IFNβ-Luc (Fig. 4.7F). To exclude the influence by nsp1β-inhibited mRNA export, mutations R128A or R129A were introduced to the mutant K18AE32A to generate mutants K18AE32AR128A and K18AE32AR129A, designed as NuR128A and NuR129A, respectively. The mutant NuR128A showed a partial suppression which was comparable to the R128A-meidated suppression (Fig. 4.7G), indicating that the nuclease motif was not essential to suppress IFN production. To clarify if mRNA level was reduced by nsp1β, HeLa cells were co-transfected with pIFN-β-Luc and pTK-RL along with individual nsp1β mutant constructs, and mRNA levels of Firefly and Renilla were determined by qRT-PCR after poly(I:C) stimulation (Fig. 4.7H). In the presence of nsp1β and the mutant K18AE32A, both Firefly and Renilla mRNA levels were reduced by 0.6 and 0.7 folds, respectively, in comparison with controls. These results show that nsp1β decreased host cellular mRNA level along with blocking mRNA export from the nucleus.

**Characterization of SAP mutant viruses:** To verify the SAP function during virus infection, mutant viruses harboring mutations in the SAP motif were generated (Fig. 4.4B) by reverse genetics. Seven SAP mutant viruses were attempted to generate using infectious clones: vK124A, vL126A, vG134A, vL135A, vR128A, vR129A, and vL130A. Of these constructs, vR128A, vR129A, and vL130A were non-available as determined by IFA and Western blot for N protein expression in cells incubated with P1 virus. The stability of mutations was determined by sequencing after five passages in MARC-145 cells, and all mutations were maintained in the

respective mutant viruses. Individual SAP mutant viruses were titrated using P1, P2, and P3 viruses, and the titers for P3 virus of vK124A, vL126A, and vL135A reached $10^4$, $10^{3.67}$, and $10^{3.83}$ $TCID_{50}$, respectively, in comparison with the titer of $10^5$ $TCID_{50}$ for the wild type PRRSV (Fig. 4.8A). The P3 titer for vG134A was $10^{5.83}$ $TCID_{50}$ in particular. The multi-step growth kinetics analysis revealed that the mutant viruses vL126A and vL135A exhibited decreased growth kinetics with a peak titer that was approximately 100-fold and 10-fold less compared to titers of wild-type PRRSV vFL13 (Fig. 4.8B) and vK124A, respectively. The mutant virus vG134A exhibited similar growth kinetics as the parental virus (Fig. 4.8B). The mutant viruses vL126A and vL135A also produced reduced size of plaques as compared to wild-type vFL13 (Fig. 4.8C). Overall, these results suggest that the SAP motif was essential for PRRSV replication.

The subcellular localization of nsp1β was examined in MARC-145 cells infected with SAP mutant viruses (Fig. 4.8D). Nuclear staining was found in cells infected with vFL13 (panel A), vK124A (panel E), and vG134A (panel M), but not in cells infected with vL126A (panel I) and vL135A (panel Q), which was consistent with the results from gene-transfected cells. The analysis of average nuclear red (nsp1β) FIs in infected cells showed strong FIs for vFL13, vK124A, and vG134A (Fig. 4.8D, right panel). Limited amounts of nsp1β were shown in the nuclear fractions for vL126A and vL135A (Fig. 4.8E, upper panel), furthering confirming that the SAP motif was important for the nsp1β nuclear localization. HSP90 and PARP as the cytosolic and nuclear proteins markers, respectively, remained in their respective compartments (Fig. 4.8E, lower panel and second lower panel).

**mRNA nuclear export in cells with SAP mutants infection:** Since exclusive cytoplasmic distribution of nsp1β was seen for vL126A and vL135A infections, it was of interest to determine if mRNA was retained in the nucleus in vL126A-infected and vL135A-infected cells. To determine this, MARC-145 cells were infected with each of SAP mutant viruses for 24 h followed by ISH assay (Fig. 4.9A). mRNA nuclear retention was significant in cells infected with vFL13 (panel F), vK124A (panel J), and vG134A (panel R), but it was not seen in cells infected with vL126A (panel N) and vL135A (panel V). Since vL126A and vL135A did not inhibit mRNA export from the nucleus, it was assumed that these two mutant viruses were unable to suppress innate immune responses. To confirm this premise, IFNβ-Luc reporter assay was performed as described elsewhere (Li et al., 2013). As shown in Fig. 4.9B, the replication of vFL13 and vG134A significantly inhibited IFN promoter-driven luciferase activities in comparison with that of pXJ41-transfected cells. On the contrary, the suppression was reverted after transfection with the infectious clones L126A and L135A.

## 4.5. DISCUSSION

Most cellular mRNAs are translated by the cap-dependent scanning mechanism that requires the binding of mRNA with the translation apparatus. For positive-strand RNA viruses, their genomes act as mRNA to direct the synthesis of viral proteins, especially the RNA-dependent RNA polymerase (RdRp) that is used for genome replication (Ahlquist et al., 2003). For viruses containing the internal ribosome entry sequence (IRES) such as picornaviruses, they gain benefits from impaired translation of cellular mRNAs during infection, enhancing IRES-driven viral protein synthesis (Martinez-Salas et al., 2008). Arterivirus genomes are 5′-capped (Snijder et al., 2013), and thus a cap-dependent synthesis is required to produce viral proteins. To

guarantee rapid translation of arterivirus proteins, blocking access of cellular mRNA to translation apparatus is an ideal strategy for arteriviruses. Blocking interactions of cellular mRNAs and ribosomes have been identified in coronaviruses such that nsp1 degrades host cell mRNAs or inactivates ribosomes. Using the reporter system, herein we have found the PRRSV-mediated down-regulation of reporter expression and inhibition of mRNA export from the nucleus (Fig. 4.1). This finding is novel for nidoviruses. By nuclear imprisonment, host cell mRNAs hardly access the cytoplasm for translation, while PRRSV genomic RNA can recruit ribosomes for viral protein synthesis with less competition with cellular mRNAs. The mRNA nuclear retention is observed in cells infected with different strains of PRRSV representing both genotype I and genotype II, suggesting that this strategy is extensively utilized by PRRSV.

The cytoplasm is the site for PRRSV to complete its replication cycle, whereas three viral proteins, nsp1α, nsp1β, and N protein, are localized in the nucleus of infected cells or gene-transfected cells (Chen et al., 2010; Han et al., 2014; Li et al., 2012; Rowland and Yoo, 2003). The nuclear localization of N protein relies on the nuclear localization signal (NLS), which has been determined as a virulence factor (Pei et al., 2008). Infection of pigs with NLS-null mutant PRRSV induced higher titers neutralizing antibodies and the duration of viremia was shortened (Pei et al., 2008). The nuclear form of nsp1α participates in CBP degradation (Han et al., 2013), whereas the subcellular distribution of nsp1β varies between gene-transfected cells and virus-infected cell. Nsp1β is distributed predominantly in the nucleus in gene-transfected cells (Fig. 4.2A), but in virus-infected cells, the majority of nsp1β appears in the perinuclear region with lesser in the nucleus (Fig. 4.1). Such an observation in virus-infected cells is probably due to the interactions among nsp1β and other viral replicase proteins. Besides, the nsp1β nuclear localization may be time-dependent since not all infected cells show the nsp1β in the nucleus

(Fig. 4.1F). Studies are needed to investigate the basis for nsp1β nuclear distribution. In the present study, we have demonstrated that impaired mRNA export is associated with the nsp1β protein in the nucleus. In PRRSV-infected cells, mRNA nuclear retention was significant in concert with nsp1β nuclear staining (Fig. 4.1F). According to the time course experiment, mRNA retention is observed as early as 8 h post-transfection, which is coincident with the first appearance of nsp1β in the nuclear by staining (Fig. 4.1E). The molecular basis of nsp1β-mediated mRNA nuclear retention needs to be further elucidated.

The activation of several signaling pathways including the IFN production, IFN signaling, and TNF-α production pathways has shown to be suppressed by PRRSV-nsp1β (Beura et al., 2010; Patel et al., 2010; Subramaniam et al., 2010), which is likely due to the nsp1β-mediated impairment of mRNA export. All nsp1 subunits of arteriviruses contain IFN suppression activities, and the CBP degradation in particular was evident by PRRSV-nsp1α, LDV-nsp1α, and SHFV-nsp1γ (Han et al., 2014). The molecular basis for IFN suppression by PRRSV-nsp1β, LDV-nsp1β, EAV-nsp1, and SHFV-nsp1αβ still remain to be determined. By separating SHFV-nsp1αβ into SHFV-nsp1α and SHFV-nsp1β, the motif for IFN downregulation was identified to locate in the nsp1β portion (Han and Yoo, 2014). Since PRRSV-nsp1β inhibits the protein expression by blocking the mRNA export, the same strategy may be taken by other arteriviruses. LDV-nsp1β and SHFV-nsp1β suppressed the protein synthesis, and this observation was consistent with the findings from ISH assays that mRNA export was inhibited by these two proteins (Fig. 4.3). Interestingly, both LDV-nsp1β and SHFV-nsp1β are distributed in the nucleus, which is the pattern identical to that of PRRSV-nsp1β. However, mRNA nuclear accumulation is not observed for EAV-nsp1, even though EAV-nsp1 is a nuclear protein, suggesting a different mechanism for EAV-nsp1-mediated IFN suppression.

The SAP motif is found in some cellular nuclear proteins besides PRRSV-nsp1β, including the scaffold attachment factors A and B (SAF-A and -B), protein inhibitors of activated STAT (PIAS), and myocardia (Aravind and Koonin, 2000; Kipp et al., 2000; Okubo et al., 2004; Wang et al., 2002). The SAP motif is essential for binding to AT-rich DNA sequences present in scaffold-attachment region/matrix-attachment region (SAR/MAR) (Aravind and Koonin, 2000). In addition, it is reported that the signature motif of LxxLL in the N-terminal region of SAP domain of PIASy critically leads to the inhibition of STAT1-dependent transcription, whereas a SAP mutant of PIASy does not inhibit type I IFN transcription (Kubota et al., 2011; Liu et al., 2001). The SAP domain is also found in the leader proteinase ($L^{pro}$) of foot-and-mouth disease virus (FMDV), and mutations introduced into the conserved SAP motif prevent the nuclear retention of Lpro and degradation of NF-κB (de los Santos et al., 2009). Remarkably, SAP-mutant FMDV was attenuated and did not cause clinical signs, and the animals developed a strong neutralizing antibody response (Segundo et al., 2012). The composition of SAP motif found in PRRSV-nsp1β meets the SAP consensus identified in cellular proteins (Fig. 4.4), especially three hydrophobic residues of L126, L130, and L135 are highly maintained in PRRSV-nsp1β.

A highly conserved sequence of 123-GKYLQRRLQ-131 has been reported in PRRSV-nsp1β, which is partially overlapped with the SAP motif, and mutant K124A/R128A impairs nsp1β-mediated IFN suppression (Li et al., 2013). In our study, the SAP mutants L126A, R129A, L130A, and L135A also resulted in the reversion of IFN suppression but the molecular basis differs from that of K124A/R128A mutation. As summarized in Table 4.4, no mRNA nuclear retention was observed in cells expressing indicated mutants, except mutant R128A which is still localized to the nucleus. In contrast, mutants L126A, R129A, L130A, and L135A remained in

the cytoplasm and were co-localized with the mitochondria marker protein, suggesting the hydrophobic residues in the SAP motif are essential for nuclear translocation of PRRSV-nsp1β. Surprisingly, the subcellular distribution pattern of mutant R129A was identical to those of leucine mutants (Fig. 4.5). PRRSV-nsp1β suppressed innate immune responses (Han and Yoo, 2014), and the SAP mutants L126A, R129A, L130A, and L135A failed to inhibit the IFN production, IFN signaling, and TNF-α induction pathways in addition to the mRNA nuclear accumulation (Fig. 4.6 and 4.7), demonstrating that nsp1β-mediated mRNA nuclear retention is closely associated with the nsp1β-regulated innate immunity. Mutant R128A showed partial reversion of inhibition and this mutant did not block mRNA export (Fig. 4.6 and 4.7), suggesting that the inhibition of mRNA export is not the only mechanism for nsp1β-mediated suppression.

The leucine residues within the SAP motif were found to be essential for mRNA nuclear retention, and subsequently two viable mutant viruses vL126A and vL135A were generated by reverse genetics (Fig. 4.8). Mutants vR128A, vR129A, and vL130A were non-viable (Fig. 4.8). For these two mutant viruses, growth was impaired compared to wild-type PRRSV vFL13 and vG134A (Fig. 4.8). nsp1β was retained in the cytoplasm for vL126A and vL135A, and no mRNA nuclear accumulation was found, which was consistent with the findings in gene-transfected cells (Fig. 4.5). In addition, IFN suppression was decreased, indicating that mRNA nuclear retention contributes to host innate immune gene expression, which may lead to viral replication. nsp1β functions as a transactivator to induce -1/-2 frameshifting in the nsp2 region of PRRSV to produce nsp2TF and nsp2N, and nsp1β-knock out virus (1βKO) fails to express nsp2TF and nsp2N (Li et al., 2014). The SAP leucine residues are in close proximity to the mutated residues of 1βKO, and thus it is plausible that the SAP mutant viruses vL126A and vL135A may be unable to produce nsp2TF and nsp2N as well.

In summary, we have shown that PRRSV infection causes host cell mRNA retention in the nucleus and thus inhibits host cell protein synthesis, and that PRRSV-nsp1β is the viral responsible for the nuclear imprisonment. A SAP motif is identified in the nsp1β protein, and this motif is shown to be essential for the nsp1β subcellular distribution, mRNA nuclear retention, modulation of innate immunity, and PRRSV replication.

## 4.6. FIGURES AND TABLES

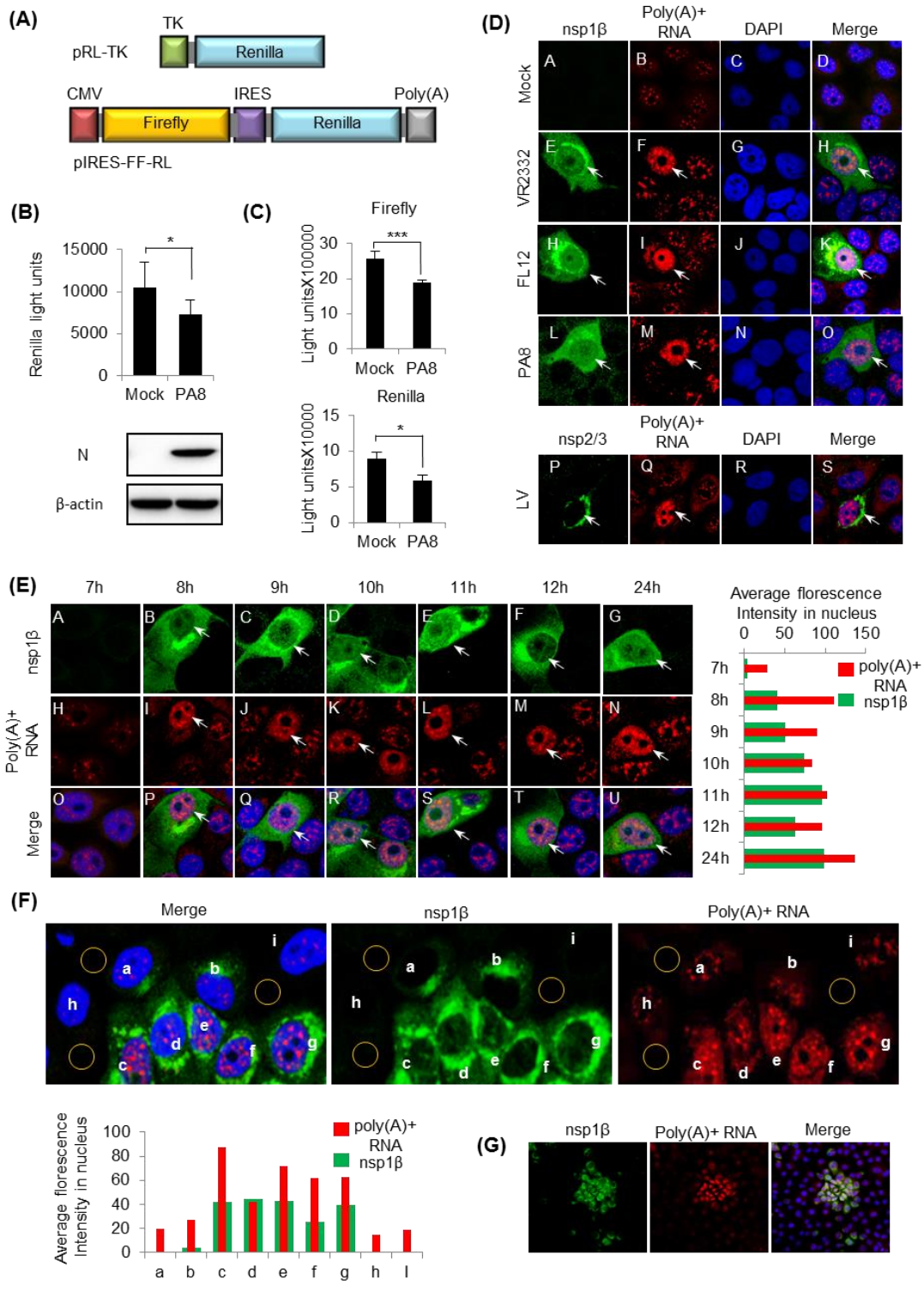


**Fig. 4.1.**

**Fig. 4.1. Inhibition of poly(A)+ RNA nuclear export by PRRSV.** (A) Schematic diagram of the reporter constructs. The Renilla luciferase plasmid pRL-TK contains the HSV-tk promoter. The bicistronic DNA plasmid pIRES-FF-RL contains a copy of the firefly gene under the CVM promoter and a copy of the Renilla gene downstream of IRES. (B) MARC-145 cells were infected with PRRSV PA8 strain for 24 h and transfected with the plasmid pRL-TK for 16 h. Luciferase activities were measured using the Dual-Glo Luciferase assay system (Promega). The data represent the means of three independent experiments, each experiment in triplicate. Statistical significance in fold changes of relative luciferase activity are indicated as follows: *, $P<0.05$; **, $P<0.01$; ***, $P<0.001$. (C) The expression of firefly and Renilla under PRRSV infection. (D) In situ hybridization (ISH) in cells infected with different strains of PRRSV. North American (NA) type PRRSV VR2332, FL12, PA8, and European (EU) type PRRSV LV were used to infect MARC-145 cells for 24 h. Anti-nsp1β and anti-nsp2/3 rabbit antisera (green) were used to stain cells infected by NA PRRSV and EU PRRSV, respectively. Poly(A)+ RNA was hybridized with the biotinylated oligo(dT) probe followed by staining with Cy3-streptavidin (in red). Arrows indicate PRRSV-infected cells. (E) Distribution of cellular poly(A)+ RNA in PRRSV-infected cells at various times. MARC-145 cells were infected with PRRSV PA8 at an m.o.i. of 5, and cells were fixed at indicated times. Average florescence intensities (FIs) in the nucleus of PRRSV-infected cells were quantified using the NIH ImageJ software (U. S. National Institutes of Health, Bethesda, Maryland; right panel). Red bars indicate the average FIs of poly(A)+ RNA and green bars indicate average FIs of nsp1β. Arrows indicate PRRSV-infected cells. (F) Distribution of cellular poly(A)+ RNA in different cells at 24 h post-infection of PRRSV. Nine individual cells were randomly chosen to examine the average FIs in the nucleus. Average FIs were calculated using the background FIs from three yellow cycles. (G) Low magnification images of the poly(A)+ RNA nuclear retention in PRRSV-infected cells.

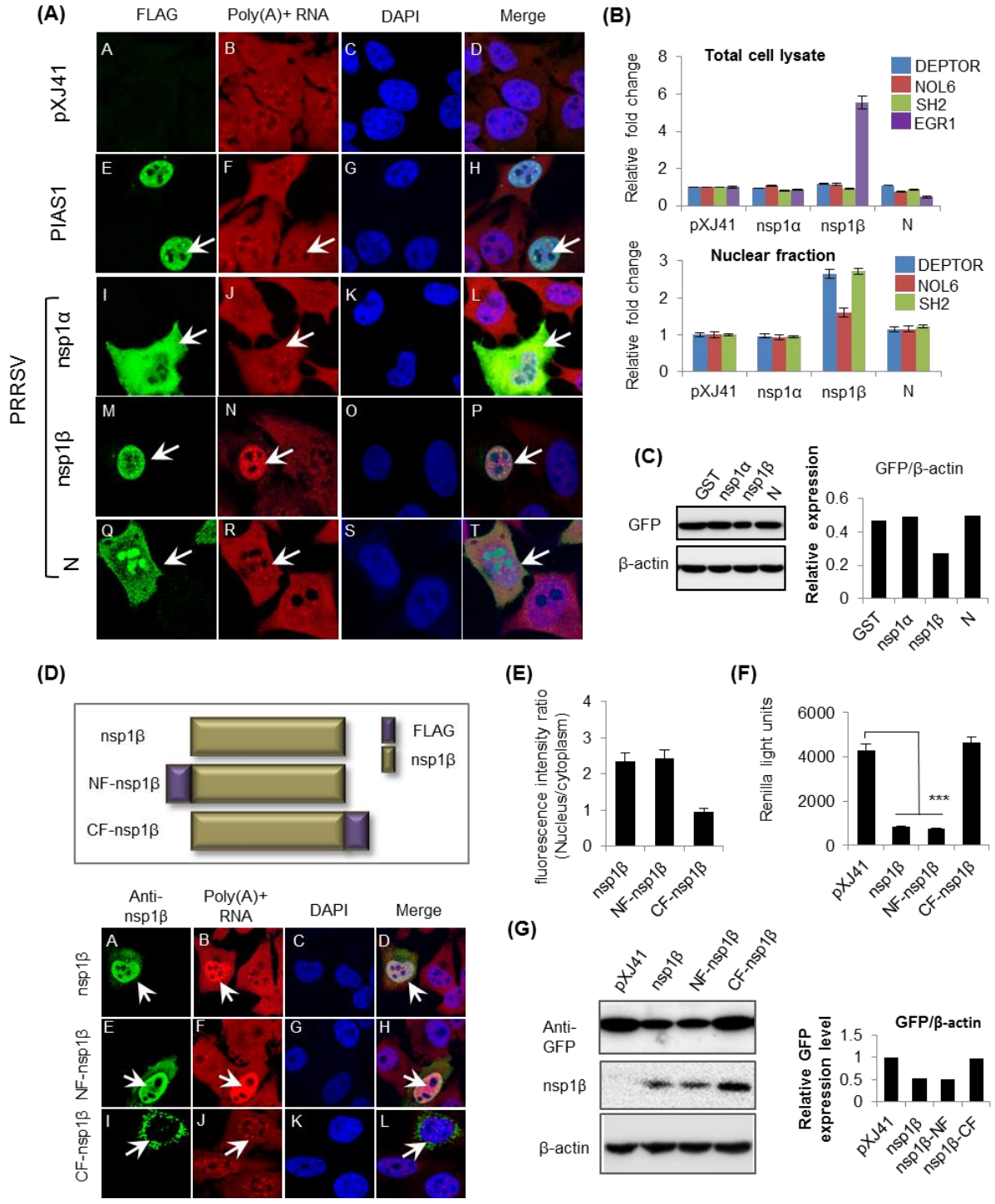
(A)
FLAG
Poly(A)+ RNA
DAPI
Merge
pXJ41
PIAS1
nsp1α
nsp1β
N
PRRSV
(B)
Total cell lysate
DEPTOR
NOL6
SH2
EGR1
Relative fold change
pXJ41
nsp1α
nsp1β
N
Nuclear fraction
(C)
GST
nsp1α
nsp1β
N
GFP
β-actin
GFP/β-actin
Relative expression
(D)
nsp1β
FLAG
NF-nsp1β
CF-nsp1β
Anti-nsp1β
Poly(A)+ RNA
DAPI
Merge
(E)
fluorescence intensity ratio (Nucleus/cytoplasm)
(F)
Renilla light units
***
(G)
pXJ41
nsp1β
NF-nsp1β
CF-nsp1β
Anti-GFP
β-actin
GFP/β-actin
Relative GFP expression level
nsp1β-NF
nsp1β-CF

**Fig. 4.2.**

**Fig. 4.2. PRRSV-nsp1β-mediated suppression of host cell protein synthesis**. (A) Inhibition of poly(A)+ RNA nuclear export in nsp1β gene-transfected cells. HeLa cells were grown to 80% confluency and transfected for 24 h with indicated genes fused with the N-terminal FLAG tag. Cells were then fixed with 4% paraformaldehyde and proceeded for ISH. Cellular localization of individual gene products (green) and poly(A)+ RNA (red) were examined by confocal microscopy (Zeiss). Arrows indicate gene-transfected cells. (C) Co-expression of GFP with nsp1β. One μg of pEGFP-N1 expressing GFP and one μg of nsp1β or other genes were co-transfected into HeLa cells for 24 h, and total cell lysates were subjected to Western blot using anti-GFP antibody (top panel). GFP expressions were quantified using the AlphaView software (Proteinsample, San Jose, California), and normalized using β-actin. (B) qRT-PCR for DEPTOR, NOL6, SH2, and EGR1 mRNAs in nsp1β gene-transfected cells. HeLa cells were individually transfected with plasmids pXJ41 (empty vector), pPRRSV-F-nsp1α, pPRRSV-F-nsp1β, and pPRRSV-F-N. At 24 h post-transfection, total cellular RNA and nuclear RNA were extracted separately, and treated with DNase I. Relative fold changes of each target mRNA in either total cell lysates (upper panel) or nuclear fraction (low panel) were calculated. (D) Nuclear export of poly(A)+ RNA by different constructs of nsp1β. pPRRSV-F-nsp1β and pPRRSV-nsp1β-F were constructed to express PRRSV-nsp1β with the N-terminal (NF-nsp1β) or C-terminal (CF-nsp1β) FLAG tags. No FLAG tag was attached for pPRRSV-nsp1β (upper panel). ISH was performed to show the distribution of poly(A)+ RNA (red) in gene-transfected cells. Anti-PRRSV-nsp1β Ab was used to examine the expression of nsp1β (green). White arrows indicate nsp1β-expressing cells. (E) Relative ratios of nuclear and cytoplasmic FIs in nsp1β-transfected cells. The total FIs of poly(A)+ RNA (red , low panel, Fig. 2D) in the nucleus and cytoplasm in nsp1β-expressing cells and non-expressing cells were analyzed using the NIH ImageJ software. Relative FI ratios (nucleus/cytoplasm) were calculated using the following formula; [(total FI nucleus/ total FI cytoplasm) nsp1β expressing cells/ (total FI nucleus/ total FI cytoplasm) nsp1β non-expressing cells]. (F) The Renilla reporter pRL-TK was co-transfected with individual nsp1β-expressing plasmids, Renilla reporter activities were determined by Dual-Glo Luciferase assay system (Promega). The data represent the means of three independent experiments, each experiment in triplicate. Statistical significance in fold changes of relative luciferase activity are indicated as follows: *, $P<0.05$; **, $P<0.01$; ***, $P<0.001$ (G) The GFP-expressing vector pEGFP-N1 was co-transfected with pXJ41, pPRRSV-nsp1β, pPRRSV-F-nsp1β, or pPRRSV-nsp1β-F in HeLa cells followed by Western blot to determine GFP expression. GFP expression was quantified using AlphaView software and normalized using β-actin expression. The quantities of GFP in nsp1β-expressing cells were normalized again using the background in pXJ41-transfected cells and the relative GFP expression was determined.

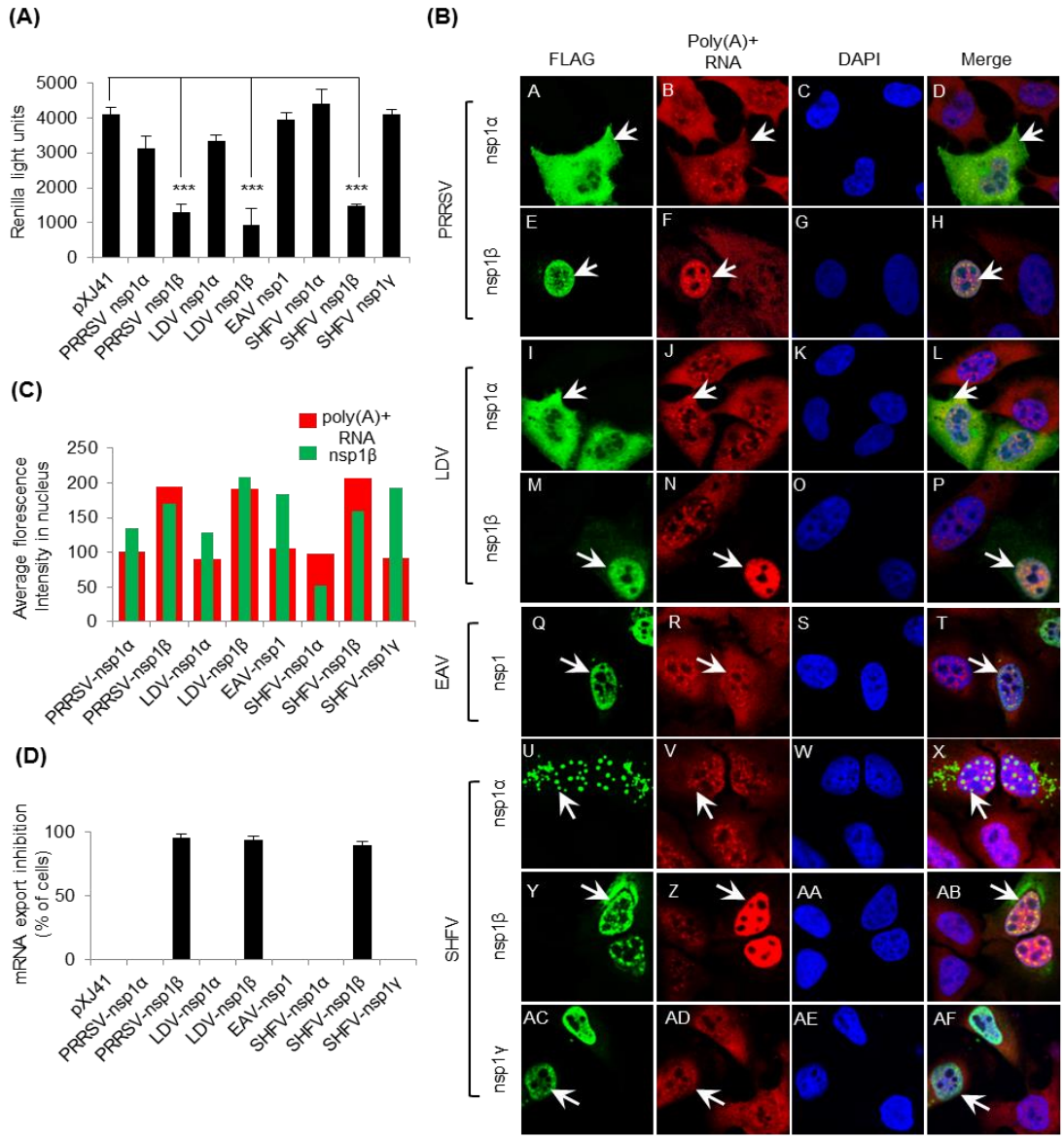


**Fig. 4.3. Inhibition of poly(A)+ RNA nuclear export by nsp1 subunits in arteriviruses.** (A) HeLa cells were co-transfected with individual constructs expressing arterivirus nsp1 subunits together with the Renilla reporter, and the Renilla activities were determined by Dual-Glo Luciferase assay system (Promega). The data represent the means of three independent experiments, each experiment in triplicate. Statistical significance in fold changes of relative luciferase activity are indicated as follows: *, $P<0.05$; **, $P<0.01$; ***, $P<0.001$. (B) ISH in cells expressing arterivirus nsp1 subunits. HeLa cells were transfected with individual arterivirus nsp1 constructs, and cellular localization of nsp1 (green) and poly(A)+ RNA (red) were examined by confocal microscopy (Zeiss). White arrows indicate nsp1-expressing cells. (C) In the nucleus of the cell expressing arterivirus nsp1 subunits, the average FIs were analyzed for green and red by NIH ImageJ software. Red and green bars indicate the average florescence intensity of poly(A)+ RNA and nsp1β, respectively. (D) The percentage of cells showing significant nuclear poly(A)+ RNA retention was calculated using the following formula; (Number of cells showing significant nuclear poly(A)+ RNA staining intensity compared to the control nuclear poly(A)+ RNA staining intensity out of 50 nsp1-expressing cells/(50 cells expressing nsp1) x 100.

.

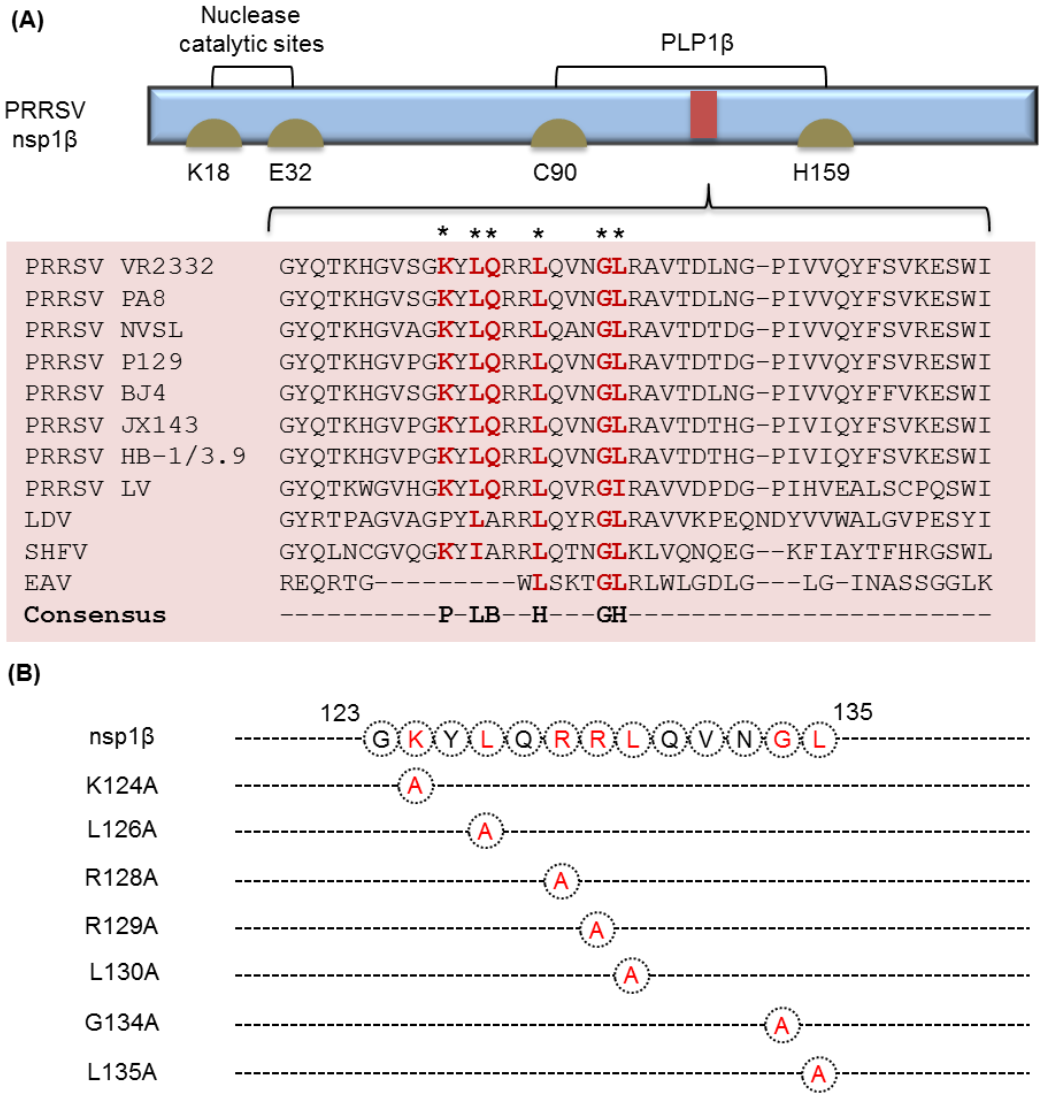


**Fig. 4.4. Identification of SAP motif in PRRSV-nsp1β and introduction of mutations.** (A) Domains in PRRSV-nsp1β and identification of SAP motif in arterivirus nsp1. The catalytic sites for nuclease and PLP1β are indicated (Fang and Snijder, 2010; Xue et al., 2010). Single letter alphabets indicate amino acids, and numbers indicate positions. Red box indicates the area of conserved sequences resembling the SAP motif. Multiple sequence alignments of the SAP motif of nsp1 of arteriviruses were constructed using Clustal X2.1. PRRSV VR2332 strain (GenBank accession no. U87392), PA8 strain (GenBank accession no. AF176348), NVSL 97-7895 strain (GenBank accession no. AY545985), P129 strain (GenBank accession no. AF494042), JX143 strain (GenBank accession no. EU708726), HB-1/3.9 strain (GenBank accession no. EU360130), LV strain (GenBank accession no. M96262), LDV Plagemann strain (GenBank accession no. U15146.1), EAV Bucyrus strain (GenBank accession no.DQ846750), and SHFV (GenBank accession no. AF180391). The SAP consensus around the first α-helix is xPLBxxHxxBxH consisting of H (hydrophobic) or L (aliphatic) residues (YFWLIVMA); P (polar) residues (STQNEDRKH); and B (bulky) residues (KREQWFYLMI) (Aravind and Koonin, 2000). Residues that meet the consensus of SAP motif are marked in red color and indicated with asterisks. (B) Encircled letters indicate the conserved sequence within the SAP motif, and the red letters indicate amino acid substitutions.

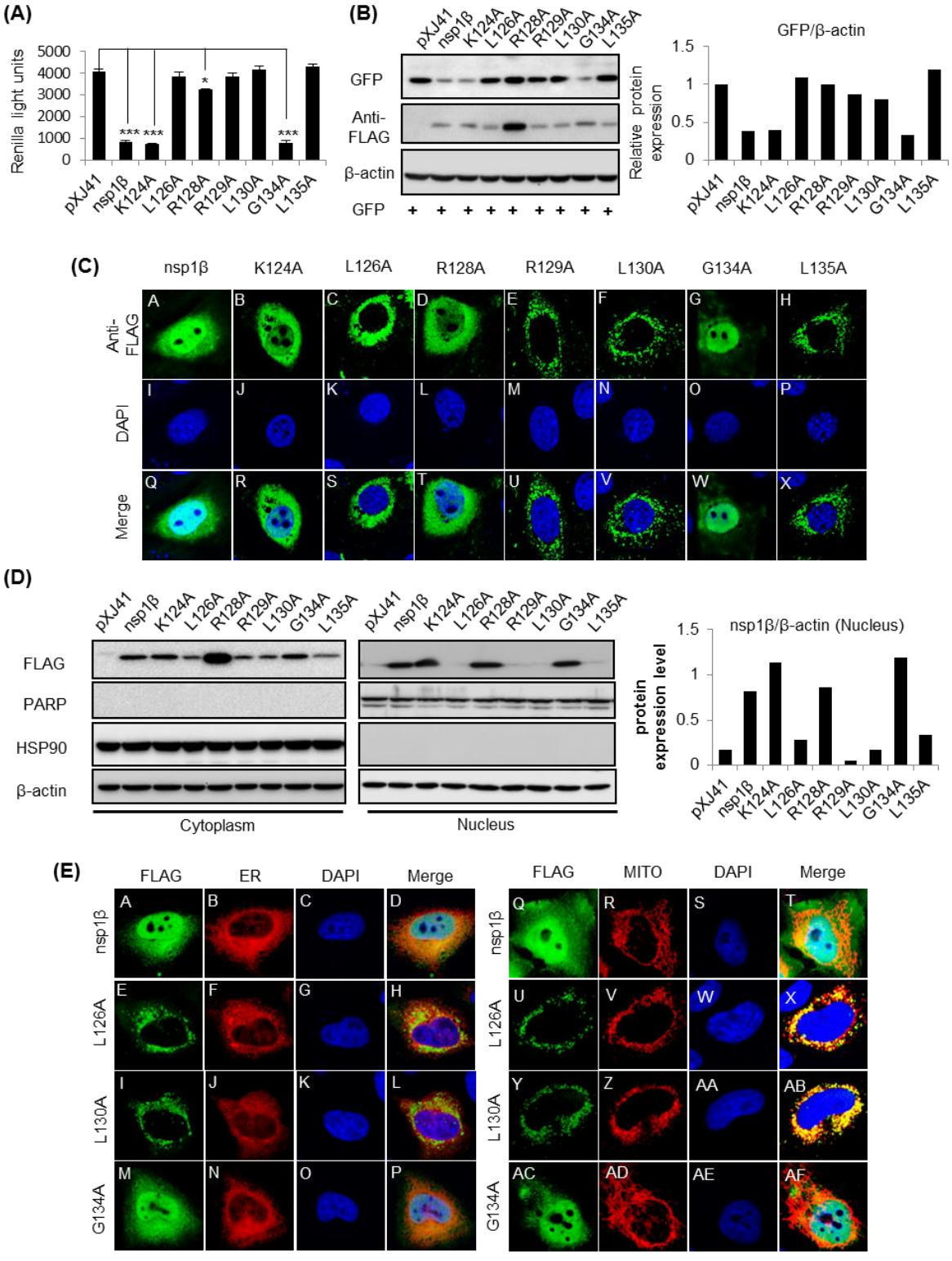
(A)
Renilla light units
5000
4000
3000
2000
1000
0
***
***
*
***
pXJ41
nsp1β
K124A
L126A
R128A
R129A
L130A
G134A
L135A
(B)
pXJ41
nsp1β
K124A
L126A
R128A
R129A
L130A
G134A
L135A
GFP
Anti-FLAG
β-actin
GFP
+ + + + + + + + +
Relative protein expression
GFP/β-actin
1.5
1
0.5
0
(C)
nsp1β
K124A
L126A
R128A
R129A
L130A
G134A
L135A
Anti-FLAG
DAPI
Merge
A
B
C
D
E
F
G
H
I
J
K
L
M
N
O
P
Q
R
S
T
U
V
W
X
(D)
pXJ41
nsp1β
K124A
L126A
R128A
R129A
L130A
G134A
L135A
FLAG
PARP
HSP90
β-actin
Cytoplasm
Nucleus
nsp1β/β-actin (Nucleus)
protein expression level
1.5
1
0.5
0
(E)
FLAG
ER
DAPI
Merge
FLAG
MITO
DAPI
Merge
nsp1β
L126A
L130A
G134A
A
B
C
D
E
F
G
H
I
J
K
L
M
N
O
P
Q
R
S
T
U
V
W
X
Y
Z
AA
AB
AC
AD
AE
AF

**Fig. 4.5.**

**Fig.4.5. Subcellular localization of nsp1β SAP mutants and inhibition of cellular protein synthesis by SAP mutants.** HeLa cells were co-transfected with the Renilla reporter pRL-TK (A) or GFP-expressing pEGFP-N1 (B), along with individual SAP mutants. Renilla activities and GFP expressions were determined by Dual-Glo Luciferase assay system (A, Promega) and Western blot using anti-GFP antibody (B). The data represent the means of three independent experiments, each experiment in triplicate. Statistical significance in fold changes of relative luciferase activity are indicated as follows: *, $P<0.05$; **, $P<0.01$; ***, $P<0.001$. GFP expression was quantified using AlphaView software (Fig. 5B, right panel) and normalized with the use of β-actin. Relative GFP expression levels for nsp1β and each SAP mutants were calculated after normalization using GFP background in pXJ41-transfected cells. (C) Cellular distribution of SAP mutant proteins in MARC-145 cells. MARC-145 cells were grown to 80% confluency and transfected with indicated SAP mutants for 24 h. Cells were stained with anti-FLAG Ab followed by staining with Alexa 488-labeled anti-mouse Ab (green) and DAPI (blue). Staining signals were examined by confocal microscopy (Zeiss). (D) Nuclear localization of SAP mutants. MARC-145 cells expressing individual SAP mutants were fractionated followed by Western blot using anti-FLAG Ab (upper panel), anti-PARP Ab (second panel) as a nuclear protein marker, and anti-HSP90 Ab as a cytosolic protein marker (third panel), and β-actin antibody as a loading control (bottom panel). The nuclear fraction of each SAP mutants was quantified by normalizing with β-actin (left panel). (E) Localization of SAP mutants in the mitochondria. MARC-145 cells were co-transfected with individual SAP mutants and pDsRed2-ER (left panel) or pDsRed2-Mito (right panel) for 24 h, and subcellular localization of individual SAP mutants was examined by confocal microscopy (Zeiss).

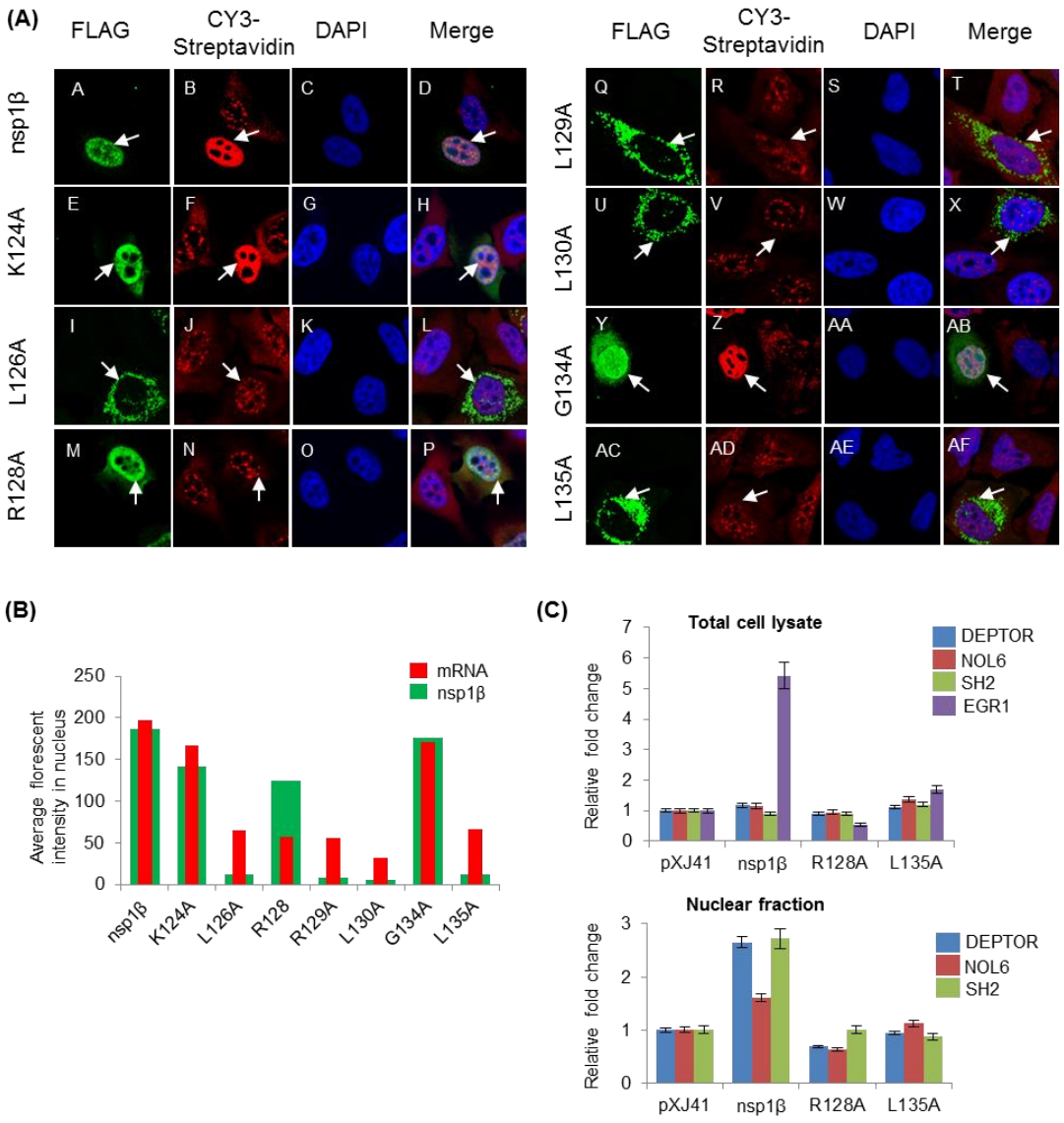


**Fig. 4.6. Nuclear retention of poly(A)+ RNA in SAP-mutant nsp1β-expressing cells.** (A) HeLa cells were transfected with individual SAP mutants for 24 h, and cellular distribution of poly(A)+ RNA was examined by ISH. (B) In the nucleus of the cell expressing SAP mutants, the average FIs for green and red were analyzed using NIH ImageJ software. Red and green bars indicate the average FIs of poly(A)+ RNA and nsp1β, respectively. (C) qRT-PCR for chosen mRNA in cells expressing the SAP mutants. HeLa cells were individually transfected with pXJ41 (empty vector), pPRRSV-F-nsp1β, R128A, and L135A. At 24 h post-transfection, total cellular RNAs and nuclear RNAs were extracted separately, and treated with DNase I. The mRNA levels of DEPTOR, NOL6, SH2, and EGR1 were examined. The relative fold changes of each target mRNA in either total cell fraction (upper panel) or nuclear fraction (low panel) were calculated.

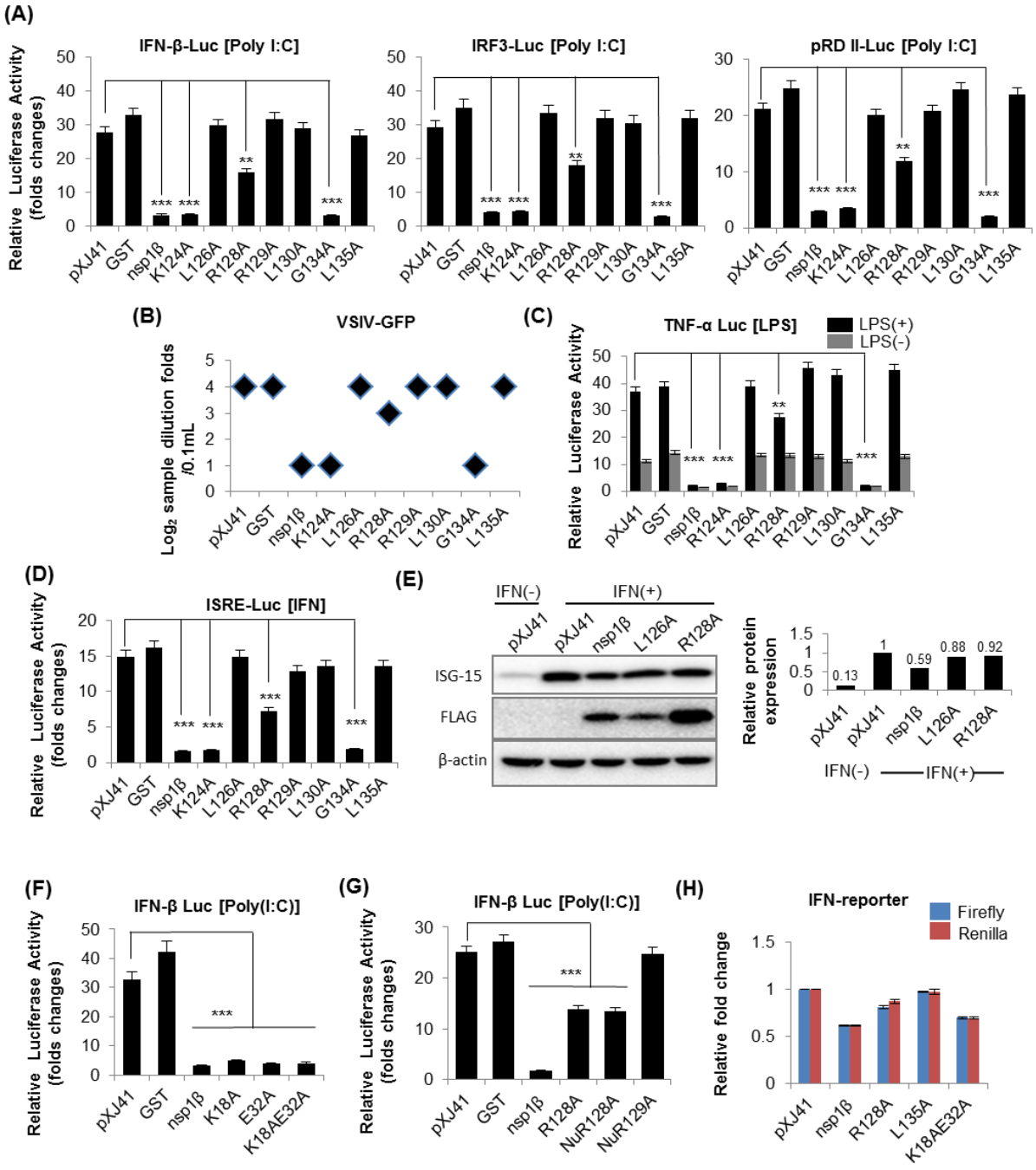
(A)
IFN-β-Luc [Poly I:C]
IRF3-Luc [Poly I:C]
pRD II-Luc [Poly I:C]
Relative Luciferase Activity (folds changes)
pXJ41 GST nsp1β K124A L126A R128A R129A L130A G134A L135A
(B)
VSIV-GFP
Log2 sample dilution folds /0.1mL
(C)
TNF-α Luc [LPS]
LPS(+)
LPS(-)
Relative Luciferase Activity
pXJ41 GST nsp1β R124A L126A R128A R129A L130A G134A L135A
(D)
ISRE-Luc [IFN]
Relative Luciferase Activity (folds changes)
(E)
IFN(-)
IFN(+)
pXJ41 pXJ41 nsp1β L126A R128A
ISG-15
FLAG
β-actin
Relative protein expression
0.13 1 0.59 0.88 0.92
(F)
IFN-β Luc [Poly(I:C)]
Relative Luciferase Activity (folds changes)
pXJ41 GST nsp1β K18A E32A K18AE32A
(G)
IFN-β Luc [Poly(I:C)]
Relative Luciferase Activity (folds changes)
pXJ41 GST nsp1β R128A NuR128A NuR129A
(H)
IFN-reporter
Firefly
Renilla
Relative fold change
pXJ41 nsp1β R128A L135A K18AE32A

**Fig. 4.7.**

**Fig. 4.7. Suppressions of innate immune signaling by SAP mutants.** (A) Regulation of type I IFN production by SAP mutants. Plasmids pIFN-β-Luc (left panel), p4×IRF3-Luc (middle panel), or pRD II-Luc (right panel) were transfected to cells to examine IFN promoter activities. Relative luciferase activities were calculated by normalizing the firefly luciferase to Renilla luciferase activities according to the manufacturer's protocol. The data represent the means of three independent experiments, each experiment in triplicate. The data represent the means of three independent experiments, each experiment in triplicate. Statistical significance in fold changes of relative luciferase activity are indicated as follows: *, $P<0.05$; **, $P<0.01$; ***, $P<0.001$. (B) IFN bioassay using VSIV-GFP. HeLa cells in 6-well plates were transfected with individual SAP mutant genes for 24 h, and stimulated with poly(I:C) for 12 h. Cell culture supernatants were collected and diluted serially by 2-folds. MARC-145 cells were grown in 96-well plates and incubated with each dilution of supernatants for 24 h, and then infected with VSIV-GFP at an m.o.i. of 0.1 for 16 h. VSIV replication was measured by monitoring the fluorescence by GFP expression. (C) TNF-α promoter activities by SAP mutants. (D) Synthesis of ISRE products. ISRE-promoter activities in cells by SAP mutants were examined by ISRE-luciferase reporter. (E) The expression of IFN-stimulated gene (ISG) 15 was analyzed (right panel upper) in cells transfected with SAP constructs after incubating with IFN (1000 units/mL) for 2 h. The expression of ISG-15 was normalized with the quantity of β-actin. The relative ISG-15 expression level was determined by comparing with the ISG-15 quantity of IFN-treated pXJ41-transfected cells. (F) Inhibition of type I IFN induction by nuclease mutants of PRRSV-nsp1β. HeLa cells were seeded in 12-well plates and co-transfected with pIFN-β-Luc, along with individual nuclease mutants of PRRSV-nsp1β (K18A, E32A, and K18AE32A) and pTK-RL as an internal control at the ratio of 1:1:0.1. At 24 h post-transfection, cells were stimulated with 1 μg/ml of poly(I:C) for 12 h, and lysed for the reporter determination using the Dual Luciferase assay system (Promega). (G) Regulation of type I IFN induction by nuclease/SAP mutants of nsp1β. (H) Quantitative RT-PCR for firefly and Renilla mRNA in cells expressing SAP mutants. HeLa cells were co-transfected with pIFN-β-Luc, along with individual mutants and pTK-RL as an internal control at the ratio of 1:1:0.1. At 24 h post-transfection, cells were stimulated with 1 μg/ml of poly(I:C) for 12 h. Total cellular RNA was extracted mRNA levels of firefly and Renilla were normalized to that of GAPDH mRNA. This data represents two separate experiments, each in triplicate.

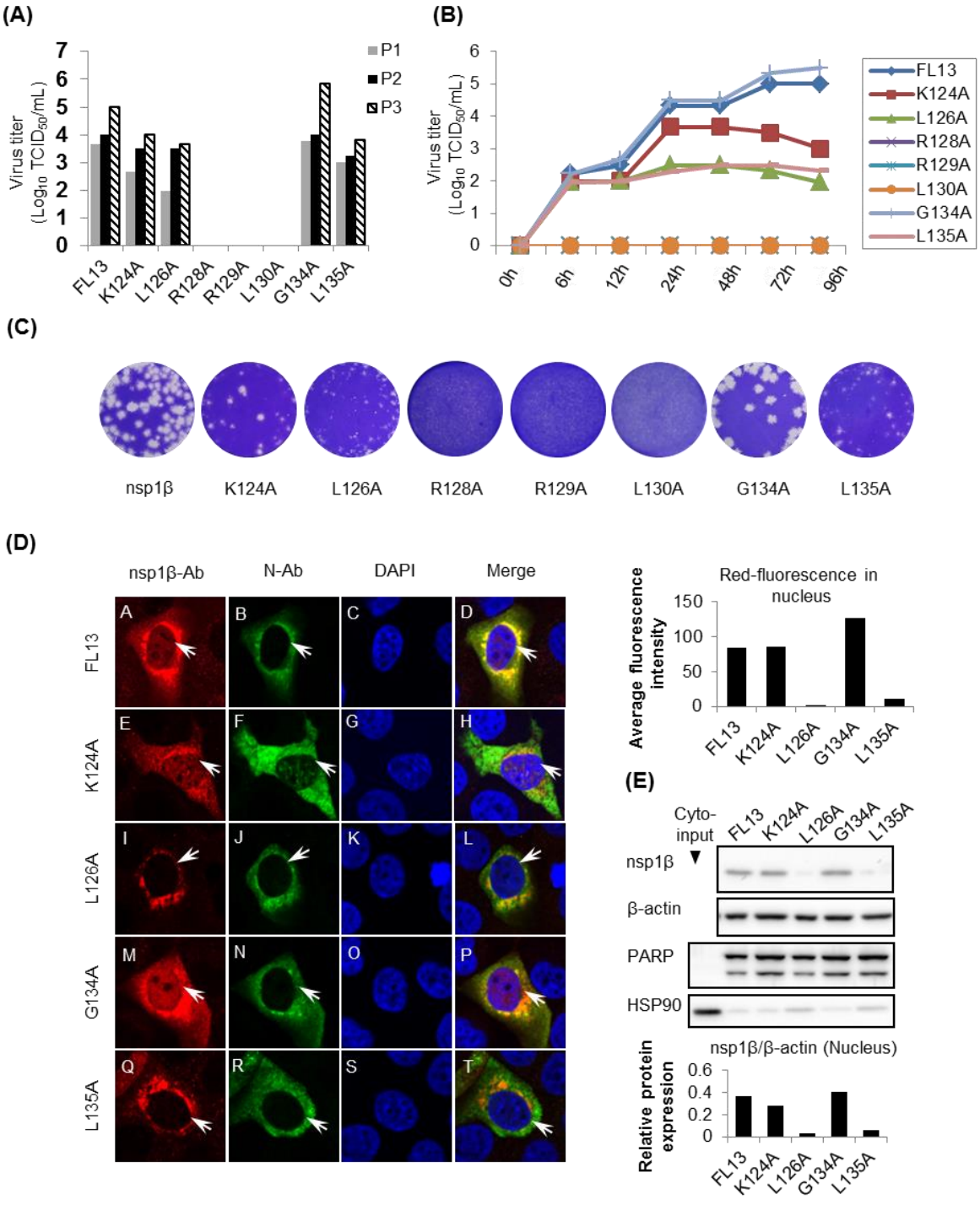
(A)
Virus titer (Log10 TCID50/mL)
P1
P2
P3
FL13
K124A
L126A
R128A
R129A
L130A
G134A
L135A
(B)
Virus titer (Log10 TCID50/mL)
0h
6h
12h
24h
48h
72h
96h
FL13
K124A
L126A
R128A
R129A
L130A
G134A
L135A
(C)
nsp1β
K124A
L126A
R128A
R129A
L130A
G134A
L135A
(D)
nsp1β-Ab
N-Ab
DAPI
Merge
FL13
K124A
L126A
G134A
L135A
Red-fluorescence in nucleus
Average fluorescence intensity
(E)
Cyto-input
nsp1β
β-actin
PARP
HSP90
nsp1β/β-actin (Nucleus)
Relative protein expression

**Fig. 4.8.**

**Fig. 4.8. Growth kinetics of SAP mutant PRRSV in MARC-145 cells.** (A) Titers of wild-type and SAP mutant viruses during the first three passages. MARC-145 cell were transfected with corresponding full-length genomic cDNA clones using Lipofectamine (Invitrogen), and CPE was monitored daily. At day 5 post-transfection, cells were harvested when CPE was extensive. The FL13-WT and SAP mutant viruses were passaged three times in MARC-145 cells and titrated. The titers are expressed as log10 TCID50/ml. The culture supernatants from DNA-transfected cells were designated passage-1. (B) One-step growth curves for FL13-WT and SAP mutant viruses. Cells were infected at an m.o.i. of 0.1 with the passage-3 preparation of indicated virus in duplicate. Samples were taken at the indicated times, and virus titers were determined. The results are expressed as mean values from two independent experiments, and error bars represent standard errors of mean values from two experiments. (C) Plaque morphology of SAP mutants viruses. (D) Subcellular localizations of nsp1β in SAP mutant virus-infected cells. MARC-145 cells were infected with FL13-WT or its SAP mutant viruses at an m.o.i. of 0.1 for 24 h. PRRSV-nsp1β was detected by anti-PRRSV-nsp1β rabbit antiserum followed by staining with anti-rabbit secondary antibody (red). Anti-N protein MAbs (SDOW17) was used to examine the expression of N protein (green). The average red FIs in virus-infected cell were analyzed by ImageJ software. (E) MARC-145 cells infected with FL13-WT or SAP mutant viruses were fractionated to obtain nucleus, and the nuclear nsp1β level was determined by Western-blot using anti-PRRSV-nsp1β rabbit antiserum. The expression of nsp1β was normalized using β-actin.

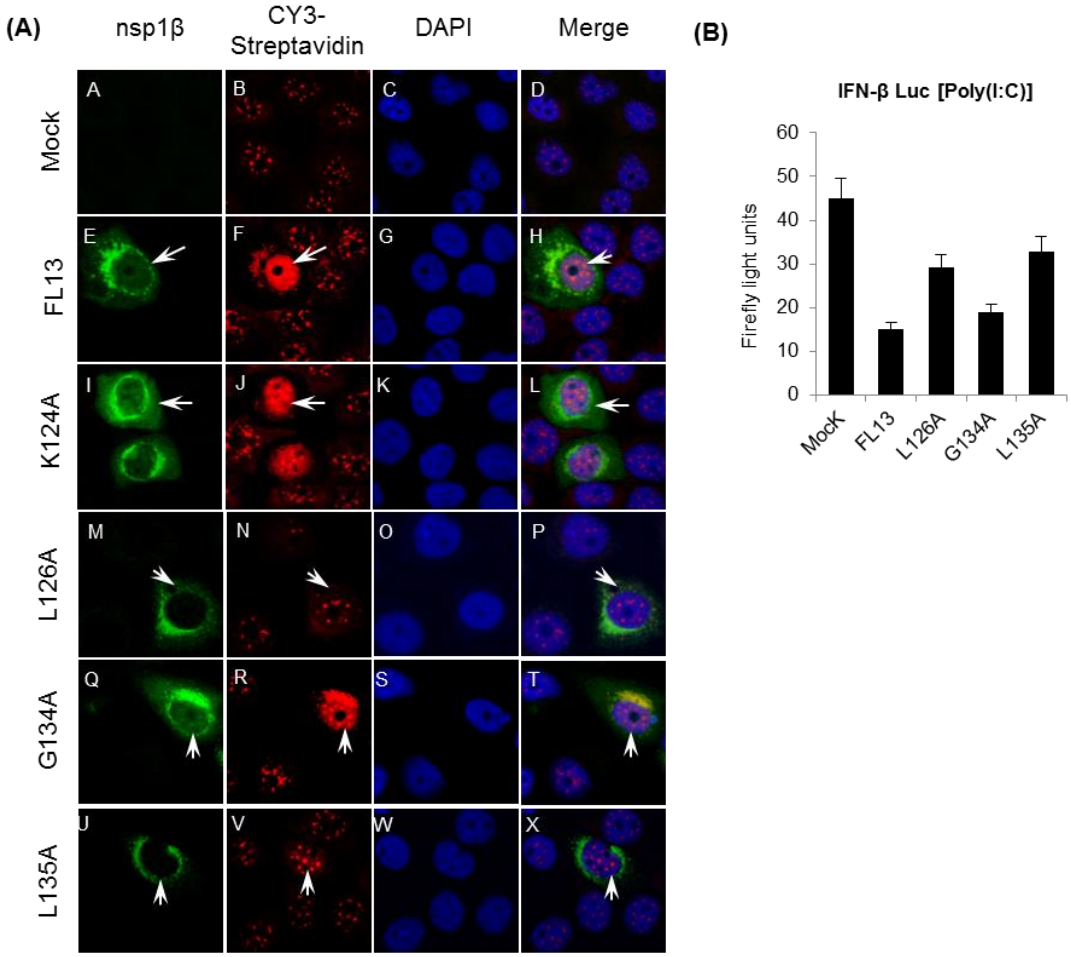


**Fig.4.9. Inhibition of mRNA export and IFN production by SAP mutant viruses.** (A) ISH in cells infected by SAP mutant viruses. PRRSV vFL13, vK124A, vL126A, vG134A and vL135A were used to infect MARC-145 cells for 24 h. Anti-nsp1β rabbit antiserum were used to stain cells infected by PRRSV (green, left column); poly(A)+ RNA was hybridized with biotinylated oligo(dT) followed by staining by Cy3-streptavidin (red, left middle column). White arrows indicate PRRSV-infected cells. (B) Regulation of type I IFN production by SAP mutant viruses. HeLa cells were seeded in 12-well plates and co-transfected with 500 ng of pIFN-β-Luc and 500 ng of pFL13 or individual indicated SAP mutant infectious cDNA clones along with 50 ng of pTK-RL as an internal control. At 24 h post-transfection, cells were either stimulated with 1 μg/ml of poly(I:C) or untreated for 8 h. Relative luciferase activities were calculated by normalizing the firefly luciferase to Renilla luciferase activities according to the manufacturer's protocol. The data represent the means of three independent experiments, each experiment in triplicate. The data represent the means of three independent experiments, each experiment in triplicate.

## Table 4.1. Oligonucleotides used for cloning nsp1 genes and their sequences

| Oligonucleotides | Primer sequence |
|---|---|
| PRRSV-nsp1β-Fwd | 5′-GCCGAATTCACCATGGCTACTGTCTATGACATTGG-3′ |
| PRRSV-nsp1β-Rev | 5′-GCCCTCGAGCTACCACTTGTGACTGCCAAACC-3′ |
| PRRSV-nsp1β-F-Fwd | 5′-GCCGAATTCACCATGGCTACTGTCTATGACATTGG-3′ |
| PRRSV-nsp1β-F-Rev | 5′-GCCCTCGAGCTA*CTTATCGTCGTCATCCTTGTAATC*CCACTTGTGACTGCCAAACC-3′ |
| Firefly-Fwd | 5′-GGCGAATTCATGGAAGACGCCAAAAACATTAAG-3′ |
| Firefly-Rev | 5′-GGCGGATCCTTACACGGCGATCTTT-3′ |
| *Renilla*-Fwd | 5′-GCCCCCGGGATGACTTCGAAAGTTTATGATC-3′ |
| *Renilla*-Rev | 5′-GCCTCTAGATTATTGTTCATTTTTGAGA-3′ |

Fwd, forward primer; Rev, reverse primer. Restriction enzyme recognition sequences are underlined. The FLAG tag is italicized and underlined.

## TABLE 4.2. Mutagenic oligonucleotides and their sequences

| Oligonucleotides | Primer sequence |
|---|---|
| K18A-Fwd | 5′-TATGTGGCCGAAAGGGCAGTCTCCTGGGCCCC-3′ |
| K18A-Rev | 5′-GGGGCCCAGGAGACTGCCCTTTCGGCCACATA-3′ |
| E32A-Fwd | 5′-GGGATGAAGTGAAATTTGCAGCTGTCCCCGGG-3′ |
| E32A-Rev | 5′-CCCGGGGACAGCTGCAAATTTCACTTCATCCC-3′ |
| C90A-Fwd | 5′-CTGTCCCTGAAGGCAACGCCTGGTGGAGCTTGTTTG-3′ |
| C90A-Rev | 5′-CAAACAAGCTCCACCAGGCGTTGCCTTCAGGGACAG-3′ |
| H159A-Fwd | 5′-GGAGAGTTGGATCCGCGCTTTGAAACTGGCGGGA-3′ |
| H159A-Rev | 5′-TCCCGCCAGTTTCAAAGCGCGGATCCAACTCTCC-3′ |
| K124A-Fwd | 5′-GCATGGTGTCGCTGGCGCGTACCTACAACGGAGG-3′ |
| K124A-Rev | 5′-CCTCCGTTGTAGGTACGCGCCAGCGACACCATGC-3′ |
| L126A-Fwd | 5′-TGCAGCCTCCGTTGTGCGTACTTGCCAGCGAC-3′ |
| L126A-Rev | 5′-GTCGCTGGCAAGTACGCACAACGGAGGCTGCA-3′ |
| R128A-Fwd | 5′-CTTGCAGCCTCGCTTGTAGGTACTTGCCAGCGA-3′ |
| R128A-Rev | 5′-TCGCTGGCAAGTACCTACAAGCGAGGCTGCAAG-3′ |
| R129A-Fwd | 5′-GACCATTAGCTTGCAGCGCCCGTTGTAGGTACTTGC-3′ |
| R129A-Rev | 5′-GCAAGTACCTACAACGGGCGCTGCAAGCTAATGGTC-3′ |
| L130A-Fwd | 5′-GGAGACCATTAGCTTGCGCCCTCCGTTGTAGGTACT-3′ |
| L130A-Rev | 5′-AGTACCTACAACGGAGGGCGCAAGCTAATGGTCTCC-3′ |
| G134A-Fwd | 5′-AGGCTGCAAGCTAATGCTCTCCGAGCGG-3′ |
| G134A-Rev | 5′-CCGCTCGGAGAGCATTAGCTTGCAGCCT-3′ |
| L135A-Fwd | 5′-CACCGCTCGGGCACCATTAGCTTGCAGCCTC-3′ |
| L135A-Rev | 5′-GAGGCTGCAAGCTAATGGTGCCCGAGCGGTG-3′ |

## TABLE 4.3. Summary of various phenotypes of nsp1β and SAP mutants

| | SAP mutant proteins | | | | | SAP mutant viruses | | | | |
|---|---|---|---|---|---|---|---|---|---|---|
| | Cellular distribution | | Activity suppression | | | | Cellular distribution | | Activity suppression | |
| | Cyto-plasm | Nucleus | mRNA nuclear export | Host protein synthesis | Innate immune responses | Viability | Cyto-plasm | Nucleus | mRNA nuclear export | IFNβ-Luc |
| **nsp1β** | + | +++ | +++ | +++ | +++ | +++ | +++ | ++ | +++ | +++ |
| **K124A** | + | +++ | +++ | +++ | +++ | ++ | +++ | ++ | +++ | ++ |
| **L126A** | +++ | - | - | - | - | + | +++ | - | - | + |
| **R128A** | + | +++ | - | - | + | - | NA | NA | NA | NA |
| **R129A** | +++ | - | - | - | - | - | NA | NA | NA | NA |
| **L130A** | +++ | - | - | - | - | - | NA | NA | NA | NA |
| **G134A** | + | +++ | +++ | +++ | +++ | +++ | +++ | ++ | +++ | +++ |
| **L135A** | +++ | - | - | - | - | + | +++ | - | - | + |

The symbols denotes the presence (+) or absence (-) of indicated phenotypes. Intensities are expressed as + (weak), ++ (medium), and +++ (strong). NA is the abbreviation of not applicable.

## TABLE 4.4. Updated biological functions of individual subunits of arterivirus nsp1

| Virus | subunits | Cellular distribution | | Activity suppression | | | |
|---|---|---|---|---|---|---|---|
| | | Cytoplasm | Nucleus | Protein synthesis | IFN | CBP | mRNA nuclear export |
| PRRSV | nsp1α | +++ | + | - | +++ | +++ | - |
| | nsp1β | + | +++ | +++ | +++ | - | +++ |
| LDV | nsp1α | +++ | + | - | +++ | +++ | - |
| | nsp1β | + | +++ | +++ | +++ | - | +++ |
| EAV | nsp1 | + | +++ | - | +++ | - | - |
| SHFV | nsp1α | ++ | ++ | - | + | - | - |
| | nsp1β | + | +++ | +++ | +++ | - | +++ |
| | nsp1γ | + | +++ | - | +++ | + | - |

The symbols denotes the presence (+) or absence (-) of indicated phenotypes. Intensities are expressed as + (weak), ++ (medium), and +++ (strong). Information is updated in accordance with and results in this study and recent reports (Han et al., 2014; Han and Yoo, 2014). .

# CHAPTER 5: GENERAL CONCLUSION

PRRSV has evolved to evade the host innate immune system for efficient survival and long-term infection in their hosts. PRRSV nsp1 has been studied extensively for its role for innate immune modulation, and accumulating evidence show the alteration of pro-inflammatory cytokines and type I IFNs production during infection. Type I IFNs are the most potent antiviral cytokines required for both innate and adaptive responses, and PRRSV suppresses the IFN production in pigs and cells. This is probably the most important mechanism for persistence of PRRSV in pigs for a prolonged time. At least six viral proteins have been identified as IFN antagonists for PRRSV: nsp1α, nsp1β, nsp2, nsp4, nsp11, and N proteins, and their mechanisms of action have been studied to a certain extent. Understanding viral strategies for immune modulation and evasion from host immune system is important, and balancing in vivo and in vitro analyses is needed to affirm each effect.

As the first viral products during infection, both nsp1α and nsp1β subunits of PRRSV inhibit the IFN and TNF-α induction, leading to the suppression of IFN-stimulated genes (ISGs) and the establishment of anti-viral state. PRRSV nsp1α but nsp1β induces CBP degradation in cells which prevents the formation of enhanceosome. The CBP degradation by PRRSV nsp1 is proteasome-dependent, and thus degradation of CBP by the nsp1α subunit is likely proteasome-dependent. Since proteasome-mediated CBP degradation is a nuclear event and because nsp1α exists in both the cytoplasm and nucleus, it is presumed that the nuclear form of nsp1α is responsible for CBP degradation. Structure and function study indicates the indispensable role of ZF1 motif of nsp1α in IFN suppression. ZF1 mutants with reversed IFN phenotype fail to induce CBP degradation, indicating its participation in regulating CBP functions.

PRRSV nsp1β inhibits productions of IFN, TNF-α, and ISGs, as well as other foreign genes like GFP and *Renilla,* whose suppressive activity is believed to be universal. Impairment of nuclear-cytoplasmic trafficking of mRNA has been proved to be associated with PRRSV nsp1β, and is highly correlated with the nuclear fraction of nsp1β. This unveils the molecular basis for nsp1β-mediated innate immune suppression, and answers the reason for nsp1β nuclear distribution. Cellular mRNA nuclear retention is significant in PRRSV-infected cells and it is in concert with nsp1β nuclear localization. Genomes of positive-strand RNA viruses act as mRNA to direct the synthesis of viral proteins, especially the RNA-dependent RNA polymerase (RdRp). Unlike IRES containing viruses, whose viral genome translation benefits from impaired cap-dependent translation, arterivirus genome contains 5′-cap structure and requires cap-dependent synthesis. PRRSV-impaired mRNA export enhances viral protein translation by blocking the access of cellular mRNA to translation apparatus. This finding is novel for nidoviruses.

The study of innate immune suppression has been expanded to nsp1 subunits of other member viruses in the family Arteriviridae. CBP degradation is evident in cells expressing PRRSV-nsp1α, LDV-nsp1α and SHFV-nsp1γ, but no such degradation is observed for EAV-nsp1. Impairment of nuclear-cytoplasmic trafficking of mRNA is evident in the presence of PRRSV-nsp1β, LDV-nsp1β, and SHFV-nsp1β, all of which have predominant nuclear distribution. It is apparent that nsp1 subunits of all member viruses in the family *Arteriviridae* are important IFN antagonists, and their IFN modulatory function seems to be a common strategy of this group of viruses for evading the host immune system.

Reverse genetic systems are available for PRRSV, and the information from structure-function studies allows us to disable the suppressive function of the virus. By sequence analysis, a SAP motif has been identified in PRRSV-nsp1β, and this motif appears essential for nsp1β-

mediated innate immune suppression, whereas SAP mutants do not block the mRNA nuclear export. Two SAP mutant viruses, vL126A and vL135A, are fully infectious and both mutants are unable to block mRNA nuclear export and thus do not suppress IFN promoter activities.

In summary, we have shown that both PRRSV nsp1α and PRRSV nsp1β inhibit innate immune responses, and their mechanism of action differs. CBP is degraded by nsp1α, whereas the SAP motif is essential for nsp1β to maintain its biological function. SAP-negative mutant viruses have been generated to eliminate the IFN antagonistic function from PRRSV, and these mutant viruses may be useful to further develop as a new generation PRRS vaccine candidate.

## REFERENCES


Aasted, B., Bach, P., Nielsen, J., Lind, P., 2002. Cytokine profiles in peripheral blood mononuclear cells and lymph node cells from piglets infected in utero with porcine reproductive and respiratory syndrome virus. Clin. Diagn. Lab. Immunol. 9, 1229-1234

Abraham, T.M., Sarnow, P., 2011. RNA virus harnesses microRNAs to seize host translation control. Cell Host Microbe 9, 5-7.

Ahlquist, P., Noueiry, A.O., Lee, W.M., Kushner, D.B., Dye, B.T., 2003. Host factors in positive-strand RNA virus genome replication. J. Virol. 77, 8181-8186.

Ait-Ali, T., Wilson, A.D., Westcott, D.G., Clapperton, M., Waterfall, M., Mellencamp, M.A., Drew, T.W., Bishop, S.C., Archibald, A.L., 2007. Innate immune responses to replication of porcine reproductive and respiratory syndrome virus in isolated swine alveolar macrophages. Viral Immunol. 20, 105-118.

Albina, E., Carrat, C., Charley, B., 1998. Interferon-alpha response to swine arterivirus (PoAV), the porcine reproductive and respiratory syndrome virus. J. Interf. Cytok. Res. 18, 485-490.

Allende, R., Laegreid, W.W., Kutish, G.F., Galeota, J.A., Wills, R.W., Osorio, F.A., 2000. Porcine reproductive and respiratory syndrome virus: description of persistence in individual pigs upon experimental infection. J. Virol. 74, 10834-10837.

Allende, R., Lewis, T.L., Lu, Z., Rock, D.L., Kutish, G.F., Ali, A., Doster, A.R., Osorio, F.A., 1999. North American and European porcine reproductive and respiratory syndrome viruses differ in non-structural protein coding regions. J. Gen. Virol. 80, 307-315.

Almazan, F., Gonzalez, J.M., Penzes, Z., Izeta, A., Calvo, E., Plana-Duran, J., Enjuanes, L., 2000. Engineering the largest RNA virus genome as an infectious bacterial artificial chromosome. Proc. Natl. Acad. Sci. USA. 97, 5516-5521.

Ammann, C.G., Messer, R.J., Peterson, K.E., Hasenkrug, K.J., 2009. Lactate dehydrogenase-elevating virus induces systemic lymphocyte activation via TLR7-dependent IFNalpha responses by plasmacytoid dendritic cells. PLoS One 4, e6105.

Anderson, G.W., Rowland, R.R.R., Palmer, G.A., Even, C., Plagemann, P.G.W., 1995. Lactate dehydrogenase-elevating virus-replication persists in liver, spleen, lymph-node, and testis tissues and results in accumulation of viral-RNA in germinal-centers, concomitant with polyclonal activation of B-cells. J. Virol. 69, 5177-5185.

Ansari, I.H., Kwon, B., Osorio, F.A., Pattnaik, A.K., 2006. Influence of N-linked glycosylation of porcine reproductive and respiratory syndrome virus GP5 on virus infectivity, antigenicity, and ability to induce neutralizing antibodies. J. Virol. 80, 3994-4004.

Aravind, L., Koonin, E.V., 2000. SAP - a putative DNA-binding motif involved in chromosomal organization. Trends Biochem. Sci. 25(3), 112-114.

Baccala, R., Hoebe, K., Kono, D.H., Beutler, B., Theofilopoulos, A.N., 2007. TLR-dependent and TLR-independent pathways of type I interferon induction in systemic autoimmunity. Nat. Med. 13, 543-551.

Balasuriya, U.B.R., Dobbe, J.C., Heidner, H.W., Smalley, V.L., Navarrette, A., Snijder, E.J., MacLachlan, N.J., 2004. Characterization of the neutralization determinants of equine arteritis virus using recombinant chimeric viruses and site-specific mutagenesis of an infectious cDNA clone (vol 321, pg 235, 2004). Virology 327, 318-319.

Balvay, L., Rifo, R.S., Ricci, E.P., Decimo, D., Ohlmann, T., 2009. Structural and functional diversity of viral IRESes. Bba-Gene Regul Mech 1789, 542-557.

Bauhofer, O., Summerfield, A., Sakoda, Y., Tratschin, J.D., Hofmann, M.A., Ruggli, N., 2007. Classical swine fever virus Npro interacts with interferon regulatory factor 3 and induces its proteasomal degradation. J. Virol. 81, 3087-3096.

Baumann, A., Mateu, E., Murtaugh, M.P., Summerfield, A., 2013. Impact of genotype 1 and 2 of porcine reproductive and respiratory syndrome viruses on interferon-alpha responses by plasmacytoid dendritic cells. Vet. Res. 44, 33.

Bedford, D.C., Brindle, P.K., 2012. Is histone acetylation the most important physiological function for CBP and p300? Aging-US 4, 247-255.

Bedford, D.C., Kasper, L.H., Fukuyama, T., Brindle, P.K., 2010. Target gene context influences the transcriptional requirement for the KAT3 family of CBP and p300 histone acetyltransferases. Epigenetics 5, 9-15.

Benfield, D.A., Nelson, E., Collins, J.E., Harris, L., Goyal, S.M., Robison, D., Christianson, W.T., Morrison, R.B., Gorcyca, D., Chladek, D., 1992. Characterization of swine infertility and respiratory syndrome (SIRS) virus (Isolate ATCC VR-2332). J. Vet. Diagn. Invest. 4, 127-133.

Beura, L.K., Sarkar, S.N., Kwon, B., Subramaniam, S., Jones, C., Pattnaik, A.K., Osorio, F.A., 2010. Porcine reproductive and respiratory syndrome virus nonstructural protein 1beta modulates host innate immune response by antagonizing IRF3 activation. J. Virol. 84, 1574-1584.

Beura, L.K., Subramaniam, S., Vu, H.L., Kwon, B., Pattnaik, A.K., Osorio, F.A., 2012. Identification of amino acid residues important for anti-IFN activity of porcine reproductive and respiratory syndrome virus nonstructural protein 1. Virology 433, 431-439.

Boyer, J.C., Haenni, A.L., 1994. Infectious transcripts and cDNA clones of RNA viruses. Virology 198, 415-426.

Bramel-Verheije, M.H.G., Rottier, P.J.M., Meulenberg, J.J.M., 2000. Expression of a foreign epitope by porcine reproductive and respiratory syndrome virus. Virology 278, 380-389.

Buddaert, W., Van Reeth, K., Pensaert, M., 1998. In vivo and in vitro interferon (IFN) studies with the porcine reproductive and respiratory syndrome virus (PRRSV). Advs. Exp. Medicine, Biology 440, 461-467.

Calzada-Nova, G., Schnitzlein, W.M., Husmann, R.J., Zuckermann, F.A., 2011. North American porcine reproductive and respiratory syndrome viruses inhibit type I interferon production by plasmacytoid dendritic cells. J. Virol. 85, 2703-2713.

Castello, A., Izquierdo, J.M., Welnowska, E., Carrasco, L., 2009. RNA nuclear export is blocked by poliovirus 2A protease and is concomitant with nucleoporin cleavage. J Cell Sci 122(20), 3799-3809.

Chakraborty, P., Satterly, N., Fontoura, B.M., 2006. Nuclear export assays for poly(A) RNAs. Methods 39(4), 363-369.

Chand, R.J., Trible, B.R., Rowland, R.R., 2012. Pathogenesis of porcine reproductive and respiratory syndrome virus. Curr. Opin. Virol. 2, 256-263.

Chang, H.C., Peng, Y.T., Chang, H.L., Chaung, H.C., Chung, W.B., 2008. Phenotypic and functional modulation of bone marrow-derived dendritic cells by porcine reproductive and respiratory syndrome virus. Vet. Microbiol.129, 281-293.

Chaung, H.C., Chen, C.W., Hsieh, B.L., Chung, W.B., 2010. Toll-Like Receptor expressions in porcine alveolar macrophages and dendritic cells in responding to poly IC stimulation

and porcine reproductive and respiratory syndrome virus (PRRSV) infection. Comp. Immunol. Microbiol. Infect. Dis. 33, 197-213.
Chelbi-Alix, M.K., Pelicano, L., Quignon, F., Koken, M.H., Venturini, L., Stadler, M., Pavlovic, J., Degos, L., de The, H., 1995. Induction of the PML protein by interferons in normal and APL cells. Leukemia 9, 2027-2033.
Chen, J.P., Strauss, J.H., Strauss, E.G., Frey, T.K., 1996. Characterization of the rubella virus nonstructural protease domain and its cleavage site. Journal of Virology 70, 4707-4713.
Chen, Z., Lawson, S., Sun, Z., Zhou, X., Guan, X., Christopher-Hennings, J., Nelson, E.A., Fang, Y., 2010a. Identification of two auto-cleavage products of nonstructural protein 1 (nsp1) in porcine reproductive and respiratory syndrome virus infected cells: nsp1 function as interferon antagonist. Virology 398, 87-97.
Chen, Z.B., Wang, Y.H., Ratia, K., Mesecar, A.D., Wilkinson, K.D., Baker, S.C., 2007. Proteolytic processing and deubiquitinating activity of papain-like proteases of human coronavirus NL63. J. Virol. 81, 6007-6018.
Chen, Z.H., Zhou, X.X., Lunney, J.K., Lawson, S., Sun, Z., Brown, E., Christopher-Hennings, J., Knudsen, D., Nelson, E., Fang, Y., 2010b. Immunodominant epitopes in nsp2 of porcine reproductive and respiratory syndrome virus are dispensable for replication, but play an important role in modulation of the host immune response. J. Gen. Virol. 91, 1047-1057.
Choi, C., Cho, W.S., Kim, B., Chae, C., 2002. Expression of Interferon-gamma and tumour necrosis factor-alpha in pigs experimentally infected with Porcine Reproductive and Respiratory Syndrome Virus (PRRSV). J. Comp. Pathol. 127, 106-113.
Clark, G.J., Angel, N., Kato, M., Lopez, J.A., MacDonald, K., Vuckovic, S., Hart, D.N., 2000. The role of dendritic cells in the innate immune system. Microbes Infect. 2, 257-272.
Clementz, M.A., Chen, Z.B., Banach, B.S., Wang, Y.H., Sun, L., Ratia, K., Baez-Santos, Y.M., Wang, J., Takayama, J., Ghosh, A.K., Li, K., Mesecar, A.D., Baker, S.C., 2010. Deubiquitinating and Interferon Antagonism Activities of Coronavirus Papain-Like Proteases. J. Virol. 84, 4619-4629.
Coleman, J.R., Papamichail, D., Skiena, S., Futcher, B., Wimmer, E., Mueller, S., 2008. Virus attenuation by genome-scale changes in codon pair bias. Science 320, 1784-1787.
Collins, J.E., Benfield, D.A., Christianson, W.T., Harris, L., Hennings, J.C., Shaw, D.P., Goyal, S.M., McCullough, S., Morrison, R.B., Joo, H.S., et al., 1992. Isolation of swine infertility and respiratory syndrome virus (isolate ATCC VR-2332) in North America and experimental reproduction of the disease in gnotobiotic pigs. J. Vet. Diagn. Invest. 4, 117-126.
Conti, P., Kempuraj, D., Kandere, K., Di Gioacchino, M., Barbacane, R.C., Castellani, M.L., Felaco, M., Boucher, W., Letourneau, R., Theoharides, T.C., 2003. IL-10, an inflammatory/inhibitory cytokine, but not always. Immunol. Lett. 86, 123-129.
Dalton, K.P., Rose, J.K., 2001. Vesicular stomatitis virus glycoprotein containing the entire green fluorescent protein on its cytoplasmic domain is incorporated efficiently into virus particles. Virology 279, 414-421.
Darwich, L., Diaz, I., Mateu, E., 2010. Certainties, doubts and hypotheses in porcine reproductive and respiratory syndrome virus immunobiology. Virus Res. 154, 123-132.
de Breyne, S., Bonderoff, J.M., Chumakov, K.M., Lloyd, R.E., Hellen, C.U., 2008. Cleavage of eukaryotic initiation factor eIF5B by enterovirus 3C proteases. Virology 378, 118-122.
de Lima, M., Kwon, B., Ansari, I.H., Pattnaik, A.K., Flores, E.F., Osorio, F.A., 2008. Development of a porcine reproductive and respiratory syndrome virus differentiable

(DIVA) strain through deletion of specific immunodominant epitopes. Vaccine 26, 3594-3600.
de Lima, M., Pattnaik, A.K., Flores, E.F., Osorio, F.A., 2006. Serologic marker candidates identified among B-cell linear epitopes of Nsp2 and structural proteins of a North American strain of porcine reproductive and respiratory syndrome virus. Virology 353, 410-421.
de los Santos, T., Segundo, F.D., Zhu, J., Koster, M., Dias, C.C., Grubman, M.J., 2009. A conserved domain in the leader proteinase of foot-and-mouth disease virus is required for proper subcellular localization and function. J. Virol. , 1800-1810.
de Vries, A.A., Glaser, A.L., Raamsman, M.J., de Haan, C.A., Sarnataro, S., Godeke, G.J., Rottier, P.J., 2000. Genetic manipulation of equine arteritis virus using full-length cDNA clones: separation of overlapping genes and expression of a foreign epitope. Virology 270, 84-97.
Dea, S., Gagnon, C.A., Mardassi, H., Pirzadeh, B., Rogan, D., 2000. Current knowledge on the structural proteins of porcine reproductive and respiratory syndrome (PRRS) virus: comparison of the North American and European isolates. Arch. Virol. 145, 659-688.
den Boon, J.A., Faaberg, K.S., Meulenberg, J.J., Wassenaar, A.L., Plagemann, P.G., Gorbalenya, A.E., Snijder, E.J., 1995. Processing and evolution of the N-terminal region of the arterivirus replicase ORF1a protein: identification of two papainlike cysteine proteases. J. Virol. 69, 4500-4505.
den Boon, J.A., Snijder, E.J., Chirnside, E.D., de Vries, A.A., Horzinek, M.C., Spaan, W.J., 1991. Equine arteritis virus is not a togavirus but belongs to the coronaviruslike superfamily. J. Virol. 65, 2910-2920.
Diaz, I., Darwich, L., Pappaterra, G., Pujols, J., Mateu, E., 2005. Immune responses of pigs after experimental infection with a European strain of porcine reproductive and respiratory syndrome virus. J. Gen. Virol. 86, 1943-1951.
Doan, D.N., Dokland, T., 2003. Structure of the nucleocapsid protein of porcine reproductive and respiratory syndrome virus. Structure 11, 1445-1451.
Dobbe, J.C., van der Meer, Y., Spaan, W.J.M., Snijder, E.J., 2001. Construction of chimeric arteriviruses reveals that the ectodomain of the major glycoprotein is not the main determinant of equine arteritis virus tropism in cell culture. Virology 288, 283-294.
Dunowska, M., Biggs, P.J., Zheng, T., Perrott, M.R., 2012. Identification of a novel nidovirus associated with a neurological disease of the Australian brushtail possum (Trichosurus vulpecula). Vet. Microbiol.156, 418-424.
Dyck, J.A., Maul, G.G., Miller, W.H., Chen, J.D., Kakizuka, A., Evans, R.M., 1994. A novel macromolecular structure is a target of the promyelocyte-retinoic acid receptor oncoprotein. Cell 76, 333-343.
Ehrhardt, C., Kardinal, C., Wurzer, W.J., Wolff, T., von Eichel-Streiber, C., Pleschka, S., Planz, O., Ludwig, S., 2004. Rac1 and PAK1 are upstream of IKK-epsilon and TBK-1 in the viral activation of interferon regulatory factor-3. FEBS Lett. 567, 230-238.
Ehrhardt, C., Kardinal, C., Wurzer, W.J., Wolff, T., von Eichel-Streiber, C., Pleschka, S., Planz, O., Ludwig, S., 2004. Rac1 and PAK1 are upstream of IKK-epsilon and TBK-1 in the viral activation of interferon regulatory factor-3. FEBS letters 567(2-3), 230-238.
Fang, Y., Christopher-Hennings, J., Brown, E., Liu, H., Chen, Z., Lawson, S.R., Breen, R., Clement, T., Gao, X., Bao, J., Knudsen, D., Daly, R., Nelson, E., 2008. Development of genetic markers in the non-structural protein 2 region of a US type 1 porcine reproductive

and respiratory syndrome virus: implications for future recombinant marker vaccine development. J. Gen. Virol. 89, 3086-3096.
Fang, Y., Faaberg, K.S., Rowland, R.R., Christopher-Hennings, J., Pattnaik, A.K., Osorio, F., Nelson, E.A., 2006a. Construction of a full-length cDNA infectious clone of a European-like type 1 PRRSV isolated in the U.S. Adv. Exp. Med. Biol. 581, 605-608.
Fang, Y., Fang, L., Wang, Y., Lei, Y., Luo, R., Wang, D., Chen, H., Xiao, S., 2012a. Porcine reproductive and respiratory syndrome virus nonstructural protein 2 contributes to NF-kappaB activation. Virol. J. 9, 83.
Fang, Y., Kim, D.Y., Ropp, S., Steen, P., Christopher-Hennings, J., Nelson, E.A., Rowland, R.R., 2004. Heterogeneity in Nsp2 of European-like porcine reproductive and respiratory syndrome viruses isolated in the United States. Virus Res. 100, 229-235.
Fang, Y., Rowland, R.R., Roof, M., Lunney, J.K., Christopher-Hennings, J., Nelson, E.A., 2006b. A full-length cDNA infectious clone of North American type 1 porcine reproductive and respiratory syndrome virus: expression of green fluorescent protein in the Nsp2 region. J. Virol. 80, 11447-11455.
Fang, Y., Snijder, E.J., 2010. The PRRSV replicase: exploring the multifunctionality of an intriguing set of nonstructural proteins. Virus Res. 154, 61-76.
Fang, Y., Treffers, E.E., Li, Y., Tas, A., Sun, Z., van der Meer, Y., de Ru, A.H., van Veelen, P.A., Atkins, J.F., Snijder, E.J., Firth, A.E., 2012. Efficient -2 frameshifting by mammalian ribosomes to synthesize an additional arterivirus protein. Proc. Natl. Acad. Sci. USA 109, E2920-2928.
Feng, W.H., Tompkins, M.B., Xu, J.S., Zhang, H.X., McCaw, M.B., 2003. Analysis of constitutive cytokine expression by pigs infected in-utero with porcine reproductive and respiratory syndrome virus. Vet. Immunol. Immunop. 94, 35-45.
Firth, A.E., Zevenhoven-Dobbe, J.C., Wills, N.M., Go, Y.Y., Balasuriya, U.B.R., Atkins, J.F., Snijder, E.J., Posthuma, C.C., 2011. Discovery of a small arterivirus gene that overlaps the GP5 coding sequence and is important for virus production. J. Gen. Virol. 92, 1097-1106.
Flores-Mendoza, L., Silva-Campa, E., Resendiz, M., Osorio, F.A., Hernandez, J., 2008. Porcine reproductive and respiratory syndrome virus infects mature porcine dendritic cells and up-regulates interleukin-10 production. Clin. Vaccine. Immunol. 15, 720-725.
Frias-Staheli, N., Giannakopoulos, N.V., Kikkert, M., Taylor, S.L., Bridgen, A., Paragas, J., Richt, J.A., Rowland, R.R., Schmaljohn, C.S., Lenschow, D.J., Snijder, E.J., Garcia-Sastre, A., Virgin, H.W., 2007. Ovarian tumor domain-containing viral proteases evade ubiquitin- and ISG15-dependent innate immune responses. Cell Host Microbe 2, 404-416.
Fu, Y., Quan, R., Zhang, H., Hou, J., Tang, J., and Feng, W.H. 2012. Porcine reproductive and respiratory syndrome virus induces interleukin-15 through the NF-kB signaling pathway. J. Virol. 86, 7625-7636.
Gao, F., Lu, J.Q., Yao, H.C., Wei, Z.Z., Yang, Q., Yuan, S.S., 2012. Cis-acting structural element in 5 ′ UTR is essential for infectivity of porcine reproductive and respiratory syndrome virus. Virus Res. 163, 108-119.
Gao, F., Yao, H., Lu, J., Wei, Z., Zheng, H., Zhuang, J., Tong, G., Yuan, S., 2013. Replacement of the heterologous 5′ untranslated region allows preservation of the fully functional activities of type 2 porcine reproductive and respiratory syndrome virus. Virology 439, 1-12.

Gao, Z.Q., Guo, X., Yang, H.C., 2004. Genomic characterization of two Chinese isolates of porcine respiratory and reproductive syndrome virus. Arch. Virol. 149, 1341-1351.

Genini, S., Delputte, P.L., Malinverni, R., Cecere, M., Stella, A., Nauwynck, H.J., Giuffra, E., 2008. Genome-wide transcriptional response of primary alveolar macrophages following infection with porcine reproductive and respiratory syndrome virus. J. Gen. Virol. 89, 2550-2564.

Gimeno, M., Darwich, L., Diaz, I., de la Torre, E., Pujols, J., Martin, M., Inumaru, S., Cano, E., Domingo, M., Montoya, M., Mateu, E., 2011. Cytokine profiles and phenotype regulation of antigen presenting cells by genotype-I porcine reproductive and respiratory syndrome virus isolates. Vet. Res.42, 9.

Gingras, A.C., Svitkin, Y., Belsham, G.J., Pause, A., Sonenberg, N., 1996. Activation of the translational suppressor 4E-BP1 following infection with encephalomyocarditis virus and poliovirus. Proc. Natl. Acad. Sci. USA. 93(11), 5578-5583.

Go,Y.Y., Li, Y., Chen, Z., Han, M., Yoo, D., Fang, Y., Balasuriya, U.B.R., 2014. Equine arteritis virus does not induce interferon production in equine endothelial cells: identification of nonstructural protein 1 as a main interferon antagonist. Biomed Res Int., 2014, Article ID 420658, 13 pages. http://dx.doi.org/10.1155/2014/420658

Godeny, E.K., de Vries, A.A., Wang, X.C., Smith, S.L., de Groot, R.J., 1998. Identification of the leader-body junctions for the viral subgenomic mRNAs and organization of the simian hemorrhagic fever virus genome: evidence for gene duplication during arterivirus evolution. J. Virol. 72, 862-867.

Goodman, R.H., Smolik, S., 2000. CBP/p300 in cell growth, transformation, and development. Genes Dev. 14, 1553-1577.

Gorbalenya, A.E., Koonin, E.V., Donchenko, A.P., Blinov, V.M., 1989. Coronavirus genome: prediction of putative functional domains in the nonstructural polyprotein by comparative amino acid sequence analysis. Nuc. Acids Res. 17, 4847-4861.

Gorbalenya, A.E., Koonin, E.V., Lai, M.M., 1991. Putative papain-related thiol proteases of positive-strand RNA viruses. Identification of rubi- and aphthovirus proteases and delineation of a novel conserved domain associated with proteases of rubi-, alpha- and coronaviruses. FEBS lett. 288, 201-205.

Guarne, A., Hampoelz, B., Glaser, W., Carpena, X., Tormo, J., Fita, I., Skern, T., 2000. Structural and biochemical features distinguish the foot-and-mouth disease virus leader proteinase from other papain-like enzymes. J. Mol. Biol. 302, 1227-1240.

Guarne, A., Tormo, J., Kirchweger, R., Pfistermueller, D., Fita, I., Skern, T., 1998. Structure of the foot-and-mouth disease virus leader protease: a papain-like fold adapted for self-processing and eIF4G recognition. EMBO Journal 17, 7469-7479.

Guo, B.Q., Lager, K.M., Henningson, J.N., Miller, L.C., Schlink, S.N., Kappes, M.A., Kehrli, M.E., Brockmeier, S.L., Nicholson, T.L., Yang, H.C., Faaberg, K.S., 2013. Experimental infection of United States swine with a Chinese highly pathogenic strain of porcine reproductive and respiratory syndrome virus. Virology 435, 372-384.

Gustin, K.E., Sarnow, P., 2001. Effects of poliovirus infection on nucleo-cytoplasmic trafficking and nuclear pore complex composition. Embo J 20(1-2), 240-249.

Gustin, K.E., Sarnow, P., 2002. Inhibition of nuclear import and alteration of nuclear pore complex composition by rhinovirus. J. Virol. 76(17), 8787-8796.

Han, J., Liu, G., Wang, Y., Faaberg, K.S., 2007. Identification of nonessential regions of the nsp2 replicase protein of porcine reproductive and respiratory syndrome virus strain VR-2332 for replication in cell culture. J. Virol. 81, 9878-9890.

Han, J., Rutherford, M.S., Faaberg, K.S., 2009. The porcine reproductive and respiratory syndrome virus nsp2 cysteine protease domain possesses both trans- and cis-cleavage activities. J. Virol. 83, 9449-9463.

Han, J., Wang, Y., Faaberg, K.S., 2006. Complete genome analysis of RFLP 184 isolates of porcine reproductive and respiratory syndrome virus. Virus Res. 122, 175-182.

Han, M., Du, Y., Song, C., Yoo, D., 2013. Degradation of CREB-binding protein and modulation of type I interferon induction by the zinc finger motif of the porcine reproductive and respiratory syndrome virus nsp1alpha subunit. Virus Res. 172(1-2), 54-65.

Han, M., Kim, C.Y., Rowland, R.R., Fang, Y., Kim, D., Yoo, D., 2014. Biogenesis of nonstructural protein 1 (nsp1) and nsp1-mediated type I interferon modulation in arteriviruses. Virology 458-459C, 136-150.

Han, M., Yoo, D., 2014. Modulation of innate immune signaling by nonstructural protein 1 (nsp1) in the family Arteriviridae. Virus Res. 194, 100-109.

Harcourt, B.H., Jukneliene, D., Kanjanahaluethai, A., Bechill, J., Severson, K.M., Smith, C.M., Rota, P.A., Baker, S.C., 2004. Identification of severe acute respiratory syndrome coronavirus replicase products and characterization of papain-like protease activity. J. Virol. 78, 13600-13612.

Hawiger, J., 2001. Innate immunity and inflammation: A transcriptional paradigm. Immunol. Res. 23, 99-109.

Honda, K., Takaoka, A., Taniguchi, T., 2006. Type I inteferon gene induction by the interferon regulatory factor family of transcription factors. Immunity 25, 349-360.

Hou, J., Wang, L., He, W., Zhang, H., Feng, W.H., 2012. Highly pathogenic porcine reproductive and respiratory syndrome virus impairs LPS- and poly(I:C)-stimulated tumor necrosis factor-alpha release by inhibiting ERK signaling pathway. Virus Res.167, 106-111.

Huang, C., Lokugamage, K.G., Rozovics, J.M., Narayanan, K., Semler, B.L., Makino, S., 2011a. Alphacoronavirus transmissible gastroenteritis virus nsp1 protein suppresses protein translation in mammalian cells and in cell-free HeLa cell extracts but not in rabbit reticulocyte lysate. J. Virol. 85(1), 638-643.

Huang, C., Lokugamage, K.G., Rozovics, J.M., Narayanan, K., Semler, B.L., Makino, S., 2011b. SARS coronavirus nsp1 protein induces template-dependent endonucleolytic cleavage of mRNAs: viral mRNAs are resistant to nsp1-induced RNA cleavage. PLoS pathog. 7(12), e1002433.

Hwang, S., Kim, K.S., Flano, E., Wu, T.T., Tong, L.M., Park, A.N., Song, M.J., Sanchez, D.J., O′Connell, R.M., Cheng, G., Sun, R., 2009. Conserved herpesviral kinase promotes viral persistence by inhibiting the IRF-3-mediated type I interferon response. Cell Host Microbe. 5, 166-178.

Iuchi, S., 2001. Three classes of C2H2 zinc finger proteins. Cell Mol. Life Sci.58, 625-635.

Johnsen, C.K., Botner, A., Kamstrup, S., Lind, P., Nielsen, J., 2002. Cytokine mRNA profiles in bronchoalveolar cells of piglets experimentally infected in utero with porcine reproductive and respiratory syndrome virus: association of sustained expression of IFN-gamma and IL-10 after viral clearance. Viral. Immunol. 15, 549-556.

Johnson, C.R., Griggs, T.F., Gnanandarajah, J., Murtaugh, M.P., 2011. Novel structural protein in porcine reproductive and respiratory syndrome virus encoded by an alternative ORF5 present in all arteriviruses. J. Gen. Virol. 92, 1107-1116.

Kamitani, W., Huang, C., Narayanan, K., Lokugamage, K.G., Makino, S., 2009. A two-pronged strategy to suppress host protein synthesis by SARS coronavirus Nsp1 protein. Nature structural & molecular biology 16(11), 1134-1140.

Kamitani, W., Narayanan, K., Huang, C., Lokugamage, K., Ikegami, T., Ito, N., Kubo, H., Makino, S., 2006. Severe acute respiratory syndrome coronavirus nsp1 protein suppresses host gene expression by promoting host mRNA degradation. Proc. Natl. Acad. Sci. USA. 103(34), 12885-12890.

Kapur, V., Elam, M.R., Pawlovich, T.M., Murtaugh, M.P., 1996. Genetic variation in porcine reproductive and respiratory syndrome virus isolates in the midwestern United States. J. Gen. Virol. 77, 1271-1276.

Karpe, Y.A., Lole, K.S., 2011. Deubiquitination activity associated with hepatitis E virus putative papain-like cysteine protease. J. Gen. Virol. 92, 2088-2092.

Kim, D.Y., Calvert, J.G., Chang, K.O., Horlen, K., Kerrigan, M., Rowland, R.R.R., 2007. Expression and stability of foreign tags inserted into nsp2 of porcine reproductive and respiratory syndrome virus (PRRSV). Virus Res. 128, 106-114.

Kim, H.S., Kwang, J., Yoon, I.J., Joo, H.S., Frey, M.L., 1993. Enhanced replication of porcine reproductive and respiratory syndrome (PRRS) virus in a homogeneous subpopulation of MA-104 cell line. Arch. Virol. 133, 477-483.

Kim, O., Sun, Y., Lai, F.W., Song, C., Yoo, D., 2010. Modulation of type I interferon induction by porcine reproductive and respiratory syndrome virus and degradation of CREB-binding protein by non-structural protein 1 in MARC-145 and HeLa cells. Virology 402, 315-326.

Kim, W.I., Yoon, K.J., 2008. Molecular assessment of the role of envelope-associated structural proteins in cross neutralization among different PRRS viruses. Virus Genes 37, 380-391.

Kipp, M., Gohring, F., Ostendorp, T., van Drunen, C.M., van Driel, R., Przybylski, M., Fackelmayer, F.O., 2000. SAF-Box, a conserved protein domain that specifically recognizes scaffold attachment region DNA. Mol. Cell. Biol. 20(20), 7480-7489.

Koyama, S., Ishii, K.J., Coban, C., Akira, S., 2008. Innate immune response to viral infection. Cytokine 43, 336-341.

Kroese, M.V., Zevenhoven-Dobbe, J.C., Bos-de Ruijter, J.N., Peeters, B.P., Meulenberg, J.J., Cornelissen, L.A., Snijder, E.J., 2008. The nsp1alpha and nsp1 papain-like autoproteinases are essential for porcine reproductive and respiratory syndrome virus RNA synthesis. J. Gen. Virol. 89, 494-499.

Kroese, M.V., Zevenhoven-Dobbe, J.C., Ruijter, J.N.A.B.D., Peeters, B.P.H., Meulenberg, J.J.M., Cornelissen, L.A.H.M., Snijder, E.J., 2008. The nsp1 alpha and nsp1 beta papain-like autoproteinases are essential for porcine reproductive and respiratory syndrome virus RNA synthesis. J. Gen. Virol. 89, 494-499.

Kubota, T., Matsuoka, M., Xu, S., Otsuki, N., Takeda, M., Kato, A., Ozato, K., 2011. PIASy inhibits virus-induced and interferon-stimulated transcription through distinct mechanisms. J. Biol. Chem. 286, 8165-8175.

Kuo, H.Y., Chang, C.C., Jeng, J.C., Hu, H.M., Lin, D.Y., Maul, G.G., Kwok, R.P.S., Shih, H.M., 2005. SUMO modification negatively modulates the transcriptional activity of CREB-

binding protein via the recruitment of Daxx. Proc. Natl. Acad. Sci. USA. 102, 16973-16978.
Kuss, S.K., Mata, M.A., Zhang, L., Fontoura, B.M., 2013. Nuclear imprisonment: viral strategies to arrest host mRNA nuclear export. Viruses 5, 1824-1849.
Kuzemtseva, L., de la Torre, E., Martin, G., Soldevila, F., Ait-Ali, T., Mateu, E., Darwich, L., 2014. Regulation of toll-like receptors 3, 7 and 9 in porcine alveolar macrophages by different genotype 1 strains of porcine reproductive and respiratory syndrome virus. Vet. Immunol. Immunop. 158, 189-198.
Kwon, B., Ansari, I.H., Osorio, F.A., Pattnaik, A.K., 2006. Infectious clone-derived viruses from virulent and vaccine strains of porcine reproductive and respiratory syndrome virus mimic biological properties of their parental viruses in a pregnant sow model. Vaccine 24, 7071-7080.
Kwon, B., Ansari, I.H., Pattnaik, A.K., Osorio, F.A., 2008. Identification of virulence determinants of porcine reproductive and respiratory syndrome virus through construction of chimeric clones. Virology 380, 371-378.
Laity, J.H., Lee, B.M., Wright, P.E., 2001. Zinc finger proteins: new insights into structural and functional diversity. Curr. Opin. Struct. Biol. 11, 39-46.
Lauck, M., Hyeroba, D., Tumukunde, A., Weny, G., Lank, S.M., Chapman, C.A., O′Connor, D.H., Friedrich, T.C., Goldberg, T.L., 2011. Novel, Divergent Simian Hemorrhagic Fever Viruses in a Wild Ugandan Red Colobus Monkey Discovered Using Direct Pyrosequencing. PLoS One 6, e19056.
Lauck, M., Sibley, S.D., Hyeroba, D., Tumukunde, A., Weny, G., Chapman, C.A., Ting, N., Switzer, W.M., Kuhn, J.H., Friedrich, T.C., O′Connor, D.H., Goldberg, T.L., 2013. Exceptional simian hemorrhagic fever virus diversity in a wild African primate community. J. Virol. 87, 688-691.
Lee, C., Calvert, J.G., Welich, S.K.W., Yoo, D., 2005. A DNA-launched reverse genetics system for porcine reproductive and respiratory syndrome virus reveals that homodimerization of the nucleocapsid protein is essential for virus infectivity. Virology 331, 47-62.
Lee, C., Hodgins, D., Calvert, J.G., Welch, S.K.W., Jolie, R., Yoo, D., 2006. Mutations within the nuclear localization signal of the porcine reproductive and respiratory syndrome virus nucleocapsid protein attenuate virus replication. Virology 346, 238-250.
Lee, C., Yoo, D., 2005. Cysteine residues of the porcine reproductive and respiratory syndrome virus small envelope protein are non-essential for virus infectivity. J. Gen. Virol. 86, 3091-3096.
Lee, C., Yoo, D., 2006. The small envelope protein of porcine reproductive and respiratory syndrome virus possesses ion channel protein-like properties. Virology 355, 30-43.
Lee, S.M., Kleiboeker, S.B., 2005. Porcine arterivirus activates the NF-kappaB pathway through IkappaB degradation. Virology 342, 47-59.
Lee, S.M., Schommer, S.K., Kleiboeker, S.B., 2004. Porcine reproductive and respiratory syndrome virus field isolates differ in in vitro interferon phenotypes. Vet. Immunol. Immunopath. 102, 217-231.
Lee, Y.J., Lee, C., 2010. Porcine reproductive and respiratory syndrome virus replication is suppressed by inhibition of the extracellular signal-regulated kinase (ERK) signaling pathway. Virus Res. 152, 50-58.

Lee, Y.J., Lee, C., 2012. Stress-activated protein kinases are involved in porcine reproductive and respiratory syndrome virus infection and modulate virus-induced cytokine production. Virology 427, 80-89.

Li, Y., Tas, A., Snijder, E.J., Fang, Y., 2012. Identification of porcine reproductive and respiratory syndrome virus ORF1a-encoded non-structural proteins in virus-infected cells. J. Gen. Virol. 93, 829-839.

Li, Y., Treffers, E.E., Napthine, S., Tas, A., Zhu, L., Sun, Z., Bell, S., Mark, B.L., van Veelen, P.A., van Hemert, M.J., Firth, A.E., Brierley, I., Snijder, E.J., Fang, Y., 2014. Transactivation of programmed ribosomal frameshifting by a viral protein. Proc. Natl. Acad. Sci. USA.111, E2172-2181.

Li, Y., Zhou, L., Zhang, J., Ge, X., Zhou, R., Zheng, H., Geng, G., Guo, X., Yang, H., 2014. Nsp9 and Nsp10 contribute to the fatal virulence of highly pathogenic porcine reproductive and respiratory syndrome virus emerging in China. PLoS Pathog 10, e1004216

Li, Y., Zhu, L., Lawson, S.R., Fang, Y., 2013. Targeted mutations in a highly conserved motif of the nsp1beta protein impair the interferon antagonizing activity of porcine reproductive and respiratory syndrome virus. J. Gen. Virol. 94, 1972-1983.

Lidsky, P.V., Hato, S., Bardina, M.V., Aminev, A.G., Palmenberg, A.C., Sheval, E.V., Polyakov, V.Y., van Kuppeveld, F.J.M., Agol, V.I., 2006. Nucleocytoplasmic traffic disorder induced by cardioviruses. J. Virol. 80(6), 2705-2717.

Lim, K.P., Ng, L.F., Liu, D.X., 2000. Identification of a novel cleavage activity of the first papain-like proteinase domain encoded by open reading frame 1a of the coronavirus Avian infectious bronchitis virus and characterization of the cleavage products. J. Virol. 74, 1674-1685.

Lindner, H.A., Fotouhi-Ardakani, N., Lytvyn, V., Lachance, P., Sulea, T., Menard, R., 2005. The papain-like protease from the severe acute respiratory syndrome coronavirus is a deubiquitinating enzyme. J. Virol. 79, 15199-15208.

Liu, B., Gross, M., ten Hoeve, J., Shuai, K., 2001. A transcriptional corepressor of Stat1 with an essential LXXLL signature motif. Proc. Natl. Acad. Sci. USA. 98(6), 3203-3207.

Liu, C.H., Chaung, H.C., Chang, H.L., Peng, Y.T., Chung, W.B., 2009. Expression of Toll-like receptor mRNA and cytokines in pigs infected with porcine reproductive and respiratory syndrome virus. Vet. Microbiol.136, 266-276.

Lloyd, R.E., 2006. Translational control by viral proteinases. Virus Res. 119(1), 76-88.

Long, J.Y., Wang, G.N., Matsuura, I., He, D.M., Liu, F., 2004. Activation of Smad transcriptional activity by protein inhibitor of activated STAT3 (PIAS3). Proc. Natl. Acad. Sci. USA. 101, 99-104.

Lopez-Fuertes, L., Campos, E., Domenech, N., Ezquerra, A., Castro, J.M., Dominguez, J., Alonso, F., 2000. Porcine reproductive and respiratory syndrome (PRRS) virus down-modulates TNF-alpha production in infected macrophages. Virus Res. 69, 41-46.

Loving, C.L., Brockmeier, S.L., Sacco, R.E., 2007. Differential type I interferon activation and susceptibility of dendritic cell populations to porcine arterivirus. Immunology 120, 217-229.

Lu, Z., Zhang, J., Huang, C.M., Go, Y.Y., Faaberg, K.S., Rowland, R.R., Timoney, P.J., Balasuriya, U.B., 2012. Chimeric viruses containing the N-terminal ectodomains of GP5 and M proteins of porcine reproductive and respiratory syndrome virus do not change the cellular tropism of equine arteritis virus. Virology 432, 99-109.

Luo, R., Fang, L., Jiang, Y., Jin, H., Wang, Y., Wang, D., Chen, H., Xiao, S., 2011. Activation of NF-kappaB by nucleocapsid protein of the porcine reproductive and respiratory syndrome virus. Virus Genes 42, 76-81.

Luo, R., Xiao, S., Jiang, Y., Jin, H., Wang, D., Liu, M., Chen, H., Fang, L., 2008. Porcine reproductive and respiratory syndrome virus (PRRSV) suppresses interferon-beta production by interfering with the RIG-I signaling pathway. Mol. Immunol. 45, 2839-2846.

Lv, J., Zhan, J.W., Sun, Z., Liu, W.Q., Yuan, S.S., 2008. An infectious cDNA clone of a highly pathogenic porcine reproductive and respiratory syndrome virus variant associated with porcine high fever syndrome. J. Gen. Virol. 89, 2075-2079.

Martinez-Salas, E., Pacheco, A., Serrano, P., Fernandez, N., 2008. New insights into internal ribosome entry site elements relevant for viral gene expression. J. Gen. Virol. 89(Pt 3), 611-626.

Mathur, R.K., Awasthi, A., Wadhone, P., Ramanamurthy, B., Saha, B., 2004. Reciprocal CD40 signals through p38MAPK and ERK-1/2 induce counteracting immune responses. Nat. Med. 10, 540-544.

Meulenberg, J.J., Hulst, M.M., de Meijer, E.J., Moonen, P.L., den Besten, A., de Kluyver, E.P., Wensvoort, G., Moormann, R.J., 1993. Lelystad virus, the causative agent of porcine epidemic abortion and respiratory syndrome (PEARS), is related to LDV and EAV. Virology 192, 62-72.

Meulenberg, J.J.M., BosDeRuijter, J.N.A., vandeGraaf, R., Wensvoort, G., Moormann, R.J.M., 1998. Infectious transcripts from cloned genome-length cDNA of porcine reproductive and respiratory syndrome virus. J. Virol. 72, 380-387.

Meyers, G., Tautz, N., Becher, P., Thiel, H.J., Kummerer, B.M., 1997. Recovery of cytopathogenic and noncytopathogenic bovine viral diarrhea viruses from cDNA constructs. J. Virol. 71, 1735.

Mielech, A.M., Chen, Y., Mesecar, A.D., Baker, S.C., 2014a. Nidovirus papain-like proteases: Multifunctional enzymes with protease, deubiquitinating and deISGylating activities. Virus Res. S0168-1702, 40-49 .

Mielech, A.M., Kilianski, A., Baez-Santos, Y.M., Mesecar, A.D., Baker, S.C., 2014b. MERS-CoV papain-like protease has deISGylating and deubiquitinating activities. Virology 450-451, 64-70.

Miguel, J.C., Chen, J., Van Alstine, W.G., Johnson, R.W., 2010. Expression of inflammatory cytokines and Toll-like receptors in the brain and respiratory tract of pigs infected with porcine reproductive and respiratory syndrome virus. Vet. Immunol. Immunop. 135, 314-319.

Mildner, A., Jung, S., 2014. Development and function of dendritic cell subsets. Immunity 40, 642-656.

Miller, L.C., Laegreid, W.W., Bono, J.L., Chitko-McKown, C.G., Fox, J.M., 2004. Interferon type I response in porcine reproductive and respiratory syndrome virus-infected MARC-145 cells. Arch. Virol. 149, 2453-2463.

Miller, L.C., Lager, K.M., Kehrli, M.E., Jr., 2009. Role of Toll-like receptors in activation of porcine alveolar macrophages by porcine reproductive and respiratory syndrome virus. Clin. Vaccine. Immunol. 16, 360-365.

Moore, B.D., Balasuriya, U.B., Watson, J.L., Bosio, C.M., MacKay, R.J., MacLachlan, N.J., 2003. Virulent and avirulent strains of equine arteritis virus induce different quantities of

TNF-alpha and other proinflammatory cytokines in alveolar and blood-derived equine macrophages. Virology 314, 662-670.
Moormann, R.J., van Gennip, H.G., Miedema, G.K., Hulst, M.M., van Rijn, P.A., 1996. Infectious RNA transcribed from an engineered full-length cDNA template of the genome of a pestivirus. J. Virol. 70, 763-770.
Moura, G., Pinheiro, M., Arrais, J., Gomes, A.C., Carreto, L., Freitas, A., Oliveira, J.L., Santos, M.A., 2007. Large scale comparative codon-pair context analysis unveils general rules that fine-tune evolution of mRNA primary structure. PLoS One 2, e847.
Mueller, S., Coleman, J.R., Papamichail, D., Ward, C.B., Nimnual, A., Futcher, B., Skiena, S., Wimmer, E., 2010. Live attenuated influenza virus vaccines by computer-aided rational design. Nature Biotechnol. 28, 723-726.
Murakami, Y., Kato, A., Tsuda, T., Morozumi, T., Miura, Y., Sugimura, T., 1994. Isolation and serological characterization of porcine reproductive and respiratory syndrome (PRRS) viruses from pigs with reproductive and respiratory disorders in Japan. J. Vet. Med. Sci. 56, 891-894.
Murray, P.J., 2007. The JAK-STAT signaling pathway: input and output integration. J. Immunol. 178, 2623-2629.
Murtaugh, M.P., Elam, M.R., Kakach, L.T., 1995. Comparison of the structural protein-coding sequences of the VR-2332 and Lelystad virus-strains of the PRRS virus. Arch. Virol. 140, 1451-1460.
Music, N., Gagnon, C.A., 2010. The role of porcine reproductive and respiratory syndrome (PRRS) virus structural and non-structural proteins in virus pathogenesis. Animal. Health. Res. Rev. 11, 135-163.
Nan, Y., Wang, R., Shen, M., Faaberg, K.S., Samal, S.K., Zhang, Y.J., 2012. Induction of type I interferons by a novel porcine reproductive and respiratory syndrome virus isolate. Virology 432, 261-270.
Narayananj, K., Huang, C., Lokugamage, K., Kamitani, W., Ikegami, T., Tseng, C.T.K., Makino, S., 2008. Severe acute respiratory syndrome coronavirus nsp1 suppresses host gene expression, including that of type I interferon, in infected cells. J. Virol. 82(9), 4471-4479.
Nedialkova, D.D., Gorbalenya, A.E., Snijder, E.J., 2010. Arterivirus np1 modulates the accumulation of minus-strand templates to control the relative abundance of viral mRNAs. Plos Pathog. 6. e1000772.
Nelsen, C.J., Murtaugh, M.P., Faaberg, K.S., 1999. Porcine reproductive and respiratory syndrome virus comparison: divergent evolution on two continents. J. Virol. 73, 270-280.
Nga, P.T., Parquet, M.D., Lauber, C., Parida, M., Nabeshima, T., Yu, F.X., Thuy, N.T., Inoue, S., Ito, T., Okamoto, K., Ichinose, A., Snijder, E.J., Morita, K., Gorbalenya, A.E., 2011. Discovery of the first insect Nidovirus, a missing evolutionary link in the emergence of the largest RNA virus genomes. PLoS Pathog. 7, e1002215.
Ni, Y.Y., Huang, Y.W., Cao, D.J., Opriessnig, T., Meng, X.J., 2011. Establishment of a DNA-launched infectious clone for a highly pneumovirulent strain of type 2 porcine reproductive and respiratory syndrome virus: Identification and in vitro and in vivo characterization of a large spontaneous deletion in the nsp2 region. Virus Res. 160, 264-273.
Ni, Y.Y., Opriessnig, T., Zhou, L., Cao, D.J., Huang, Y.W., Halbur, P.G., Meng, X.J., 2013. Attenuation of porcine reproductive and respiratory syndrome virus by molecular breeding of virus envelope genes from genetically divergent strains. J. Virol. 87, 304-313.

Ni, Y.Y., Zhao, Z., Opriessnig, T., Subramaniam, S., Zhou, L., Cao, D., Cao, Q., Yang, H., Meng, X.J., 2014. Computer-aided codon-pairs deoptimization of the major envelope GP5 gene attenuates porcine reproductive and respiratory syndrome virus. Virology 450-451, 132-139.

Nielsen, H.S., Liu, G., Nielsen, J., Oleksiewicz, M.B., Botner, A., Storgaard, T., Faaberg, K.S., 2003. Generation of an infectious clone of VR-2332, a highly virulent North American type isolate of porcine reproductive and respiratory syndrome virus. J. Virol. 77, 3702-3711.

Okubo, S., Hara, F., Tsuchida, Y., Shimotakahara, S., Suzuki, S., Hatanaka, H., Yokoyama, S., Tanaka, H., Yasuda, H., Shindo, H., 2004. NMR structure of the N-terminal domain of SUMO ligase PIAS1 and its interaction with tumor suppressor p53 and A/T-rich DNA oligomers. J. Biol. Chem. 279(30), 31455-31461.

Okumura, A., Alce, T., Lubyova, B., Ezelle, H., Strebel, K., Pitha, P.M., 2008. HIV-1 accessory proteins VPR and Vif modulate antiviral response by targeting IRF-3 for degradation. Virology 373, 85-97.

Oleksiewicz, M.B., Botner, A., Toft, P., Normann, P., Storgaard, T., 2001. Epitope mapping porcine reproductive and respiratory syndrome virus by phage display: the nsp2 fragment of the replicase polyprotein contains a cluster of B-cell epitopes. J. Virol. 75, 3277-3290.

Panne, D., McWhirter, S.M., Maniatis, T., Harrison, S.C., 2007. Interferon regulatory factor 3 is regulated by a dual phosphorylation-dependent switch. J. Biol. Chem. 282, 22816-22822.

Park, N., Skern, T., Gustin, K.E., 2010. Specific Cleavage of the Nuclear Pore Complex Protein Nup62 by a Viral Protease. J. Biol. Chem. 285(37), 28796-28805.

Pasternak, A.O., Spaan, W.J.M., Snijder, E.J., 2006. Nidovirus transcription: how to make sense ... ? J. Gen. Virol. 87, 1403-1421.

Patel, D., Nan, Y., Shen, M., Ritthipichai, K., Zhu, X., Zhang, Y.J., 2010. Porcine reproductive and respiratory syndrome virus inhibits type I interferon signaling by blocking STAT1/STAT2 nuclear translocation. J. Virol. 84, 11045-11055.

Pei, Y., Hodgins, D.C., Lee, C., Calvert, J.G., Welch, S.K.W., Jolie, R., Keith, M., Yoo, D., 2008. Functional mapping of the porcine reproductive and respiratory syndrome virus capsid protein nuclear localization signal and its pathogenic association. Virus Res. 135, 107-114.

Pei, Y.L., Hodgins, D.C., Wu, J.Q., Welch, S.K.W., Calvert, J.G., Li, G., Du, Y.J., Song, C., Yoo, D.W., 2009. Porcine reproductive and respiratory syndrome virus as a vector: Immunogenicity of green fluorescent protein and porcine circovirus type 2 capsid expressed from dedicated subgenomic RNAs. Virology 389, 91-99.

Plagemann, P.G.W., Rowland, R.R.R., Even, C., Faaberg, K.S., 1995. Lactate dehydrogenase-elevating virus - an ideal persistent virus. Springer. Semin. Immun. 17, 167-186.

Porter, F.W., Bochkov, Y.A., Albee, A.J., Wiese, C., Palmenberg, A.C., 2006. A picornavirus protein interacts with Ran-GTPase and disrupts nucleocytoplasmic transport. Proc. Natl. Acad. Sci. USA. 103(33), 12417-12422.

Pu, S.Y., Wu, R.H., Yang, C.C., Jao, T.M., Tsai, M.H., Wang, J.C., Lin, H.M., Chao, Y.S., Yueh, A., 2011. Successful propagation of flavivirus infectious cDNAs by a novel method to reduce the cryptic bacterial promoter activity of virus genomes. J. Virol. 85, 2927-2941.

Pujhari, S., Baig, T.T., Zakhartchouk, A.N., 2014. Potential role of porcine reproductive and respiratory syndrome virus structural protein GP2 in apoptosis inhibition. Biomed Res Int., 2014, Article ID 160505, http://dx.doi.org/10.1155/2014/160505

Racaniello, V.R., Baltimore, D., 1981. Cloned Ppliovirus complementary-DNA is infectious in mammalian-cells. Science 214, 916-919.

Ran, Z.G., Chen, X.Y., Guo, X., Ge, X.N., Yoon, K.J., Yang, H.C., 2008. Recovery of viable porcine reproductive and respiratory syndrome virus from an infectious clone containing a partial deletion within the Nsp2-encoding region. Arch. Virol. 153, 899-907.

Randall, R.E., Goodbourn, S., 2008. Interferons and viruses: an interplay between induction, signalling, antiviral responses and virus countermeasures. J. Gen. Virol. 89, 1-47.

Ren, J., Liu, T., Pang, L., Li, K., Garofalo, R.P., Casola, A., Bao, X., 2011. A novel mechanism for the inhibition of interferon regulatory factor-3-dependent gene expression by human respiratory syncytial virus NS1 protein. J. Gen. Virol. 92, 2153-2159.

Ricour, C., Delhaye, S., Hato, S.V., Olenyik, T.D., Michel, B., van Kuppeveld, F.J.M., Gustin, K.E., Michiels, T., 2009. Inhibition of mRNA export and dimerization of interferon regulatory factor 3 by Theiler′s virus leader protein. J. Gen. Virol. 90, 177-186.

Rowland, R.R., Kervin, R., Kuckleburg, C., Sperlich, A., Benfield, D.A., 1999. The localization of porcine reproductive and respiratory syndrome virus nucleocapsid protein to the nucleolus of infected cells and identification of a potential nucleolar localization signal sequence. Virus Res. 64, 1-12.

Rowland, R.R., Robinson, B., Stefanick, J., Kim, T.S., Guanghua, L., Lawson, S.R., Benfield, D.A., 2001. Inhibition of porcine reproductive and respiratory syndrome virus by interferon-gamma and recovery of virus replication with 2-aminopurine. Arch.Virol. 146, 539-555.

Rowland, R.R., Yoo, D., 2003. Nucleolar-cytoplasmic shuttling of PRRSV nucleocapsid protein: a simple case of molecular mimicry or the complex regulation by nuclear import, nucleolar localization and nuclear export signal sequences. Virus Res. 95, 23-33.

Rowland, R.R.R., Schneider, P., Fang, Y., Wootton, S., Yoo, D., Benfield, D.A., 2003. Peptide domains involved in the localization of the porcine reproductive and respiratory syndrome virus nucleocapsid protein to the nucleolus. Virology 316, 135-145.

Rowland, R.R.R., Yoo, D., 2003. Nucleolar-cytoplasmic shuttling of PRRSV nucleocapsid protein: a simple case of molecular mimicry or the complex regulation by nuclear import, nucleolar localization and nuclear export signal sequences. Virus Res. 95, 23-33.

Ryan, C.M., Kindle, K.B., Collins, H.M., Heery, D.M., 2010. SUMOylation regulates the nuclear mobility of CREB binding protein and its association with nuclear bodies in live cells. Biochem. Biophys. Res. Commun. 391, 1136-1141.

Saccani, S., Pantano, S., Natoli, G., 2002. p38-Dependent marking of inflammatory genes for increased NF-kappa B recruitment. Nat. Immunol. 3, 69-75.

Sadler, A.J., Williams, B.R.G., 2008. Interferon-inducible antiviral effectors. Nat. Rev. Immunol. 8, 559-568.

Sagong, M., Lee, C., 2011. Porcine reproductive and respiratory syndrome virus nucleocapsid protein modulates interferon-beta production by inhibiting IRF3 activation in immortalized porcine alveolar macrophages. Arch. Virol. 156(12), 2187-2195.

Samuel, C.E., 2001. Antiviral actions of interferons. Clin. Microbiol. Rev. 14, 778-809.

Sanchez-Molina, S., Oliva, J.L., Garcia-Vargas, S., Valls, E., Rojas, J.M., Martinez-Balbas, M.A., 2006. The histone acetyltransferases CBP/p300 are degraded in NIH 3T3 cells by activation of Ras signalling pathway. Biochem. J. 398, 215-224.

Sang, Y.M., Shi, J.S., Sang, W.J., Rowland, R.R.R., Blecha, F., 2012. Replication-competent recombinant porcine reproductive and respiratory syndrome (PRRS) viruses expressing indicator proteins and antiviral cytokines. Viruses (Basel) 4, 102-116.

Sawicki, S.G., Sawicki, D.L., Siddell, S.G., 2007. A contemporary view of coronavirus transcription. J. Virol. 81, 20-29.

Schindler, C., Darnell, J.E., Jr., 1995. Transcriptional responses to polypeptide ligands: the JAK-STAT pathway. Ann. Rev. Biochem. 64, 621-651.

Scobey, T., Yount, B.L., Sims, A.C., Donaldson, E.F., Agnihothram, S.S., Menachery, V.D., Graham, R.L., Swanstrom, J., Bove, P.F., Kim, J.D., Grego, S., Randell, S.H., Baric, R.S., 2013. Reverse genetics with a full-length infectious cDNA of the Middle East respiratory syndrome coronavirus. Proc. Natl. Acad. Sci. USA. 110, 16157-16162.

Segundo, F.D., Weiss, M., Perez-Martin, E., Dias, C.C., Grubman, M.J., Santos Tde, L., 2012. Inoculation of swine with foot-and-mouth disease SAP-mutant virus induces early protection against disease. J. Virol. 86(3), 1316-1327.

Sen, A., Feng, N.G., Ettayebi, K., Hardy, M.E., Greenberg, H.B., 2009. IRF3 inhibition by rotavirus NSP1 is host cell and virus strain dependent but independent of NSP1 proteasomal degradation. J. Virol. 83, 10322-10335.

Sen, N., Sommer, M., Che, X., White, K., Ruyechan, W.T., Arvin, A.M., 2010. Varicella-zoster virus immediate-early protein 62 blocks interferon regulatory factor 3 (IRF3) phosphorylation at key serine residues: a novel mechanism of IRF3 inhibition among herpesviruses. J. Virol. 84, 9240-9253.

Shen, S., Kwang, J., Liu, W., Liu, D.X., 2000. Determination of the complete nucleotide sequence of a vaccine strain of porcine reproductive and respiratory syndrome virus and identification of the Nsp2 gene with a unique insertion. Arch. Virol. 145, 871-883.

Shi, X., Wang, L., Zhi, Y., Xing, G., Zhao, D., Deng, R., Zhang, G., 2010. Porcine reproductive and respiratory syndrome virus (PRRSV) could be sensed by professional beta interferon-producing system and had mechanisms to inhibit this action in MARC-145 cells. Virus Res. 153, 151-156.

Shi, X., Zhang, G., Wang, L., Li, X., Zhi, Y., Wang, F., Fan, J., Deng, R., 2011. The nonstructural protein 1 papain-like cysteine protease was necessary for porcine reproductive and respiratory syndrome virus nonstructural protein 1 to inhibit interferon-beta induction. DNA. Cell. Biol. 30, 355-362.

Shimizu, M., Yamada, S., Murakami, Y., Morozumi, T., Kobayashi, H., Mitani, K., Ito, N., Kubo, M., Kimura, K., Kobayashi, M., et al., 1994. Isolation of porcine reproductive and respiratory syndrome (PRRS) virus from Heko-Heko disease of pigs. J. Vet. Med. Sci. 56, 389-391.

Smith, R.W., Gray, N.K., 2010. Poly(A)-binding protein (PABP): a common viral target. The Biochem. J. 426(1), 1-12.

Snijder, E.J., Kikkert, M., Fang, Y., 2013. Arterivirus molecular biology and pathogenesis. J. Gen. Virol. 94, 2141-2163.

Snijder, E.J., Meulenberg, J.J., 1998. The molecular biology of arteriviruses. Journal of General Virology 79, 961-979.

Snijder, E.J., van Tol, H., Pedersen, K.W., Raamsman, M.J.B., de Vries, A.A.F., 1999. Identification of a novel structural protein of arteriviruses. J. Virol. 73, 6335-6345.

Snijder, E.J., Wassenaar, A.L., Spaan, W.J., 1992. The 5′ end of the equine arteritis virus replicase gene encodes a papainlike cysteine protease. J. Virol. 66, 7040-7048.

Snijder, E.J., Wassenaar, A.L., Spaan, W.J., 1993. Proteolytic processing of the N-terminal region of the equine arteritis virus replicase. Adv. Exp. Med. Biol. 342, 227-232.
Snijder, E.J., Wassenaar, A.L., Spaan, W.J., Gorbalenya, A.E., 1995. The arterivirus Nsp2 protease. An unusual cysteine protease with primary structure similarities to both papain-like and chymotrypsin-like proteases. J. Biol. Chem. 270, 16671-16676.
Snijder, E.J., Wassenaar, A.L.M., Spaan, W.J.M., 1994. Proteolytic Processing of the Replicase Orf1a Protein of Equine Arteritis Virus. J. Virol. 68, 5755-5764.
Sokoloski, K.J., Chaskey, E.L., Wilusz, J., 2009. Virus-mediated mRNA decay by hyperadenylation. Genome Biol. 10(8), 234.
Sola, I., Mateos-Gomez, P.A., Almazan, F., Zuniga, S., Enjuanes, L., 2011. RNA-RNA and RNA-protein interactions in coronavirus replication and transcription. RNA Biol 8, 237-248.
Song, C., Krell, P., Yoo, D., 2010. Nonstructural protein 1alpha subunit-based inhibition of NF-kappaB activation and suppression of interferon-beta production by porcine reproductive and respiratory syndrome virus. Virology 407, 268-280.
Song, S., Bi, J., Wang, D., Fang, L., Zhang, L., Li, F., Chen, H., Xiao, S., 2013. Porcine reproductive and respiratory syndrome virus infection activates IL-10 production through NF-kappaB and p38 MAPK pathways in porcine alveolar macrophages. Dev. Comp. Immunol. 39, 265-272.
Sosnovtsev, S., Green, K.Y., 1995. RNA transcripts derived from a cloned full-length copy of the feline calicivirus genome do not require VpG for infectivity. Virology 210, 383-390.
Spilman, M.S., Welbon, C., Nelson, E., Dokland, T., 2009. Cryo-electron tomography of porcine reproductive and respiratory syndrome virus: organization of the nucleocapsid. J. Gen. Virol. 90, 527-535.
Steinberger, J., Kontaxis, G., Rancan, C., Skern, T., 2013. Comparison of self-processing of foot-and-mouth disease virus leader proteinase and porcine reproductive and respiratory syndrome virus leader proteinase nsp1α. Virology 443, 271-277.
Subramaniam, S., Beura, L.K., Kwon, B., Pattnaik, A.K., Osorio, F.A., 2012. Amino acid residues in the nonstructural protein 1 of porcine reproductive and respiratory syndrome virus involved in down-regulation of TNF-alpha expression in vitro and attenuation in vivo. Virology 432, 241-249.
Subramaniam, S., Kwon, B., Beura, L.K., Kuszynski, C.A., Pattnaik, A.K., Osorio, F.A., 2010. Porcine reproductive and respiratory syndrome virus non-structural protein 1 suppresses tumor necrosis factor-alpha promoter activation by inhibiting NF-kappaB and Sp1. Virology 406, 270-279.
Sumiyoshi, H., Hoke, C.H., Trent, D.W., 1992. Infectious japanese encephalitis-virus RNA can be synthesized from in vitro-ligated cDNA templates. J. Virol. 66, 5425-5431.
Sun, Y., Han, M.Y., Kim, C., Calvert, J.G., Yoo, D., 2012. Interplay between interferon-mediated innate immunity and porcine reproductive and respiratory syndrome virus. Viruses 4, 424-446.
Sun, Y., Li, D., Giri, S., Prasanth, S.G., Yoo, D., 2014. Differential host cell gene expression and regulation of cell cycle progression by nonstructural protein 11 of porcine reproductive and respiratory syndrome virus. BioMed Res. Int. 2014, 430508.
Sun, Y., Xue, F., Guo, Y., Ma, M., Hao, N., Zhang, X.C., Lou, Z., Li, X., Rao, Z., 2009. Crystal structure of porcine reproductive and respiratory syndrome virus leader protease nsp1-alpha. J. Virol. 83, 10931-10940.

Sun, Z., Chen, Z.H., Lawson, S.R., Fang, Y., 2010a. The cysteine protease domain of porcine reproductive and respiratory syndrome virus nonstructural protein 2 possesses deubiquitinating and interferon antagonism functions. J. Virol. 84, 7832-7846.

Sun, Z., Li, Y.H., Ransburgh, R., Snijder, E.J., Fang, Y., 2012b. Nonstructural protein 2 of porcine reproductive and respiratory syndrome virus inhibits the antiviral function of interferon-simulated gene 15. J. Virol. 86, 3839-3850.

Sun, Z., Liu, C.L., Tan, F.F., Gao, F., Liu, P., Qin, A.J., Yuan, S.S., 2010b. Identification of dispensable nucleotide sequence in 3′ untranslated region of porcine reproductive and respiratory syndrome virus. Virus Res. 154, 38-47.

Suradhat, S., Thanawongnuwech, R., Poovorawan, Y., 2003. Upregulation of IL-10 gene expression in porcine peripheral blood mononuclear cells by porcine reproductive and respiratory syndrome virus. J. Gen. Virol. 84, 453-459.

Takahasi, K., Horiuchi, M., Fujii, K., Nakamura, S., Noda, N.N., Yoneyama, M., Fujita, T., Inagaki, F., 2010. Ser386 phosphorylation of transcription factor IRF-3 induces dimerization and association with CBP/p300 without overall conformational change. Genes to Cells 15, 901-910.

Tan, F.F., Wei, Z.Z., Li, Y.H., Zhang, R., Zhuang, J.S., Sun, Z., Yuan, S.S., 2011. Identification of non-essential regions in nucleocapsid protein of porcine reproductive and respiratory syndrome virus for replication in cell culture. Virus Res. 158, 62-71.

Tanaka, T., Nishimura, D., Wu, R.C., Amano, M., Iso, T., Kedes, L., Nishida, H., Kaibuchi, K., Hamamori, Y., 2006. Nuclear Rho kinase, ROCK2, targets p300 acetyltransferase. J. Biol. Chem. 281, 15320-15329.

Thanawongnuwech, R., Young, T.F., Thacker, B.J., Thacker, E.L., 2001. Differential production of proinflammatory cytokines: in vitro PRRSV and Mycoplasma hyopneumoniae co-infection model. Vet. Immunol. Immunop. 79, 115-127.

Thompson, P.R., Wang, D., Wang, L., Fulco, M., Pediconi, N., Zhang, D., An, W., Ge, Q., Roeder, R.G., Wong, J., Levrero, M., Sartorelli, V., Cotter, R.J., Cole, P.A., 2004. Regulation of the p300 HAT domain via a novel activation loop. Nat. Struct. Mol. Biol. 11, 308-315.

Tian, D.B., Wei, Z.Z., Zevenhoven-Dobbe, J.C., Liu, R.X., Tong, G.Z., Snijder, E.J., Yuan, S.S., 2012. Arterivirus minor envelope proteins are a major determinant of viral tropism in cell culture. J. Virol. 86, 3701-3712.

Tian, D.B., Zheng, H.H., Zhang, R., Zhuang, J.S., Yuan, S.S., 2011. Chimeric porcine reproductive and respiratory syndrome viruses reveal full function of genotype 1 envelope proteins in the backbone of genotype 2. Virology 412, 1-8.

Tian, K.G., Yu, X.L., Zhao, T.Z., Feng, Y.J., Cao, Z., Wang, C.B., Hu, Y., Chen, X.Z., Hu, D.M., Tian, X.S., Liu, D., Zhang, S.O., Deng, X.Y., Ding, Y.Q., Yang, L., Zhang, Y.X., Xiao, H.X., Qiao, M.M., Wang, B., Hou, L.L., Wang, X.Y., Yang, X.Y., Kang, L.P., Sun, M., Jin, P., Wang, S.J., Kitamura, Y., Yan, J.H., Gao, G.F., 2007. Emergence of fatal PRRSV variants: Unparalleled outbreaks of atypical PRRS in China and molecular dissection of the unique hallmark. PLoS One 2. e526.

Tijms, M.A., Nedialkova, D.D., Zevenhoven-Dobbe, J.C., Gorbalenya, A.E., Snijder, E.J., 2007. Arterivirus subgenomic mRNA synthesis and virion biogenesis depend on the multifunctional nsp1 autoprotease. J. Virol. 81, 10496-10505.

Tijms, M.A., van der Meer, Y., Snijder, E.J., 2002. Nuclear localization of non-structural protein 1 and nucleocapsid protein of equine arteritis virus. J. Gen. Virol. 83, 795-800.

Tijms, M.A., van Dinten, L.C., Gorbalenya, A.E., Snijder, E.J., 2001. A zinc finger-containing papain-like protease couples subgenomic mRNA synthesis to genome translation in a positive-stranded RNA virus. Proc. Natl. Acad. Sci. USA. 98, 1889-1894.

Tohya, Y., Narayanan, K., Kamitani, W., Huang, C., Lokugamage, K., Makino, S., 2009. Suppression of host gene expression by nsp1 proteins of group 2 bat coronaviruses. J. Virol. 83(10), 5282-5288.

Truong, H.M., Lu, Z., Kutish, G.F., Galeota, J., Osorio, F.A., Pattnaik, A.K., 2004. A highly pathogenic porcine reproductive and respiratory syndrome virus generated from an infectious cDNA clone retains the in vivo virulence and transmissibility properties of the parental virus. Virology 325, 308-319.

van Aken, D., Zevenhoven-Dobbe, J., Gorbalenya, A.E., Snijder, E.J., 2006. Proteolytic maturation of replicase polyprotein pp1a by the nsp4 main proteinase is essential for equine arteritis virus replication and includes internal cleavage of nsp7. J. Gen. Virol. 87, 3473-3482.

Van Hemert, M.J., Snijder, E. J. 2007. Nidoviruses, the arterivirus replicase. Charpter 6, 83-101.

van Kasteren, P.B., Bailey-Elkin, B.A., James, T.W., Ninaber, D.K., Beugeling, C., Khajehpour, M., Snijder, E.J., Mark, B.L., Kikkert, M., 2013. Deubiquitinase function of arterivirus papain-like protease 2 suppresses the innate immune response in infected host cells. Proc. Natl. Acad. Sci. USA.110(9), E838-847.

van Kasteren, P.B., Beugeling, C., Ninaber, D.K., Frias-Staheli, N., van Boheemen, S., Garcia-Sastre, A., Snijder, E.J., Kikkert, M., 2012. Arterivirus and nirovirus ovarian tumor domain-containing deubiquitinases target activated RIG-I to control innate immune signaling. J. Virol. 86, 773-785.

Van Reeth, K., Labarque, G., Nauwynck, H., Pensaert, M., 1999. Differential production of proinflammatory cytokines in the pig lung during different respiratory virus infections: correlations with pathogenicity. Res. Vet. Science 67, 47-52.

vanDinten, L.C., denBoon, J.A., Wassenaar, A.L.M., Spaan, W.J.M., Snijder, E.J., 1997. An infectious arterivirus cDNA clone: Identification of a replicase point mutation that abolishes discontinuous mRNA transcription. Proc. Natl. Acad. Sci. USA. 94, 991-996.

Vatter, H.A., Brinton, M.A., 2014. Differential responses of disease-resistant and disease-susceptible primate macrophages and myeloid dendritic cells to simian hemorrhagic fever virus infection. J. Virol. 88, 2095-2106.

Verheije, M.H., Kroese, M.V., Rottier, P.J.M., Meulenberg, J.J.M., 2001. Viable porcine arteriviruses with deletions proximal to the 3 ′ end of the genome. J. Gen. Virol. 82, 2607-2614.

Verheije, M.H., Welting, T.J.M., Jansen, H.T., Rottier, P.J.M., Meulenberg, J.J.M., 2002. Chimeric arteriviruses generated by swapping of the M protein ectodomain rule out a role of this domain in viral targeting. Virology 303, 364-373.

Vogt, C., Preuss, E., Mayer, D., Weber, F., Schwemmle, M., Kochs, G., 2008. The interferon antagonist ML protein of Thogoto virus targets general transcription factor IIB. J. Virol. 82, 11446-11453.

Vu, H.L.X., Kwon, B., de Lima, M., Pattnaik, A.K., Osorio, F.A., 2013. Characterization of a serologic marker candidate for development of a live-attenuated DIVA vaccine against porcine reproductive and respiratory syndrome virus. Vaccine 31, 4330-4337.

Vu, H.L.X., Kwon, B., Yoon, K.J., Laegreid, W.W., Pattnaik, A.K., Osorio, F.A., 2011. Immune evasion of porcine reproductive and respiratory syndrome virus through glycan shielding involves both glycoprotein 5 as well as glycoprotein 3. J. Virol. 85, 5555-5564.

Walsh, D., Mohr, I., 2011. Viral subversion of the host protein synthesis machinery. Nat. Rev. Micro. 9, 860-875.

Wang, D.Z., Li, S., Hockemeyer, D., Sutherland, L., Wang, Z., Schratt, G., Richardson, J.A., Nordheim, A., Olson, E.N., 2002. Potentiation of serum response factor activity by a family of myocardin-related transcription factors. Proc. Natl. Acad. Sci. USA. 99(23), 14855-14860.

Wang, R., Nan, Y.C., Yu, Y., Zhang, Y.J., 2013. Porcine reproductive and respiratory syndrome virus nsp1 beta inhibits interferon-activated JAK/STAT signal transduction by inducing karyopherin-alpha 1 degradation. J. Virol. 87, 5219-5228.

Wang, X., Eaton, M., Mayer, M., Li, H., He, D., Nelson, E., Christopher-Hennings, J., 2007. Porcine reproductive and respiratory syndrome virus productively infects monocyte-derived dendritic cells and compromises their antigen-presenting ability. Arch. Virol. 152, 289-303.

Weaver, B.K., Kumar, K.P., Reich, N.C., 1998. Interferon regulatory factor 3 and CREB-binding protein/p300 are subunits of double-stranded RNA-activated transcription factor DRAF1. Mol. Cell. Biol. 18, 1359-1368.

Wei, Z.Z., Lin, T., Sun, L.C., Li, Y.H., Wang, X.M., Gao, F., Liu, R.X., Chen, C.Y., Tong, G.Z., Yuan, S.S., 2012. N-Linked glycosylation of GP5 of porcine reproductive and respiratory syndrome virus is critically important for virus replication in vivo. J. Virol. 86, 9941-9951.

Welch, S.K.W., Jolie, R., Pearce, D.S., Koertje, W.D., Fuog, E., Shields, S.L., Yoo, D., Calvert, J.G., 2004. Construction and evaluation of genetically engineered replication-defective porcine reproductive and respiratory syndrome virus vaccine candidates. Vet. Immunol. Immunopathol. 102, 277-290.

Wensvoort, G., Terpstra, C., Pol, J.M., ter Laak, E.A., Bloemraad, M., de Kluyver, E.P., Kragten, C., van Buiten, L., den Besten, A., Wagenaar, F., et al., 1991. Mystery swine disease in The Netherlands: the isolation of Lelystad virus. Vet. Quart. 13(3), 121-130.

Wojciak, J.M., Martinez-Yamout, M.A., Dyson, H.J., Wright, P.E., 2009. Structural basis for recruitment of CBP/p300 coactivators by STAT1 and STAT2 transactivation domains. EMBO J. 28, 948-958.

Wojdyla, J.A., Manolaridis, I., van Kasteren, P.B., Kikkert, M., Snijder, E.J., Gorbalenya, A.E., Tucker, P.A., 2010. Papain-like protease 1 from transmissible gastroenteritis virus: crystal structure and enzymatic activity toward viral and cellular substrates. J. Virol. 84, 10063-10073.

Wongyanin, P., Buranapraditkul, S., Yoo, D., Thanawongnuwech, R., Roth, J.A., Suradhat, S., 2012. Role of porcine reproductive and respiratory syndrome virus nucleocapsid protein in induction of interleukin-10 and regulatory T-lymphocytes (Treg). J. Gen. Virol. 93, 1236-1246.

Wootton, S., Koljesar, G., Yang, L.Z., Yoon, K.J., Yoo, D., 2001. Antigenic importance of the carboxy-terminal beta-strand of the porcine reproductive and respiratory syndrome virus nucleocapsid protein. Clin. Diag. Lab. Immunol. 8, 598-603.

Wootton, S., Yoo, D., Rogan, D., 2000. Full-length sequence of a Canadian porcine reproductive and respiratory syndrome virus (PRRSV) isolate. Arch. Virol. 145, 2297-2323.

Wootton, S.K., Rowland, R.R., Yoo, D., 2002. Phosphorylation of the porcine reproductive and respiratory syndrome virus nucleocapsid protein. J. Virol. 76, 10569-10576.

Xiao, J.H., Davidson, I., Matthes, H., Garnier, J.M., Chambon, P., 1991. Cloning, expression, and transcriptional properties of the human enhancer factor TEF-1. Cell 65, 551-568.

Xing, Y.L., Chen, J.F., Tu, J., Zhang, B.L., Chen, X.J., Shi, H.Y., Baker, S.C., Feng, L., Chen, Z.B., 2013. The papain-like protease of porcine epidemic diarrhea virus negatively regulates type I interferon pathway by acting as a viral deubiquitinase. J. Gen. Virol. 94, 1554-1567.

Xu, Y.Z., Zhou, Y.J., Zhang, S.R., Jiang, Y.F., Tong, W., Yu, H., Tong, G.Z., 2012a. Stable expression of foreign gene in nonessential region of nonstructural protein 2 (nsp2) of porcine reproductive and respiratory syndrome virus: Applications for marker vaccine design. Vet. Microbiol. 159, 1-10.

Xu, Y.Z., Zhou, Y.J., Zhang, S.R., Tong, W., Li, L., Jiang, Y.F., Tong, G.Z., 2012b. Identification of nonessential regions of the nsp2 protein of an attenuated vaccine strain (HuN4-F112) of highly pathogenic porcine reproductive and respiratory syndrome virus for replication in MARC-145 cell. Virol J 9.

Xue, F., Sun, Y., Yan, L., Zhao, C., Chen, J., Bartlam, M., Li, X., Lou, Z., Rao, Z., 2010. The crystal structure of porcine reproductive and respiratory syndrome virus nonstructural protein nsp1beta reveals a novel metal-dependent nuclease. J. Virol. 84, 6461-6471.

Yoo, D., Song, C., Sun, Y., Du, Y., Kim, O., Liu, H.C., 2010. Modulation of host cell responses and evasion strategies for porcine reproductive and respiratory syndrome virus. Virus Res. 154, 48-60.

Yoo, D., Wootton, S.K., Li, G., Song, C., Rowland, R.R., 2003. Colocalization and interaction of the porcine arterivirus nucleocapsid protein with the small nucleolar RNA-associated protein fibrillarin. J. Virol. 77, 12173-12183.

Yoo, D.W., Welch, S.K.W., Lee, C.H., Calvert, J.G., 2004. Infectious cDNA clones of porcine reproductive and respiratory syndrome virus and their potential as vaccine vectors. Vet Immunol Immunop 102, 143-154.

Yount, B., Curtis, K.M., Fritz, E.A., Hensley, L.E., Jahrling, P.B., Prentice, E., Denison, M.R., Geisbert, T.W., Baric, R.S., 2003. Reverse genetics with a full-length infectious cDNA of severe acute respiratory syndrome coronavirus. Proc. Natl. Acad. Sci. USA. 100, 12995-13000.

Yu, D.D., Lv, J., Sun, Z., Zheng, H.H., Lu, J.Q., Yuan, S.S., 2009. Reverse genetic manipulation of the overlapping coding regions for structural proteins of the type II porcine reproductive and respiratory syndrome virus. Virology 383, 22-31.

Yuan, S., Wei, Z., 2008. Construction of infectious cDNA clones of PRRSV: separation of coding regions for nonstructural and structural proteins. Science in China. Series C, Life sciences / Chinese Academy of Sciences 51, 271-279.

Zhang, H., Guo, X., Nelson, E., Christopher-Hennings, J., Wang, X., 2012. Porcine reproductive and respiratory syndrome virus activates the transcription of interferon alpha/beta (IFN-alpha/beta) in monocyte-derived dendritic cells (Mo-DC). Vet. Microbiol.159, 494-498.

Zhang, R., Chen, C., Sun, Z., Tan, F., Zhuang, J., Tian, D., Tong, G., Yuan, S., 2012. Disulfide linkages mediating nucleocapsid protein dimerization are not required for porcine arterivirus infectivity. J. Virol. 86, 4670-4681.

Zhang, S.R., Zhou, Y.J., Jiang, Y.F., Li, G.X., Yan, L.P., Yu, H., Tong, G.Z., 2011. Generation of an infectious clone of HuN4-F112, an attenuated live vaccine strain of porcine reproductive and respiratory syndrome virus. Virol. J. 8:410.

Zhang, Z., Zheng, Z., Luo, H., Meng, J., Li, H., Li, Q., Zhang, X., Ke, X., Bai, B., Mao, P., Hu, Q., Wang, H., 2012. Human Bocavirus NP1 inhibits IFN-beta production by blocking association of IFN regulatory factor 3 with IFNβ promoter. J. Immunol. 189, 1144-1153.

Zheng, D.H., Chen, G., Guo, B.C., Cheng, G.H., Tang, H., 2008. PLP2, a potent deubiquitinase from murine hepatitis virus, strongly inhibits cellular type I interferon production. Cell Res. 18, 1105-1113.

Zhou, H.X., Perlman, S., 2007. Mouse hepatitis virus does not induce beta interferon synthesis and does not inhibit its induction by double-stranded RNA. J. Virol. 81, 568-574.

Zhou, L., Ni, Y.Y., Pineyro, P., Cossaboom, C.M., Subramaniam, S., Sanford, B.J., Dryman, B.A., Huang, Y.W., Meng, X.J., 2013. Broadening the heterologous cross-neutralizing antibody inducing ability of porcine reproductive and respiratory syndrome virus by breeding the GP4 or M genes. PloS One 8, e66645.

Zhou, L., Ni, Y.Y., Pineyro, P., Sanford, B.J., Cossaboom, C.M., Dryman, B.A., Huang, Y.W., Cao, D.J., Meng, X.J., 2012. DNA shuffling of the GP3 genes of porcine reproductive and respiratory syndrome virus (PRRSV) produces a chimeric virus with an improved cross-neutralizing ability against a heterologous PRRSV strain. Virology 434, 96-109.

Zhou, L., Zhang, J., Zeng, J., Yin, S., Li, Y., Zheng, L., Guo, X., Ge, X., Yang, H., 2009. The 30-amino-acid deletion in the Nsp2 of highly pathogenic porcine reproductive and respiratory syndrome virus emerging in China is not related to its virulence. J. Virol. 83, 5156-5167.

Zhu, H., Zheng, C., Xing, J., Wang, S., Li, S., Lin, R., Mossman, K.L., 2011. Varicella-zoster virus immediate-early protein ORF61 abrogates the IRF3-mediated innate immune response through degradation of activated IRF3. J. Virol. 85, 11079-11089.

Ziebuhr, J., Snijder, E.J., Gorbalenya, A.E., 2000. Virus-encoded proteinases and proteolytic processing in the Nidovirales. J. Gen. Virol. 81, 853-879.

Zirkel, F., Kurth, A., Quan, P.L., Briese, T., Ellerbrok, H., Pauli, G., Leendertz, F.H., Lipkin, W.I., Ziebuhr, J., Drosten, C., Junglen, S., 2011. An insect nidovirus emerging from a primary tropical rainforest. MBio 2, e00077-11.

Zust, R., Cervantes-Barragan, L., Kuri, T., Blakqori, G., Weber, F., Ludewig, B., Thiel, V., 2007. Coronavirus non-structural protein 1 is a major pathogenicity factor: Implications for the rational design of coronavirus vaccines. PLoS pathog. 3(8), 1062-1072.